

Dynamics and Control of Lattice Boom Cranes as Spatial Rigid-Flexible Multibody Systems

Dynamik und Steuerung von Gitterauslegerkranen als
Räumlich Starr-Flexible Mehrkörpersysteme

Wissenschaftliche Arbeit zur Erlangung des Grades
M.Sc.
an der Fakultät für Maschinenwesen der Technischen Universität München.

Themenstellende/r Prof. Dr.-Ing. Johannes Fottner
Lehrstuhl für Fördertechnik Materialfluss Logistik

Betreuer/Betreuerin M.Sc. Lingchong Gao

Eingereicht von Xiaobing Dai
Tumblingerstraße 56, 315
80337 München
+49 15257535182

Eingereicht am 31, Mai, 2021 in Garching

Inventarnr. fml 2020116

Anhang I

Erklärung

Ich versichere hiermit, dass ich die von mir eingereichte Abschlussarbeit selbstständig verfasst und keine anderen als die angegebenen Quellen und Hilfsmittel benutzt habe.

München, 31. Mai, 2021

Ort, Datum, Unterschrift

Dai-xiaobing

Appendix I

Statement

I hereby affirm that I wrote the thesis by myself and that I did not use any other sources or aids than those in bibliography.

München, 31, Mai, 2021

Place, Date, Signature

Dai Xianbing

Vorwort

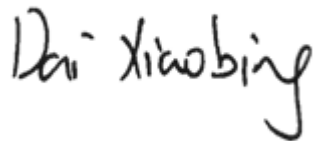
Die vorliegende Arbeit entstand unter der wissenschaftlichen und inhaltlichen Anleitung von M.Sc. Lingchong Gao, wissenschaftlicher Mitarbeiter am Lehrstuhl für Fördertechnik Materialfluss Logistik (fml) der Technischen Universität München.

Vereinbarung zum Urheberrecht

Hiermit gestatte ich dem Lehrstuhl für Fördertechnik Materialfluss Logistik diese Studienarbeit bzw. Teile davon nach eigenem Ermessen an Dritte weiterzugeben, zu veröffentlichen oder anderweitig zu nutzen. Mein persönliches Urheberrecht ist über diese Regelung hinaus nicht beeinträchtigt.

Eventuelle Geheimhaltungsvereinbarungen über den Inhalt der Arbeit zwischen mir bzw. dem Lehrstuhl für Fördertechnik Materialfluss Logistik und Dritten bleiben von dieser Vereinbarung unberührt.

31, Mai, 2021 München
Ort, Datum, Unterschrift

Lin Xianbing

Foreword

The present work was created under the scientific and content-related guidance of M.Sc. Lingchong Gao, research assistant at the Chair for Materials Handling, Material Flow, Logistics (fml) at the Technical University of Munich.

Copyright Agreement

I hereby permit the Chair of Materials Handling, Material Flow, Logistics to pass on, publish or otherwise use this thesis or parts of it to third parties at its own discretion. My personal copyright is not affected beyond this regulation.

Any non-disclosure agreements between myself or the Chair of Materials Handling, Material Flow, Logistics and third parties regarding the content of the work remain unaffected by this agreement.

31, Mai, 2021 München
Place, Date, Signature

Ling Xiaobing

Abstract

A mobile crane equipped with a boom system is widely used to lift the heavy load on construction sites. Lattice boom with lower self-mass is designed to lift larger load and move. Therefore, the dynamic response of the lattice boom is important but also time-consuming due to a large number of degrees of freedom.

In this thesis, several flexible models are established to simulate the beam elements, rod elements and rope elements. In addition, a detailed super truss element formulation for nonlinear truss element is proposed to reduce the number of degrees of freedom of complex lattice boom.

According to the control requirements of the lattice boom crane, a quasi-static control method is designed to realize the optimal control for specified complex system. This method combines the static mapping relationship with the target optimal trajectory to generate the optimal control trajectory.

Several experiments for different beam elements are performed to do the cross verification. A dynamic calculation of the lattice boom crane is performed to simulate the lifting, luffing and slewing stages.

Keywords: non-linear dynamics, mobile crane, lattice boom, optimal control

Nomenclature

Symbol	Explanation
$\underline{\underline{I}}^*$	Variable $*$ in inertial coordinate
$\underline{\underline{B}}^*$	Variable $*$ in local body coordinate
$*^i$	Variable $*$ of body i
$*_e$	Variable $*$ for element
$\underline{\underline{R}}_B, \underline{\underline{R}}_B$	Rotation matrix from local body coordinate to inertial coordinate
$\dot{*} = d(*)/dt$	First-order total derivative of the variable $*$ to time
$\ddot{*} = d^2(*)/dt^2$	Second-order total derivative of the variable $*$ to time
$*' = d(*)/ds$	First-order total derivative of the variable $*$ to arc coordinate
$*'' = d^2(*)/ds^2$	Second-order total derivative of the variable $*$ to arc coordinate
$*^T$	Transpose of a matrix or vector $*$
$\underline{\underline{I}}, \underline{\underline{0}}, \underline{\underline{0}}$	Identity matrix, zero matrix and zero vector
$\underline{\varphi}$	Rotation vector
$\underline{\underline{\tilde{s}}} = \text{skew}(\underline{\underline{*}})$	Skew symmetric matrix of vector $*$
$\underline{\underline{R}}_{x_1}, \underline{\underline{R}}_{x_2}, \underline{\underline{R}}_{x_3}$ or $\underline{\underline{R}}_x, \underline{\underline{R}}_y, \underline{\underline{R}}_z$	elementary rotation matrix
$\underline{\underline{g}}_{x_1}, \underline{\underline{g}}_{x_2}, \underline{\underline{g}}_{x_3}$ or $\underline{\underline{g}}_x, \underline{\underline{g}}_y, \underline{\underline{g}}_z$	base vector of the global coordinate system
$\underline{\underline{n}}_{x_1}, \underline{\underline{n}}_{x_2}, \underline{\underline{n}}_{x_3}$ or $\underline{\underline{n}}_x, \underline{\underline{n}}_y, \underline{\underline{n}}_z$	base vector of the local body coordinate system
$j\omega^i$	angular velocity of body i in the coordinate system j
$j\kappa^i$	curvature of body i in the coordinate system j
$\underline{\underline{T}}$	Transformation matrix
$m, J, \underline{\underline{\Theta}}$	Mass, Moment of inertia, Moment of inertia
ρ	Density of body
V	Volume of body
L	Length of beam or rod or rope
A	Area of section
$\underline{\underline{F}}, \underline{\underline{M}}$	Force vector, Moment vector
$\underline{\underline{K}}, \underline{\underline{K}_E}, \underline{\underline{K}_T}$	Stiffness or Constitutive matrix, normal stiffness, shear stiffness
$\underline{\varepsilon}, \underline{\tau}$	(Normal) strain, shear strain
$\underline{\sigma}$	Stress
$\delta *$	Virtual variable $*$
$\underline{\underline{g}}$	Gravity vector
p	Power
$\underline{q}, \underline{dq}$	Generalized coordinate and generalized velocity
$\underline{\Phi}$	Constraint vector
$\underline{\lambda}$	Lagrange operator
\underline{u}	Deformation vector

Symbol	Explanation
$\underline{\underline{N}}$	Shape function or shape matrix
$\nabla(\cdot)$	Nabla operator
$\underline{\underline{F}}$	Deformation Gradient Tensor
$\underline{\underline{C}}$	Right Cauchy-Green Tensors
$\underline{\underline{B}}$	Left Cauchy-Green Tensors
$\underline{\underline{f}}$	Finger Deformation Tensor
$\underline{\underline{c}}$	Cauchy Deformation Tensor
$\underline{\underline{\sigma}}$	Cauchy Stress
$\underline{\underline{\tau}}$	1 st Piola-Kirchhoff Stress
$\underline{\underline{S}}$	2 nd Piola-Kirchhoff Stress
J	Cost function
$L(\underline{x}(t), \underline{u}(t), t)$	Running cost
$\Phi(x_e, t_e)$	Terminal cost
t_0, t_e	Start time and end time
t_s, t_f	Sampling time and simulation time
\underline{x}	State variable

All units used in this thesis are based on SI (Système International d'Unités).

Catalogue

1	Introduction	1
1.1	Background of Lattice Boom Crane	1
1.2	Technical Route	2
2	State of Technology	3
2.1	Spatial Kinematics and Rotations	3
2.1.1	Relative Kinematics and Rotation Matrices	3
2.1.2	Spatial Angle Representation	3
2.1.3	Derivative Laws of Rotation Matrix	4
2.2	Dynamics Modeling Method	5
2.2.1	Virtual Power Principle	5
2.2.2	Minimum DoF Method (Lagrange's Equation of Second Kind)	6
2.2.3	Multibody Dynamics Method (Lagrange's Equation of First Kind)	6
2.3	Mechanics of Flexible Element	7
2.3.1	Modeling Method based on Co-rotational Coordinate	7
2.3.2	Modeling Method based on Absolute Coordinate	7
2.3.3	Deformation and Strain Tensor	8
2.3.4	Stress Tensor	9
2.4	Optimal Control Theory	9
2.4.1	Classical Optimal Control Theory	9
2.4.2	Non-linear Model Predictive Control	10
3	Dynamic Models of different Types of Elements	11
3.1	Rigid Body Dynamic Model	11
3.1.1	Generalized Coordination and Generalized Velocity	11
3.1.2	Kinematics of Points on Rigid Body	11
3.1.3	The Virtual Power of Rigid Body	11
3.2	Two Nodes Strut Tie Dynamic Model	12
3.2.1	Assumption for Ideal Strut Tie Model	12
3.2.2	Generalized Coordinate and Generalized Velocity	12
3.2.3	Kinematics and Deformation of Points on the Beam	13
3.2.4	Discretization and Shape Function	14
3.2.5	The Virtual Power of Strut Tie Model	15

3.2.6	Body Parameter of Strut Tie Model after Deformation	16
3.3	Spatial Timoshenko Beam Dynamic Model	16
3.3.1	Generalized Coordination, Velocity and Co-rotational Coordinate	16
3.3.2	Assumptions and Formulation of Deformation	17
3.3.3	Kinematics of Points on Timoshenko Beam	18
3.3.4	The Formulation of Strain and Stress	19
3.3.5	The Virtual Power of Timoshenko Beam	19
3.3.6	Discretization and Shape Function	20
3.4	Cubic Spline Beam Dynamic Model	22
3.4.1	Assumptions for Cubic Spline Beam	22
3.4.2	Generalized Coordinate and Generalized Velocity	22
3.4.3	Discretization and Shape Function	23
3.4.4	Kinematics and Deformation of Points on the Beam	25
3.4.5	The Virtual Power of Cubic Spline Beam	25
3.5	Super Truss Element Dynamic Model	26
3.5.1	Assumptions for Super Truss Element	26
3.5.2	Parameterization of Super Truss Element	27
3.5.3	Dynamics Calculation of Super Truss Element	30
4	Multi-Body Dynamics Method	35
4.1	Multi-Body Dynamics Function	35
4.2	Joint Configuration	36
4.3	System Generalized External Forces	36
4.4	Formulation of Different Constraints	37
4.4.1	Fixed Constraint	37
4.4.2	Revolute Constraint	38
4.4.3	Prismatic Constraint	39
4.4.4	Spherical Constraint	40
4.5	Solving Multibody Dynamics Equation	41
4.5.1	Baumgartner stability method	41
4.5.2	State Space Representation	41
4.5.3	Runge-Kutta Integrator	42
5	Rigid-Flexible Hybrid Multibody Dynamics Program	45
5.1	Functions of the Program	45
5.1.1	Main Functions	45

5.1.2 Additional Modules and Auxiliary Modules	46
5.2 Data Input and Parameter Setting	48
5.2.1 Parameters for Dynamics Model	48
5.2.2 Parameters for Solving Route	49
5.3 Display and Analysis of Result	50
5.3.1 Video Generation	50
5.3.2 Specified Analysis Method	50
6 Optimal Control of Lattice Boom Crane	51
6.1 Quasi-Static Optimal Trajectory Tracking Strategy	51
6.2 Static State Mapping	51
6.3 NMPC for Optimal State Trajectory Generation	53
6.4 Generation of Optimal Control Trajectory	55
7 Detailed Modeling of Lattice Boom Crane	57
7.1 Lattice Boom	57
7.1.1 Main Boom	57
7.1.2 Derrick Boom	58
7.2 Rope and Rope Systems	59
7.2.1 Rope Model	59
7.2.2 Rope System	59
7.3 Pedestal and Load	59
7.4 Constraints and Drives	60
7.4.1 Constraints	60
7.4.2 Drives	61
8 Analysis and Evaluation of Simulation Results	63
8.1 Cross-validation of Single Flexible Beam Element	63
8.1.1 Cantilever Beam Static Bending Test	63
8.1.2 Vibration Test of Cantilever Beam under Self-gravity	64
8.1.3 Fixed Axis Rotation under Torque Control and Angle Control	65
8.2 Simulation for Single Super Truss Element	66
8.2.1 Vibration Test of Cantilever Truss Boom under Self-gravity	67
8.2.2 Fixed Axis Rotation under Torque Control and Angle Control	67
8.2.3 Equivalent Stiffness and Mass	68
8.3 Simulation for Lattice Boom Crane	69

8.3.1 Elementary Movement	69
8.3.2 Combined Motion	72
8.4 Quasi-Static Optimal Control of Crane	73
8.4.1 Quasi-Static Mapping	73
8.4.2 Optimal Trajectory of End Point	74
8.4.3 Optimal Control Trajectory and Verification	75
9 Conclusion and Future Development	79
9.1 Conclusion	79
9.2 Future Development	80
Bibliography	81
List of Figures	85
List of Tables	87
Appendix A Mathematical Convention	A-1
Appendix B Spatial Rotation and Kinematics	B-1
Appendix C Detailed Dynamics Models of Different Types of Elements	C-1
Appendix D Detailed Modelling Information of Lattice Boom Crane	D-1
Appendix E Specified Drive Function	E-1

1 Introduction

1.1 Background of Lattice Boom Crane

Among the large number of cranes developed for various tasks, mobile cranes are particularly flexible in their application possibilities. Truck-mounted cranes, mobile cranes, railway cranes, and crawler cranes are different cranes equipped with a boom system, which can be designed as telescopic or truss boom. Compared with the continuous boom structure, the crane with a truss boom has a higher load capacity under the same mass due to the optimization of its structure. It is suitable for lifting tasks with special requirements of lifting height and radius. It is mainly used for large-scale factory construction, steel industry, and building construction [Kle-1996].

The form and boom configuration of cranes is diverse and complex. In the design process, simulation and proofreading for different types of cranes under different load cases are required, which causes many calculations. As a kind of engineering machinery, mobile cranes need to lift a large load and move (crawler crane). Considering the mass of the hoisting cargo and the boom structure, dynamics calculations should be done, especially for some extreme conditions in the lifting capacity sheet. The dynamic modeling of lattice boom becomes difficult due to the unevenness of cross-section and a large number of nodes and elements. Previously there are mainly two modeling methods: 1. Modeling of each element of the lattice boom [Gün-1997]; 2. Modeling the entire lattice boom with a continuous flexible beam element.

Therefore, a scientific reduction method that accelerates the model calculation and makes the number of degrees of freedom small is urgently needed. For truss boom, there is a static condensation method, which condenses the stiffness and gravity of the truss beam to the nodes on the end section. This method is only suitable for the static reduction of linear models [Kle-2006]. For dynamics reduction, the Craig-Bampton method is often used. It converts the dynamic equations from the time domain into the frequency domain to obtain information such as the natural frequency of the system [Kou-2007]. However, for nonlinear models, it is very difficult to convert them to the frequency domain [Kam-2015].

The vibration of flexible large structures is a severe test for the stability and safety of large structures [Arn-2003]. In order to reduce the impact of dynamic loads on the crane structure, a controller is needed which can reduce the vibration while meeting specific operation objects [Neu-2010]. In addition, the movement of such large

machinery is very energy consuming, it is necessary to investigate the optimal trajectory to meet the requirements of moving time, mechanical stability and energy consumption. Currently, general optimal control algorithms are only used for simpler models. The research on optimal control algorithms for large-scale dynamics models is very necessary.

1.2 Technical Route

In chapter 1, the research background, research goals and research framework of this thesis are clarified. In chapter 2, the modeling methods (kinematics, materials properties, dynamics modeling methods) and control methods (iterative format, optimal control algorithm) are introduced.

In chapter 3, different types of dynamics models are introduced, including rigid body model, spatial Timoshenko beam, strut tie model, Cubic Spline Beam and the super truss element. And in Chapter 4, through multi-body dynamics, these simple dynamics models are connected through constraints to form the final model. In addition, the Baumgartner stability method, state space expression, and explicit and implicit Runge-Kutta integrator are also introduced to solve the dynamic equations.

In chapter 5, the traditional optimal control algorithm and the optimal control based on deep reinforcement learning are introduced.

In chapter 6, a rigid-flexible hybrid multi-body dynamics program platform based on MatLab is introduced. The functions, operation method and basic logics of the program are described. And in chapter 7, based on this platform, several commonly used crane models are created by defining the composition, connection and driving mode.

In chapter 8, some experimental results are shown. Firstly cross-validation experiments with different flexible beam models are conducted. Secondly, the vibration tests of cantilever truss beam and approximate static deformation calculation for super truss element are performed, to get the dynamics and statics response. Finally, the motion response of the crane model without control and with optimal control is analyzed.

Finally, in chapter 9, the main content and the results obtained are summarized. Based on the research results and actual engineering application scenarios, the further research direction is proposed.

2 State of Technology

2.1 Spatial Kinematics and Rotations

2.1.1 Relative Kinematics and Rotation Matrices

The position vector of a certain point has different representations in different coordinate systems, they can be transformed by the rotation matrix $\underline{\underline{R}}_B$.

$$\underline{\underline{r}} = \underline{\underline{R}}_{BB} \underline{\underline{r}} \quad \text{with} \quad \underline{\underline{R}}_B \triangleq \underline{\underline{R}}_B \quad (2-1)$$

where $\underline{\underline{r}}$ is the position vector in inertial coordinate and $\underline{\underline{r}}_B$ is the position vector in local body coordinate. The absolute speed and absolute acceleration of the point must consider the relative movement in the certain coordinate system as well as the movement of the coordinate system, which can be written as

$$\underline{\dot{r}} = \underline{\dot{\underline{\underline{R}}}_{BB}} \underline{\underline{r}} + \underline{\underline{R}}_{BB} \dot{\underline{\underline{r}}} \quad \underline{\ddot{r}} = \underline{\ddot{\underline{\underline{R}}}_{BB}} \underline{\underline{r}} + 2\underline{\dot{\underline{\underline{R}}}_{BB}} \dot{\underline{\underline{r}}} + \underline{\underline{R}}_{BB} \ddot{\underline{\underline{r}}} \quad (2-2)$$

2.1.2 Spatial Angle Representation

Axis-Angle Representation

The Cartesian rotation vector is used to describe the rotation vector through the axis and angle. The direction of the vector \underline{n} represents the direction of the rotation axis, and the norm of the vector θ represents the angle of rotation along the rotation axis [Die-2006]. Since the direction of the rotation vector is consistent with the rotation axis, the expression of the vector in the two coordinate systems before and after the rotation is the same, which is represented by $\underline{\varphi}$.

$$\underline{\varphi} = \underline{\varphi}_B = \underline{\varphi} \quad \theta = \|\underline{\varphi}\| \quad \underline{n} = \underline{\varphi}/\theta \quad (2-3)$$

The rotation matrix under the axis angle representation can be obtained by Rodrigues' rotation formula [Kov-2012].

$$\underline{\underline{R}}_B = \underline{\underline{I}} + \frac{\sin \theta}{\theta} \tilde{\underline{\underline{\varphi}}} + \frac{1 - \cos \theta}{\theta^2} \underline{\underline{\varphi}} \tilde{\underline{\underline{\varphi}}} \quad (2-4)$$

The relationship between angular velocity or curvature and the derivative of angle can be obtained by

$$\underline{\underline{T}}(\underline{\varphi}) = \underline{\underline{I}} + \frac{\cos \|\underline{\varphi}\| - 1}{\|\underline{\varphi}\|^2} \underline{\underline{\tilde{\varphi}}} + \frac{\|\underline{\varphi}\| - \sin \|\underline{\varphi}\|}{\|\underline{\varphi}\|^3} \underline{\underline{\tilde{\varphi}}}\underline{\underline{\tilde{\varphi}}} \quad (2-5)$$

Cardan Angles and Euler Angles

Both the Cardan angle [Tup-1987] and the Euler angle [Pio-1966] are compounded by successive elementary rotation around the x_i , x_j and x_k axes. The angle vector with $i \neq j \neq k$ is called the Cardan angle; and with $i = k \neq j$ is called the Euler angle. The rotation sequence of the Cardan angle and Euler angle must be defined before use.

$$\begin{array}{ccc} I \xrightarrow[\varphi_i]{} {}^1x_i & \xrightarrow[\varphi_j]{} {}^1x_j & \xrightarrow[\varphi_k]{} {}^2x_k \\ & & \end{array} \Rightarrow \begin{array}{l} \underline{\underline{R}}_B = {}^I\underline{\underline{R}}_1 {}^1\underline{\underline{R}}_2 {}^2\underline{\underline{R}}_B \\ = \underline{\underline{R}}_{x_i}(\varphi_i) \underline{\underline{R}}_{x_j}(\varphi_j) \underline{\underline{R}}_{x_k}(\varphi_k) \end{array} \quad (2-6)$$

The relationship between angular velocity or curvature and the derivative of angle can be obtained by

$$\underline{\underline{T}} = \underline{\underline{g}}_{x_k} \underline{\underline{g}}_x^T + {}^B\underline{\underline{R}}_2 \underline{\underline{g}}_{x_j} \underline{\underline{g}}_y^T + {}^B\underline{\underline{R}}_2 {}^2\underline{\underline{R}}_1 \underline{\underline{g}}_{x_i} \underline{\underline{g}}_z^T \quad \text{with} \quad \underline{\varphi} = [\varphi_i \quad \varphi_j \quad \varphi_k]^T \quad (2-7)$$

2.1.3 Derivative Laws of Rotation Matrix

Angular velocity is defined as the first derivative of the rotation matrix with time

$${}_I\underline{\underline{\tilde{\omega}}}^B = {}^I\underline{\underline{R}}_B {}^B\underline{\underline{R}}_I \quad {}^B\underline{\underline{\tilde{\omega}}}^B = {}^B\underline{\underline{R}}_I {}^I\underline{\underline{R}}_B \quad (2-8)$$

where $\underline{\underline{\tilde{\omega}}}$ is the skew symmetric matrix of vector $\underline{\omega}$. Curvature is defined by the first derivative of the rotation matrix along the x_i axis

$${}_I\underline{\underline{\tilde{\kappa}}}^B = {}^I\underline{\underline{R}}'_B {}^B\underline{\underline{R}}_I \quad {}^B\underline{\underline{\tilde{\kappa}}}^B = {}^B\underline{\underline{R}}_I {}^I\underline{\underline{R}}'_B \quad (2-9)$$

where here $(')' = \partial(\partial)/\partial x_i$. Normally, the angular velocity and curvature in the local body coordinate can be written in the form of the derivative of angle.

$${}_{\text{B}}\underline{\omega}^{\text{B}} = \underline{T}(\underline{\varphi}) \dot{\underline{\varphi}} \quad {}_{\text{B}}\underline{\kappa}^{\text{B}} = \underline{T}(\underline{\varphi}) \underline{\varphi}' \quad (2-10)$$

The specific formular is related to the spatial angle representation method.

2.2 Dynamics Modeling Method

2.2.1 Virtual Power Principle

The description of virtual power principle [Ger-1973] is, that for a balanced system, the sum of the virtual power of the internal force between two elements is zero.

According to D'Alembert's principle [Vuj-1978], a dynamic system can be turned into a static system by introducing inertial force. Furthermore, internal forces are introduced to transform the flexible dynamics system.

$$\begin{cases} \underline{F}_{\text{ine}} = -m\ddot{\underline{r}} \\ \underline{M}_{\text{ine}} = -J\dot{\underline{\omega}} \end{cases} \quad \begin{cases} \underline{F}_{\text{int}} = -\underline{\underline{K}}_e \underline{\varepsilon} \\ \underline{M}_{\text{int}} = -\underline{\underline{K}}_r \underline{\tau} \end{cases} \quad (2-11)$$

Therefore, the virtual power of the rigid-flexible dynamics system consists of three parts: virtual inertial power, virtual internal power and virtual external power [Jon-1990]. The virtual power of the element can be written as

$$\begin{aligned} \delta p_e &= \delta p_{\text{int}} + \delta p_{\text{ine}} + \delta p_{\text{ext}} = \delta p_{\text{int}} + \delta p_{\text{ine}} + \delta p_{\text{ext,g}} + \delta p_{\text{ext,N}} \\ \delta p_{\text{ine,e}} &= -\rho \iiint_V \delta \dot{\underline{r}}^T \ddot{\underline{r}} dV \quad \delta p_{\text{int,e}} = - \iiint_V \delta \dot{\underline{\varepsilon}}^T \underline{\sigma} dV \\ \delta p_{\text{ext,e,g}} &= \rho \iiint_V \delta \dot{\underline{r}}^T dV \underline{g} \quad \delta p_{\text{ext,e,N}} = \sum_N \delta \dot{\underline{r}}^T \underline{F} \end{aligned} \quad (2-12)$$

According to the virtual power principle, the sum of the virtual power generated by all the forces on the element should be zero. Since the sum of the virtual power produced by the interaction force (I. F.) between the elements is zero, there is no need to consider the interaction force, and the virtual power of the entire system is also zero.

$$\delta p_e = 0 \text{ with I. F.} \quad \delta p = \sum_e \delta p_e = 0 \text{ without I. F.} \quad (2-13)$$

2.2.2 Minimum DoF Method (Lagrange's Equation of Second Kind)

The mechanism is generally composed of multiple elements, and the interconnection between the elements is called a constraint. There are generally two methods for dynamics modeling with constraints: the minimum degree of freedom method and the multi-body dynamics method.

In the minimum degree of freedom method, the system generalized coordinates are the minimum degree of freedom that can describe the state of mechanism. Through the constraint, the generalized coordinates of the elements can be expressed by the system generalized coordinates. Generally, the generalized coordinates, velocity and acceleration of the element can be written as

$$\underline{q}_e = \underline{q}_e(\underline{q}) \quad \underline{dq}_e = \underline{T}_e \underline{dq} \quad \underline{d\dot{q}}_e = \underline{T}_e \underline{d\dot{q}} + \dot{\underline{T}}_e \underline{dq} \quad (2-14)$$

The virtual power of the system can be written through the system virtual generalized velocity. Since the system virtual generalized velocity can be arbitrary, the dynamics equation of the system can be obtained, which is also called the Lagrange's equation of second kind [Hen-2017].

$$\delta p = \sum_e \delta p_e = \delta \underline{dq}^T \sum_e \underline{T}_e^T \frac{\partial p_e}{\partial \underline{q}_e} = 0 \Rightarrow \sum_e \underline{T}_e^T \frac{\partial p_e}{\partial \underline{q}_e} = \underline{0} \quad (2-15)$$

2.2.3 Multibody Dynamics Method (Lagrange's Equation of First Kind)

In the multi-body dynamics method, the system generalized coordinates are composed by the element generalized coordinates without the consideration of the constraints.

$$\underline{q} = [\underline{q}_1^T \quad \underline{q}_2^T \quad \cdots \quad \underline{q}_N^T]^T \quad \underline{T}_e = [0 \quad \cdots \quad I \quad \cdots \quad 0] \quad \dot{\underline{T}}_e = \underline{0} \quad (2-16)$$

Constraints $\underline{\Phi}$ will be written as binding force and introduced into the virtual power of the system through Lagrange operator $\underline{\lambda}$ [Bau-2010].

$$\begin{aligned} \delta p &= \sum_e \delta p_e + \delta \underline{\Phi}^T \underline{\lambda} \\ &= \delta \underline{dq}^T \left(\sum_e \underline{T}_e^T \frac{\partial p_e}{\partial \underline{q}_e} + \frac{\partial \underline{\Phi}}{\partial \underline{q}} \underline{\lambda} \right) = 0 \end{aligned} \Rightarrow \begin{cases} \sum_e \underline{T}_e^T \frac{\partial p_e}{\partial \underline{q}_e} + \frac{\partial \underline{\Phi}}{\partial \underline{q}} \underline{\lambda} = \underline{0} \\ \underline{\Phi} = \underline{0} \end{cases} \quad (2-17)$$

The resultant dynamics equation is called Lagrange's equation of first kind [Yus-1998].

2.3 Mechanics of Flexible Element

2.3.1 Modeling Method based on Co-rotational Coordinate

The co-rotational coordinate is used to describe the base of deformation, which is considered as the position and posture of the element in the undeformed state [Elk-1995; Cri-1990]. The difference between the actual state and the state in the co-rotational coordinate is the deformation of the element.

$$\underline{r} = \underline{r}^* + \underline{u} = \underline{r}^B + \underline{r}^{B,*} + \underline{u} \quad \text{with} \quad \underline{r}^{B,*} = \text{constant} \quad (2-18)$$

where \underline{r} is the actual state after deformation and \underline{r}^* the state before deformation [Li-2007]. \underline{r}^* can also be written through the co-rotational coordinate (base coordinate) \underline{r}^B and the undeformed relative position vector to this point $\underline{r}^{B,*}$. \underline{u} represents the deformation, which can be written through the deformation on the boundary \underline{u}_∂ of the element and shape function $\underline{\underline{N}}_u$.

$$\underline{u} = \underline{\underline{N}}_u \underline{u}_\partial = \underline{\underline{N}}_u (\underline{r}_\partial - \underline{r}_\partial^*) = \underline{\underline{N}}_u (\underline{r}_\partial - \underline{r}^B + \underline{r}_\partial^{B,*}) \quad \text{with} \quad \begin{cases} \underline{r}_\partial \text{ boundary condition} \\ \underline{r}_\partial^{B,*} \text{ known, constant} \end{cases} \quad (2-19)$$

The boundary condition can either be constant or relevant to the element coordinate. Theoretically, the choice of co-rotational coordinate can be arbitrary. By determination of the co-rotational coordinate, the overall small deformation condition and easy calculation requirement should be considered. Generally, the co-rotational coordinate can be written through element coordinate. Therefore, \underline{r} can be written as

$$\underline{r} = (\underline{\underline{I}} - \underline{\underline{N}}_u) \underline{r}^B + (\underline{r}^{B,*} + \underline{\underline{N}}_u \underline{r}_\partial^{B,*}) + \underline{\underline{N}}_u \underline{r}_\partial = \underline{r}(\underline{q}_e) \quad (2-20)$$

The strain will be calculated using the Green-Lagrangian strain tensor.

2.3.2 Modeling Method based on Absolute Coordinate

The position vector and angle vector of the point on the element is obtained directly through the boundary state and the shape function.

$$\begin{cases} \underline{r} = \underline{\underline{N}}_r (\underline{B}\underline{r}^*) \underline{r}_\partial = \underline{r}(\underline{q}_e) \\ \underline{\varphi} = \underline{\underline{N}}_\varphi (\underline{B}\underline{r}^*) \underline{\varphi}_\partial = \underline{\varphi}(\underline{q}_e) \end{cases} \quad \text{with} \quad \underline{B}\underline{r}^* = \underline{B}\underline{r}^B + \underline{B}\underline{r}^{B,*} = \underline{B}\underline{r}^{B,*} \quad (2-21)$$

where ${}_B\bar{r}^B$ represents the undeformed position vector of the origin of the rigid body base in the local coordinate system, which is generally set to $\underline{0}$; ${}_B\bar{r}^{B,*}$ represents the relative displacement in the local coordinate system between the undeformed point of the element and the base origin, which is a fixed value.

For this modeling method, the strain cannot be obtained directly through the difference of position before and after the deformation, but is defined according to the spatial derivative of the position and posture vector [Gar-2003]. For the one-dimensional beam element, the strain tensor is divided into translational and rotational part.

$${}_{B\underline{\underline{\varepsilon}}} = \underline{\underline{R}}^T \underline{\underline{I}} \underline{\underline{r}}' \quad \text{and} \quad {}_{B\underline{\underline{\tilde{\kappa}}}}^B = \underline{\underline{R}}^T \underline{\underline{R}}' \quad \text{with} \quad (\cdot)' = \partial(\cdot)/\partial s \quad (2-22)$$

The translational strain is written as the derivative of position vector along the arc-length. The rotational strain is expressed by the derivative of rotation matrix along the arc-length.

2.3.3 Deformation and Strain Tensor

The deformation and strain are defined without the consideration of the large movement and rotation of the element. There are different definition method for the deformation tensor [Bon-2001; Blu-1989; Cia-2003; Hul-1990]

Table 2-1: Deformation Tensor

	Formula
Deformation Gradient Tensor	$\underline{\underline{F}} = \nabla_{\underline{\underline{c}}^*} \underline{\underline{r}}^c \underline{\underline{r}}^c$
The Right Cauchy-Green Tensors	$\underline{\underline{C}} = \underline{\underline{F}}^T \underline{\underline{F}}$
The Left Cauchy-Green Tensors	$\underline{\underline{B}} = \underline{\underline{F}} \underline{\underline{F}}^T$
The Finger Deformation Tensor	$\underline{\underline{f}} = \underline{\underline{C}}^{-1} = \underline{\underline{F}}^{-1} \underline{\underline{F}}^{-T}$
The Cauchy Deformation Tensor	$\underline{\underline{c}} = \underline{\underline{B}}^{-1} = \underline{\underline{F}}^{-T} \underline{\underline{F}}^{-1}$

The strain describes the difference of displacement in local coordinate. For large deformation the Green-Lagrangian strain tensor (Green-St-Venant strain tensor) is often used [Ped-2005; San-2020], which can be written as

$$\begin{aligned} \underline{\underline{\varepsilon}} &= \frac{1}{2} (\underline{\underline{C}} - \underline{\underline{I}}) = \frac{1}{2} (\nabla_{\underline{\underline{r}}^*}^T \underline{\underline{r}} \nabla_{\underline{\underline{r}}^*} \underline{\underline{r}} - \underline{\underline{I}}) = \frac{1}{2} (\nabla_{\underline{\underline{r}}^*} \underline{\underline{u}} + \nabla_{\underline{\underline{r}}^*}^T \underline{\underline{u}} + \nabla_{\underline{\underline{r}}^*}^T \underline{\underline{u}} \nabla_{\underline{\underline{r}}^*} \underline{\underline{u}}), \underline{\underline{r}} = \underline{\underline{r}}^* + \underline{\underline{u}} \\ \Leftrightarrow {}_B\varepsilon_{ij} &= \frac{1}{2} \left(\frac{\partial_B r_k}{\partial_B r_i^*} \frac{\partial_B r_k}{\partial_B r_j^*} - \delta_{ij} \right) = \frac{1}{2} \left(\frac{\partial_B u_i}{\partial_B r_j^*} + \frac{\partial_B u_j}{\partial_B r_i^*} + \frac{\partial_B u_k}{\partial_B r_i^*} \frac{\partial_B u_k}{\partial_B r_j^*} \right) \end{aligned} \quad (2-23)$$

2.3.4 Stress Tensor

According to the coordinate system of the stress and its acting surface, the stress tensor has different expression [Cao-2018; Rot-1981; Sur-2016]

Table 2-2: Stress Tensor

	Coordinate of Stress	Coordinate of Area	Properties	Formula
Cauchy Stress	Current	Current	symmetric	$\underline{\underline{\sigma}}$
1st Piola-Kirchhoff Stress	Current	Reference	asymmetric	$\underline{\tau} = J\underline{\underline{\sigma}}\underline{F}^{-T}, J = \det(\underline{F})$
2nd Piola-Kirchhoff Stress	Reference	Reference	symmetric	$\underline{\underline{S}} = J\underline{F}^{-1}\underline{\underline{\sigma}}\underline{F}^{-T} = \underline{\underline{F}}^{-1}\underline{\tau}$

The 2nd Piola–Kirchhoff stress tensor matches the Green–Lagrange finite strain tensor. Usually stress-strain laws are given by Cauchy stress and left Cauchy-Green deformation tensor. However, by dynamics calculation the constitutive relationship is often established based on Cauchy stress and the Green-Lagrangian strain tensor. The constitutive relationship between the stress tensor and the strain tensor can be expressed by a fourth-order tensor.

$$\underline{\underline{\sigma}}^{(4)} = K \underline{\underline{\varepsilon}} \Leftrightarrow {}_B\varepsilon_{ij} = K_{ij}^{kl} {}_B\varepsilon_{kl} \quad (2-24)$$

2.4 Optimal Control Theory

2.4.1 Classical Optimal Control Theory

The purpose of classical optimal control is to make the state of the system change from the initial state to the final state while meeting the constraints within a specified time [Lew-2012]. The optimal control problem can be written as follows

$$\begin{aligned} \min J &= \Phi(\underline{x}_e, t_e) + \int_{t_0}^{t_e} L(\underline{x}(t), \underline{u}(t), t) dt \\ \text{s. t. } &\dot{\underline{x}}(t) = \underline{f}_t(\underline{x}(t), \underline{u}(t), t) \\ &\underline{g}_t(\underline{x}(t), \underline{u}(t), t) \leq 0 \\ &\underline{x}(t_0) = \underline{x}_0, \underline{u}(t) \in \mathcal{U}, \underline{x}(t) \in \mathcal{X} \end{aligned} \quad (2-25)$$

Cost functional J is usually composed of running cost L and terminal cost Φ . The dynamics state function is considered as the equality constraint of the optimal control problem. For special requirements such as obstacle avoidance, some inequality

constraints will be added. In addition, the control variables and the state variables of the system have corresponding limits. Normally the nonlinear optimal control problems have no analytical solution. Therefore, many approximate methods are proposed to obtain sub-optimal solutions.

2.4.2 Non-linear Model Predictive Control

Model predictive control (MPC) is a real-time model-based feedback control method, which consists of a sensor system, a model predictor, and a controller. The structure of the MPC is shown as follows

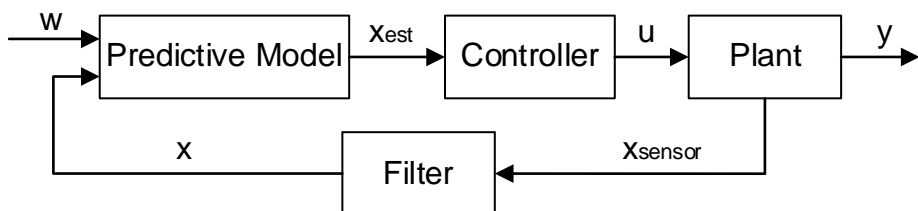


Figure 2-1: Structure of Model Predictive Control

The predictive model is a mathematical model, which is used to simulate the different states that may be produced by different control variables within a finite step time from this moment. The controller will give the suitable control signal at the moment based on these predicted states. The control signal will be input into the actual system (plant), and through the sensor and filter the obtained state of true mechanism will again go into the predictive model for the next predictive control loop.

3 Dynamic Models of different Types of Elements

3.1 Rigid Body Dynamic Model

3.1.1 Generalized Coordination and Generalized Velocity

The generalized coordinate of the rigid body can be defined by the position and posture of only one point on the body. Therefore, the generalized coordinate and generalized velocity can be written as

$$\underline{q}_e = [\underline{r}^0{}^T \quad \underline{\varphi}{}^T]^T \quad \underline{dq}_e = [\underline{\dot{r}}^0{}^T \quad {}_B\underline{\omega}{}^T]^T \quad (3-1)$$

The chosen point is called origin point of the rigid body. The choice of origin point can be arbitrary, and does not even need to be the actual point on the body.

3.1.2 Kinematics of Points on Rigid Body

The position, velocity and acceleration of any point on the rigid body can be determined through the origin point and the relative position to the origin point. They can be formulated as

$$\begin{aligned} \underline{r}^k &= \underline{r}^0 + \underline{R}_B \underline{r}^{0k} \quad \text{with } \underline{R}_B = \underline{R}(\underline{\varphi}) \\ \underline{\dot{r}}^k &= \underline{\dot{r}}^0 - \underline{R}_B \underline{\dot{r}}^{0k} {}_B\omega \\ \underline{\ddot{r}}^k &= \underline{\ddot{r}}^0 - \underline{R}_B \underline{\ddot{r}}^{0k} {}_B\dot{\omega} + \underline{R}_B \underline{\tilde{\omega}} {}_B \underline{\dot{r}}^{0k} {}_B\omega \end{aligned} \quad (3-2)$$

where ${}_B\underline{r}^{0k}$ is the constant relative position to the origin point in body coordinate.

3.1.3 The Virtual Power of Rigid Body

The virtual inertial power of the rigid body can be expressed as

$$\delta p_{ine} = - \int_{\Omega} \delta \underline{r}^k{}^T \underline{\ddot{r}}^k \rho d\Omega = - \delta \underline{dq}_e^T (\underline{M}_e \underline{d}\dot{q}_e + \underline{D}_e \underline{dq}_e) \quad (3-3)$$

where the mass matrix and damping matrix can be formulated as

$$\underline{\underline{M}}_e = \begin{bmatrix} m_{\text{tot}} \underline{\underline{I}} & -m_{\text{tot}} \underline{\underline{R}}^T \underline{\underline{B}} \tilde{\underline{\underline{r}}}^{0C} \\ m_{\text{tot}} \underline{\underline{B}} \tilde{\underline{\underline{r}}}^{0C} \underline{\underline{R}}^T & \underline{\underline{B}} \underline{\underline{\theta}}^0 \end{bmatrix} \quad \underline{\underline{D}}_e = \begin{bmatrix} 0 & m_{\text{tot}} \underline{\underline{R}}_B \tilde{\underline{\underline{\omega}}}_B \tilde{\underline{\underline{r}}}^{0C} \\ 0 & \underline{\underline{B}} \tilde{\underline{\underline{\omega}}}_B \underline{\underline{\theta}}^0 \end{bmatrix} \quad (3-4)$$

The virtual external gravity power can be written as

$$\delta p_{\text{ext}} = \int_{\Omega} \delta \underline{\underline{L}} \dot{\underline{\underline{r}}}^k \underline{\underline{I}} \underline{\underline{g}} \rho d\Omega = -m_{\text{tot}} \left[\underline{\underline{B}} \tilde{\underline{\underline{r}}}^{0C} \underline{\underline{R}}^T \right] \underline{\underline{I}} \underline{\underline{g}} = -\delta \underline{\underline{d}} \underline{\underline{q}}_e^T \underline{\underline{V}}_{\text{ext},g} \underline{\underline{I}} \underline{\underline{g}} \quad (3-5)$$

There is no deformation in rigid body, so that the virtual internal power is zero. The total virtual power of rigid body only consists of virtual inertial and external power.

$$\begin{aligned} \delta p_e &= \delta p_{\text{ine}} + \delta p_{\text{int}} + \delta p_{\text{ext}} = \delta p_{\text{ine}} + \delta p_{\text{ext},g} \\ &= -\delta \underline{\underline{d}} \underline{\underline{q}}_e^T \left(\underline{\underline{M}}_e \underline{\underline{d}} \dot{\underline{\underline{q}}}_e + \underline{\underline{D}}_e \underline{\underline{d}} \underline{\underline{q}}_e + \underline{\underline{V}}_{\text{ext},g} \underline{\underline{I}} \underline{\underline{g}} \right) = -\delta \underline{\underline{d}} \underline{\underline{q}}_e^T \left(\underline{\underline{M}}_e \underline{\underline{d}} \dot{\underline{\underline{q}}}_e + \underline{\underline{F}}_e \right) \end{aligned} \quad (3-6)$$

3.2 Two Nodes Strut Tie Dynamic Model

3.2.1 Assumption for Ideal Strut Tie Model

The strut tie model described in this part is an ideal strut tie model, which satisfies the following assumptions:

1. Only the normal stress from axial tension and compression is considered, and other internal forces that may exist in the real rod are ignored;
2. the normal stress is evenly distributed with the length of the rod;
3. the cross section of the rod is symmetrical about the y- and z-axis of the section local coordinate;
4. the density and total mass of the rod remain unchanged.

3.2.2 Generalized Coordinate and Generalized Velocity

According to the above assumptions, the generalized coordinates and generalized velocity of the two nodes strut tie model can be expressed by the position vectors and translational velocity of the two nodes.

$$\underline{q}_e = [\underline{r}^1{}^T \quad \underline{r}^2{}^T]^T \quad d\underline{q}_e = \dot{\underline{q}}_e = [\underline{\dot{r}}^1{}^T \quad \underline{\dot{r}}^2{}^T]^T \quad (3-7)$$

Since only the x-axis is determined (parallel to the line connected the two end nodes), according to the third assumption the posture can be obtained only through the x-axis.

$$\underline{\varphi}^B = \varphi^B \underline{n}_\varphi^B \quad \underline{\underline{R}}_B = \underline{\underline{R}}(\underline{\varphi}^B) \quad (3-8)$$

where

$$\begin{aligned} \sin \varphi^B &= \left\| \underline{\underline{g}}_x \underline{n}_x \right\| / l_{\varphi,B} & \cos \varphi^B &= \underline{g}_x^T \underline{n}_x / l_{\varphi,B} \\ \underline{n}_\varphi^B &= \underline{\underline{g}}_x \underline{n}_x / \left\| \underline{\underline{g}}_x \underline{n}_x \right\| & l_{\varphi,B} &= \sqrt{\left\| \underline{\underline{g}}_x \underline{n}_x \right\|^2 + (\underline{g}_x^T \underline{n}_x)^2} \end{aligned} \quad (3-9)$$

According to the relationship between the translational velocities of the two end nodes, the angular velocity of the rod and the velocity of the axial deformation can be obtained.

$$\begin{aligned} \underline{\dot{r}}^{12} &= \underline{g}_x \underline{n}_x^T \begin{bmatrix} -I & I \end{bmatrix} \underline{d}q_e = \underline{T}_x \underline{d}q_e \\ {}_B \underline{\omega}^B &= 1 / \left\| \underline{\underline{r}}^{12} \right\| \underline{\underline{R}}_{x,90^\circ} \left(\underline{\underline{R}}_B^T - \underline{g}_x \underline{n}_x^T \right) \begin{bmatrix} -I & I \end{bmatrix} \underline{d}q_e = \underline{T}_\varphi \underline{d}q_e \end{aligned} \quad (3-10)$$

where

$$\underline{\underline{r}}^{12} = \underline{r}^2 - \underline{r}^1 \quad \underline{n}_x = \underline{n}_x = \underline{r}^{12} / \left\| \underline{\underline{r}}^{12} \right\| \quad \underline{\underline{R}}_{x,90^\circ} = \underline{\underline{R}}([\pi/2 \quad 0 \quad 0]^T) \quad (3-11)$$

The angular acceleration of the rod can be written as

$${}_B \underline{\dot{\omega}}^B = \left[\underline{\underline{R}}_{x,90^\circ} \left(\frac{\underline{r}^{12}{}^T \underline{\dot{r}}^{12}}{\left\| \underline{\underline{r}}^{12} \right\|^2} I - {}_B \underline{\underline{\widetilde{\omega}}}^B \right) \underline{\underline{g}}_x \underline{\underline{T}}_\varphi \right] \underline{d}q_e + \underline{\underline{T}}_\varphi \underline{d}\dot{q}_e = \underline{\dot{T}}_\varphi \underline{d}q_e + \underline{\underline{T}}_\varphi \underline{d}\dot{q}_e \quad (3-12)$$

where $\underline{\dot{r}}^{12} = \underline{\dot{r}}^2 - \underline{\dot{r}}^1$.

3.2.3 Kinematics and Deformation of Points on the Model

Since for the strut tie model only the axial deformation is considered, there is no relative rotation with the local coordinate on any cross section. The position, velocity and acceleration of any point on any section of the rod can be expressed as

$$\begin{aligned}\underline{\underline{r}} &= \underline{\underline{r}}^c + \underline{\underline{R}}_{Bc} \underline{t} & \dot{\underline{\underline{r}}} &= \dot{\underline{\underline{r}}}^c + \underline{\underline{R}}_{Bc} \dot{\underline{\underline{\omega}}}^B_c \underline{t} \\ \ddot{\underline{\underline{r}}} &= \ddot{\underline{\underline{r}}}^c + \underline{\underline{R}}_{Bc} \dot{\underline{\underline{\omega}}}^B_c \underline{t} + \underline{\underline{R}}_{Bc} \dot{\underline{\underline{\omega}}}^B_B \dot{\underline{\underline{\omega}}}^B_c \underline{t}\end{aligned}\quad (3-13)$$

According to the definition of strain in absolute coordinates, the axial strain of the rod can be written as

$$I\varepsilon = \| \underline{\underline{r}}^c \| - 1 = \underline{n}_x^T \underline{\underline{r}}^c - \underline{n}_x^T \underline{n}_x \quad (3-14)$$

The velocity and acceleration of the axial strain can be expressed as

$$\begin{aligned}I\dot{\varepsilon} &= \frac{1}{\| \underline{\underline{r}}^c \|} \underline{\underline{r}}'^T \underline{\underline{N}}' d\underline{q}_e = \frac{1}{\| \underline{\underline{r}}^c \|} \underline{q}_e^T \underline{\underline{N}}'^T \underline{\underline{N}}' d\underline{q}_e \triangleq \underline{T}_e^T d\underline{q}_e \\ I\ddot{\varepsilon} &= \frac{1}{\| \underline{\underline{r}}^c \|} \underline{q}_e^T \underline{\underline{N}}'^T \underline{\underline{N}}' d\dot{\underline{q}}_e + \underline{\underline{r}}'^T \frac{1}{\| \underline{\underline{r}}^c \|} \left(\underline{\underline{I}} - \frac{\underline{\underline{r}}' \underline{\underline{r}}'^T}{\| \underline{\underline{r}}^c \|^2} \right) \underline{\underline{N}}' d\underline{q}_e \triangleq \underline{T}_e^T d\dot{\underline{q}}_e + \dot{\underline{T}}_e^T d\underline{q}_e\end{aligned}\quad (3-15)$$

The stress can be obtained from the constitutive relationship with strain. In order to avoid the high-frequency oscillation of the rod caused by strain, the average stress is used to replace the instantaneous stress by introducing smooth factor h . The average stress in inertial coordinate can be expressed as

$$I\bar{\sigma} = E_I \bar{\varepsilon} = E \left(I\varepsilon + \frac{h}{2} I\dot{\varepsilon} + \frac{h^2}{6} I\ddot{\varepsilon} \right) = E_I \varepsilon + E \left(\frac{h}{2} \underline{T}_e^T + \frac{h^2}{6} \dot{\underline{T}}_e^T \right) d\underline{q}_e + E \frac{h^2}{6} \underline{T}_e^T d\dot{\underline{q}}_e \quad (3-16)$$

3.2.4 Discretization and Shape Function

In order to satisfy the second assumption, the first derivative of the position vector of the center of any section on the rod should be constant. Therefore, its position vector can be expressed by linear interpolation of position vectors of two end section. The position, velocity and acceleration of this center point can be expressed as

$$\underline{\underline{r}}^c \triangleq \underline{\underline{N}} \underline{q}_e \quad \underline{\underline{r}}^c = \underline{\underline{N}} d\underline{q}_e \quad \dot{\underline{\underline{r}}}^c = \underline{\underline{N}} d\dot{\underline{q}}_e \quad (3-17)$$

Where $\underline{\underline{N}}$ is the shape function, and its specific expression is

$$\underline{\underline{N}} = [(1 - \xi) \underline{\underline{I}} \quad \xi \underline{\underline{I}}] \quad \underline{\underline{N}}' = 1/L [-\underline{\underline{I}} \quad \underline{\underline{I}}] \quad (3-18)$$

with $\xi = s/L$. The first derivative of its position and velocity vector with respect to the arc length coordinate s can be written as

$$\underline{\underline{r}}^c \triangleq \underline{\underline{N}}' \underline{q}_e \quad \underline{\underline{\dot{r}}}^c = \underline{\underline{N}}' \dot{\underline{q}}_e \quad (3-19)$$

3.2.5 The Virtual Power of Strut Tie Model

The virtual inertial power of strut tie model can be written as

$$\begin{aligned} \delta p_{\text{ine}} &= - \iiint_V \delta \underline{\underline{I}} \underline{\underline{\dot{r}}}^T \underline{\underline{I}} \underline{\underline{\ddot{r}}} \rho dV = - \delta \underline{d}\underline{q}_e^T (\underline{\underline{M}}_{e,\text{ine}} \underline{d}\dot{\underline{q}}_e + \underline{\underline{D}}_{e,\text{ine}} \underline{d}\underline{q}_e) \\ &= - \delta \underline{d}\underline{q}_e^T (\underline{\underline{M}}_{e,\text{ine}} \underline{d}\dot{\underline{q}}_e + \underline{\underline{F}}_{\text{ine}}) \end{aligned} \quad (3-20)$$

The mass matrix and damping matrix generated from the virtual inertial power can be expressed as

$$\underline{\underline{M}}_{e,\text{ine}} = \rho L \left(\frac{A}{6} \begin{bmatrix} 2I & I \\ I & 2I \end{bmatrix} + \underline{\underline{T}}_{\varphi}^T \underline{\underline{J}} \underline{\underline{T}}_{\varphi} \right) \quad \underline{\underline{D}}_{e,\text{ine}} = -\rho L \underline{\underline{T}}_{\varphi}^T \left(\underline{\underline{J}} \dot{\underline{\underline{T}}}_{\varphi} + \dot{\underline{\underline{T}}}_{\varphi} \right) \quad (3-21)$$

where $\underline{\underline{J}}$ is the moment of inertia of section

$$\underline{\underline{J}} = \text{diag}([I_y + I_z \quad I_z \quad I_y]) \quad \dot{\underline{\underline{J}}}_B \underline{\omega}^B = \underline{\underline{\widetilde{\omega}}}^B \underline{\underline{J}}_B \underline{\omega}^B \quad (3-22)$$

The virtual internal power with the smooth factor can be written as

$$\begin{aligned} \delta p_{\text{int}} &= - \int_0^L \delta \underline{\dot{I}} \underline{\dot{\varepsilon}} \underline{\bar{\sigma}} A ds = - \delta \underline{d}\underline{q}_e^T (\underline{\underline{M}}_{e,\text{int}} \underline{d}\dot{\underline{q}}_e + \underline{\underline{D}}_{e,\text{int}} \underline{d}\underline{q}_e + \underline{\underline{K}}_e \underline{q}_e) \\ &= - \delta \underline{d}\underline{q}_e^T (\underline{\underline{M}}_{e,\text{int}} \underline{d}\dot{\underline{q}}_e + \underline{\underline{F}}_{\text{int}}) \end{aligned} \quad (3-23)$$

The mass matrix, the damping matrix and the stiffness matrix obtained through the virtual internal power can be expressed as

$$\begin{aligned} \underline{\underline{M}}_{e,\text{int}} &= \frac{h^2}{6} EAL \underline{\underline{T}}_{\varepsilon} \underline{\underline{T}}_{\varepsilon}^T \quad \underline{\underline{D}}_{e,\text{int}} = EAL \left(\frac{h}{2} \underline{\underline{T}}_{\varepsilon} \underline{\underline{T}}_{\varepsilon}^T + \frac{h^2}{6} \underline{\underline{T}}_{\varepsilon} \dot{\underline{\underline{T}}}_{\varepsilon}^T \right) \\ \underline{\underline{K}}_e &= (1/\|\underline{\underline{r}}'\|) \underline{\underline{N}}'^T \underline{\underline{N}}' EA_I \varepsilon L \end{aligned} \quad (3-24)$$

As the external force here only gravity is considered. The virtual power of gravity can be written as

$$\delta p_{\text{ext},g} = \iiint_V \delta \underline{\underline{I}} \dot{\underline{\underline{r}}}^T \underline{\underline{I}} \underline{\underline{g}} \rho dV = \delta \underline{\underline{d}} \underline{\underline{q}}_e^T \rho A \int_0^L \underline{\underline{N}}^T ds \underline{\underline{I}} \underline{\underline{g}} = -\delta \underline{\underline{d}} \underline{\underline{q}}_e^T \underline{\underline{F}}_{\text{ext},g} \quad (3-25)$$

The virtual power of strut tie model is

$$\begin{aligned} \delta p_e &= \delta p_{\text{ine}} + \delta p_{\text{int}} + \delta p_{\text{ext},g} = -\delta \underline{\underline{d}} \underline{\underline{q}}_e^T (\underline{\underline{M}}_e \underline{\underline{d}} \dot{\underline{\underline{q}}}_e + \underline{\underline{F}}_e) \\ &= -\delta \underline{\underline{d}} \underline{\underline{q}}_e^T [(\underline{\underline{M}}_{e,\text{ine}} + \underline{\underline{M}}_{e,\text{int}}) \underline{\underline{d}} \dot{\underline{\underline{q}}}_e + (\underline{\underline{F}}_{\text{ine}} + \underline{\underline{F}}_{\text{int}} + \underline{\underline{F}}_{\text{ext},g})] \end{aligned} \quad (3-26)$$

3.2.6 Body Parameter of Strut Tie Model after Deformation

According to the fourth assumption, the density ρ and the total mass m are assumed to be constant under the deformation. When the cross section of the rod is circular with outer diameter r_a and inner diameter r_i , the ratio of outer to inner diameter remains unchanged, the section parameters after the deformation can be expressed as

$$r_a = \sqrt{\frac{m}{\rho \pi \| \underline{\underline{I}} \underline{\underline{r}}^{12} \| (r_a^{*2} - r_i^{*2})}} r_a^* \quad r_i = \sqrt{\frac{m}{\rho \pi \| \underline{\underline{I}} \underline{\underline{r}}^{12} \| (r_a^{*2} - r_i^{*2})}} r_i^* \quad (3-27)$$

where r_a^* and r_i^* is the outer diameter and inner diameter before deformation.

3.3 Spatial Timoshenko Beam Dynamic Model

3.3.1 Generalized Coordination, Velocity and Co-rotational Coordinate

The generalized coordinate of the Timoshenko beam is defined by the position and posture of the end section. The generalized velocity is defined as the translational velocity and the angular velocity in the local coordinate system of the end section.

$$\begin{aligned} \underline{\underline{q}}_e &= [\underline{\underline{q}}_1^T \quad \underline{\underline{q}}_2^T]^T = [\underline{\underline{I}} \dot{\underline{\underline{r}}}^1^T \quad \underline{\underline{\varphi}}^1^T \quad \underline{\underline{I}} \dot{\underline{\underline{r}}}^2^T \quad \underline{\underline{\varphi}}^2^T]^T \\ \underline{\underline{d}} \underline{\underline{q}}_e &= [\underline{\underline{d}} \underline{\underline{q}}_1^T \quad \underline{\underline{d}} \underline{\underline{q}}_2^T]^T = [\underline{\underline{I}} \dot{\underline{\underline{r}}}^1^T \quad {}_1 \underline{\underline{\omega}}^1^T \quad \underline{\underline{I}} \dot{\underline{\underline{r}}}^2^T \quad {}_2 \underline{\underline{\omega}}^2^T]^T \end{aligned} \quad (3-28)$$

The co-rotational coordinate describes the position of the element without deformation, which means that, the deformation of any point on the element is based on the co-16

rotational coordinate. The co-rotational coordinate can be defined through the coordinates of the two ends of the beam.

$$\underline{q}_B = \begin{bmatrix} \underline{r}^{B^T} & \underline{\varphi}^{B^T} \end{bmatrix}^T = \underline{q}_B(\underline{q}_e) \quad (3-29)$$

where \underline{r}^B is the position vector of the origin point of co-rotational coordinate expressed in inertial coordinate, and posture is represented by the Cartesian vector. The relationship between the generalized velocity and acceleration of the co-rotational coordinate and the generalized velocity and acceleration of the end-point coordinates can be expressed as

$$\begin{aligned} \underline{dq}_B &= [\underline{r}^{B^T} \quad {}_B\underline{\omega}^{B^T}]^T = \underline{dq}_B(\underline{q}_e, \underline{dq}_e) = \underline{T}_B \underline{dq}_e \\ \underline{d}\dot{q}_B &= [\underline{\ddot{r}}^{B^T} \quad {}_B\underline{\dot{\omega}}^{B^T}]^T = \underline{d}\dot{q}_B(\underline{q}_e, \underline{dq}_e, \underline{d}\dot{q}_e) = \underline{T}_B \underline{d}\dot{q}_e + \underline{\dot{T}}_B \underline{dq}_e \end{aligned} \quad (3-30)$$

3.3.2 Assumptions and Formulation of Deformation

According to the Timoshenko beam assumption, the deformation of any point on the section c is caused by the centroid translational deformation of the section ${}_B\underline{u}^c$ and the section rotational deformation. The actual deformation of this point ${}_B\underline{u}$ can be obtained by the difference between the position vector before deformation \underline{r}^* and the after deformation \underline{r} .

$$\begin{aligned} \underline{r}^* &= \underline{r}^c + \underline{R}_{Bc}\underline{t} = \underline{r}^B + \underline{R}_B({}_Br^{r,c} + {}_ct) \quad \text{with} \quad \underline{R}_B = \underline{R}(\underline{\varphi}^B) \\ \underline{r} &= \underline{r}^c + \underline{R}_{Bd,cc}\underline{t} = \underline{r}^B + \underline{R}_B({}_Br^{r,c} + {}_B\underline{u}^c + \underline{R}_{d,cc}\underline{t}) \end{aligned} \quad (3-31)$$

where ${}_Br^{r,c}$ is the relative position of cross-section c to the original point of co-rotational coordinate, and ${}_ct^T = [0 \quad {}_cy \quad {}_cz]$ is the relative position of any point on cross-section c to the sectional center. ${}_Br^{r,c}$ and ${}_ct$ are constant for each cross-section. The hypothesis of small rotational deformation is applied, so that the rotation matrix for axis-angle rotation vector ${}_B\underline{\psi}^c$ and the deformation can be written as:

$$\begin{aligned} \underline{R}_{d,c} &= \underline{R}({}_B\underline{\psi}^c) \approx \underline{I} + {}_B\underline{\tilde{\psi}}^c \\ {}_B\underline{u} &= \underline{R}_B^T(\underline{r} - \underline{r}^*) = {}_B\underline{u}^c + (\underline{R}_{d,c} - \underline{I}) {}_ct \approx {}_B\underline{u}^c + {}_B\underline{\tilde{\psi}}^c {}_ct \end{aligned} \quad (3-32)$$

The deformation coordinate $\underline{q}_{d,c}$ is defined as

$$\underline{q}_{d,c} = \begin{bmatrix} {}_B\underline{u}^c \\ {}_B\underline{\psi}^c \end{bmatrix}^T \quad (3-33)$$

The deformation coordinate at the end point can be expressed by the following formula

$$\begin{cases} {}_B\underline{u}^e = \underline{R}_B^T (\underline{l}r^e - {}_l\underline{r}^B) - {}_B\underline{r}^{r,e} \\ {}_B\underline{\psi}^e = {}_B\underline{\psi}^e (\underline{R}_B^T \underline{R}_e) = {}_B\underline{\psi}^e (\underline{R}_{d,e}) \end{cases}, \quad e = 1, 2 \quad (3-34)$$

$$\underline{q}_{d,end} = \begin{bmatrix} {}_B\underline{u}^{1T} & {}_B\underline{\psi}^{1T} & {}_B\underline{u}^{2T} & {}_B\underline{\psi}^{2T} \end{bmatrix}^T$$

The velocity and acceleration of the end deformation coordinate can be expressed as

$$\begin{aligned} \underline{dq}_{d,end} &= [{}_B\dot{\underline{u}}^{1T} \quad {}_1\bar{\omega}^{1T} \quad {}_B\dot{\underline{u}}^{2T} \quad {}_2\bar{\omega}^{2T}]^T = \underline{T}_{d,end} \underline{dq}_e \\ \underline{d\dot{q}}_{d,end} &= [{}_B\ddot{\underline{u}}^{1T} \quad {}_1\ddot{\omega}^{1T} \quad {}_B\ddot{\underline{u}}^{2T} \quad {}_2\ddot{\omega}^{2T}]^T = \underline{T}_{d,end} \underline{d\dot{q}}_e + \underline{\dot{T}}_{d,end} \underline{dq}_e \end{aligned} \quad (3-35)$$

where ${}_e\bar{\omega}^e$ represent the angular velocity of the angular deformation ${}_B\underline{\psi}^e$.

3.3.3 Kinematics of Points on Timoshenko Beam

The velocity and acceleration of the point on the beam after the deformation is depend on the generalized velocity and acceleration of co-rotational coordinate and deformation coordinate, which can be formulated as

$$\begin{aligned} {}_l\dot{\underline{r}} &= {}_l\dot{\underline{r}}^c + \underline{\Omega}_{c,c}\underline{t} = (\underline{H}_t + \underline{H}_{r,t}) [\underline{dq}_B^T \quad \underline{dq}_{d,c}^T]^T \\ {}_l\ddot{\underline{r}} &= {}_l\ddot{\underline{r}}^c + \underline{A}_{c,c}\underline{t} = (\underline{H}_t + \underline{H}_{r,t}) [\underline{d\dot{q}}_B^T \quad \underline{d\dot{q}}_{d,c}^T]^T + (\underline{D}_t + \underline{D}_{r,t}) [\underline{dq}_B^T \quad \underline{dq}_{d,c}^T]^T \end{aligned} \quad (3-36)$$

Where the translational part can be formulated as

$$\begin{aligned} \underline{H}_t &= \begin{bmatrix} I & -\underline{R}_B (\underline{B}\tilde{r}^{r,c} + {}_B\underline{\tilde{u}}^c) & \underline{R}_B & 0 \end{bmatrix} \\ \underline{D}_t &= \begin{bmatrix} 0 & -\underline{R}_B \underline{\tilde{\omega}}^B (\underline{B}\tilde{r}^{r,c} + {}_B\underline{\tilde{u}}^c) & 2\underline{R}_B \underline{\tilde{\omega}}^B & 0 \end{bmatrix} \end{aligned} \quad (3-37)$$

And the rotational part around the c -axis can be written as

$$\begin{aligned}\underline{\underline{H}}_{r,t} &= \begin{bmatrix} 0 & -\underline{\underline{R}}_{cc} \tilde{t} \underline{\underline{R}}_{d,c}^T & 0 & -\underline{\underline{R}}_{cc} \tilde{t} \\ 0 & -\underline{\underline{R}}_{BB} \tilde{\omega}^B \underline{\underline{R}}_{d,c} \tilde{t} \underline{\underline{R}}_{d,c}^T & 0 & -\left(2\underline{\underline{R}}_{BB} \tilde{\omega}^B \underline{\underline{R}}_{d,c} + \underline{\underline{R}}_{cc} \tilde{\omega}^c\right) c \tilde{t} \end{bmatrix} \\ \underline{\underline{D}}_{r,t} &= \begin{bmatrix} 0 & -\underline{\underline{R}}_{BB} \tilde{\omega}^B \underline{\underline{R}}_{d,c} \tilde{t} \underline{\underline{R}}_{d,c}^T & 0 & -\left(2\underline{\underline{R}}_{BB} \tilde{\omega}^B \underline{\underline{R}}_{d,c} + \underline{\underline{R}}_{cc} \tilde{\omega}^c\right) c \tilde{t} \end{bmatrix}\end{aligned}\quad (3-38)$$

3.3.4 The Formulation of Strain and Stress

The strain at this point is defined using linear Green-Lagrange strains, which is defined as the derivative of the deformation with respect to the coordinate.

$$\begin{aligned}_{B}\varepsilon_{ij} = {}_B\varepsilon_{ji} &= \frac{1}{2} \left(\frac{\partial_B u_i}{\partial_B x_j} + \frac{\partial_B u_j}{\partial_B x_i} \right) \approx \frac{1}{2} \left(\frac{\partial_B u_i}{\partial_c x_j} + \frac{\partial_B u_j}{\partial_c x_i} \right) \\ \Rightarrow \begin{cases} {}_B\varepsilon_{xx} = {}_B u^{c'} - {}_B \theta^{c'} c y + {}_B \psi^{c'} c z \\ {}_B\varepsilon_{xy} = 1/2 ({}_B v^{c'} - {}_B \varphi^{c'} c z - {}_B \theta^{c'}) \\ {}_B\varepsilon_{xz} = 1/2 ({}_B w^{c'} + {}_B \varphi^{c'} c y + {}_B \psi^{c'}) \\ {}_B\varepsilon_{yy} = {}_B \varepsilon_{yz} = {}_B \varepsilon_{zz} = 0 \end{cases} &\quad (3-39)\end{aligned}$$

where $(*)' = \partial(*)/\partial_c x$ and

$${}_B\underline{u}^c = [{}_B u^c \quad {}_B v^c \quad {}_B w^c]^T \quad {}_B\underline{\psi}^c = [{}_B \varphi^c \quad {}_B \psi^c \quad {}_B \theta^c]^T \quad (3-40)$$

Through the constitutive relationship between stress and strain, instantaneous stress can be obtained as

$${}_B\sigma_{ij} = \begin{cases} E {}_B\varepsilon_{ij}, i = j \\ G {}_B\varepsilon_{ij}, i \neq j \end{cases} \quad (3-41)$$

3.3.5 The Virtual Power of Timoshenko Beam

The virtual internal power of the element can be expressed as

$$\begin{aligned}\delta p_{int} &= - \iiint_V \sum_i \sum_j \delta_B \dot{\varepsilon}_{ij} {}_B \sigma_{ij} dV = - \int_0^L \iint_{A(s)} \sum_i \sum_j \delta_B \dot{\varepsilon}_{ij} {}_B \sigma_{ij} dA ds \\ &= - \int_0^L \left[\delta \dot{\underline{q}}_{d,c}'^T (\underline{\underline{H}}_1 \underline{q}'_{d,c} + \underline{\underline{H}}_2 \underline{q}_{d,c}) - \delta \dot{\underline{q}}_{d,c}^T (\underline{\underline{H}}_3 \underline{q}'_{d,c} + \underline{\underline{H}}_4 \underline{q}_{d,c}) \right] ds\end{aligned}\quad (3-42)$$

where

$$\begin{aligned}\underline{\underline{H}}_1 &= \text{diag}([EA \quad GA/4 \quad GA/4 \quad G(I_y + I_z)/4 \quad EI_z \quad EI_y]) \\ \underline{\underline{H}}_2 &= \underline{\underline{H}}_3^T = \frac{GA}{4} \begin{bmatrix} 0 & \tilde{g}_x \\ 0 & 0 \\ 0 & 0 \end{bmatrix} \\ \underline{\underline{H}}_4 &= \text{diag}([0 \quad 0 \quad 0 \quad 0 \quad GA/4 \quad GA/4])\end{aligned}\quad (3-43)$$

The integration by parts is used to deal with the first part of the integration

$$\begin{aligned}\delta p_{\text{int}} &= -\delta \dot{\underline{q}}_{d,c}^T (\underline{\underline{H}}_1 \underline{q}'_{d,c} + \underline{\underline{H}}_2 \underline{q}_{d,c}) \Big|_0^L \\ &\quad + \int_0^L \delta \dot{\underline{q}}_{d,c}^T \left[-\underline{\underline{H}}_1 \underline{q}''_{d,c} + (\underline{\underline{H}}_3 - \underline{\underline{H}}_2) \underline{q}'_{d,c} + \underline{\underline{H}}_4 \underline{q}_{d,c} \right] ds\end{aligned}\quad (3-44)$$

The virtual inertial power of the beam element can be expressed as

$$\delta p_{\text{ine}} = - \iiint_V \delta \underline{\underline{I}} \dot{\underline{I}}^T \underline{\underline{I}} \ddot{\rho} dV = - \int_0^L \delta \left[\frac{dq_B}{dq_{d,c}} \right]^T \left(\underline{\underline{M}}_{B,c} \left[\frac{d\dot{q}_B}{dq_{d,c}} \right] + \underline{\underline{D}}_{B,c} \left[\frac{dq_B}{dq_{d,c}} \right] \right) ds \quad (3-45)$$

The mass matrix and damping matrix regarding to co-rotational coordinate and deformation coordinate of cross-section c can be formulated as

$$\begin{aligned}\underline{\underline{M}}_{B,c} &= \rho A \underline{\underline{H}}_t^T \underline{\underline{H}}_t + \rho I_y \underline{\underline{H}}_{r,y}^T \underline{\underline{H}}_{r,y} + \rho I_z \underline{\underline{H}}_{r,z}^T \underline{\underline{H}}_{r,z} \\ \underline{\underline{D}}_{B,c} &= \rho A \underline{\underline{H}}_t^T \underline{\underline{D}}_t + \rho I_y \underline{\underline{H}}_{r,y}^T \underline{\underline{D}}_{r,y} + \rho I_z \underline{\underline{H}}_{r,z}^T \underline{\underline{D}}_{r,z}\end{aligned}\quad (3-46)$$

The virtual external power of the Timoshenko beam caused by gravity $\underline{\underline{I}} g$ can be expressed as

$$\delta p_{\text{ext}} = \iiint_V \delta \underline{\underline{I}} \dot{\underline{I}}^T \underline{\underline{I}} g \rho dV = \int_0^L \delta \underline{\underline{I}} \dot{\underline{I}}^c \rho A ds \underline{\underline{I}} g = \int_0^L \delta \left[\frac{dq_B}{dq_{d,c}} \right]^T \underline{\underline{H}}_t^T \underline{\underline{I}} g \rho A ds \quad (3-47)$$

3.3.6 Discretization and Shape Function

To avoid shear lock, one complex shape function is proposed [Baz-2003]. The deformation coordinate of any cross section can be written as

$$\underline{q}_{d,c} = \underline{\underline{N}}_c \underline{q}_{d,\text{end}} \quad (3-48)$$

The detailed description of the shape function is in the appendix. With this shape function, the integration part of internal power become zero [Luo-2008], so that the virtual internal power can be written as

$$\delta p_{\text{int}} = -\delta \underline{\dot{q}}_{d,c}^T \left(\underline{\underline{H}}_1 \underline{q}'_{d,c} + \underline{\underline{H}}_2 \underline{q}_{d,c} \right) \Big|_0^L = -\delta \underline{\dot{q}}_{d,\text{end}}^T \underline{\underline{N}}_c^T \left(\underline{\underline{H}}_1 \underline{\underline{N}}'_c + \underline{\underline{H}}_2 \underline{\underline{N}}_c \right) \Big|_0^L \underline{q}_{d,\text{end}} \quad (3-49)$$

Additionally, the relationship between deformation coordinate of end point, co-rotational coordinate and generalized coordinate of the beam can be written as

$$\begin{aligned} \begin{bmatrix} \underline{dq}_B \\ \underline{dq}_{d,c} \end{bmatrix} &= \begin{bmatrix} \underline{dq}_B \\ \underline{\dot{q}}_{d,c} \end{bmatrix} = \begin{bmatrix} \underline{\underline{I}} & \underline{\underline{0}} \\ \underline{\underline{0}} & \underline{\underline{N}}_c \end{bmatrix} \begin{bmatrix} \underline{\underline{T}}_B \\ \underline{\underline{T}}_{d,\text{end}} \end{bmatrix} \underline{dq}_e = \underline{\underline{N}}_{B,\text{end}} \underline{\underline{T}}_{B,\text{end}} \underline{dq}_e \\ \begin{bmatrix} \underline{d\dot{q}}_B \\ \underline{d\dot{q}}_{d,c} \end{bmatrix} &= \begin{bmatrix} \underline{d\dot{q}}_B \\ \underline{\ddot{q}}_{d,c} \end{bmatrix} = \begin{bmatrix} \underline{\underline{I}} & \underline{\underline{0}} \\ \underline{\underline{0}} & \underline{\underline{N}}_c \end{bmatrix} \begin{bmatrix} \underline{\underline{T}}_B \\ \underline{\underline{T}}_{d,\text{end}} \end{bmatrix} \underline{d\dot{q}}_e + \begin{bmatrix} \underline{\underline{I}} & \underline{\underline{0}} \\ \underline{\underline{0}} & \underline{\underline{N}}_c \end{bmatrix} \begin{bmatrix} \underline{\underline{\dot{T}}}_B \\ \underline{\underline{\dot{T}}}_{d,\text{end}} \end{bmatrix} \underline{dq}_e \\ &= \underline{\underline{N}}_{B,\text{end}} \underline{\underline{T}}_{B,\text{end}} \underline{d\dot{q}}_e + \underline{\underline{N}}_{B,\text{end}} \underline{\underline{\dot{T}}}_{B,\text{end}} \underline{dq}_e \end{aligned} \quad (3-50)$$

The virtual total power of spatial Timoshenko beam can be written as

$$\delta p_e = \delta p_{\text{ine}} + \delta p_{\text{int}} + \delta p_{\text{ext,g}} = -\delta \underline{dq}_e^T \left(\underline{\underline{M}}_e \underline{d\dot{q}}_e + \underline{F}_e \right) \quad (3-51)$$

The generalized mass and force regarding to generalized coordinate can be written as

$$\begin{aligned} \underline{\underline{M}}_e &= \underline{\underline{T}}_{B,\text{end}}^T \int_0^L \underline{\underline{N}}_{B,\text{end}}^T \underline{\underline{M}}_{B,c} \underline{\underline{N}}_{B,\text{end}} ds \underline{\underline{T}}_{B,\text{end}} \\ \underline{F}_e &= \underline{\underline{D}}_e \underline{dq}_e + \underline{F}_{\text{int},e} + \underline{F}_{\text{ext},e,g} \end{aligned} \quad (3-52)$$

where

$$\begin{aligned} \underline{\underline{D}}_e &= \underline{\underline{T}}_{B,\text{end}}^T \int_0^L \underline{\underline{N}}_{B,\text{end}}^T \left(\underline{\underline{M}}_{B,c} \underline{\underline{N}}_{B,\text{end}} \underline{\underline{\dot{T}}}_{B,\text{end}} + \underline{\underline{D}}_{B,c} \underline{\underline{N}}_{B,\text{end}} \underline{\underline{T}}_{B,\text{end}} \right) ds \\ \underline{F}_{\text{int},e} &= \underline{\underline{T}}_{d,\text{end}} \underline{\underline{N}}_c^T \left(\underline{\underline{H}}_1 \underline{\underline{N}}'_c + \underline{\underline{H}}_2 \underline{\underline{N}}_c \right) \Big|_0^L \underline{q}_{d,\text{end}} \\ \underline{F}_{\text{ext},g} &= -\underline{\underline{T}}_{B,\text{end}}^T \int_0^L \underline{\underline{N}}_{B,\text{end}}^T \underline{\underline{H}}_t^T \rho A ds \underline{g} \end{aligned} \quad (3-53)$$

3.4 Cubic Spline Beam Dynamic Model

3.4.1 Assumptions for Cubic Spline Beam

The cubic spline beam is a kind of exact geometry beam based on absolute coordinate, which also satisfies the Euler-Bernoulli beam assumptions. The assumptions are as follows:

1. The axis after deformation is smooth and continuous in the absolute coordinate system, and satisfies the positions and posture of the two end points;
2. the axial deformation is smaller than the bending deformation, so the parameters of the cross section remain unchanged after the deformation;
3. only the axial strain at the two ends of the beam is considered.

3.4.2 Generalized Coordinate and Generalized Velocity

According to the third assumption, in addition to the position and direction angle of the end point, the generalized coordinates also include the norm of the first derivative of the position to the arc length coordinate s to represent the axial strain of the end point. Therefore, the generalized coordinates and generalized velocity of the cubic spline beam are defined as follows:

$$\underline{q}_e = \begin{bmatrix} q_1^T & q_2^T \end{bmatrix}^T = \begin{bmatrix} \underline{r}^{1T} & \underline{\varphi}^{1T} & \|\underline{r}'^1\| & \underline{r}^{2T} & \underline{\varphi}^{2T} & \|\underline{r}'^2\| \end{bmatrix}^T$$

$$\underline{dq}_e = \begin{bmatrix} dq_1^T & dq_2^T \end{bmatrix}^T = \begin{bmatrix} \dot{\underline{r}}^{1T} & \underline{\omega}^{1T} & \|\dot{\underline{r}}'^1\| & \dot{\underline{r}}^{2T} & \underline{\varphi}^{2T} & \|\dot{\underline{r}}'^2\| \end{bmatrix}^T \quad (3-54)$$

In general, the deformation in a single beam element is not large, so the relative rotation angle between the two end-sections can be represented by the unique cardan angle ${}_1\underline{\varphi}^{12}$ through the respective rotation matrix.

$$\underline{\underline{R}}^{\text{cardan}} \left({}_1\underline{\varphi}^{12} \right) = {}_1\underline{\underline{R}}_2 = \underline{\underline{R}}_1^T \underline{\underline{R}}_2 \quad {}_1\underline{\varphi}^{12} = [{}_1\varphi^{12} \quad {}_1\psi^{12} \quad {}_1\theta^{12}]^T \quad (3-55)$$

The order of the cardan angles from end section 1 to any section c is defined as follows

$$\begin{array}{c} z \quad y \quad x \\ 1 \longrightarrow \longrightarrow \longrightarrow 2 \\ {}_1\theta^{12} \quad {}_1\psi^{12} \quad {}_1\varphi^{12} \end{array} \quad \begin{array}{c} z \quad y \quad x \\ 1 \longrightarrow \longrightarrow \longrightarrow c \\ {}_1\theta \quad {}_1\psi \quad {}_1\varphi \end{array} \quad (3-56)$$

According to the monotonicity of the sin function near 0, the rotation angle along the x-axis ${}_1\varphi^{12}$ can be expressed as [Gao-2020]

$${}_1\varphi^{12} = \sin^{-1} \left(\underline{g}_z^T \underline{R}_2 \underline{g}_y / \cos {}_1\psi^{12} \right) \quad \text{with} \quad {}_1\psi^{12} = -\sin^{-1} \underline{g}_z^T \underline{R}_2 \underline{g}_x \quad (3-57)$$

Through the angular velocity and angular acceleration of the two end sections, the angular velocity and acceleration of the relative rotation angle can be determined

$$\begin{aligned} {}_2\underline{\omega}^2 &= {}_1\underline{R}_2^T {}_1\underline{\omega}^1 + \underline{T}_{12}^{\text{cardan}} {}_1\dot{\underline{\varphi}}^{12} \quad \text{with} \quad \underline{T}_{12}^{\text{cardan}} = \underline{T}^{\text{cardan}} \left({}_1\varphi^{12} \right) \\ {}_2\dot{\underline{\omega}}^2 &= \underline{\underline{R}}_2^T \underline{\underline{R}}_1 {}_1\dot{\underline{\omega}}^1 + \underline{\underline{T}}_{12}^{\text{cardan}} {}_1\ddot{\underline{\varphi}}^{12} - {}_2\tilde{\underline{\omega}}^2 {}_1\underline{R}_2^T {}_1\underline{\omega}^1 + \underline{\dot{T}}_{12}^{\text{cardan}} {}_1\dot{\underline{\varphi}}^{12} \\ &\quad \Downarrow \\ {}_1\dot{\underline{\varphi}}^{12} &= \underline{T}_{12}^{\text{cardan}}{}^{-1} \left(\underline{T}_{\omega 2} - \underline{\underline{R}}_2^T \underline{\underline{R}}_1 \underline{T}_{\omega 1} \right) d\underline{q}_e = \underline{T}_{\varphi 12} d\underline{q}_e \\ {}_1\ddot{\underline{\varphi}}^{12} &= \underline{T}_{\varphi 12} d\dot{\underline{q}}_e + \underline{\dot{T}}_{\varphi 12} d\underline{q}_e \end{aligned} \quad (3-58)$$

where

$$\begin{aligned} \underline{\underline{T}}_{\omega 1} &= \begin{bmatrix} 0 & I & 0 & 0 & 0 & 0 \end{bmatrix} & \underline{\underline{T}}_{\omega 2} &= \begin{bmatrix} 0 & 0 & 0 & 0 & I & 0 \end{bmatrix} \\ \underline{\dot{T}}_{12}^{\text{cardan}} &= \underline{T}^{\text{cardan}} \left({}_1\varphi^{12}, {}_1\dot{\underline{\varphi}}^{12} \right) \\ \underline{\dot{T}}_{\varphi 12} &= \underline{T}_{12}^{\text{cardan}}{}^{-1} \left({}_2\tilde{\underline{\omega}}^2 \underline{\underline{R}}_2^T \underline{\underline{R}}_1 \underline{T}_{\omega 1} - \underline{\dot{T}}_{12}^{\text{cardan}} \underline{T}_{\varphi 12} \right) \end{aligned} \quad (3-59)$$

3.4.3 Discretization and Shape Function

In order to ensure the geometric continuity of the cubic spline beam in the absolute coordinate system, Hermite interpolation is used to determine the position of the center of the section [Wan-2015]. Therefore, the position vector of section c and its derivative along the arc length coordinate can be written as

$$\underline{r}^{(s)c} = N_0^{1(s)} \underline{r}^1 + N_0^{2(s)} \underline{r}^2 + N_1^{1(s)} \underline{r}'^1 + N_1^{2(s)} \underline{r}'^2 \quad (3-60)$$

where $(*)^{(s)} = d^{(s)}(*)/ds^{(s)}$, $s = 0, 1, 2, \dots$ and

$$\underline{r}'^1 = \|\underline{r}'^1\| \underline{n}_x^1 = \|\underline{r}'^1\| \underline{R}_1 \underline{g}_x \quad \underline{r}'^2 = \|\underline{r}'^2\| \underline{n}_x^2 = \|\underline{r}'^2\| \underline{R}_2 \underline{g}_x \quad (3-61)$$

Velocity and acceleration can be written as

$$\underline{\dot{r}}^{(s)c} = \underline{\underline{N}}^{(s)} \underline{\underline{D}} d\underline{q}_e \quad \underline{\ddot{r}}^{(s)c} = \underline{\underline{N}}^{(s)} \underline{\underline{D}} d\underline{q}_e + \underline{\underline{N}}^{(s)} \underline{\underline{D}} d\dot{\underline{q}}_e \quad (3-62)$$

where

$$\begin{aligned}
 \underline{\underline{N}}^{(s)} &= \begin{bmatrix} N_0^1(s) & N_1^1(s) & N_0^2(s) & N_1^2(s) \end{bmatrix} \\
 \underline{\underline{D}} &= \begin{bmatrix} I & 0 & 0 & 0 \\ 0 & -\underline{\underline{r}}'^1 R_1 & \underline{n}_x^1 & 0 \\ 0 & 0 & I & 0 \\ 0 & 0 & 0 & -\underline{\underline{r}}'^2 R_2 \end{bmatrix} \\
 \underline{\underline{\dot{D}}} &= \begin{bmatrix} 0 & 0 & 0 & 0 & 0 & 0 \\ 0 & -\|\underline{\underline{r}}'^1\| R_1 \underline{\underline{\tilde{\omega}}}^1 \underline{\underline{\tilde{g}}}_x & -2 \underline{n}_x^1 \omega^1 & 0 & 0 & 0 \\ 0 & 0 & 0 & 0 & 0 & 0 \\ 0 & 0 & 0 & 0 & -\|\underline{\underline{r}}'^2\| R_2 \underline{\underline{\tilde{\omega}}}^2 \underline{\underline{\tilde{g}}}_x & -2 \underline{n}_x^2 \omega^2 \end{bmatrix} \tag{3-63}
 \end{aligned}$$

The direction of the tangential vector $\underline{\underline{r}}'^c$ reflects the x-axis of the section. In addition, the x-axis of the section can also be defined by the rotation matrix of the section

$$\underline{n}_x = 1/\|\underline{\underline{r}}'^c\| \underline{\underline{r}}'^c = \underline{\underline{R}}_1 \underline{\underline{R}}_z (\underline{\theta}) \underline{\underline{R}}_y (\underline{\psi}) \underline{\underline{g}}_x \tag{3-64}$$

Therefore, the y-axis and z-axis components of the relative rotation angle to the section 1 can be obtained, which reflect the bending of the beam.

$$\underline{\psi} = -\sin^{-1} \underline{g}_z^T \underline{\underline{R}}_1^T \underline{n}_x \quad \underline{\theta} = \sin^{-1} (\underline{g}_y^T \underline{\underline{R}}_1^T \underline{n}_x / \cos \underline{\psi}) \tag{3-65}$$

The x-axis component of the relative rotation angle reflects the torsion of the section relative to section 1, which can be obtained by linear interpolation

$$\underline{\varphi} = \xi \underline{\varphi}^{12} \quad \text{with} \quad \xi = x/L \tag{3-66}$$

Therefore, the relative rotation cardan angle from section 1 to section c can be expressed as

$$\underline{\underline{\varphi}} = [\underline{\varphi} \quad \underline{\psi} \quad \underline{\theta}]^T \quad \underline{\underline{\varphi}}' = [\underline{\varphi}' \quad \underline{\psi}' \quad \underline{\theta}']^T \tag{3-67}$$

The velocity and acceleration of relative cardan angle and its derivative with respect to the arc length can be written as

$$\begin{aligned} {}_1\dot{\underline{\phi}} &= \underline{T}_{\text{Angle}} d\underline{q}_e \\ {}_1\ddot{\underline{\phi}} &= \underline{T}_{\text{Angle}} d\dot{\underline{q}}_e + \dot{\underline{T}}_{\text{Angle}} d\underline{q}_e \end{aligned} \quad (3-68)$$

The detailed expressions are shown in appendix [Fan-2016].

3.4.4 Kinematics and Deformation of Points on the Beam

The angular velocity and angular acceleration of section c can be written as

$$\begin{aligned} {}_c\omega^c &= \left(\underline{R}_d^T \underline{T}_{\omega 1} + \underline{T}_d \underline{T}_{\text{Angle}} \right) d\underline{q}_e = \underline{T}_{\omega} d\underline{q}_e \\ {}_c\dot{\omega}^c &= \underline{T}_{\omega} d\dot{\underline{q}}_e + \left(\dot{\underline{T}}_d \underline{T}_{\text{Angle}} + \underline{T}_d \dot{\underline{T}}_{\text{Angle}} - {}_c\tilde{\omega}_d^c \underline{R}_d^T \underline{T}_{\omega 1} \right) d\underline{q}_e = \underline{T}_{\omega} d\dot{\underline{q}}_e + \dot{\underline{T}}_{\omega} d\underline{q}_e \end{aligned} \quad (3-69)$$

in which

$$\underline{R}_d = \underline{R}({}_1\phi) \quad \underline{T}_d = \underline{T}({}_1\phi) \quad \dot{\underline{T}}_d = \dot{\underline{T}}({}_1\phi, {}_1\dot{\phi}) \quad {}_c\omega_d^c = \underline{T}({}_1\phi) {}_1\dot{\phi} \quad (3-70)$$

According to the Euler Bernoulli beam assumption, the shear strain on the section is ignored. The principal strain along the x-axis of section c can be written as

$$\begin{aligned} {}_1\varepsilon &= {}_c\varepsilon = \|{}_1r'^c\| - 1 \\ {}_1\dot{\varepsilon} &= {}_c\dot{\varepsilon} = 1/\|{}_1r'^c\| {}_1r'^{cT} \underline{N}' \underline{D} d\underline{q}_e = \underline{T}_{\varepsilon}^T d\underline{q}_e \end{aligned} \quad (3-71)$$

Bending and torsional strains are expressed by the curvature of the section

$$\begin{aligned} {}_c\kappa &= \underline{T}_d {}_1\phi' \\ {}_c\dot{\kappa} &= \left[\underline{T}_d \underline{T}_{\text{dAngle}} + \underline{T}'({}_1\phi, {}_1\phi') \underline{T}_{\text{Angle}} - {}_c\tilde{\kappa} \underline{T}_{\omega} \right] d\underline{q}_e = \underline{T}_{\kappa} d\underline{q}_e \end{aligned} \quad (3-72)$$

3.4.5 The Virtual Power of Cubic Spline Beam

The virtual inertial power can be written as the summation of the translational and rotational part. The virtual translational inertial power can be formulated as

$$\delta p_{\text{ine,tra}} = -\rho A \int_0^L \delta {}_1\dot{r}^c {}_1\dot{r}^c ds = -\delta d\underline{q}_e^T \left(\underline{M}_{e,\text{ine,tra}} d\dot{\underline{q}}_e + \underline{F}_{e,\text{ine,tra}} \right) \quad (3-73)$$

where

$$\begin{aligned}\underline{\underline{M}}_{e,\text{ine,tra}} &= \rho A \underline{\underline{D}}^T \int_0^L \underline{\underline{N}}^T \underline{\underline{N}} ds \underline{\underline{D}} \\ \underline{F}_{e,\text{ine,tra}} &= \underline{\underline{D}}_{e,\text{ine,tra}} \underline{dq}_e = \rho A \underline{\underline{D}}^T \int_0^L \underline{\underline{N}}^T \underline{\underline{N}} ds \underline{\underline{D}} \dot{\underline{dq}}_e\end{aligned}\quad (3-74)$$

The virtual rotational inertial power can be formulated as

$$\begin{aligned}\delta p_{\text{ine,rot}} &= -\rho \int_0^L \delta_c \underline{\underline{\omega}}^c T \left(\underline{\underline{J}}_c \dot{\underline{\underline{\omega}}}^c + c \widetilde{\underline{\underline{\omega}}}^c \underline{\underline{J}}_c \underline{\underline{\omega}}^c \right) ds \\ &= -\delta \underline{dq}_e^T \left(\underline{\underline{M}}_{e,\text{ine,rot}} \underline{dq}_e + \underline{F}_{e,\text{ine,rot}} \right)\end{aligned}\quad (3-75)$$

where

$$\begin{aligned}\underline{\underline{M}}_{e,\text{ine,rot}} &= \rho \int_0^L \underline{\underline{T}}_\omega^T \underline{\underline{T}}_\omega ds \\ \underline{F}_{e,\text{ine,rot}} &= \underline{\underline{D}}_{e,\text{ine,rot}} \underline{dq}_e = \rho \int_0^L \underline{\underline{T}}_\omega^T \left(\underline{\underline{J}} \dot{\underline{\underline{T}}}_\omega + c \widetilde{\underline{\underline{\omega}}}^c \underline{\underline{J}} \underline{\underline{T}}_\omega \right) ds \underline{dq}_e\end{aligned}\quad (3-76)$$

The virtual internal power of the cubic spline beam can be expressed as

$$\begin{aligned}\delta p_{\text{int}} &= - \int_0^L \delta_c \underline{\underline{\varepsilon}}^c \underline{\underline{\sigma}} ds = -\delta \underline{dq}_e^T \int_0^L \underline{\underline{T}}_{\text{strain}}^T \underline{\underline{K}}_e \underline{\underline{\varepsilon}} ds = -\delta \underline{dq}_e^T \underline{F}_{e,\text{int}} \\ \underline{\underline{T}}_{\text{strain}} &= [\underline{\underline{T}}_e \quad \underline{\underline{T}}_k^T]^T \quad \underline{\underline{K}}_e = \text{diag}([EA \quad GJ \quad EI_y \quad EI_z])\end{aligned}\quad (3-77)$$

The virtual external power of the cubic spline beam caused by gravity $\underline{\underline{g}}$ can be expressed as

$$\delta p_{\text{ext,g}} = \rho A \int_0^L \delta \underline{\underline{I}}^c \underline{\underline{g}} ds \underline{\underline{g}} = \delta \underline{dq}_e^T \rho A \underline{\underline{D}}^T \int_0^L \underline{\underline{N}}^T ds \underline{\underline{g}} = -\delta \underline{dq}_e^T \underline{V}_e \underline{\underline{g}} \quad (3-78)$$

3.5 Super Truss Element Dynamic Model

3.5.1 Assumptions for Super Truss Element

In order to reduce the number of degrees of freedom of the truss element, three assumptions are proposed, so that each beam in the truss element can be expressed by

the coordinates of the two end sections. These assumptions can be acceptable when the truss is long and the deformation is uniform and small.

Assumption 1: Rigid End Section

When the truss is long, the deformation is mainly along the length of the truss, while the deformation of the end section is relatively small. In reality, the truss is often strengthened on the end section, making the stiffness of the end section larger, so the end section of the truss can be considered as rigid. The rigid end section of the truss means the position vector from the section node to any point on the end section in this section coordinate is constant.

Assumption 2: Geometric Continuity of Main Beam

The position vector of the cross-section center of the main beam is assumed to be geometric continuous after the deformation. Moreover, the arc-length derivative of position vector remains parallel to the normal direction of the cross-section.

Assumption 3: Rigid Connection

The rigid connection hypothesis refers to the relative rotation angles of different beam elements connected to the same node in the local coordinate, which remain unchanged before and after deformation. In reality, riveting or welding is often used to connect the beam element, and the stiffness of the nodes will be strengthened, so this assumption is in line with the actual situation.

In addition, all truss elements here are regular, which means the shape satisfies the following conditions:

1. The end section of the truss element is a plane, and the two sections are parallel to each other and perpendicular to the virtual main axis;
2. All beam members are straight before the deformation

3.5.2 Parameterization of Super Truss Element

Truss Elements and Truss Order

The configuration of the sub-beams is defined by the connection form and the truss order. The sub-beam connection form refers to the position of the internal nodes connected by the sub-beam. Truss order refers to the ratio of the total length of the main beam to the minimum element length divided by the sub-beams.

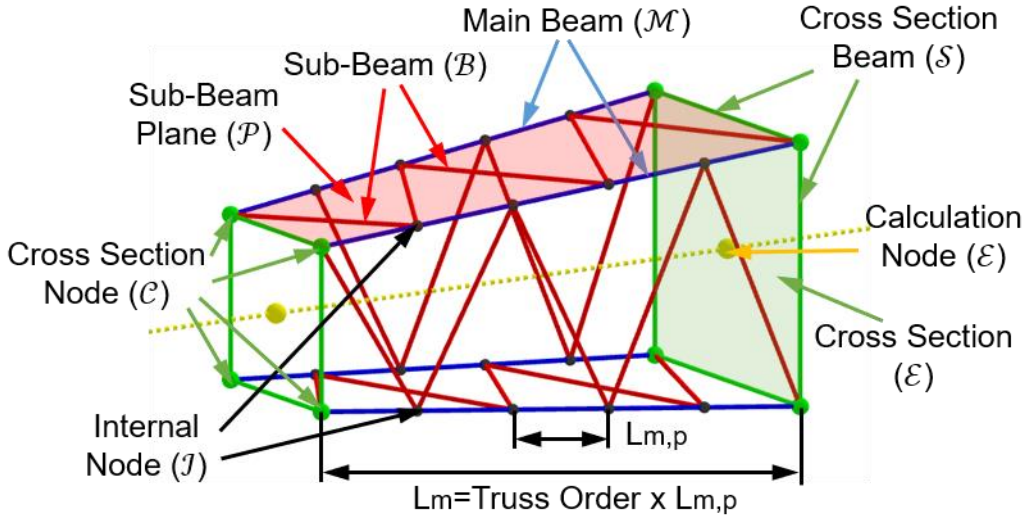


Figure 3-1: Definition of truss elements and truss order

The truss here is defined by nodes (cross section nodes, internal nodes), planes (cross section, sub-beam planes) and beam elements (cross section beams, main beams, sub-beams).

Parameters of Cross Section Nodes

According to the rigid end section assumption, only the position vector from the section node to any point on the end section in this section coordinate should be defined. Moreover, the posture of the section node can be expressed by the angle of the end section.

Parameters of Cross Section Beams

The cross section beams in a certain cross section s can be defined by the cross-section nodes. According to the definition of beam element above, it is required that the x-axis of the beam must be parallel to the line connecting the two ends of the beam when there is no deformation. In addition, the z-axis of cross section beam is defined to be perpendicular to the cross section, which is the same as the x-axis of the cross-section coordinate. Therefore, the rotation matrix of the nodes at both ends of the end beam can be defined as

$$\underline{\underline{R}}_s = [\underline{n}_x^s \quad \underline{n}_y^s \quad \underline{n}_z^s] \quad \text{with} \quad \underline{\underline{R}}_s^i = \underline{\underline{R}}_s^T \underline{\underline{R}}_s = \text{const. } \forall i, s \quad (3-79)$$

where

$$\underline{n}_x^s = (\underline{r}^k - \underline{r}^l) / \| \underline{r}^k - \underline{r}^l \| \quad \underline{n}_z^s = \underline{n}_x^i \quad (3-80)$$

in which $s \in \mathcal{S}_i$, $k, l \in \mathcal{C}_i$, $i \in \mathcal{E}$. According to assumption of rigid end section or rigid connection, the relative rotation matrix between the coordinate system of the nodes at both ends of the cross-section beam and the coordinate system of the end section is constant under deformation.

Parameters of Main Beams, Sub-beam Planes and Internal Nodes

Main beam is defined by the two cross section nodes of different end section. The x-axis of the main beam is along the length of the main beam.

$$\underline{n}_x^m = (\underline{r}^k - \underline{r}^l) / \| \underline{r}^k - \underline{r}^l \| \quad (3-81)$$

in which $m \in \mathcal{M}$, $k \in \mathcal{C}_i$, $l \in \mathcal{C}_j$. The sub-beams must be located on the surface formed by the two main beams. According to the assumptions above, only the situation where two main beams form a plane is discussed, which is basically the same in practical applications. The direction of the sub-beam plane and the z-axis of the main beam in this sub-beam plane is defined by its normal vector.

$$\underline{n}_z^{m,g} = \underline{n}_z^{n,g} = \underline{k}^g = \underline{\hat{n}}_x^m \underline{n}_x^n \quad (3-82)$$

in which $m, n \in \mathcal{M}_g$, $g \in \mathcal{P}$. The main beams belonging to different sub-beam planes will have different directions defined in each sub-beam plane. According to the rigid connection assumption, the relative rotation between the end node of the main beam and the cross-section node is constant.

$$\underline{\underline{R}}_{m,g} = [\underline{n}_x^m \quad \underline{n}_y^m \quad \underline{n}_z^{m,g}] \quad \text{with} \quad \underline{\underline{R}}_{m,g}^i = \underline{\underline{R}}_i^T \underline{\underline{R}}_{m,g} = \text{const. } \forall i, m, g \quad (3-83)$$

With the assumption of geometric continuity of the main beam, the direction of the internal nodes on the main beam is the same as the direction of the main beam when it is not deformed.

Parameters of Sub-beams

The sub-beam is defined by the main beam and the location of end nodes on the main beam. The x-axis of the sub-beam is defined as the unit vector between the internal nodes on two main beams. The z-axis of the sub-beam is defined as the normal direction of the sub-beam plane.

$$\underline{n}_x^h = (\underline{r}^{m,p} - \underline{r}^{n,q}) / \| \underline{r}^{m,p} - \underline{r}^{n,q} \| \quad \underline{n}_z^h = \underline{k}^g \quad (3-84)$$

in which $h \in \mathcal{B}_g$, $p \in \mathcal{I}_m$, $q \in \mathcal{I}_n$. According to the rigid connection assumption, the relative rotation angle between the end point coordinate of the sub-beam and the corresponding main beam coordinate is constant and must be along the normal direction of the sub-beam plane.

$$\underline{\underline{R}}_h = [\underline{m}_x^h \quad \underline{n}_y^h \quad \underline{n}_z^h] \quad \text{with} \quad \underline{\underline{R}}_h^{m,g} = \underline{\underline{R}}_{m,g}^T \underline{\underline{R}}_h = \text{const. } \forall m, g, h \quad (3-85)$$

3.5.3 Dynamics Calculation of Super Truss Element

The dynamics calculation of the super truss element is composed of the following modules: cross section node, internal node, cross section beam, main beam and sub-beam.

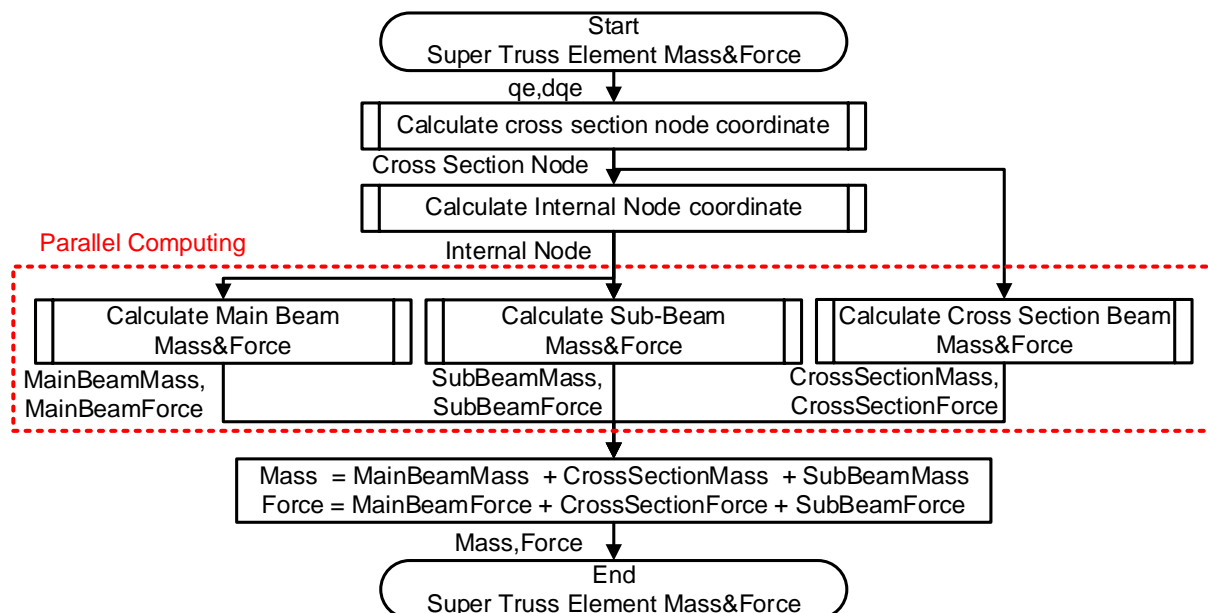


Figure 3-2: Flow chart of dynamic calculation of super truss element

From the flow chart above, it can be found that the calculations of the cross-section beam, the main beam and the sub-beams do not affect each other. Parallel computation can effectively reduce the single-step calculation time of the super truss element.

Generalized Coordinate and Generalized Velocity

According to the above assumptions and parameter definitions, the generalized coordinates and velocity of the super truss element can be defined only by two end sections.

$$\underline{q}_e = \begin{bmatrix} q_1^T & q_2^T \end{bmatrix}^T = \begin{bmatrix} \underline{r}^1^T & \underline{\varphi}^1^T & \underline{r}^2^T & \underline{\varphi}^2^T \end{bmatrix}^T \quad 1,2 \in \mathcal{E}$$

$$\underline{dq}_e = \begin{bmatrix} dq_1^T & dq_2^T \end{bmatrix}^T = \begin{bmatrix} \underline{\dot{r}}^1^T & \underline{\omega}^1^T & \underline{\dot{r}}^2^T & \underline{\omega}^2^T \end{bmatrix}^T \quad (3-86)$$

Cross Section Nodes

The position and the posture of the cross-section nodes will be calculated according to the assumption of rigid end section.

$$\underline{r}^k = \underline{r}^i + \underline{\underline{R}}_{ji} \underline{r}^{i,k} \quad \underline{\underline{R}}_k = \underline{\underline{R}}_j \quad (3-87)$$

The generalized velocity and generalized acceleration of the cross-section is composed of translational and angular velocity, which can be written as

$$\underline{dq}_k = \begin{bmatrix} \underline{\dot{r}}^k^T & k\underline{\omega}^k^T \end{bmatrix}^T = \underline{\underline{T}}_k \underline{\underline{T}}_j \underline{dq}_e = \underline{\underline{T}}_k \underline{dq}_e$$

$$\underline{d\dot{q}}_k = \begin{bmatrix} \underline{\ddot{r}}^k^T & k\underline{\dot{\omega}}^k^T \end{bmatrix}^T = \underline{\underline{T}}_k \underline{\underline{T}}_j \underline{d\dot{q}}_e + \underline{\underline{\dot{T}}}_k \underline{\underline{T}}_j \underline{dq}_e = \underline{\underline{T}}_k \underline{dq}_e + \underline{\underline{\dot{T}}}_k \underline{dq}_e \quad (3-88)$$

where

$$\underline{\underline{T}}_k^i = \begin{bmatrix} I & -\underline{\underline{R}}_{ji} \underline{\underline{\tilde{r}}}^{i,k} \\ 0 & I \end{bmatrix} \quad \underline{\underline{\dot{T}}}_k^i = \begin{bmatrix} 0 & -\underline{\underline{R}}_{ji} \underline{\underline{\tilde{\omega}}}^i \underline{\underline{\tilde{r}}}^{i,k} \\ 0 & 0 \end{bmatrix} \quad \underline{\underline{T}}_i = \begin{cases} \begin{bmatrix} I & 0 \\ 0 & I \end{bmatrix}, & i = 1 \\ \begin{bmatrix} 0 & I \\ 0 & 0 \end{bmatrix}, & i = 2 \end{cases} \quad (3-89)$$

Internal Nodes

The internal node is defined by the main beam on the sub-beam plane to which the internal node belongs. The coordinates of the end point of the main beam can be obtained by the corresponding cross section node and the relative rotation angle to the main beam in a certain sub-beam plane g .

$$\underline{r}_{m,g}^k = \underline{r}^k \quad \underline{\underline{R}}_{m,g}^k = \underline{\underline{R}}_j \underline{\underline{R}}_{m,g}^i \quad (3-90)$$

The generalized velocity and acceleration of the end point of the main beam is

$$\underline{dq}_{m,g}^k = \begin{bmatrix} \underline{\dot{r}}_{m,g}^k^T & m,g \underline{\omega}_k^{m,g T} \end{bmatrix}^T = \underline{\underline{T}}_{m,g}^k \underline{\underline{T}}_k \underline{dq}_e = \underline{\underline{T}}_{m,g,k} \underline{dq}_e$$

$$\underline{d\dot{q}}_s^k = \begin{bmatrix} \underline{\ddot{r}}_{m,g}^k^T & m,g \underline{\dot{\omega}}_k^{m,g T} \end{bmatrix}^T = \underline{\underline{T}}_{m,g}^k \left(\underline{\underline{T}}_k \underline{d\dot{q}}_e + \underline{\underline{\dot{T}}}_k \underline{dq}_e \right) = \underline{\underline{T}}_{m,g,k} \underline{d\dot{q}}_e + \underline{\underline{\dot{T}}}_{m,g,k} \underline{dq}_e \quad (3-91)$$

where $\underline{\underline{T}}_{m,g}^k = \text{diag} \left(\begin{bmatrix} I & \underline{\underline{R}}_{m,g}^i \end{bmatrix}^T \right)$.

Here the main deformation of the main beam is considered to be caused by bending. Thus, the deformation in axial direction is ignored. The position vector, rotation matrix as well as the generalized velocity and generalized acceleration can be obtained by using cubic spline beam model, whose axis is also assumed to be geometric continuous. Thus, the generalized velocity and generalized acceleration can be formulated as

$$\begin{aligned}\underline{dq}_g^p &= \begin{bmatrix} \underline{\dot{r}}_g^{pT} & {}^p_g\omega_p^{gT} \end{bmatrix}^T = \underline{T}_{p,g}^{m,g} \underline{T}_{m,g} \underline{dq}_e = \underline{T}_{p,g} \underline{dq}_e \\ \underline{d\dot{q}}_g^p &= \begin{bmatrix} \underline{\ddot{r}}_g^{pT} & {}^p_g\dot{\omega}_p^g \end{bmatrix}^T = \underline{T}_{p,g}^{m,g} \underline{T}_{m,g} \underline{d\dot{q}}_e + \left(\underline{\dot{T}}_{p,g}^{m,g} \underline{T}_{m,g} + \underline{T}_{p,g}^{m,g} \underline{\dot{T}}_{m,g} \right) \underline{dq}_e \\ &= \underline{T}_{p,g} \underline{d\dot{q}}_e + \underline{\dot{T}}_{p,g} \underline{dq}_e\end{aligned}\quad (3-92)$$

in which $\underline{T}_{p,g}^{m,g}$ and $\underline{\dot{T}}_{p,g}^{m,g}$ can be obtained through cubic spline beam model.

The Jacobian matrix between generalized coordinate of super truss element and generalized coordinate of main beam can be written as

$$\underline{T}_{m,g} = \begin{bmatrix} \underline{T}_{m,g,k}^T & \underline{T}_{m,g,l}^T \end{bmatrix}^T \quad \underline{\dot{T}}_{m,g} = \begin{bmatrix} \underline{\dot{T}}_{m,g,k}^T & \underline{\dot{T}}_{m,g,l}^T \end{bmatrix}^T \quad (3-93)$$

Cross Section Beam Elements

According to the parameters of the definition of cross section nodes, the coordinate of the end point of the cross-section beam is depend only on cross section node.

$$\underline{r}_s^k = \underline{r}^k \quad \underline{R}_s^k = \underline{\underline{R}}_i \underline{\underline{R}}_s^i \quad (3-94)$$

The generalized velocity and acceleration of the end point can be expressed as

$$\begin{aligned}\underline{dq}_s^k &= \begin{bmatrix} \underline{\dot{r}}_s^k \\ {}_s^k\omega_k^s \end{bmatrix} = \underline{T}_{s,k}^k \underline{T}_k \underline{dq}_e = \underline{T}_{s,k} \underline{dq}_e \quad \text{with} \quad \underline{T}_{s,k}^k = \begin{bmatrix} \underline{\underline{I}} & \underline{\underline{0}} \\ \underline{\underline{0}} & \underline{\underline{R}}_s^i {}^T \end{bmatrix} \\ \underline{d\dot{q}}_s^k &= \begin{bmatrix} \underline{\ddot{r}}_s^k & {}_s^k\dot{\omega}_k^s {}^T \end{bmatrix}^T = \underline{T}_{s,k}^k \underline{T}_k \underline{d\dot{q}}_e + \underline{T}_{s,k}^k \underline{\dot{T}}_k \underline{dq}_e = \underline{T}_{s,k} \underline{d\dot{q}}_e + \underline{\dot{T}}_{s,k} \underline{dq}_e\end{aligned}\quad (3-95)$$

According to the definition of end beam, the generalized coordinate, velocity and acceleration of end beam can be expressed as

$$\begin{aligned} \underline{\underline{r}}_s^k &= \underline{\underline{r}}^k & \underline{\underline{r}}_s^l &= \underline{\underline{r}}^l & \underline{\underline{R}}_s^k &= \underline{\underline{R}}_i^k \underline{\underline{R}}_s^l & \underline{\underline{R}}_s^l &= \underline{\underline{R}}_i^l \underline{\underline{R}}_s^k \\ \underline{dq}_s &= \begin{bmatrix} \underline{dq}_s^{k^T} & \underline{dq}_s^{l^T} \end{bmatrix}^T = \begin{bmatrix} \underline{T}_{s,k}^T & \underline{T}_{s,l}^T \end{bmatrix}^T \underline{dq}_e = \underline{\underline{T}}_s \underline{dq}_e & & & & & & (3-96) \\ \underline{d\dot{q}}_s &= \begin{bmatrix} \underline{d\dot{q}}_s^{k^T} & \underline{d\dot{q}}_s^{l^T} \end{bmatrix}^T = \begin{bmatrix} \underline{\underline{T}}_{s,k}^T & \underline{\underline{T}}_{s,l}^T \end{bmatrix}^T \underline{d\dot{q}}_e + \begin{bmatrix} \underline{\dot{T}}_{s,k}^T & \underline{\dot{T}}_{s,l}^T \end{bmatrix}^T \underline{dq}_e = \underline{\underline{T}}_s \underline{d\dot{q}}_e + \underline{\dot{T}}_s \underline{dq}_e \end{aligned}$$

The mass matrix and force vector of the cross-section beam need to be calculated through the generalized coordinates of the cross-section beam, and then converted to the super truss element coordinate. The virtual power of the cross-section beam can be written as

$$\begin{aligned} \delta p_e^s &= -\delta \underline{dq}_s^T (\underline{\underline{M}}_s^s \underline{d\dot{q}}_s + \underline{F}_s^s) = -\delta \underline{dq}_e^T [\underline{\underline{T}}_s^T \underline{\underline{M}}_s^s \underline{\underline{T}}_s \underline{d\dot{q}}_e + (\underline{\underline{T}}_s^T \underline{\underline{M}}_s^s \dot{\underline{\underline{T}}}_s \underline{dq}_e + \underline{\underline{T}}_s^T \underline{F}_s^s)] \\ &= -\delta \underline{dq}_e^T (\underline{\underline{M}}_e^s \underline{d\dot{q}}_e + \underline{F}_e^s) \end{aligned} \quad (3-97)$$

Main Beam Elements

Considering that internal nodes will transmit force and moment, it is necessary to segment the main beam according to the position of the internal nodes (sub main beam), in order to meet the virtual power principle. The generalized coordinate of sub main beam can be obtained directly using the generalized coordinate of internal nodes.

$$\begin{aligned} \underline{dq}_m &= \begin{bmatrix} \underline{\underline{T}}_p^T & \underline{\underline{T}}_q^T \end{bmatrix}^T \underline{dq}_e = \underline{\underline{T}}_m \underline{dq}_e \\ \underline{d\dot{q}}_m &= \begin{bmatrix} \underline{\underline{T}}_p^T & \underline{\underline{T}}_q^T \end{bmatrix}^T \underline{d\dot{q}}_e + \begin{bmatrix} \dot{\underline{\underline{T}}}_p^T & \dot{\underline{\underline{T}}}_q^T \end{bmatrix}^T \underline{dq}_e = \underline{\underline{T}}_m \underline{d\dot{q}}_e + \dot{\underline{\underline{T}}}_m \underline{dq}_e \end{aligned} \quad (3-98)$$

The virtual power of sub main beam can be written as

$$\begin{aligned} \delta p_e^m &= -\delta \underline{dq}_m^T (\underline{\underline{M}}_m^m \underline{d\dot{q}}_m + \underline{F}_m^m) = -\delta \underline{dq}_e^T (\underline{\underline{M}}_e^m \underline{d\dot{q}}_e + \underline{F}_e^m) \\ &= -\delta \underline{dq}_e^T [\underline{\underline{T}}_m^T \underline{\underline{M}}_m^m \underline{\underline{T}}_m \underline{d\dot{q}}_e + (\underline{\underline{T}}_m^T \underline{\underline{M}}_m^m \dot{\underline{\underline{T}}}_m \underline{dq}_e + \underline{\underline{T}}_m^T \underline{F}_m^m)] \end{aligned} \quad (3-99)$$

Sub-beam Elements

According to the internal nodes connected by the sub-beam and the constant relative rotation between the end points of the sub-beam and the internal nodes, the generalized coordinates of the end points of the sub-beam can be obtained through the internal nodes. The generalized velocity and acceleration of the sub-beam endpoint can be expressed as

$$\underline{dq}_h^p = \begin{bmatrix} I_h^{pT} & p \underline{\omega}_p^{hT} \end{bmatrix}^T = \underline{T}_{h,p}^p \underline{T}_p \underline{dq}_e = \underline{T}_{h,p} \underline{dq}_e \quad \text{with} \quad \underline{T}_{h,p}^p = \begin{bmatrix} I & 0 \\ 0 & \underline{R}_h^{m,gT} \end{bmatrix} \quad (3-100)$$

$$\underline{d\dot{q}}_h^p = \begin{bmatrix} I_h^{pT} & p \underline{\dot{\omega}}_p^{hT} \end{bmatrix}^T = \underline{T}_{h,p}^p \underline{T}_p \underline{d\dot{q}}_e + \underline{T}_{h,p}^p \dot{\underline{T}}_p \underline{dq}_e = \underline{T}_{h,p} \underline{d\dot{q}}_e + \dot{\underline{T}}_{h,p} \underline{dq}_e$$

in which $p \in \mathcal{M}_g$. Therefore, the generalized velocity and acceleration of sub-beam can be written as

$$\underline{dq}_h = \begin{bmatrix} \underline{T}_{h,p}^T & \underline{T}_{h,q}^T \end{bmatrix}^T \underline{dq}_e = \underline{T}_h \underline{dq}_e$$

$$\underline{d\dot{q}}_h = \begin{bmatrix} \underline{T}_{h,p}^T & \underline{T}_{h,q}^T \end{bmatrix}^T \underline{d\dot{q}}_e + \begin{bmatrix} \dot{\underline{T}}_{h,p}^T & \dot{\underline{T}}_{h,q}^T \end{bmatrix}^T \underline{dq}_e = \underline{T}_h \underline{d\dot{q}}_e + \dot{\underline{T}}_h \underline{dq}_e \quad (3-101)$$

The virtual power of sub-beam can be written as

$$\delta p_e^h = -\delta \underline{dq}_h^T (\underline{M}_h^h \underline{d\dot{q}}_h + \underline{F}_h^h) = -\delta \underline{dq}_e^T (\underline{M}_e^h \underline{d\dot{q}}_e + \underline{F}_e^h)$$

$$= -\delta \underline{dq}_e^T \left[\underline{T}_h^T \underline{M}_h^h \underline{T}_h \underline{d\dot{q}}_e + \left(\underline{T}_h^T \underline{M}_h^h \dot{\underline{T}}_h \underline{dq}_e + \underline{T}_h^T \underline{F}_h^h \right) \right] \quad (3-102)$$

4 Multi-Body Dynamics Method

4.1 Multi-Body Dynamics Function

According to the Lagrangian equation of the first kind, the dynamic equation with constraints can be written as follows

$$\begin{cases} \underline{\underline{M}}(\underline{\underline{q}}) \underline{\underline{d}\dot{q}} + \underline{\underline{F}}(\underline{\underline{q}}, \underline{\underline{dq}}) + \underline{\underline{B}}(\underline{\underline{q}}) \underline{\lambda} = \underline{0} \\ \underline{\underline{dq}} = \underline{\underline{J}}(\underline{\dot{q}}), \quad \underline{\underline{\Phi}}(\underline{\underline{q}}) = \underline{0} \end{cases} \quad \text{with } \underline{\dot{\Phi}} = \underline{\underline{B}}^T \underline{\underline{dq}} \quad (4-1)$$

The mechanism must always satisfy its constraint equation when it is moving, so the derivative of the constraint equation with respect to time must always be zero. When the mechanism satisfies the constraints in the initial state, according to its constant and zero time derivative, it can be ensured that the mechanism still meets the constraints in the subsequent movement.

$$\begin{aligned} \underline{\underline{\Phi}} \equiv \underline{0} &\Rightarrow \underline{\dot{\Phi}} \equiv \underline{0} \Rightarrow \underline{\ddot{\Phi}} \equiv \underline{0} \\ \underline{\ddot{\Phi}} \equiv \underline{0} &\Rightarrow \underline{\dot{\Phi}} \equiv \underline{0} \Rightarrow \underline{\Phi} \equiv \underline{0}, \quad \text{if } \underline{\Phi}(t_0) = \underline{0}, \underline{\dot{\Phi}}(t_0) = \underline{0} \end{aligned} \quad (4-2)$$

According to the above characteristics of the constraint, the multi-body dynamic equation can be written as

$$\begin{cases} \underline{\underline{M}} \underline{\underline{d}\dot{q}} + \underline{\underline{F}} + \underline{\underline{B}} \underline{\lambda} = \underline{0} \\ \underline{\underline{dq}} = \underline{\underline{J}}(\underline{\dot{q}}) \\ \underline{\underline{B}}^T \underline{\underline{d}\dot{q}} + \underline{\underline{\Gamma}} = \underline{0} \end{cases} \Leftrightarrow \begin{cases} \begin{bmatrix} \underline{\underline{M}} & \underline{\underline{B}} \\ \underline{\underline{B}}^T & \underline{0} \end{bmatrix} \begin{bmatrix} \underline{\underline{d}\dot{q}} \\ \underline{\lambda} \end{bmatrix} + \begin{bmatrix} \underline{\underline{F}} \\ \underline{\underline{\Gamma}} \end{bmatrix} = \underline{0} \\ \underline{\underline{dq}} = \underline{\underline{J}}(\underline{\dot{q}}) \end{cases} \quad \text{with } \begin{cases} \underline{\dot{\Phi}} = \underline{\underline{B}}^T \underline{\underline{dq}} \\ \underline{\ddot{\Phi}} = \underline{\underline{B}}^T \underline{\underline{d}\dot{q}} + \underline{\underline{\Gamma}} \end{cases} \quad (4-3)$$

The generalized mass matrix and generalized force vector with constraints can be formulated in the following form. $\underline{\lambda}$ represents the magnitude of the generalized constraint forces in the certain constraint directions $\underline{\underline{B}}$.

$$\begin{cases} \underline{\lambda} = (\underline{\underline{B}}^T \underline{\underline{M}}^{-1} \underline{\underline{B}})^{-1} (-\underline{\underline{B}}^T \underline{\underline{M}}^{-1} \underline{\underline{F}} + \underline{\underline{\Gamma}}) \\ \underline{\underline{d}\dot{q}} = -\underline{\underline{M}}^{*-1} \underline{\underline{F}}^* \end{cases} \quad \text{with } \begin{cases} \underline{\underline{M}}^* = \underline{\underline{M}} \\ \underline{\underline{F}}^* = \underline{\underline{F}} + \underline{\underline{B}} \underline{\lambda} \end{cases} \quad (4-4)$$

4.2 Joint Configuration

A joint refers to a point that has a fixed relative position and angle with a certain generalized coordinate of the body. Joints are used to connect other bodies or bear generalized external nodal forces. The generalized coordinates of the joint can be represented by the position vector and the rotation matrix.

$$\begin{cases} \underline{l}^J = \underline{l}^B + \underline{\underline{R}}_{BB} \underline{r}^{BJ} \\ \underline{R}_J = \underline{\underline{R}}_B \underline{\underline{R}}_J^B \end{cases} \quad \text{with} \quad \begin{cases} \underline{B} \underline{r}^{BJ} = \text{const.} \\ \underline{R}_J^B = \text{const.} \end{cases}, \quad \underline{\underline{R}}_B = \underline{\underline{R}}(\varphi^B) \quad (4-5)$$

The generalized velocity and generalized acceleration of a joint can be expressed by the generalized coordinate of the body.

$$\underline{dq}_J = [\underline{l}\dot{r}^J^T \quad \underline{\omega}^J^T]^T = \underline{T}_{J,B} \underline{dq}_B \quad \underline{d\dot{q}}_J = [\underline{l}\ddot{r}^J^T \quad \underline{\dot{\omega}}^J^T]^T = \underline{T}_{J,B} \underline{d\dot{q}}_B + \underline{\dot{T}}_{J,B} \underline{dq}_B \quad (4-6)$$

where

$$\begin{aligned} \underline{q}_B &= [\underline{l}^B^T \quad \underline{\varphi}^B^T]^T & \underline{dq}_B &= [\underline{l}\dot{r}^B^T \quad \underline{\omega}^B^T]^T & \underline{d\dot{q}}_B &= [\underline{l}\ddot{r}^B^T \quad \underline{\dot{\omega}}^B^T]^T \\ \underline{T}_{J,B} &= \begin{bmatrix} I & -\underline{\underline{R}}_{BB} \underline{\underline{r}}^{BJ} \\ 0 & \underline{\underline{B}} \underline{\underline{R}}_J^T \end{bmatrix} & \underline{\dot{T}}_{J,B} &= \begin{bmatrix} 0 & -\underline{\underline{R}}_{BB} \underline{\dot{\omega}}^B \underline{\underline{r}}^{BJ} \\ 0 & 0 \end{bmatrix} \end{aligned} \quad (4-7)$$

4.3 System Generalized External Forces

The virtual external nodal power of generalized external forces applied on the joints can be formulated as

$$\delta p_{\text{ext}} = \sum_J \delta \underline{dq}_J^T \underline{F}_{\text{ext},J} = \delta \underline{dq}^T \sum_B \underline{T}_B^T \sum_{J \in B} \underline{T}_{J,B}^T \underline{F}_{\text{ext},J} \quad (4-8)$$

It should be noted, that the translational velocity is defined in inertial coordinate system, while the angular velocity in body local coordinate system. This means the generalized external force should be converted to the corresponding coordinate system.

$$\underline{F}_{\text{ext},J} = \begin{bmatrix} {}_I\underline{F}^J \\ {}_J\underline{M}^J \end{bmatrix}^T \quad \text{with} \quad {}_I\underline{F}^J = \underline{R}_{J,I}\underline{F}^J \quad \text{and} \quad {}_J\underline{M}^J = \underline{R}_{J,I}^T \underline{M}^J \quad (4-9)$$

4.4 Formulation of Different Constraints

The constraint equation is established by the generalized coordinates of the two joints.

$$\underline{\Phi}_{J1,J2} \left({}_I\underline{r}^{J1}, \underline{R}_{J1}, {}_I\underline{r}^{J2}, \underline{R}_{J2} \right) = \underline{0} \quad (4-10)$$

The first-time derivative of the constraint equation in the joint coordinate system, the body coordinate system and the global coordinate system can be written as

$$\begin{aligned} \dot{\underline{\Phi}}_{J1,J2} &\triangleq \underline{B}_{J1,J2}^T \underline{dq}_{J12} = \underline{B}_{B1,B2}^T \underline{dq}_{B12} = \underline{B}^T \underline{dq} = \underline{0} \\ \underline{B}_{B1,B2}^T &= \underline{B}_{J1,J2}^T \underline{B}_{J2,B12}^T \quad \underline{B}^T = \underline{B}_{B1,B2}^T \underline{T}_{B12} \quad \underline{T}_{J1J2} = \underline{B}_{J12,B12}^T \underline{T}_{B12} \end{aligned} \quad (4-11)$$

where

$$\underline{dq}_{J12} = \begin{bmatrix} dq_{J1} \\ dq_{J2} \end{bmatrix} \quad \underline{dq}_{B12} = \begin{bmatrix} dq_{B1} \\ dq_{B2} \end{bmatrix} \quad \underline{T}_{B12} = \begin{bmatrix} \underline{T}_{B1} \\ \underline{T}_{B2} \end{bmatrix} \quad \underline{B}_{J12,B12}^T = \begin{bmatrix} \underline{T}_{J1,B1} & \underline{0} \\ \underline{0} & \underline{T}_{J2,B2} \end{bmatrix} \quad (4-12)$$

4.4.1 Fixed Constraint

Fixed constraint means that the positions and rotation angles of the two joints are exactly the same. Therefore, there is no possibility of relative movement between these two joints.

The position constraint and angle constraint can be written as

$$\begin{aligned} {}_I\underline{r}^{J1} - {}_I\underline{r}^{J2} &= \underline{0} \\ \underline{\varphi}^{J1} - \underline{\varphi}^{J2} = \underline{0} &\Leftrightarrow \underline{e}_i^{J1} \underline{e}_j^{J2} = 0 \quad \text{with} \quad {}_I\underline{e}_i^J = \underline{R}_J \underline{g}_i, \forall i \neq j \in (x, y, z) \end{aligned} \quad (4-13)$$

The constraint equation and its first and second derivatives over time can be formulated as

$$\underline{\Phi}_{\text{FIX}} = \begin{bmatrix} \underline{r}^{J1} - \underline{r}^{J2} \\ \underline{R}_{J1}^T \underline{R}_{J2} \end{bmatrix} \quad \dot{\underline{\Phi}}_{\text{FIX}} = \underline{B}_{J1,J2}^{\text{FIX} T} \underline{dq}_{J12} \quad \ddot{\underline{\Phi}}_{\text{FIX}} = \underline{B}_{J1,J2}^{\text{FIX} T} \underline{d\dot{q}}_{J12} + \underline{\Gamma}_{\text{FIX}} \quad (4-14)$$

where

$$\begin{aligned} \underline{B}_{J1,J2}^{\text{FIX} T} &= \begin{bmatrix} \underline{\underline{I}} & \underline{\underline{0}} & -\underline{\underline{I}} & \underline{\underline{0}} \\ \underline{\underline{0}}^T & -\underline{\underline{g}}_z^T \underline{\underline{R}}_{J2}^T \underline{\underline{R}}_{J1} \underline{\underline{\tilde{g}}}_x & \underline{\underline{0}}^T & -\underline{\underline{g}}_x^T \underline{\underline{R}}_{J1}^T \underline{\underline{R}}_{J2} \underline{\underline{\tilde{g}}}_z \\ \underline{\underline{0}}^T & -\underline{\underline{g}}_z^T \underline{\underline{R}}_{J2}^T \underline{\underline{R}}_{J1} \underline{\underline{\tilde{g}}}_y & \underline{\underline{0}}^T & -\underline{\underline{g}}_y^T \underline{\underline{R}}_{J1}^T \underline{\underline{R}}_{J2} \underline{\underline{\tilde{g}}}_z \\ \underline{\underline{0}}^T & -\underline{\underline{g}}_y^T \underline{\underline{R}}_{J2}^T \underline{\underline{R}}_{J1} \underline{\underline{\tilde{g}}}_x & \underline{\underline{0}}^T & -\underline{\underline{g}}_x^T \underline{\underline{R}}_{J1}^T \underline{\underline{R}}_{J2} \underline{\underline{\tilde{g}}}_y \end{bmatrix} \\ \underline{\Gamma}_{\text{FIX}} &= \underline{B}_{J1,J2}^{\text{FIX} T} \underline{dq}_{J12} = \begin{bmatrix} \underline{\underline{0}} & \underline{\underline{0}} & \underline{\underline{0}} & \underline{\underline{0}} \\ \underline{\underline{0}}^T & \underline{\underline{g}}_z^T \underline{\underline{D}}_{21} \underline{\underline{\tilde{g}}}_x & \underline{\underline{0}}^T & \underline{\underline{g}}_x^T \underline{\underline{D}}_{12} \underline{\underline{\tilde{g}}}_z \\ \underline{\underline{0}}^T & \underline{\underline{g}}_z^T \underline{\underline{D}}_{21} \underline{\underline{\tilde{g}}}_y & \underline{\underline{0}}^T & \underline{\underline{g}}_y^T \underline{\underline{D}}_{12} \underline{\underline{\tilde{g}}}_z \\ \underline{\underline{0}}^T & \underline{\underline{g}}_y^T \underline{\underline{D}}_{21} \underline{\underline{\tilde{g}}}_x & \underline{\underline{0}}^T & \underline{\underline{g}}_x^T \underline{\underline{D}}_{12} \underline{\underline{\tilde{g}}}_y \end{bmatrix} \underline{dq}_{J12} \quad (4-15) \\ \underline{\underline{D}}_{12} &= J_1 \underline{\underline{\tilde{\omega}}}^{J1} \underline{\underline{R}}_{J1}^T \underline{\underline{R}}_{J2} - \underline{\underline{R}}_{J1}^T \underline{\underline{R}}_{J2} \underline{\underline{\tilde{\omega}}}^{J2} \quad \underline{\underline{D}}_{21} = J_2 \underline{\underline{\tilde{\omega}}}^{J2} \underline{\underline{R}}_{J2}^T \underline{\underline{R}}_{J1} - \underline{\underline{R}}_{J2}^T \underline{\underline{R}}_{J1} \underline{\underline{\tilde{\omega}}}^{J1} \end{aligned}$$

4.4.2 Revolute Constraint

Revolute constraint means that two joints can only rotate relative to one another around a body fixed axis. For the revolute constraint described here, the position vectors of the two joints are the same, and the i -axis of joint 1 and the j -axis of joint 2 are the same. Therefore, the two joints can rotate relatively around this axis. The position and angle constraint can be written as

$$\begin{aligned} \underline{r}^{J1} &= \underline{r}^{J2} \\ \underline{e}_i^{J1} = \underline{e}_j^{J2} &\Leftrightarrow \underline{e}_p^{J1 T} \underline{e}_j^{J2} = 0, \quad i, j \in (x, y, z), \forall p \neq i \in (x, y, z) \end{aligned} \quad (4-16)$$

The constraint equation can be formulated as

$$\underline{\Phi}_{\text{REV}} = \begin{bmatrix} \underline{r}^{J1} - \underline{r}^{J2} \\ \underline{e}_p^{J1 T} \underline{e}_j^{J2} \\ \underline{e}_q^{J1 T} \underline{e}_j^{J2} \end{bmatrix} = \begin{bmatrix} \underline{r}^{J1} - \underline{r}^{J2} \\ \underline{g}_p^T \underline{R}_{J1}^T \underline{R}_{J2} \underline{g}_j \\ \underline{g}_q^T \underline{R}_{J1}^T \underline{R}_{J2} \underline{g}_j \end{bmatrix}, \quad p \neq q \in (x, y, z), (p, q) \neq i \quad (4-17)$$

The first and second derivatives of the revolute constraint over time can be written as

$$\dot{\underline{\Phi}}_{\text{REV}} = \underline{\underline{B}}_{\text{REV}}^T \underline{dq}_{J12} \quad \ddot{\underline{\Phi}}_{\text{REV}} = \underline{\underline{B}}_{\text{REV}}^T \underline{d\dot{q}}_{J12} + \underline{\Gamma}_{\text{REV}} \quad (4-18)$$

where

$$\begin{aligned} \underline{\underline{B}}_{\text{REV}}^T &= \begin{bmatrix} \underline{\underline{I}} & \underline{\underline{0}} & -\underline{\underline{I}} & \underline{\underline{0}} \\ \underline{\underline{0}}^T & -\underline{\underline{g}}_j^T \underline{\underline{R}}_{J2}^T \underline{\underline{R}}_{J1} \underline{\underline{\tilde{g}}}_p & \underline{\underline{0}}^T & -\underline{\underline{g}}_p^T \underline{\underline{R}}_{J1}^T \underline{\underline{R}}_{J2} \underline{\underline{\tilde{g}}}_j \\ \underline{\underline{0}}^T & -\underline{\underline{g}}_j^T \underline{\underline{R}}_{J2}^T \underline{\underline{R}}_{J1} \underline{\underline{\tilde{g}}}_q & \underline{\underline{0}}^T & -\underline{\underline{g}}_q^T \underline{\underline{R}}_{J1}^T \underline{\underline{R}}_{J2} \underline{\underline{\tilde{g}}}_j \end{bmatrix} \\ \underline{\Gamma}_{\text{REV}} &= \underline{\underline{B}}_{\text{REV}}^T \underline{dq}_{J12} = \begin{bmatrix} \underline{\underline{0}} & \underline{\underline{0}} & \underline{\underline{0}} & \underline{\underline{0}} \\ \underline{\underline{0}}^T & \underline{\underline{g}}_j^T \underline{\underline{D}}_{21} \underline{\underline{\tilde{g}}}_p & \underline{\underline{0}}^T & \underline{\underline{g}}_p^T \underline{\underline{D}}_{12} \underline{\underline{\tilde{g}}}_j \\ \underline{\underline{0}}^T & \underline{\underline{g}}_j^T \underline{\underline{D}}_{21} \underline{\underline{\tilde{g}}}_q & \underline{\underline{0}}^T & \underline{\underline{g}}_q^T \underline{\underline{D}}_{12} \underline{\underline{\tilde{g}}}_j \end{bmatrix} \underline{dq}_{J12} \end{aligned} \quad (4-19)$$

4.4.3 Prismatic Constraint

Prismatic constraint means that two joints can only slide relative to each other along a fixed route. Here it is only considered, that the relative sliding route is a straight line. It is also assumed that when the two joints are sliding, their rotation angles remain unchanged, and the relative sliding direction is along $\underline{\underline{e}}_i^{J1} = \underline{\underline{e}}_i^{J2}, i \in (x, y, z)$. Therefore, the position and angle constraint of the prismatic constraint can be written as

$$(\underline{\underline{r}}^{J1} - \underline{\underline{r}}^{J2}) \parallel \underline{\underline{e}}_i^{J2} \Leftrightarrow (\underline{\underline{r}}^{J1} - \underline{\underline{r}}^{J2})^T \underline{\underline{e}}_p^{J1} = 0, \quad \forall p \neq i \in (x, y, z) \quad \underline{\underline{\varphi}}^{J1} - \underline{\underline{\varphi}}^{J2} = \underline{\underline{0}} \quad (4-20)$$

The constraint equation of the prismatic constraint can be written as

$$\underline{\Phi}_{\text{PRI}} = \begin{bmatrix} (\underline{\underline{r}}^{J1} - \underline{\underline{r}}^{J2})^T \underline{\underline{R}}_{J1} \underline{\underline{g}}_p \\ (\underline{\underline{r}}^{J1} - \underline{\underline{r}}^{J2})^T \underline{\underline{R}}_{J1} \underline{\underline{g}}_q \\ \underline{\underline{R}}_{J1}^T \underline{\underline{R}}_{J2} \end{bmatrix}, \quad p \neq q \in (x, y, z), (p, q) \neq i \quad (4-21)$$

The first and second derivatives of the prismatic constraint over time can be written as

$$\dot{\underline{\Phi}}_{\text{PRI}} = \underline{\underline{B}}_{\text{PRI}}^T \underline{dq}_{J12} \quad \ddot{\underline{\Phi}}_{\text{PRI}} = \underline{\underline{B}}_{\text{PRI}}^T \underline{d\dot{q}}_{J12} + \underline{\Gamma}_{\text{PRI}} \quad (4-22)$$

where

$$\underline{\underline{B}}_{\text{PRI}}^T = \begin{bmatrix} \underline{g}_p^T \underline{R}_{J1}^T & -(\underline{l}\dot{r}^{J1} - \underline{l}\dot{r}^{J2})^T \underline{R}_{J1} \underline{\tilde{g}}_p & -\underline{g}_p^T \underline{R}_{J1}^T & \underline{0}^T \\ \underline{g}_q^T \underline{R}_{J1}^T & -(\underline{l}\dot{r}^{J1} - \underline{l}\dot{r}^{J2})^T \underline{R}_{J1} \underline{\tilde{g}}_q & -\underline{g}_q^T \underline{R}_{J1}^T & \underline{0}^T \\ \underline{0}^T & -\underline{g}_z^T \underline{R}_{J2}^T \underline{R}_{J1} \underline{\tilde{g}}_x & \underline{0}^T & -\underline{g}_x^T \underline{R}_{J1}^T \underline{R}_{J2} \underline{\tilde{g}}_z \\ \underline{0}^T & -\underline{g}_z^T \underline{R}_{J2}^T \underline{R}_{J1} \underline{\tilde{g}}_y & \underline{0}^T & -\underline{g}_y^T \underline{R}_{J1}^T \underline{R}_{J2} \underline{\tilde{g}}_z \\ \underline{0}^T & -\underline{g}_y^T \underline{R}_{J2}^T \underline{R}_{J1} \underline{\tilde{g}}_x & \underline{0}^T & -\underline{g}_x^T \underline{R}_{J1}^T \underline{R}_{J2} \underline{\tilde{g}}_y \end{bmatrix} \quad (4-23)$$

$$\underline{\underline{\Gamma}}_{\text{PRI}} = \dot{\underline{\underline{B}}}_{\text{PRI}}^T \underline{dq}_{J12} = \begin{bmatrix} -\underline{g}_{pJ1}^T \tilde{\omega}^{J1} \underline{R}_{J1}^T & -\underline{D}_{r1}^T \underline{\tilde{g}}_p & \underline{g}_{pJ1}^T \tilde{\omega}^{J1} \underline{R}_{J1}^T & \underline{0}^T \\ -\underline{g}_{qJ1}^T \tilde{\omega}^{J1} \underline{R}_{J1}^T & -\underline{D}_{r1}^T \underline{\tilde{g}}_q & \underline{g}_{qJ1}^T \tilde{\omega}^{J1} \underline{R}_{J1}^T & \underline{0}^T \\ \underline{0}^T & \underline{g}_z^T \underline{D}_{21} \underline{\tilde{g}}_x & \underline{0}^T & \underline{g}_x^T \underline{D}_{12} \underline{\tilde{g}}_z \\ \underline{0}^T & \underline{g}_z^T \underline{D}_{21} \underline{\tilde{g}}_y & \underline{0}^T & \underline{g}_y^T \underline{D}_{12} \underline{\tilde{g}}_z \\ \underline{0}^T & \underline{g}_y^T \underline{D}_{21} \underline{\tilde{g}}_x & \underline{0}^T & \underline{g}_x^T \underline{D}_{12} \underline{\tilde{g}}_y \end{bmatrix} \underline{dq}_{J12}$$

$$\underline{D}_{r1}^T = (\underline{l}\dot{r}^{J1} - \underline{l}\dot{r}^{J2})^T \underline{R}_{J1} + (\underline{l}\dot{r}^{J1} - \underline{l}\dot{r}^{J2})^T \underline{R}_{J1} \underline{J1} \underline{\tilde{\omega}}^{J1}$$

4.4.4 Spherical Constraint

Spherical constraint means that one joint can rotate at any angle around another joint. For spherical constraints, only the position vectors of the two joints are required to be same. Therefore, the constraint equation can be written as

$$\underline{\Phi}_{\text{SPH}} = \underline{l}\dot{r}^{J1} - \underline{l}\dot{r}^{J2} = \underline{0} \quad (4-24)$$

The first and second derivatives of the spherical constraint over time can be written as

$$\dot{\underline{\Phi}}_{\text{SPH}} = \underline{\underline{B}}_{\text{REV}}^T \underline{dq}_{J12} \quad \ddot{\underline{\Phi}}_{\text{SPH}} = \underline{\underline{B}}_{\text{SPH}}^T \underline{d}\dot{q}_{J12} + \underline{\Gamma}_{\text{SPH}} \quad (4-25)$$

where

$$\begin{aligned} \underline{\underline{B}}_{\text{SPH}}^T &= [\underline{\underline{I}} \quad \underline{\underline{0}} \quad -\underline{\underline{I}} \quad \underline{\underline{0}}] \\ \underline{\Gamma}_{\text{SPH}} &= \dot{\underline{\underline{B}}}_{\text{SPH}}^T \underline{dq}_{J12} = [\underline{\underline{0}} \quad \underline{\underline{0}} \quad \underline{\underline{0}} \quad \underline{\underline{0}}] \underline{dq}_{J12} = \underline{\underline{0}} \end{aligned} \quad (4-26)$$

4.5 Solving Multibody Dynamics Equation

4.5.1 Baumgartner stability method

According to the above, the constraint equation keeps unchanged by making the second derivative of the constraint over time equal to 0. However, due to the cumulative error of numerical integration, the constraint equation will gradually deviate from zero.

In order to maintain the stability of the constraint equation during the integration process, the Baumgartner stability method is applied. This method introduces the first derivative of the constraint equation $\dot{\underline{\Phi}}$ and the constraint equation $\underline{\Phi}$, so that the cumulative error of the constraint equation is considered in the process of numerical integration, which keeps the constraint equation always 0 during the integration. Through the Baumgartner stability method, the original $\underline{\Gamma}$ can be replaced by $\underline{\Gamma}^*$.

$$\begin{aligned}\underline{\ddot{\Phi}} = \underline{0} &\rightarrow \underline{\ddot{\Phi}} + 2\alpha\beta\underline{\dot{\Phi}} + \alpha^2\underline{\Phi} = \underline{0} \\ \underline{\underline{B}^T d\dot{q}} + \underline{\Gamma}^* = \underline{0} &\quad \text{with} \quad \underline{\Gamma}^* = \underline{\Gamma} + 2\alpha\beta\underline{\dot{\Phi}} + \alpha^2\underline{\Phi}\end{aligned}\quad (4-27)$$

where α and β are compensation coefficients, the recommended value of α is half of the system's natural frequency, and the recommended value of β is 1.

4.5.2 State Space Representation

The dynamics equation is a second-order differential equation, which needs to be converted into a first-order differential equation (equation of state) for easy calculation. The new state variables defined here are as follows

$$\underline{x} = [q^T \quad \underline{dq}^T]^T \quad \underline{\dot{x}} = [\dot{q}^T \quad \underline{d\dot{q}}^T]^T \quad (4-28)$$

Therefore, the state space representation of dynamics equation can be formulated as

$$\underline{\dot{x}} = \begin{bmatrix} \dot{q} \\ \underline{d\dot{q}} \end{bmatrix} = \begin{bmatrix} \underline{J}^{-1}(q, \underline{dq}) \\ -\underline{\underline{M}}^{*-1}(q) \underline{F}^*(q, \underline{dq}) \end{bmatrix} = \underline{f}(\underline{x}) \quad (4-29)$$

4.5.3 Runge-Kutta Integrator

Runge-Kutta Method is a high-precision single-step algorithm used to solve nonlinear ordinary differential equations (ODE). The dynamic equation is generally a nonlinear ordinary differential equation, and can be written as the following general formula

$$\begin{cases} \dot{\underline{x}} = \underline{f}(\underline{x}) + \underline{g}(\underline{x})\underline{u} = \underline{f}(\underline{t}, \underline{x}, \underline{u}) \\ \underline{x}_0 = \underline{x}(t=0) = \text{known} \end{cases} \quad (4-30)$$

According to Runge-Kutta Method, the solution of the ODE can be obtained by the following iterative formula

$$\begin{cases} \underline{x}_{k+1} = \underline{x}_k + \Delta t \sum_i b_i \underline{k}_i \\ \underline{k}_i = \underline{f}\left(t_k + c_i \Delta t, \underline{x}_k + \Delta t \sum_j a_{i,j} \underline{k}_j, \underline{u}_k\right), \forall i \end{cases} \quad (4-31)$$

The parameters $a_{i,j}$, b_i and c_i can be obtained from butcher tableau. When $a_{i,j} = 0, \forall i < j$, it is the explicit Runge-Kutta Method, when $\exists a_{i,j} \neq 0, i < j$ is the implicit Runge-Kutta Method.

c_1	$a_{1,1}$	$a_{1,2}$	\cdots	$a_{1,s}$		
c_2	$a_{2,1}$	$a_{2,2}$	\cdots	$a_{2,s}$		
\vdots	\vdots	\vdots	\ddots	\vdots		
c_s	$a_{s,1}$	$a_{s,2}$	\cdots	$a_{s,s}$		
	b_1	b_2	\cdots	b_s		

Figure 4-1: Butcher Tableau

From the butcher tableau and formula, it can be found that \underline{k}_i is difficult to be obtained directly for the implicit Runge-Kutta Method. Therefore, a first-order Taylor expansion of \underline{k}_i at $(t_k, \underline{x}_k, \underline{u}_k)$ is applied.

$$\begin{aligned} \underline{k}_i &= \underline{f}_k + c_i \Delta t \underline{f}_t + \Delta t \sum_j a_{i,j} \underline{k}_j \underline{f}_x + \mathcal{O}^2 \\ \underline{f}_k &= \underline{f}(t_k, \underline{x}_k, \underline{u}_k) & \underline{f}_t &= \partial \underline{f} / \partial t & \underline{f}_x &= \partial \underline{f} / \partial \underline{x} \end{aligned} \quad (4-32)$$

Therefore, \underline{k}_i can be obtained by solving the following equation

$$\underline{\underline{h}} = \underline{\underline{f}} + \Delta t \underline{\underline{F}}_t + \Delta t \underline{\underline{F}}_x \underline{\underline{h}} \quad \rightarrow \quad \underline{\underline{h}} = \left(\underline{\underline{I}} - \Delta t \underline{\underline{F}}_x \right)^{-1} \left(\underline{\underline{f}} + \Delta t \underline{\underline{F}}_t \right)$$

$$\underline{\underline{h}} = \begin{bmatrix} \underline{k}_1 \\ \underline{k}_2 \\ \vdots \\ \underline{k}_s \end{bmatrix} \quad \underline{\underline{F}}_t = \begin{bmatrix} c_1 \underline{\underline{f}}_t \\ c_2 \underline{\underline{f}}_t \\ \vdots \\ c_s \underline{\underline{f}}_t \end{bmatrix} \quad \underline{\underline{F}}_x = \begin{bmatrix} a_{1,1} \underline{\underline{f}}_x & a_{1,2} \underline{\underline{f}}_x & \cdots & a_{1,s} \underline{\underline{f}}_x \\ a_{2,1} \underline{\underline{f}}_x & a_{2,2} \underline{\underline{f}}_x & \cdots & a_{2,s} \underline{\underline{f}}_x \\ \vdots & \vdots & \ddots & \vdots \\ a_{s,1} \underline{\underline{f}}_x & a_{s,2} \underline{\underline{f}}_x & \cdots & a_{s,s} \underline{\underline{f}}_x \end{bmatrix} \quad (4-33)$$

Therefore, the iterative format of the general implicit Runge-Kutta method can be written as

$$\underline{x}_{k+1} = \underline{x}_k + \Delta t \underline{\underline{b}} \left(\underline{\underline{I}} - \Delta t \underline{\underline{F}}_x \right)^{-1} \underline{\underline{f}} + \Delta t^2 \underline{\underline{b}} \left(\underline{\underline{I}} - \Delta t \underline{\underline{F}}_x \right)^{-1} \underline{\underline{F}}_t$$

$$\underline{\underline{b}} = [b_1 \underline{\underline{I}} \quad b_2 \underline{\underline{I}} \quad \cdots \quad b_s \underline{\underline{I}}] \quad (4-34)$$

According to different Butcher Tableau, implicit Runge-Kutta can be divided into Lobatto, Radau, Gauss, Kutta 4, etc.

In general, the implicit Runge-Kutta Method is more accurate and stable than the explicit method, which realize a larger time step. However, the solution is more difficult:

1. $\underline{\underline{f}}_t$ and $\underline{\underline{f}}_x$ is difficult to obtain for complex models;
2. The dimension of the above equation is s times larger than the dynamic equation.

5 Rigid-Flexible Hybrid Multibody Dynamics Program

5.1 Functions of the Program

5.1.1 Main Functions

Jacobian Matrix Calculation

Jacobian matrix is obtained through the symbolic package CasADi, which is mainly used for optimal control and implicit ODE solver. In this program the Jacobian matrix of mass matrix to generalized coordinates, the Jacobian matrix of generalized force vector to generalized coordinates and generalized velocity can be calculated. In addition, the symbolic matrix relevant to symplectic solver can also be calculated.

Static Position Calculation

In this program two ways to get the equilibrium position are provided: dynamic solution under damping and nonlinear equation solution. In the method of dynamics solution under damping, a larger damping term is added to the system, so that the system gradually approaches the equilibrium position from the initial state. The equilibrium state obtained by this method has no initial error in the subsequent dynamics calculation.

In the method of solving nonlinear equations, the generalized speed of the mechanism is set to 0, and the generalized coordinates will be changed to make the generalized force to 0. Due to the differences between the nonlinear equation solver and the dynamics solver, it cannot be completely guaranteed that the mechanism will reach the equilibrium position in the initial state of the dynamics solving process. However, during the method of solving nonlinear equations, the equilibrium position of the mechanism can be obtained more quickly. The error in the initial stage of dynamics solution is also acceptable.

Dynamics Calculation

The calculation method of multibody dynamics has been described above. Here is a detailed introduction to the pre-processing of the system, the definition of the inertial coordinate system, the introduction method of driving force and the use of Baumgartner stability method. The specific process can be seen as follows

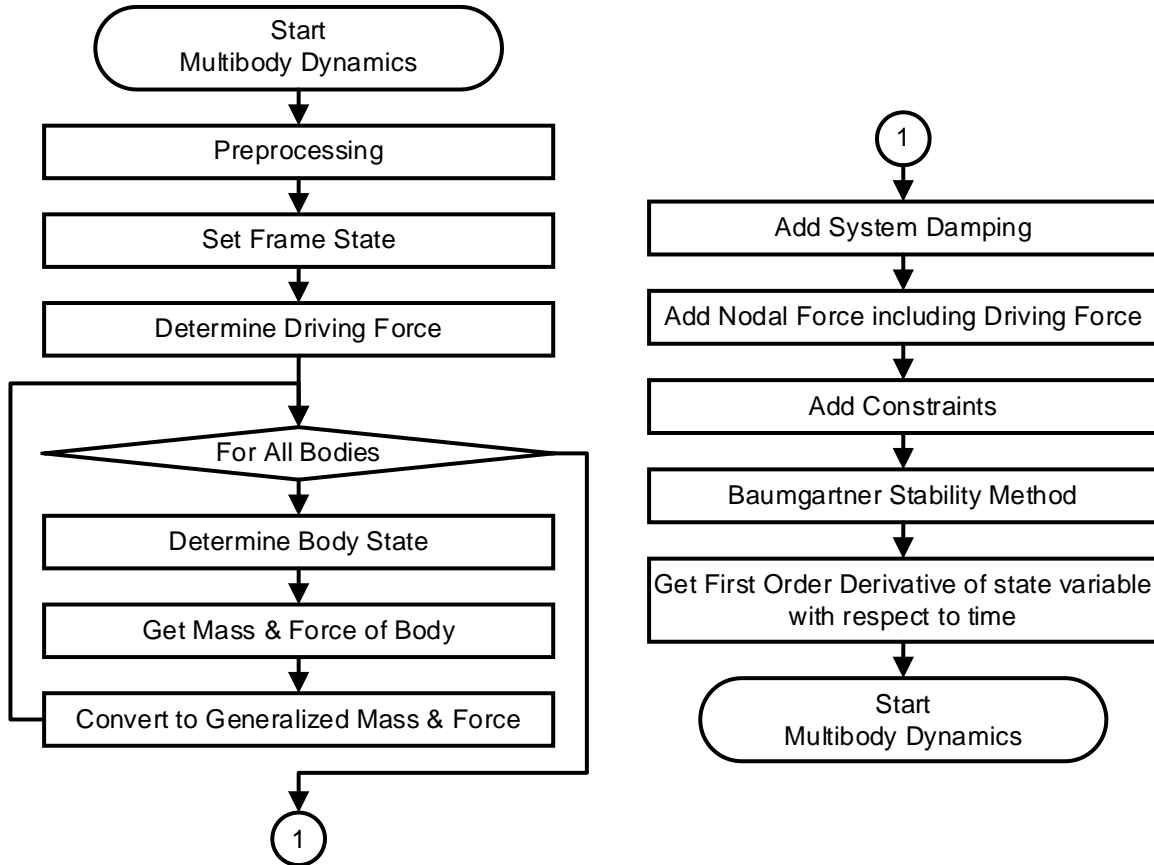


Figure 5-1: Flow Chart of Dynamics Calculation

5.1.2 Additional Modules and Auxiliary Modules

Dynamics System with Minimum Degree of Freedom

In addition to multi-body dynamics modeling for rigid-flexible hybrid models with large degrees of freedom, in this program some rigid-body minimum-degree-of-freedom models are also established such as folding boom system, multi-degree-of-freedom pendulum models, etc.

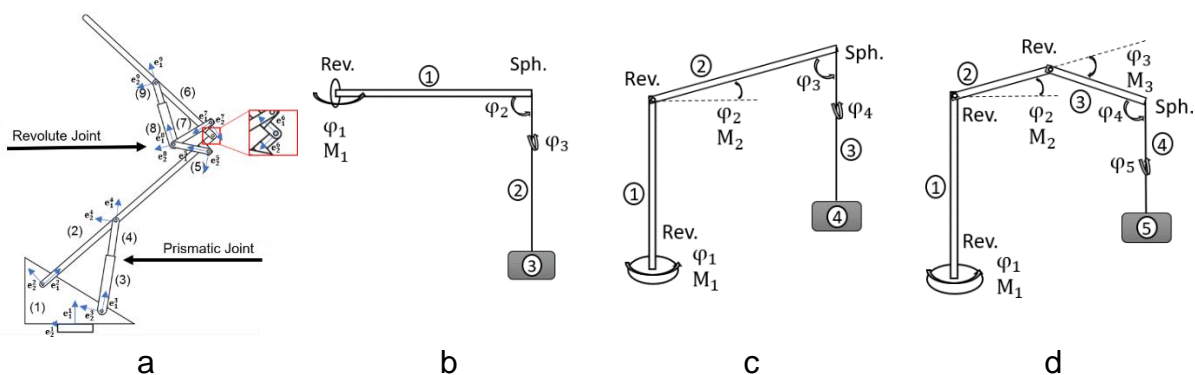


Figure 5-2: Rigid-body Minimum-Degree-of-Freedom Models a) Folding Boom System b) Single Jib Pendulum c) Double Jib Pendulum d) Triple Jib Pendulum

Hydraulic System Module

Many mechanism models need to be driven by hydraulic systems. In this program, models of hydraulic cylinder, throttle valve, back pressure valve, reversing valve, and ideal hydraulic pump with compressible fluid are established, and overall hydraulic systems with different hydraulic connections is built. The co-simulation logic of hydraulic system and mechanism dynamics system is shown as follows

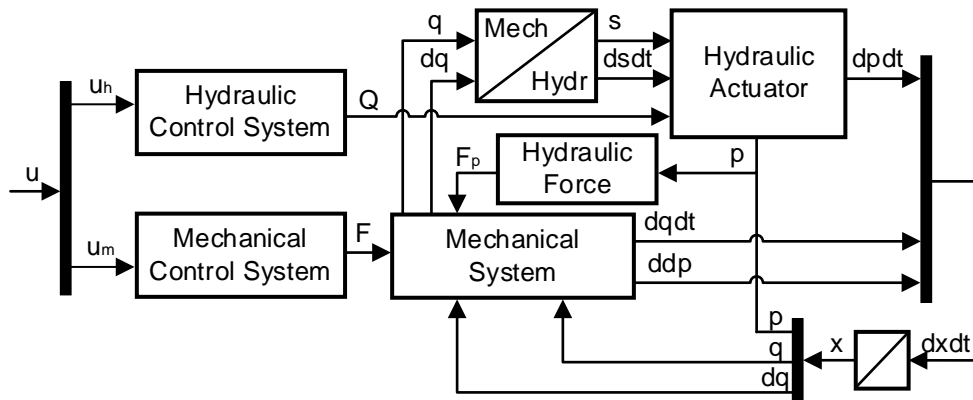


Figure 5-3: Co-Simulation Logic of Hydraulic System and Mechanism Dynamics System

Since the lattice boom crane model does not involve the hydraulic model, the hydraulic system is not explained in detail here.

Deep Reinforcement Learning based Optimal Control Module

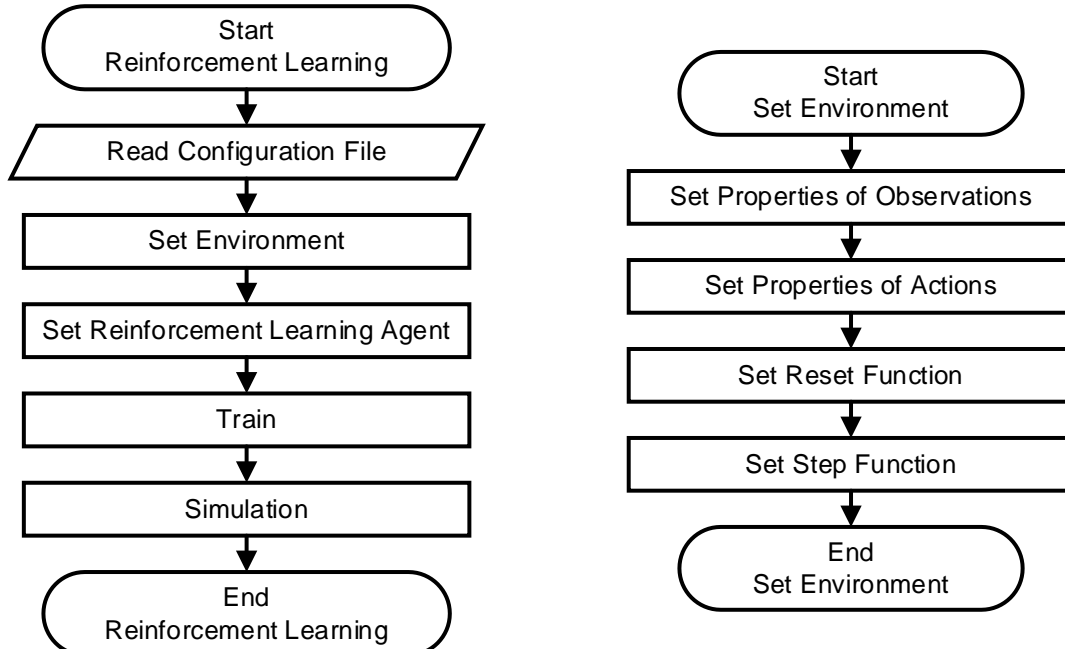


Figure 5-4: Deep Reinforcement Learning Framework for Optimal Control based on the Multi-body Dynamics Model

In this program a deep reinforcement learning framework for optimal control based on the multi-body dynamics model is created. For dynamic systems, the observations are generally continuous, and the action can be continuous or discrete according to actual needs. The agent of reinforcement learning needs to be selected according to the attributes of the observations and the actions. The reset function will reset the observations to the initial state or initial equilibrium state of the mechanism, and the step function will get the observation value at the next sampling time through the ODE solver of the dynamic model.

Nonlinear Model Predictive Control Module

This program embeds “mpctools” developed by Rawlings Group for nonlinear MPC control. The expansion package is based on the CasADi symbolic calculation. The research and development of this module is not the focus of this article, so that it will not be discussed here.

Model Recognition Module

This program also has an interface for model recognition. At present, only sparse identification of non-linear dynamics model has been established, and other model identification methods are still under study.

5.2 Data Input and Parameter Setting

This program realizes the separation of data and code for basic functions. According to the configuration Excel file, the program can perform calculations for different operations on different models. The current complete parameter modules are divided into two categories: dynamics model parameters and solving parameters.

5.2.1 Parameters for Dynamics Model

Almost all the rigid-flexible hybrid dynamics models here are created through multi-body dynamic model, which includes body parameters, joint parameters, constraints, and external nodal force parameters. In addition, the initial state of the mechanism and plot configuration is defined in the Excel file.

The minimum degree of freedom model can also call the body parameters, external nodal force parameters and display parameters in the configuration file. The parameters are shown as follows

Table 5-1: Parameters for Dynamics Model

	Parameter	Content
Body Parameter	Body Type	Model Type, Number of Degrees of Freedom, Section Type
	Material Properties	Density, Elastic Modulus, Poisson's ratio
	Length of Beam	Beam Length
	Section Size	(Round Tube) Outer Diameter, Inner Diameter (Frame) Length, Width, Thickness (Customized) Area, Moment of Inertia, Quality, Centroid position
Joint Configuration	Joint Quantity	Joint Quantity
	Single Joint	Joint Position, Joint Posture
Constraint	Constraint Quantity	Constraint Quantity
	Single Constraint	Number of Body 1 and 2, Number of Joint 1 and 2, Constraint Type
Initial State		Position, Posture, Other Initial State
Nodal Force	Force Quantity	Force Quantity
	Single Force	Number of Body, Number of Joint, Fx, Fy, Fz, Coordinate
	Single Moment	Number of Body, Number of Joint, Mx, My, Mz, Coordinate
Plot Parameter		Joint Sequence, Interpolation Number, Plot Configuration

5.2.2 Parameters for Solving Route

The solving route can be set in the configuration file, including global gravity, statics and dynamics parameters, result saving and post-processing methods.

Table 5-2: Parameters for Solving Route

	Parameter	Content
Gravity		Direction, Magnitude
Jacobian Matrix		Do Calculation Jacobian Matrix
Static Position	Manipulate	Do Calculation Static Position, Start from Static Position
	Nonlinear solver	Algorithm, Step Tolerance, Function Tolerance, Max Iterations
ODE	ODE Solver	Solver Name, Solver Method, Order, Option
Setting	Solving Parameter	Start/End Time, Absolute/Relative Tolerance, Max Step
Display by Computing	Time Display	Do Display, Display Interval, Display Start Position
Result	Mechanism Display	Do Display, Display Interval, Display Start Position
		Do Save Result, Existence, Saving Dictionary
Plot Configuration		Axes Size, Grid Configuration, Observation View
Postprocessing		Postprocessing Method

Currently, only the above parameters can be modified through the configuration file. The driving function, dynamics preprocessing function, additional system configuration and other parameters still need to be modified in the program.

5.3 Display and Analysis of Result

The post-processing of the final results can make it more intuitively to understand the entire dynamic process and simply to analyze the results. In this program, there are video generation function and general post-processing methods for specified experimental groups.

5.3.1 Video Generation

When the mechanism is complicated, generating the state diagram of each time step is a relatively time-consuming process, and it is not easy to repeat. Therefore, in this program, it can be chosen to save the generated results as a video. The display speed of the video can be consistent with the real calculation speed or proportional faster or proportional slower, so that the real dynamic response of the mechanism can be directly observed.

5.3.2 Specified Analysis Method

According to commonly used experiments, some general post-processing methods are designed. These standard experiments include the vibration of single beam, static bending of single beam, etc. The display of strain and stress within the mechanism is still under study.

6 Optimal Control of Lattice Boom Crane

6.1 Quasi-Static Optimal Trajectory Tracking Strategy

The lattice boom crane model is a complex rigid-flexible model with large degrees of freedom, which makes it difficult to meet the control requirement through the commonly used optimal control methods. However, because the movement of the lattice boom crane is realized by changing length of the luffing rope and hoisting rope, quasi-static optimal control algorithm can be used. This method combines the optimal trajectory of end point with the control variables through the quasi-static mapping relationship. The generated control trajectory can track the optimal trajectory of the end point, thereby achieving optimal control of complex systems. The specific implementation process is shown as follows

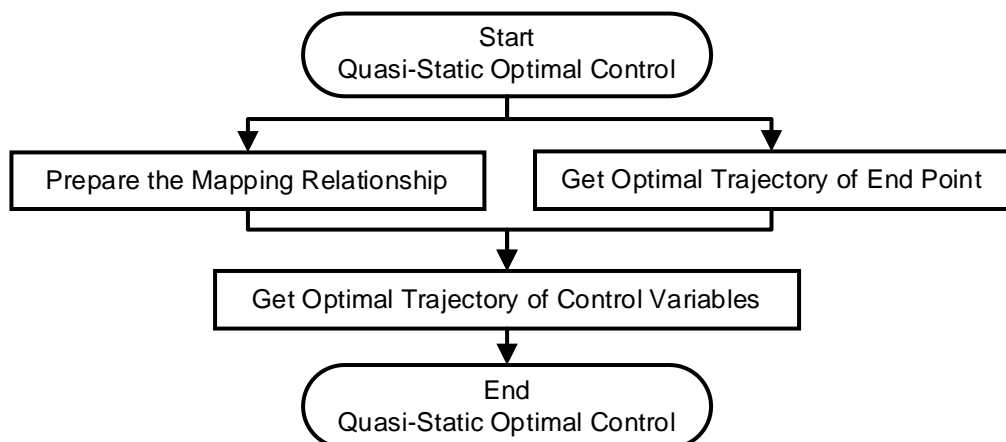


Figure 6-1: Quasi-Static Optimal Trajectory Tracking Strategy

The quasi-static optimal control method is mainly divided into three modules: the establishment of a static mapping relationship, the generation of the optimal trajectory at the end point and the generation of the optimal control trajectory.

6.2 Static State Mapping

To establish the static mapping relationship, it is required to calculate the relationship between the control variable and the control object (position of the end point) under all possible static states.

Since the dynamics system is continuous, calculating relationship of all possible positions is not realizable. Here some discrete states are selected and the mapping relationship is obtained by fitting. The detailed process is shown as follows

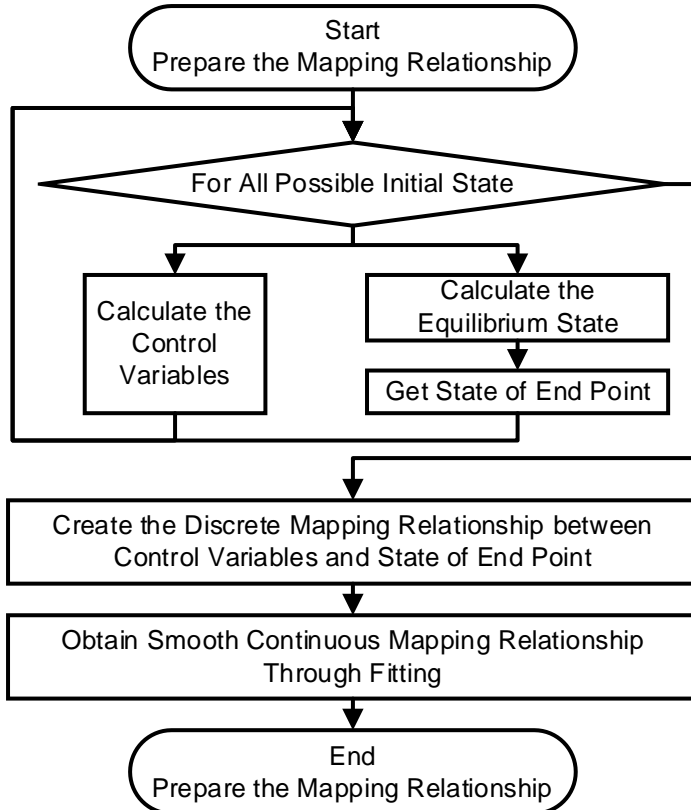


Figure 6-2: *Static State Mapping*

During the movement of the lattice boom crane, only the length of the luffing rope and the rope is changed. The change in the length of the luffing rope is reflected in the change in the angle of the main boom. In order to simplify the calculation of the state, the angle of the main boom and the change in the length of the luffing rope are taken as the characteristic state variables of the lattice boom crane.

Here the main boom angle is taken every 1 degree from 45 degrees to 85 degrees, the lifting rope length change is taken every 1m from 0m to 20m. The calculated control variables are the length of the luffing rope and the lifting rope in the initial state before deformation. The coordinates of the end point in the equilibrium state are calculated as the control object. The final experimental results can generate a discrete mapping table, which is shown as follows

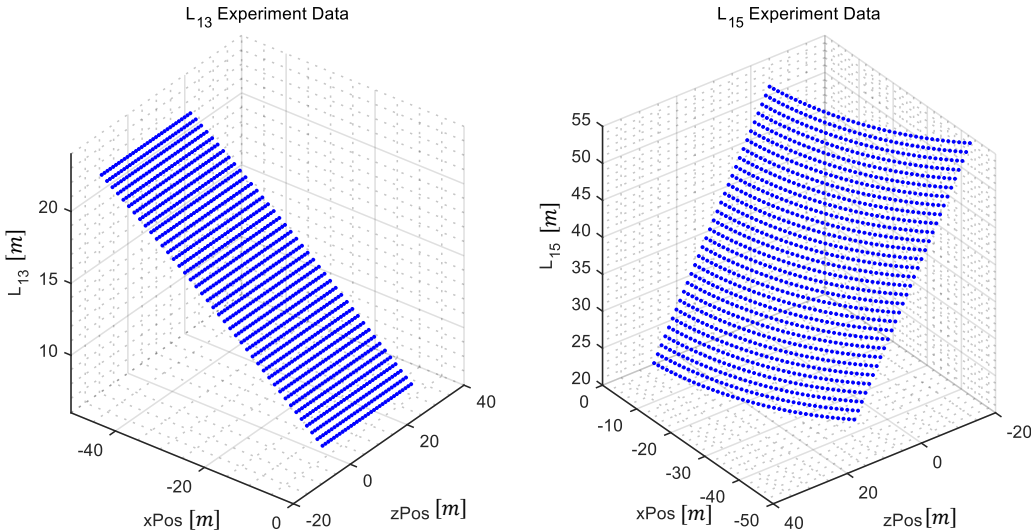


Figure 6-3: Discrete Experimental Data from Statics Calculation

In order to obtain a continuous mapping relationship, surface fitting needs to be performed on discrete data points. There are two forms of surface fitting: spline surface fitting and polynomial surface fitting.

The advantage of spline surface fitting is that its results are in good agreement with experimental data, but it is also very sensitive to experimental errors. Polynomial surface fitting can use different polynomial orders for the independent variables of each dimensions. Here only polynomial surfaces below the 5th order are supported. The fitting accuracy of the polynomial surface is not very high, but it can balance the error of the experimental data and make the fitted surface smoother and more continuous. According to the static experiment set, a polynomial surface of order 2-2 is sufficient and recommended.

6.3 NMPC for Optimal State Trajectory Generation

Discrete QR control is a commonly used optimal control method for planning the trajectory to a certain target point [Arn-2005]. QR control takes the time optimization and the minimum control cost into account. The cost function is composed of running cost and terminal cost [Cow-2006].

Terminal cost is a quadratic function of the difference between the state at the last moment and the target state. The running cost reflects two aspects, namely the difference between the current state and target state as well as the energy cost by applying

control system. The QR controller requires that all the coefficient matrix must be positive definite. The discrete QR optimal control problem can be written as

$$\begin{aligned} \min J(\underline{u}_0, \underline{u}_1, \dots, \underline{u}_{N-2}, \underline{u}_{N-1}) &= (\underline{x}_N - \underline{x}_e)^T \underline{\underline{P}}_{\text{end}} (\underline{x}_N - \underline{x}_e) \\ &\quad + \sum_{k=0}^{N-1} \left[(\underline{x}_k - \underline{x}_e)^T \underline{\underline{Q}} (\underline{x}_k - \underline{x}_e) + \underline{u}_k^T \underline{\underline{R}} \underline{u}_k \right] \\ \text{s. t. } & \underline{x}_{k+1} = \underline{f}_k(\underline{x}_k, \underline{u}_k, t_k) \\ & \underline{x}_{\min} \leq \underline{x}_k \leq \underline{x}_{\max}, \quad \underline{u}_{\min} \leq \underline{u}_k \leq \underline{u}_{\max} \\ & \underline{x}_0, \underline{x}_e \text{ known} \end{aligned} \quad (6-1)$$

The dynamic equation of discrete QR control requires a discrete iterative format. Here 4th order Runge-Kutta integrator is used to transfer the continuous state space equation into discrete state space equation.

Due to the large number of time steps in the entire simulation time, the calculation will consume a large amount of resource when considering all the time steps. Therefore, the concept of predictive horizon is proposed to calculate the optimal control variable only considering limit amount of time steps. The cost function, which is used to calculate the optimal control variable at time step m with the consideration of h steps from current time can be written as

$$\begin{aligned} \min J_m(\underline{x}_m, \underline{u}_m, \underline{u}_{m+1}, \dots, \underline{u}_{m+h-2}, \underline{u}_{m+h-1}) &= (\underline{x}_{m+h} - \underline{x}_e)^T \underline{\underline{P}}_{\text{end}} (\underline{x}_{m+h} - \underline{x}_e) \\ &\quad + \sum_{k=m}^{m+h-1} \left[(\underline{x}_k - \underline{x}_e)^T \underline{\underline{Q}} (\underline{x}_k - \underline{x}_e) + \underline{u}_k^T \underline{\underline{R}} \underline{u}_k \right], \forall m = 1, \dots, N \end{aligned} \quad (6-2)$$

The unconstrained optimal control solution can be obtained by

$$\frac{\partial J_m}{\partial \underline{u}_k} = \underline{0} \rightarrow \underline{u}_k^*, \forall k = m, \dots, (m+h-1) \quad (6-3)$$

When the control variable is constrained, the optimal solution obtained by the above formula does not necessarily satisfy the feasible range of the control variable. The optimal condition changes from a partial derivative of 0 to taking the minimum value in this range. When the cost function has no local minimum relative to the control variable, the optimal control variable with constraints can often be obtained on the constraint boundary [Lim-1999].

$$\min_{\underline{u}_m, \underline{u}_{m+1}, \dots, \underline{u}_{m+h-2}, \underline{u}_{m+h-1}} J_m = J_m(\underline{x}_m, \underline{u}_m^*, \underline{u}_{m+1}^*, \dots, \underline{u}_{m+h-2}^*, \underline{u}_{m+h-1}^*)$$

$$u_{k,i}^* = \begin{cases} u_{i,\min}, & x < u_{i,\min} \\ u_{k,i}^*, & u_{i,\min} \leq u_{k,i}^* \leq u_{i,\max} \\ u_{i,\max}, & x > u_{i,\max} \end{cases} \quad (6-4)$$

For the above prediction window, only the optimal control variable \underline{u}_m^* at the start time of the prediction window is taken as the optimal solution at that moment.

6.4 Generation of Optimal Control Trajectory

Through the optimal trajectory of end point and the mapping relationship, the optimal control trajectory can be obtained. However, since the optimal trajectory of the end obtained from NMPC is discrete, the optimal control trajectory after mapping is also discrete. It is necessary to convert the discrete control trajectory into a continuous optimal trajectory for dynamics calculation. The specific process is as follows

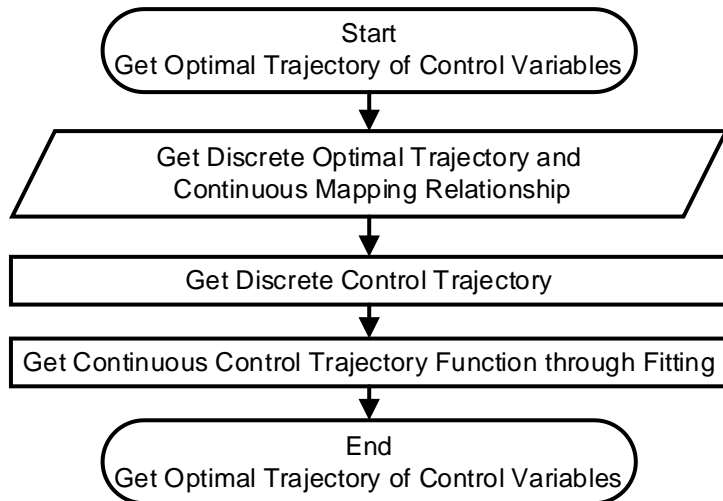


Figure 6-4: Generation of Optimal Control Trajectory

Because in this model rope length is used as the control variable, it is required that the change rate of the control variable with time is 0 in the initial and end stages. In order to obtain a continuous function that meets the requirements and reduce the error from the discrete data, the generated discrete control trajectory will be resampled, and add 5 steady-state control points will be added before and after the curve. The spline curve will be used for the fitting of the optimal control trajectory.

7 Detailed Modeling of Lattice Boom Crane

This lattice boom crane consists of a main boom, a derrick boom, a luffing cable module, a sub-cable, a hoist cable and load. The model is created using rigid-flexible multi-body dynamics method.

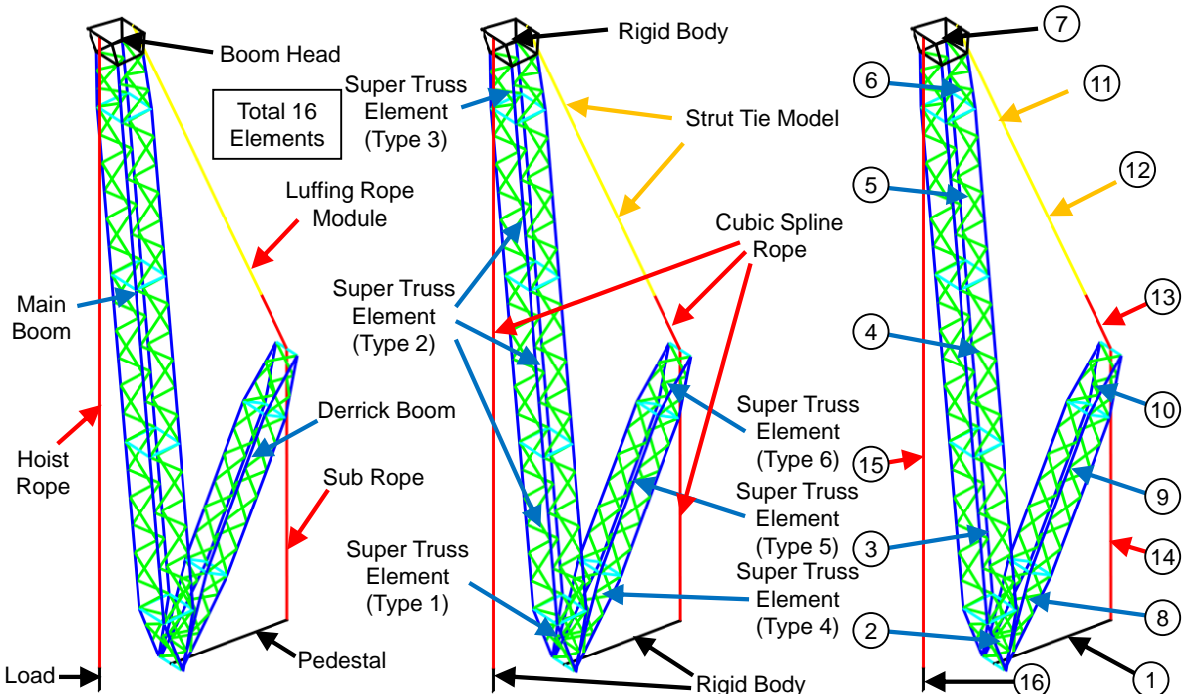


Figure 7-1: The Composition, Model Types of Elements and the number of the Elements of the Lattice Boom Crane

7.1 Lattice Boom

The lattice boom crane described here is composed of two lattice booms: the main boom and the derrick boom.

7.1.1 Main Boom

The main boom is composed of 227 beam elements. The main boom has 1362 degrees of freedom and requires 2724 state variables by using classical multi-body dynamics modeling method. Even if the fixed connections between these beam elements are considered and part of the redundant degrees of freedom is eliminated, the main boom still has 672 degrees of freedom and 1344 state variables, which also needs a lot of calculations by solving dynamics equation. In the actual situation, the truss boom

will be composed of some standard truss elements, so the super truss elements are used to model these standard truss elements. The main boom is divided into 5 super truss elements, and in 3 different types.

After using the super truss element and the elimination of the redundant degrees of freedom caused by the fixed constraints, the degree of freedom of the main boom becomes 36, and it needs 72 state variables (reduced by 97.4% and 94.6%). However, because the super truss element needs to estimate the internal nodes of the truss through the assumption of geometric continuity, the amount of calculation in single-step is increased from 227 to 339 (increased by 49.3%).

Table 7-1: Properties of different Types of Super Truss Elements

	Type 1	Type 2	Type 3
Structure			
Type	Triangular Prism	Rectangle	Shrink Rectangle
	Type 4	Type 5	Type 6
Structure			
Type	Triangular Prism	Rectangle	Anti Triangular Prism

In addition, because the shape of the boom head is complex and the size is smaller than other truss elements, the deformation of the boom head is not considered and it is treated as a rigid body.

7.1.2 Derrick Boom

The derrick boom is composed of 126 beam elements. The derrick boom has 756 degrees of freedom and requires 1512 state variables by using classical multi-body dynamics modeling method. The degrees of freedom will be reduced to 384 and state variables will be decreased to 768 after eliminating redundant degrees of freedom caused by fixed constraints. Here 3 different types of super truss elements are established for the derrick boom.

The degree of freedom of the derrick boom becomes 24, requiring 48 state variables after applying super truss elements (reduced by 96.8% and 93.8%). The amount of calculation in single-step is increased from 126 to 190 (increased by 50.8%).

7.2 Rope and Rope Systems

7.2.1 Rope Model

The rope can be regarded as a kind of beam with special stress properties: the bending and torsional stiffness are very small and is often ignored. Generally, the rope is not subject to pressure, so only the tensile stress is considered. Therefore, the virtual power of the internal force can be written as

$$\delta p_{\text{int}} = - \iiint_V \delta_B \dot{\varepsilon}_{xx} \max(B \sigma_{xx}, 0) dV \quad (7-1)$$

The rope model can be created through cubic spline beam, strut tie model or Timoshenko beam model. In order to meet the geometric continuity and smoothness under the absolute coordinate system, the rope model here will be established based on cubic spline beam.

7.2.2 Rope System

The lattice boom crane contains 3 rope systems: luffing rope module, hoisting rope and sub-rope. According to the actual model, the luffing rope module consists of two strut tie models and one rope element. The hoisting rope and the sub-rope each consist of one cubic spline rope model.

7.3 Pedestal and Load

Generally, in addition to the plane freedom provided by the hoisting rope and luffing rope, the entire boom system can also rotate along the vertical direction. Here the boom system is built on a pedestal, and will rotate with the pedestal relative to the inertial coordinate system. The rigidity of the pedestal is always relatively large and the deformation is relatively stable. Therefore, here a rigid body model is used to simulate the pedestal.

Since the sway of the load is also one of the research directions of lattice boom cranes, in this model a small rigid body is added at the end of the hoisting rope to simulate the

load. The position and posture of the load during the moving of the lattice boom crane will be studied.

In summary, the entire lattice boom crane has 168 degrees of freedom and 336 state variables before simplification through constraints. The detailed parameters of all the model can be seen in the appendix.

7.4 Constraints and Drives

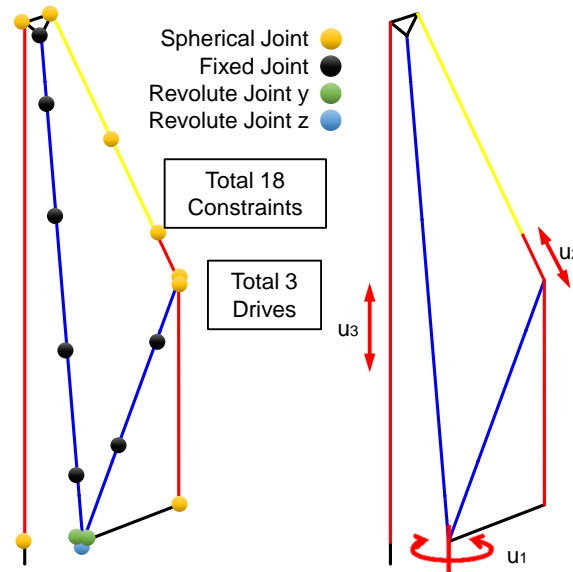


Figure 7-2: Locations and Types of Constraints and Drive Configuration displayed on the Calculation Model

7.4.1 Constraints

The lattice boom crane has original totally 18 constraints. The locations and types of these constraints are shown as follows

Table 7-2: Locations and Types of Constraints for Lattice Boom Crane

Type	Quantity	Redundant DoF	Relevant Elements (Elements Nr1/ Elements Nr2)
Fixed	7(-6)	Each 6	2/3, 3/4, 4/5, 5/6, 6/7, 8/9, 9/10
Revolute-z	1	Each 5	0/1
Revolute-y	2	Each 5	1/2, 1/8
Spherical	8(-4)	Each 3	7/11, 11/12, 12/13, 13/10, 1/14, 10/14, 7/15, 15/16

Among them, the 6 fixed constraints connecting the super truss elements can be realized by using public computing nodes, which can reduce the overall degree of freedom

by 36. Using same method, the spherical constraints in the rope model can also be eliminated, which can reduce the overall degree of freedom by 12. The final lattice boom crane model has 120 degrees of freedom, 240 state variables and 8 constraints.

7.4.2 Drives

In reality, the lattice boom crane is controlled through the hydraulic motor to change the length of hoisting and luffing rope. The overall rotation of the crane is also realized by the hydraulic motor. However, due to the complexity of the pulley rope model and the hydraulic system, these systems are not considered in this model. Here the angle of the pedestal and the length of the hoisting rope and the luffing rope are directly set to control variables.

Table 7-3: Definition of Control Variables for Lattice Crane Model

Control Variable	Unit	Description
u_1	rad	The z-axis relative rotation angle of Pedestal (Element 1)
u_2	m	The length of luffing rope model (Element 13)
u_3	m	The length of hoisting rope model (Element 15)

Because the change of the rope element length affects the Gaussian integral and the calculation of stress and strain, the influence of the control variable on the system is very complicated, and it is almost impossible to separate the control variable from the state variable. In addition, the model of lattice boom crane is too complicated, and it is difficult to implement many controllers that use symbolic calculations, which makes it difficult for classical non-linear optimal control methods. Therefore, the quasi-static control method is carried out to generate offline optimal control strategy for the lattice boom crane.

8 Analysis and Evaluation of Simulation Results

8.1 Cross-validation of Single Flexible Beam Element

A cross-validation method is used in order to verify the accuracy of the flexible beam model. The beams with the same parameters are modeled with multi-segment Timoshenko beams and cubic spline beams. A number of experimental scenarios are designed to judge the accuracy of the model through the model response. The parameters of the beams used in the experiment are shown as

Tabelle 8-1: Parameters of Single Beam

		Cubic Spline Beam Model				Timoshenko Beam Model								
		Model Type	Cubic Spline Beam (C-Beam)			Timoshenko Beam (T-Beam)								
Beam Type	Segment Quantity	1	3	5	10	1	3	5	10					
	Degrees of Freedom	14			12									
Material properties	Density	7800												
	Elastic Modulus	206000000000												
	Poisson's ratio	0.25												
Length of Beam		15												
Section size	Section Type	Round Tube												
	Outer Diameter	0.15												
	Inner Diameter	0												

8.1.1 Cantilever Beam Static Bending Test

The statics tests are set to verify the internal force of the beams. Since the bending deformation is the main deformation form of the beam, a moment is added to the non-fixed end of the cantilever beam. The relationship between the bending curvature of the beams and the external moment can be approximated by

$$M = EI\kappa = KM_{\text{circle}} \quad M_{\text{circle}} = 2\pi EI/L \quad K = M_{\text{max}}/M_{\text{circle}} \quad (8-1)$$

where M is the external moment applied to the end of the cantilever beam, M_{circle} represents the theoretical moment required to bend the beam into a circle, and $K \in [0,1]$ represents the ratio coefficient between the maximum torque M_{max} and M_{circle} . EI represents the bending stiffness of the bar section, L represents the length of the bar, and κ represents the curvature of the bar. The experimental results are as follows

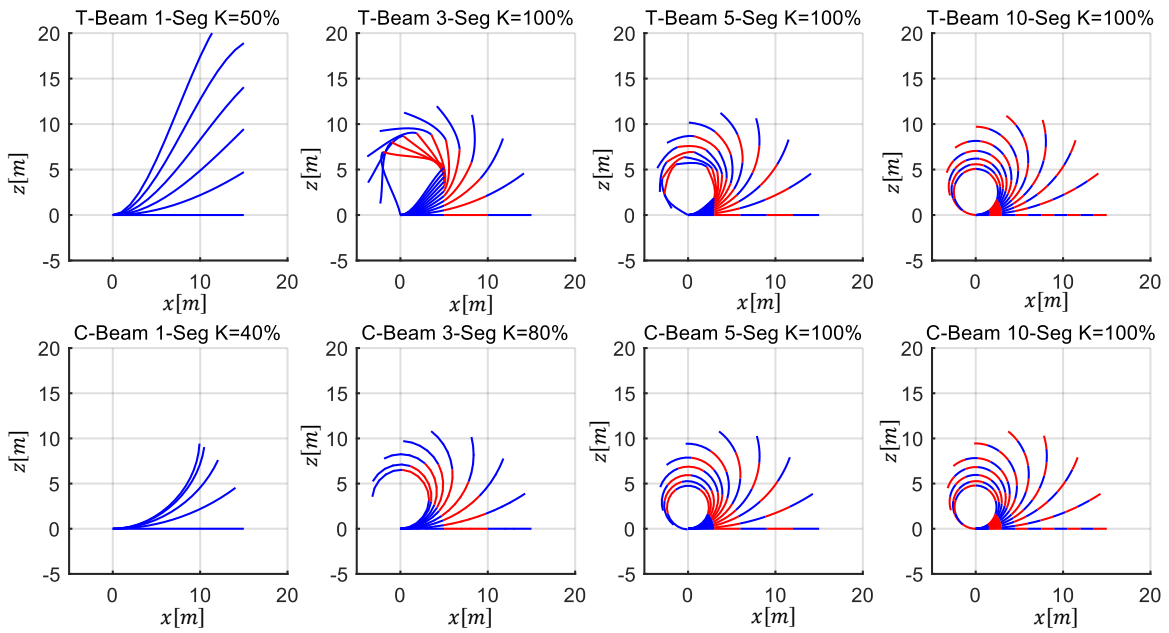


Figure 8-1: Cantilever Beam Static Bending Test

Due to the assumption of small deformation, the stiffness of the single T-beam will become smaller and the geometric continuity of the connection of each section will be lost under large deformation. Therefore, it is suggested the deformation of the T-beam should not exceed 15 degrees. The deformation of single C-beam can be slightly larger, but due to the monotonicity of the cardan angle by small rotation, the deformation cannot exceed 90 degrees. The C-beam model can maintain the geometric continuity of the entire beam.

8.1.2 Vibration Test of Cantilever Beam under Self-gravity

The undeformed flexible beam will vibrate under gravity. The amplitude of the vibration can be used to verify the gravity effect. The vibration frequency can verify the relationship between the mass matrix and the force vector.

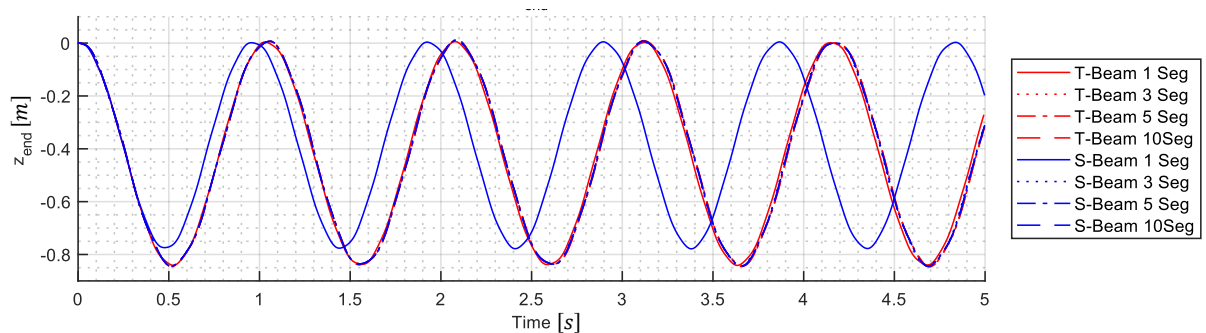


Figure 8-2: Vibration Test of Cantilever Beam under Self-gravity

In the above figure, the end displacement perpendicular to the beam axis over time is shown. The maximum deformation in z-direction is near to 0.85 meter, and the amplitude of the vibration is almost 0.42 meter. The waveform is basically symmetrical along the vertical axis of 0.42 meter. The other experimental results are relatively close except the cubic spline beam with one segment. Using the cubic spline beam with one segment the effect of gravity decreases and the frequency of vibration increases. Therefore, it is generally recommended to use at least 2 segments of cubic spline beam under small deformations.

8.1.3 Fixed Axis Rotation under Torque Control and Angle Control

Torque Control

The beams in this experiment are hinged at one end. The revolute constraint allows the beam to rotate around a fixed axis (y-axis). A constant torque (10^6) is applied to the free end to accelerated the rotation of the beam. In this experiment, the z-direction displacement at the end of the beam is measured, and the motion under different numerical integration accuracy is studied.

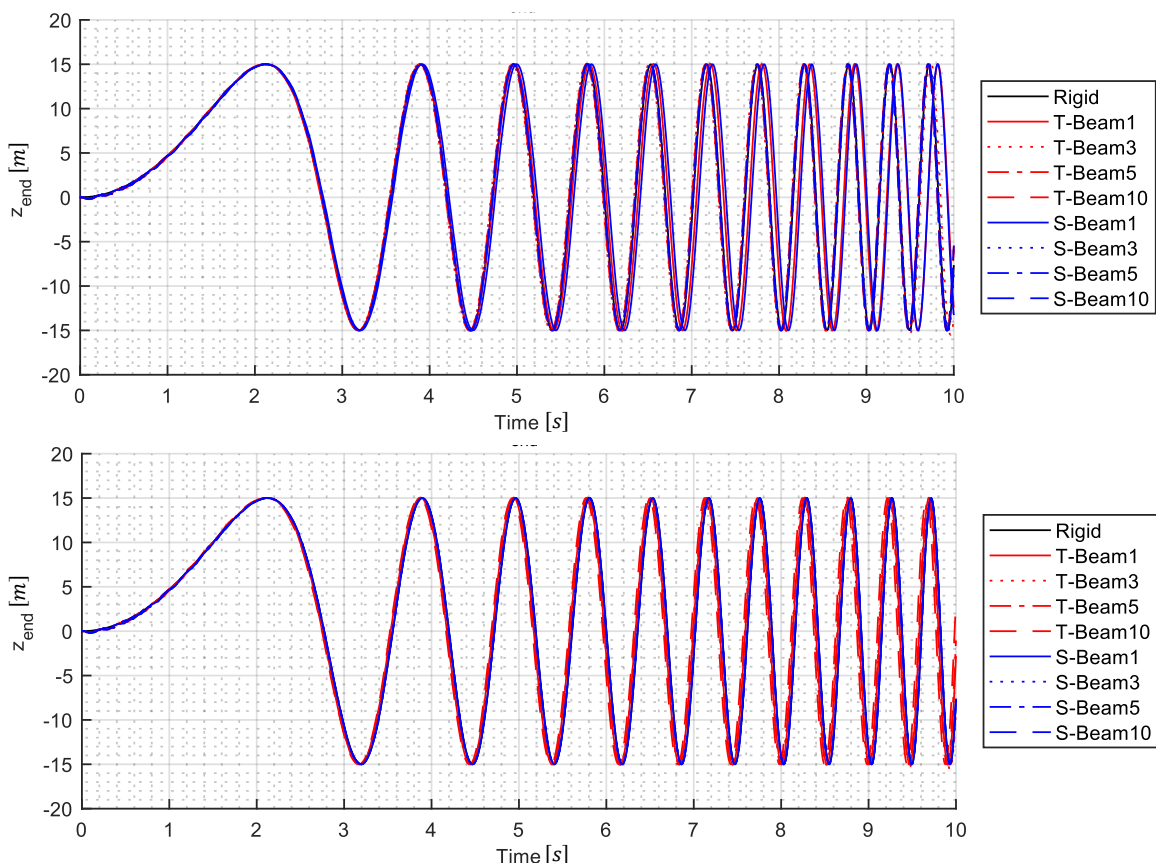


Figure 8-3: Fixed Axis Rotation under Torque Control

The maximum average rotation speed in this experiment reached nearly 120 rounds per minute. The flexible deformation is relatively small relative to the rigid rotation. Both Timoshenko beam and cubic spline beam can have better accuracy in slow rigid velocity. But the cumulative error becomes large due to calculation accuracy when the number of segments is small and the rigid body moves faster. In addition, the Timoshenko beam has a slight hysteresis when it rotates at high speed.

Angle Control

Angle drive refers to the rotation of the fixed end of the cantilever beam around a certain axis (y-axis) according to a drive function. In this experiment, a cos-function is designed to simulate the situation where the beam rotates to a certain angle and then returns to the origin. The expression of the cos-function can be written as

$$\psi = -\frac{\pi}{4} \left[1 - \cos \left(\frac{\pi}{5} t \right) \right] \quad \dot{\psi} = -\frac{\pi^2}{20} \sin \left(\frac{\pi}{5} t \right) \quad (8-2)$$

The result is as follows

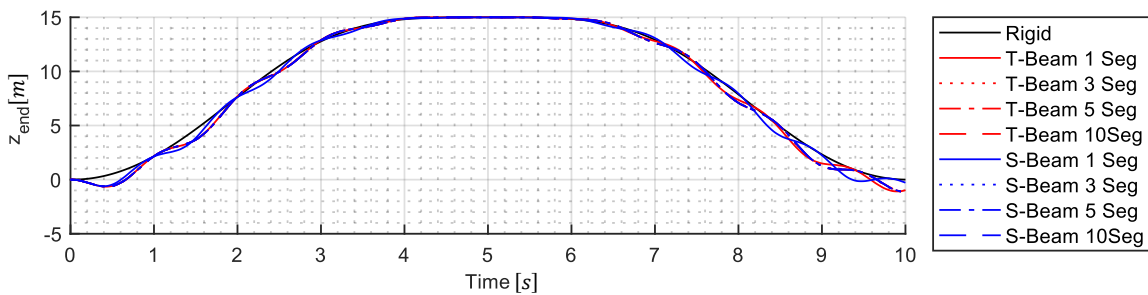


Figure 8-4: Fixed Axis Rotation under Angle Control

It can be seen from the results that the beam elements have a flexible vibration part on the basis of the original rigid motion, which is caused by the unbalance of the initial state and the acceleration step of the driving function. The results of different models are very similar except the cubic spline beam with one segment. In addition, there is a slight hysteresis in the Timoshenko beam with one segment.

8.2 Simulation for Single Super Truss Element

The structure of the truss is diverse, and its dynamic response is also different. Here super truss element in type 2 is selected as the research object.

8.2.1 Vibration Test of Cantilever Truss Boom under Self-gravity

The vibration of the super truss element under self-gravity is shown as follows

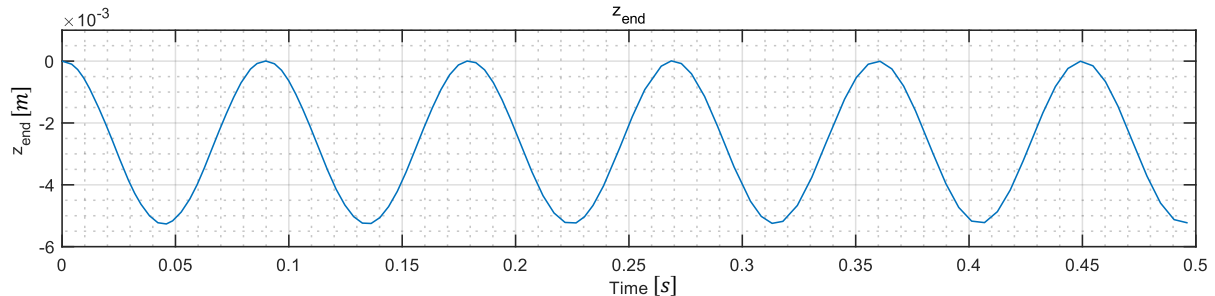


Figure 8-5: Vibration Test of Cantilever Truss Boom under Self-gravity

The super truss element under self-gravity has a similar dynamics response to the continuous flexible beam. Because the truss has a more optimal structure, the deformation under self-gravity is smaller.

8.2.2 Fixed Axis Rotation under Torque Control and Angle Control

Torque Control

Under the constant end torque (10^6), the dynamic response of the super truss element with revolute constraint is shown as follows

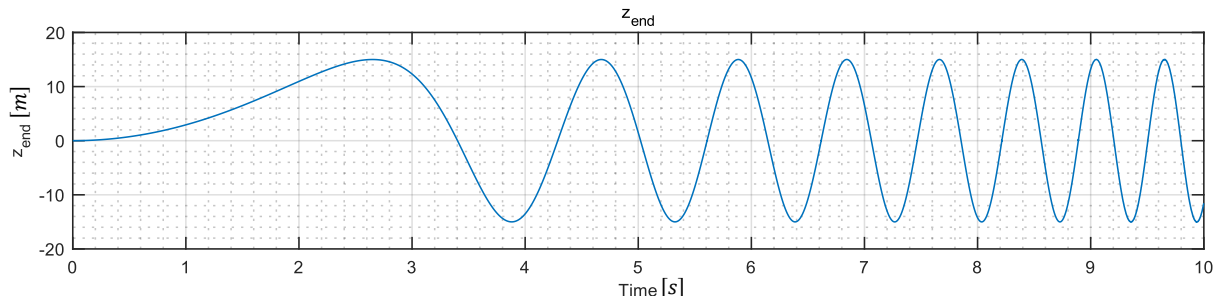


Figure 8-6: Super Truss Element Fixed Axis Rotation under Torque Control

The experimental result curve is similar to the curve of continuous beam curve, so a simplified model can be considered to simulate the rotation of the truss. And because the flexible deformation is relatively small compared to this large rotation, it can even be replaced by a rigid body model.

Angle Control

The cos- function above is used as angle drive function, and its dynamic response is shown as follows

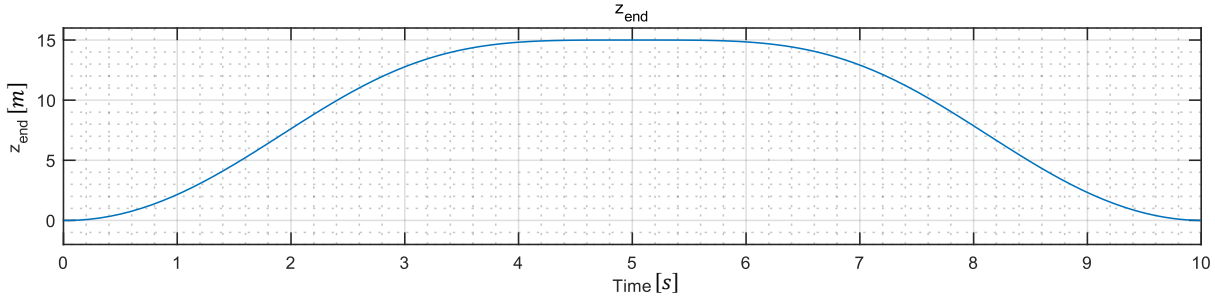


Figure 8-7: Super Truss Element Fixed Axis Rotation under Angle Control

Due to the large stiffness of the lattice structure, the deformation caused by gravity and inertial force is smaller than the large displacement and large rotation.

8.2.3 Equivalent Stiffness and Mass

Equivalent Stiffness Test

If one end of the super truss element is fixed and apply force or torque is applied on the other end, the displacement of the free end can reflect the stiffness of the truss beam.

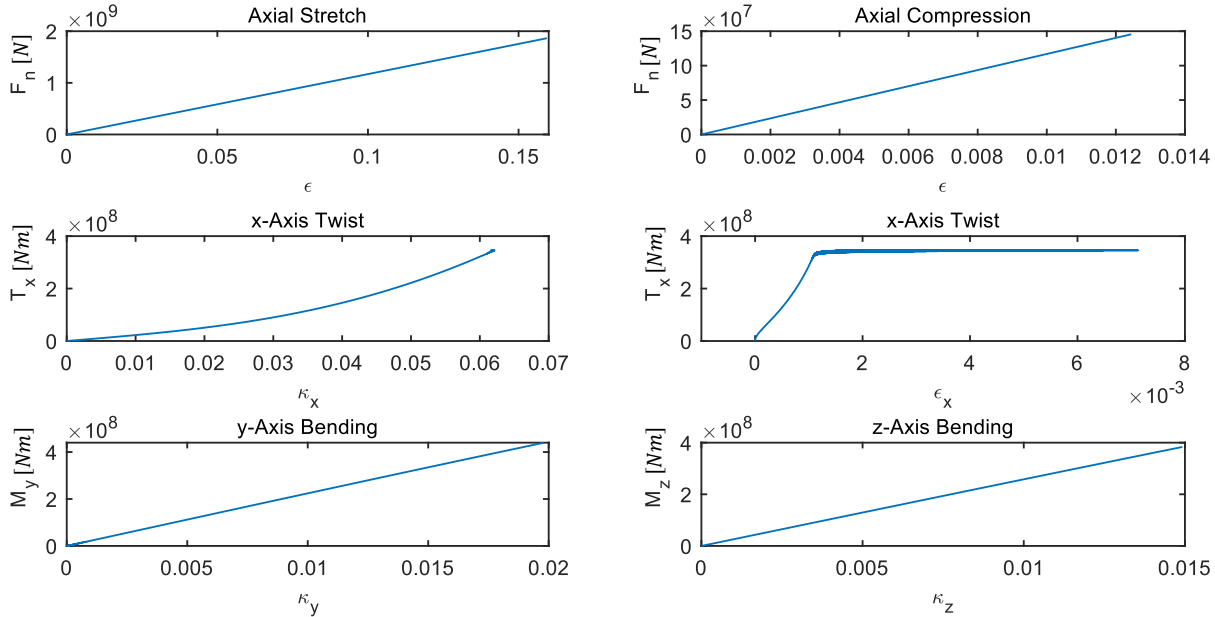


Figure 8-8: Super Truss Element Equivalent Stiffness Test

It can be seen from the curve that the stresses and strains by axial force and bending are linear. The torsion in the x-axis will cause the strain in the axial direction, which is caused by the main beam rotating around the axis of super truss element instead of its own axis. This also makes the equivalent torsional stiffness in x-axis of the truss not constant. The continuous beam model cannot express this phenomenon.

Equivalent Mass Test

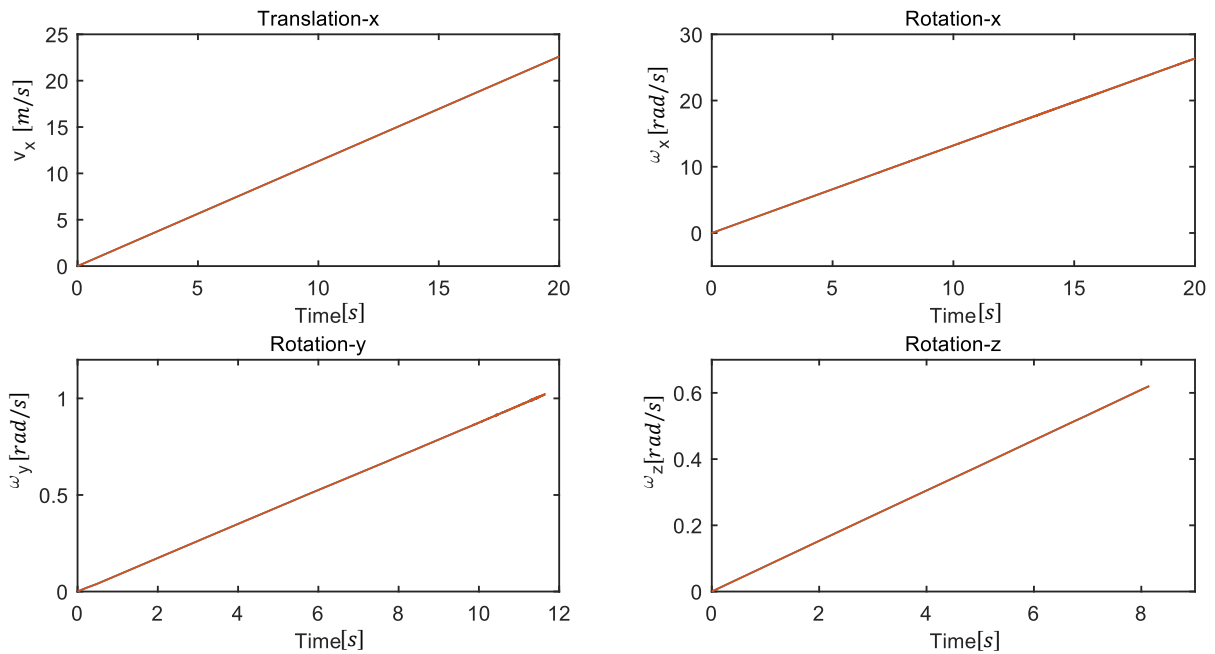


Figure 8-9: Super Truss Element Equivalent Mass Test

If the both end of the super truss element are set free and same force or torque is added on both ends. The velocity change of the super truss element can be used to determine the mass parameter. The angular velocity change can be seen as linear to time. However, only the translational velocity change in x-Axis is linear to time. In fact, due to the discontinuity and asymmetry of the truss, it is difficult to express the mass matrix of the truss through a continuous beam model. Especially for non-rectangular trusses, the determination of its equivalent mass will become very difficult.

8.3 Simulation for Lattice Boom Crane

8.3.1 Elementary Movement

In practice, the motions of the mobile cranes in the operation can be specified as three kinds, lifting, slewing, and luffing. The slewing means the boom system and the turn-table (super-structure) rotates along the vertical slewing axis. The luffing means to change the distance between the payload and the slewing axis by changing the elevation angle of the boom. In order to make the movement of the crane relatively stable, the crane will start from the equilibrium position. The driven function is a second-order smooth continuous function, which can be written as

$$s(t) = \begin{cases} 0, & t < 0 \\ \frac{1}{2}a_1 t^2, & 0 \leq t < t_1 \\ s_1 + v_{\max}(t - t_2), & t_1 \leq t < t_1 + t_2 \\ s_1 + v_{\max}(t - t_1) + \frac{1}{2}a_3(t - t_1 - t_2)^2, & t_1 \leq t < t_0 \\ s_0, & t_0 \leq t \end{cases} \quad (8-3)$$

$$s_1 = \frac{1}{2}a_1 t_1^2 \quad t_0 = t_1 + t_2 + t_3$$

$$a_1 = \frac{2s_0}{t_1(2t_0 - t_1 - t_3)} \quad a_3 = -\frac{2s_0}{t_3(2t_0 - t_1 - t_3)}$$

where t_0 represents the total movement time, t_1 represents the acceleration time, t_2 represents the time with constant speed, t_3 represents the deceleration time, and s_0 represents the total displacement.

The initial equilibrium state of the crane is set with a turning angle of 0 degrees, the original length of the luffing rope 7.0608m, and the original length of the hoisting rope 53.9937m.

Lifting Stage

The lifting stage requires the lifting rope to be shortened by 20m within 40s, including 5s acceleration time and 5s deceleration time. The result is as follows

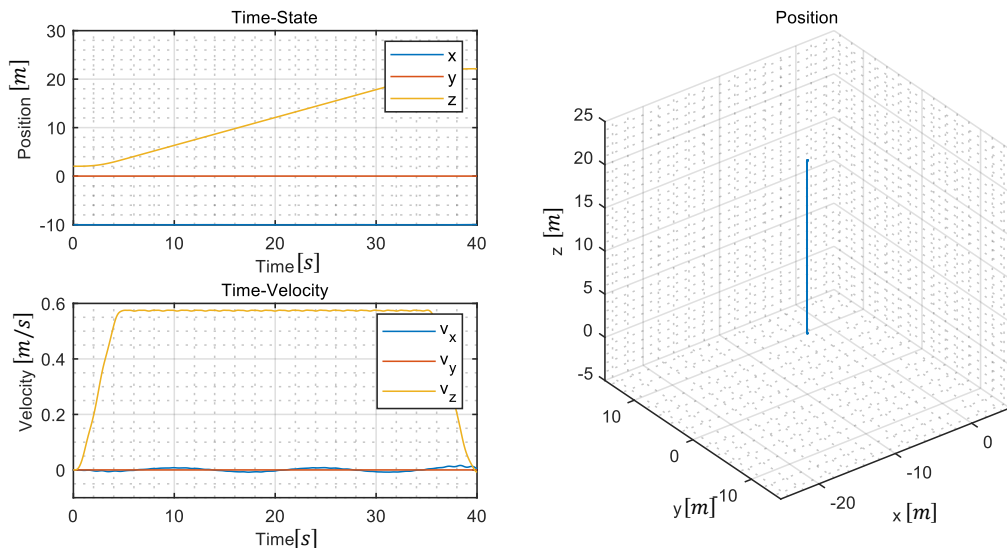


Figure 8-10: Position and Velocity of the Load by Lifting Stage of the Crane

It can be seen that the main movement trend is the lifting in the z-axis direction, and there is a small vibration of the crane in x-axis. The vibration in the z-axis is quite small,

with the vibration amplitude in the velocity curve is less than 0.05 meter per second. The vibration is caused by the reduction in the length of the lifting rope, which provides same pull force with less deformation.

The vibration in the x-axis is caused by the reduction in the mass of the lifting rope, which change the equilibrium position of the main boom. The main boom will slightly lift up and the x-position of the load will then change. The vibration will increase if the lifting speed increases. There is no vibration or movement in the y-axis, which means the lifting stage has no effect on the direction orthogonal to the crane plane.

Luffing Stage

In the luffing stage, the luffing rope extends 10m in 40s, with 5s acceleration time and 5s deceleration time.

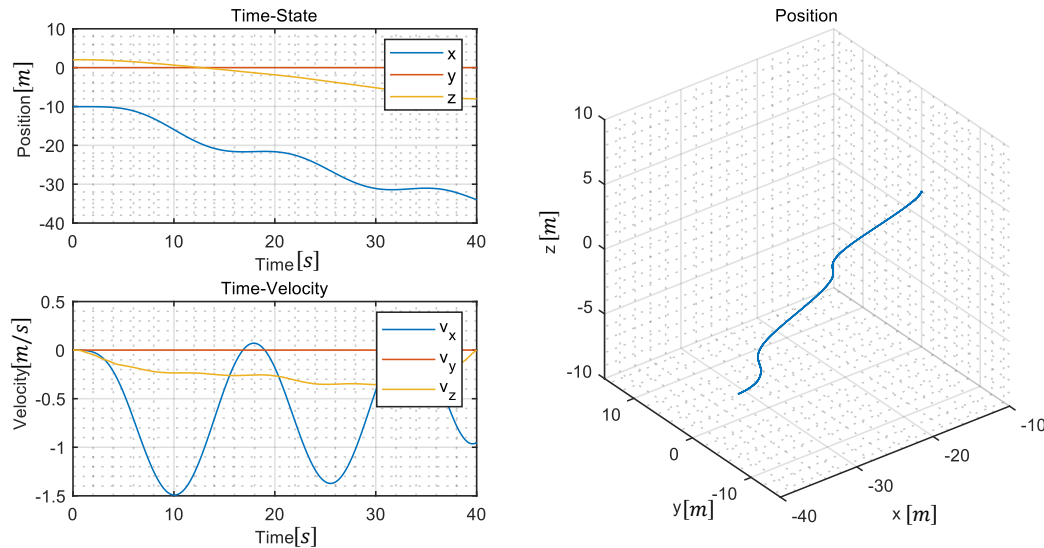


Figure 8-11: Position and Velocity of the Load by Luffing Stage of the Crane

It can be seen that luffing will cause the vibration, which is mainly caused by the sway of the load. The effect of flexible vibration of the crane is relatively small on the motion of the load. The small flexible vibration is due to the smoothness of the driving function and the large rigidity of the overall crane. In addition, due to the slow overall movement speed of the crane and the optimization of the truss boom structure, the inertia of the model has little influence.

However, the flexibility of the model caused the deviation of the mechanism state relative to the rigid body model. In order to reduce the away of the load, the change of the length of the luffing rope should not be too fast.

Slewing Stage

During the slewing stage, the crane will rotate 90 degrees along z-axis within 40s, with 5s acceleration time and 5s deceleration time. The result is as follows

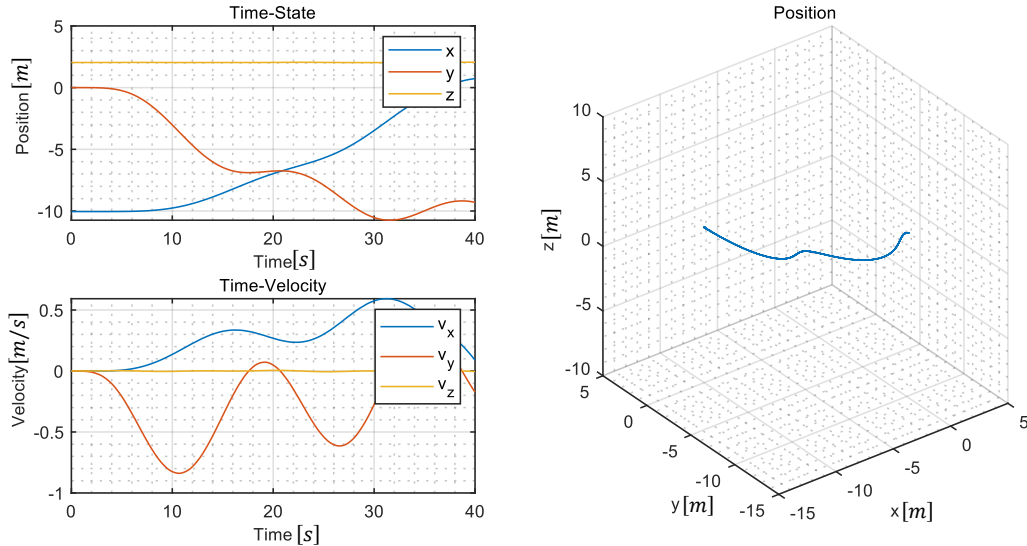


Figure 8-12: Position and Velocity of the Load by Slewing Stage of the Crane

From the result, the vibration in the x- and y-axis is most obvious. The vibration frequency in both x- and y-axis is almost 15 seconds, which is the pendulum period with the rope length 55 meters and acceleration of gravity 9.8 N/kg. This means the vibration is mainly caused by the sway of the load, and the flexible vibration from the crane itself is not obvious. So the slewing speed of the crane should be limited to reduce the centrifugal effect.

8.3.2 Combined Motion

In this section, the lifting state under the simultaneous action of multiple drives is designed. The combined motion can be divided into 4 stages:

1. 0 - 10s: lifting stage
2. 10 - 20s: lifting + slewing stage
3. 20 - 30s: lifting + slewing + luffing stage
4. 30 - 40s: lifting + luffing stage

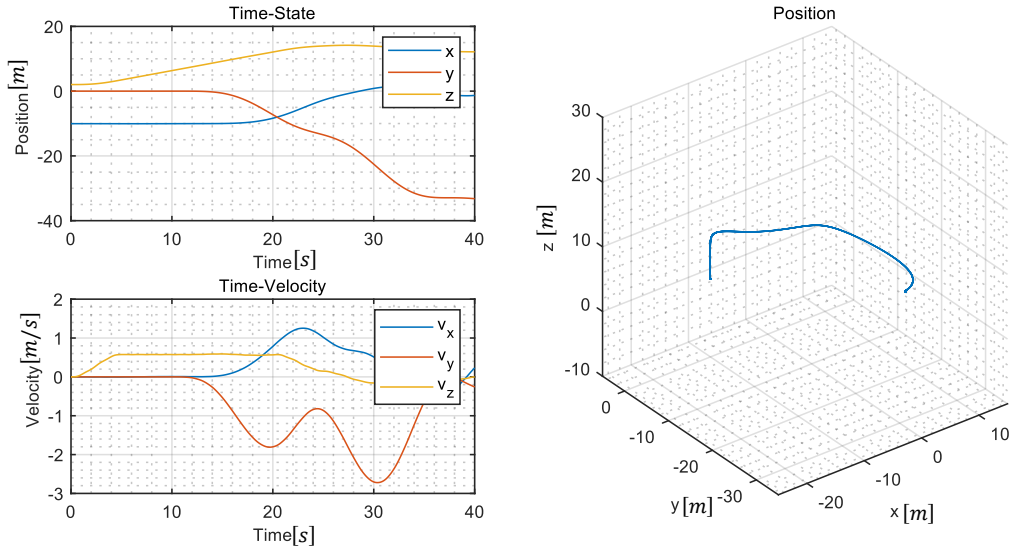


Figure 8-13: Position and Velocity of the Load by Combined Motion of the Crane

In the only lifting stage, the position of the load changes smoothly, and the speed has only a small vibration. The slewing of the crane has little effect on the vertical motion of the load. The position of the load changes smoothly in the horizontal direction, but speed begins to fluctuate greatly. The luffing motion of the crane has a greater influence on the vertical direction of the lifting, the fluctuation of the speed in the vertical direction becomes larger, and there is a big vibration in the horizontal direction.

8.4 Quasi-Static Optimal Control of Crane

8.4.1 Quasi-Static Mapping

Under different loads, the static mapping relationship between the control variable and the end position is different. Here the load with maximum weight of 400t is selected as an example. The mapping relationship is shown as follows.

The solid surface is obtained from experimental data, and the transparent surface is obtained through flat quadratic surface fitting. The fitted surface is used as the actual mapping relationship to reduce the influence of experimental errors. From the fitted surface, it is more intuitively to see the nonlinear relationship between the control variables and the end point output variables

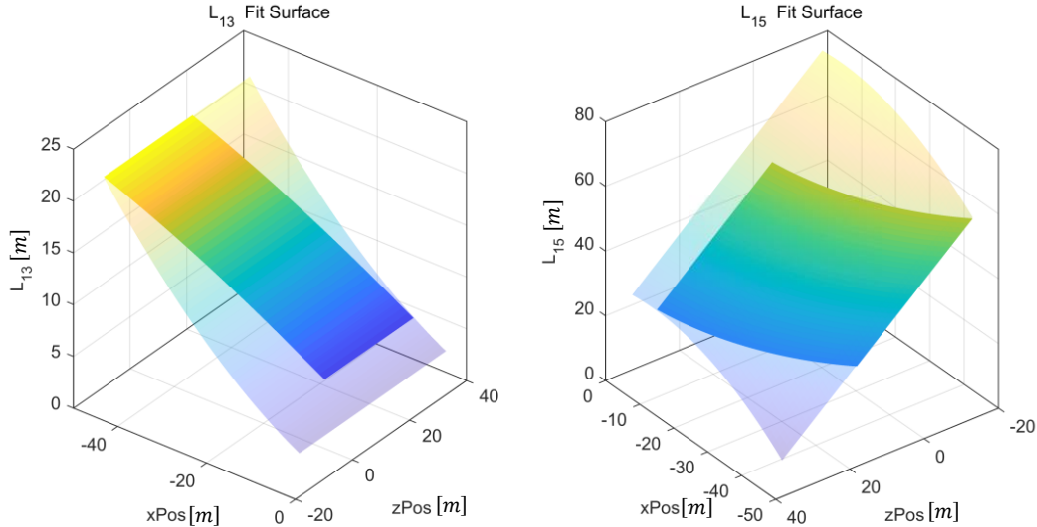


Figure 8-14: Experimental Data and Fitted Surface as Actual Mapping Relationship

8.4.2 Optimal Trajectory of End Point

When designing the optimal trajectory, the maximum absolute velocity and maximum absolute acceleration are considered. In order to make the trajectory more reasonable, the possible position of the end point is also limited. The parameters of QR optimal control are shown in the following table

Tabelle 8-2: Beschriftung der Tabelle im Hauptteil

Parameter		Value
	Initial Value	$\underline{x}_0 = [-10 \ 0 \ 0 \ 0]^T$
State	Number	$n_x = 4$
Variables	Upper Bound	$\underline{x}_{\max} = [-5 \ 30 \ 1 \ 1]^T$
	Lower Bound	$\underline{x}_{\min} = [-50 \ 0 \ -1 \ -1]^T$
Control Variables	Number	$n_u = 2$
	Upper Bound	$\underline{u}_{\max} = [0.2 \ 0.2]^T$
	Lower Bound	$\underline{u}_{\min} = [-0.2 \ -0.2]^T$
Cost	Q	$\underline{\underline{Q}} = 100 \times \text{diag}([1 \ 1 \ 1 \ 1])$
	R	$\underline{\underline{R}} = \text{diag}([1 \ 1])$
Function	Pend	$\underline{\underline{P}}_{\text{end}} = 100 \times \text{diag}([1 \ 1 \ 1 \ 1])$
	Terminal Value	$\underline{x}_e = [-35 \ 10 \ 0 \ 0]^T$
Optimal Control	Prediction Horizon	$N = 400$
	Sampling Time	$t_s = 0.1$
	Simulation Time	$t_f = 40$

The generated optimal trajectory is as follows

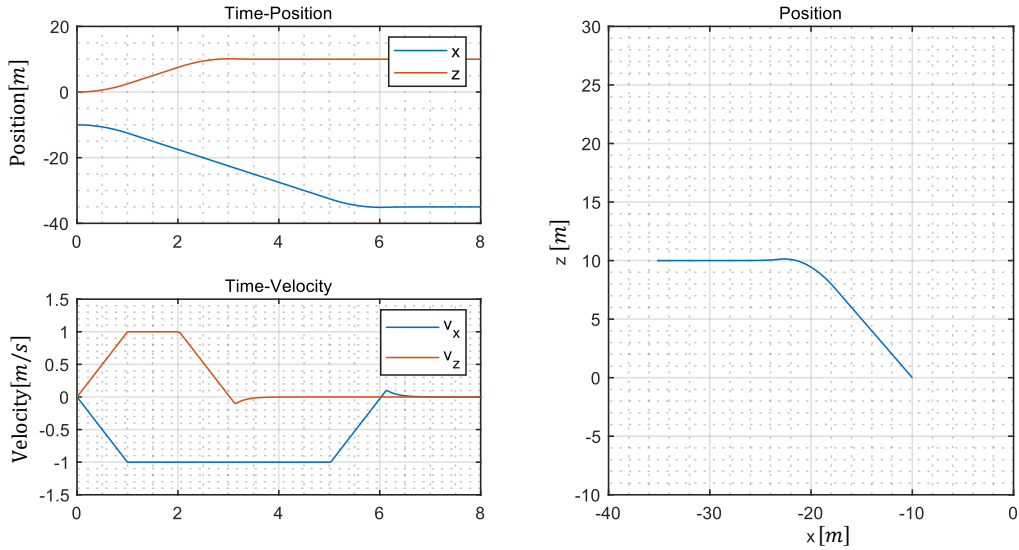


Figure 8-15: Optimal Trajectory of End Point from NMPC

From the curve, it can be seen that the end point initially accelerates to a maximum speed of 1 meter per second with a maximum acceleration of 0.2 meter per second squared, and then stabilizes at the maximum speed. When the position of the end point is close to the target point, it will decelerate with the maximum acceleration. Due to the consideration of the optimal time and minimum energy requirements, the deceleration process will have a certain fine-tuning on the speed curve, but the amount of fine-tuning reflected on the position curve is very small. The speed of the end point will gradually become 0 and finally reach the target position.

Since the distances required to move in the x direction and the z direction are different, the x axis direction first reaches the target x value, and then the z direction arrives. The performance from the path is that the x and z directions move at the same time at the beginning, and after reaching a certain point in time, the movement in the z direction gradually stops. The second half of the path is the movement along the x direction.

8.4.3 Optimal Control Trajectory and Verification

Projection and Control Trajectory

From the projection of the optimal trajectory on the mapping surface, the quasi-static control trajectory can be obtained. The control trajectory is shown as follows.

In order to reduce the error of the control curve caused by the error of the mapping relationship, it is generally required the mapping curve to lie within the experimental surface as much as possible. As shown in the left figure, most of the curves are in this range, so the accuracy of the mapping relationship is high.

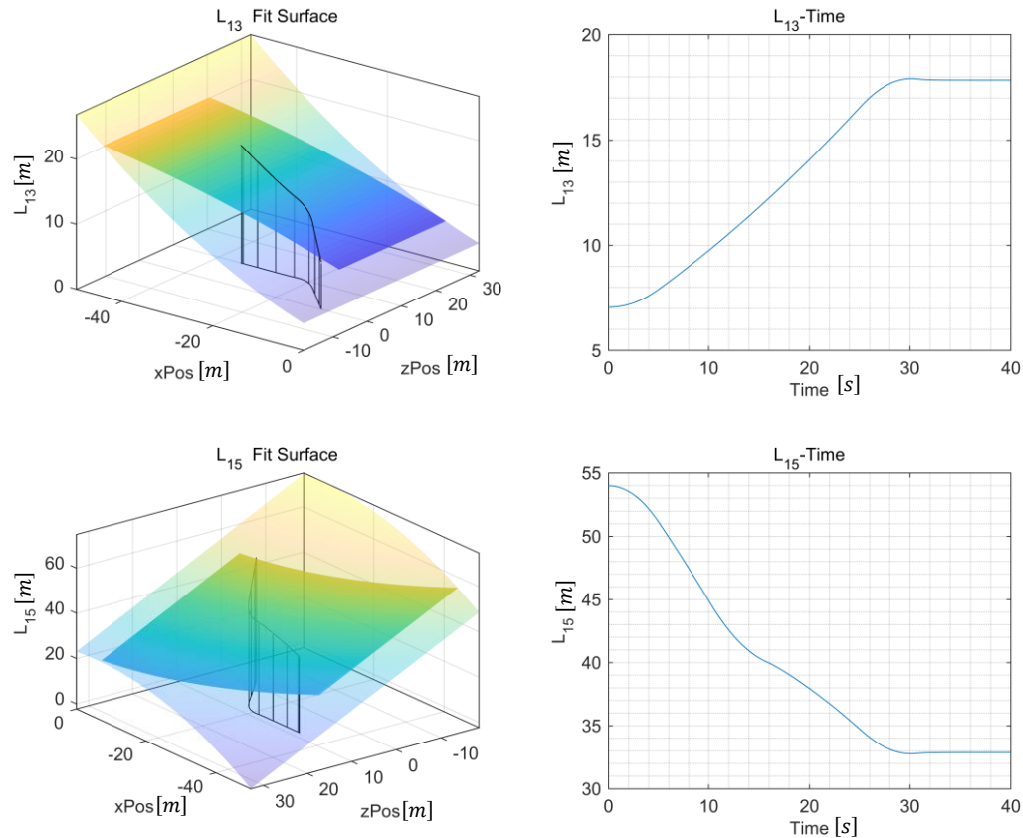


Figure 8-16: Projection of Trajectory on Mapping Surface and Optimal Control Trajectory

Expansion and Fitting of Optimal Control Trajectory

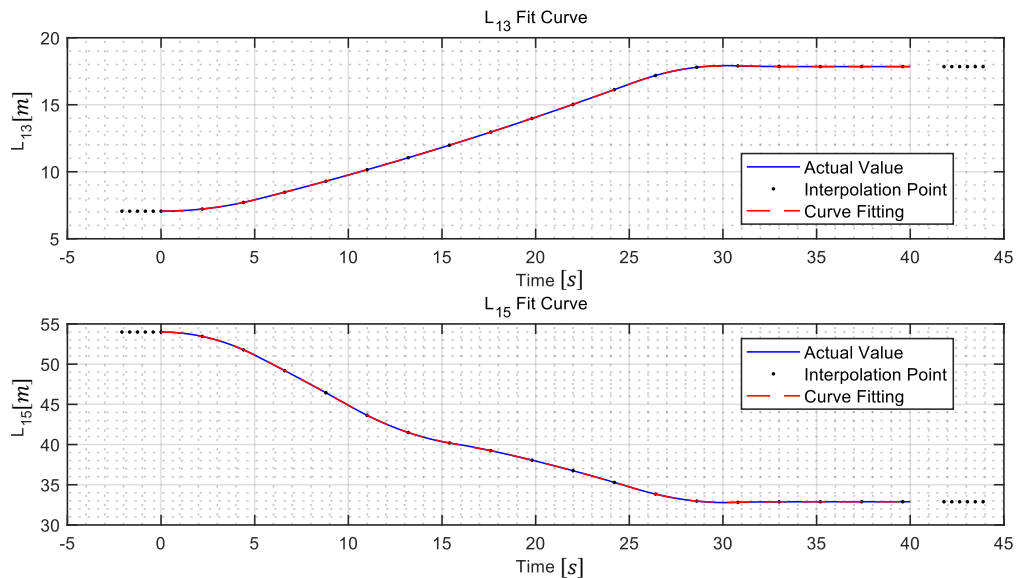


Figure 8-17: Expansion and Fitting of Optimal Control Trajectory

The control data generated by the mapping relationship is discrete. In order to be used in a solver with an indefinite time step, the generated data will be fitted. In order to ensure the stability of the start and end stages of the control trajectory, in addition to the 20 interpolation points taken at the same distance in the control data, 5 steady-state control points are added at each end. Spline curve is used as the fitting method.

Verification through Experiment

In order to verify the quasi-static optimal control method, the generated continuous control trajectory is applied to the crane model to obtain the dynamic response. The results are as follows

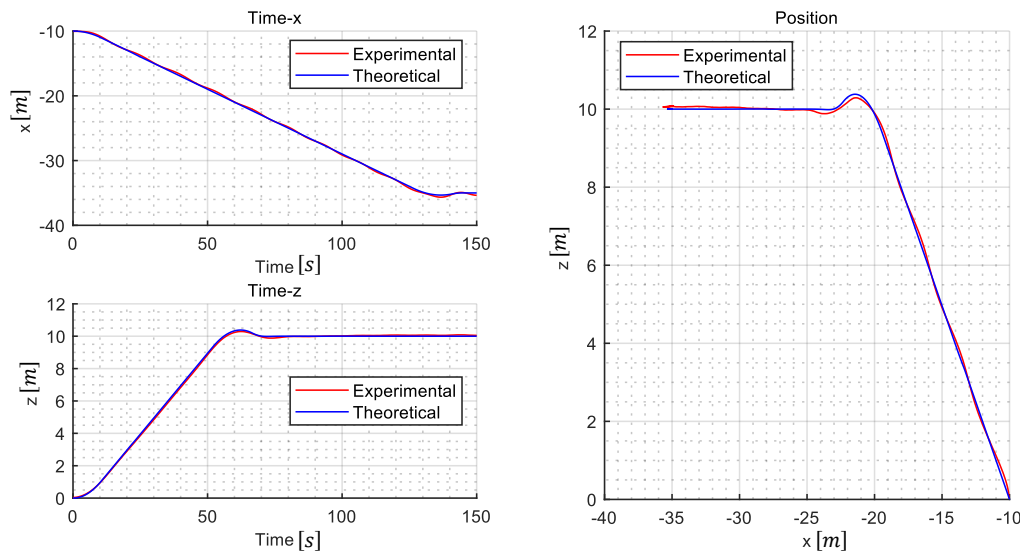


Figure 8-18: Theoretical Optimal Trajectory and Experimental Trajectory using Quasi-Static Optimal Control

According to the experimental results, the actual trajectory is basically close to the theoretical trajectory with slight vibration. This proves that the quasi-static control method can track the optimal path. The vibration is mainly caused by the inertia of the crane and the load. To suppress vibration, feedback control of the crane is required, such as PID [Kha-2014], real-time MPC etc [Sch-2014]. The feedback controller for suppressing flexible vibration is the future research direction.

9 Conclusion and Future Development

9.1 Conclusion

In this thesis the modeling and control method for lattice boom cranes is studied, and some experiments are done for the verification.

In order to model the lattice boom crane efficiently and accurately, several flexible models for dynamic calculation are proposed, such as spatial Timoshenko beam, cubic spline beam, strut tie model. Super truss elements based on three assumptions are proposed to simulate the lattice boom with the minimum number of degrees of freedoms. To combine all relevant elements of the crane, the functions for different kinds of constraint are established and the multibody dynamics method with Baumgartner stability method is applied. In addition, different types of lattice boom, the detailed modeling and driving approach of the lattice boom crane are also described.

According to the special control variables and control requirements of the lattice boom crane, a quasi-static control method is designed. This method combines the static mapping relationship with the target optimal trajectory to generate the optimal control trajectory. The static mapping relationship is obtained through experiments and data post-processing, which can reflect the relationship between the control object and the control variable under slow motion. The optimal trajectory of the target is obtained through the nonlinear model predictive control (NMPC). Because of the QR control method applied in NMPC, the optimal trajectory satisfies the time optimal and minimum control cost.

As the verification, some experiments are designed to verify the modeling accuracy of each flexible model, such as static bending, vibration under self-gravity, controlled motion. Experiments on super truss elements can not only observe the dynamic response of the model, but also reflect some characteristics that continuous beams do not have, which provides a theoretical basis for further simplification. For the crane model, the dynamic response of the crane in the motion of lifting, luffing and slewing is obtained through the simulation. In addition, the control effect of the quasi-static optimal control algorithm on the control of lattice boom crane is also verified.

In order to make modeling, control and experiment more convenient, in this thesis a rigid-flexible hybrid multibody dynamics platform is established, which can do the statics and dynamics calculation of the complex mechanism.

9.2 Future Development

Modeling Part

Although the super truss element can greatly reduce the number of degrees of freedom, it is still needed to calculate each member of the truss beam in each time step. This makes the single-step calculation time of the ODE solver very large. Parallel computing and other methods of accelerating computing to reduce computing time will be studied in the future.

The parameterization method in this paper is only suitable for general simple truss models. At present, in the direction of lighter and miniaturized machinery, more complex truss models are widely used. These trusses may no longer meet the three assumptions in this paper when they are deformed. Therefore, a completer and more general truss model is urgently needed.

Control Part

The current control method is difficult to control the sway of the load swing during fast movement. Therefore, it is necessary to increase the feedback structure into the control theory and carry out real-time adjustment by using real-time MPC or PID controller.

For the generation of the optimal trajectory at the end point, only the time and energy optimization under barrier-free conditions are currently considered. However, there are often many obstacles in actual work scenarios. The identification of obstacles and the design of optimal trajectory to avoid obstacles need to be studied.

Bibliography

- [Arn-2003] Arnold, E and Sawodny, O and Hildebrandt, A and Schneider, K (Hrsg.): Anti-sway system for boom cranes based on an optimal control approach, 2003.
- [Arn-2005] Arnold, E., Sawodny, O., Neupert, J., & Schneider, K. (Hrsg.): Anti-sway system for boom cranes based on a model predictive control approach, 2005.
- [Bau-2010] Bauchau, O. A.: Flexible multibody dynamics. In: 94007033 (2010)
- [Baz-2003] Bazoune, A.; Khulief, Y. A.; Stephen, N. G.: Shape functions of three-dimensional Timoshenko beam element. In: Journal of Sound and Vibration, Jg. 259 (2003) Nr. 2, S. 473–480.
- [Blu-1989] Blume, J. A.: Compatibility conditions for a left Cauchy-Green strain field. In: Journal of elasticity, Jg. 21 (1989) Nr. 3, S. 271–308.
- [Bon-2001] Bonet, J.; Marriott, H.; Hassan, O.: An averaged nodal deformation gradient linear tetrahedral element for large strain explicit dynamic applications. In: Communications in Numerical Methods in Engineering, Jg. 17 (2001) Nr. 8, S. 551–561.
- [Cao-2018] Cao, T.; Cuffari, D.; Bongiorno, A.: First-principles calculation of third-order elastic constants via numerical differentiation of the second Piola-Kirchhoff stress tensor. In: Physical review letters, Jg. 121 (2018) Nr. 21, S. 216001.
- [Cia-2003] Ciarlet, P. G.; Laurent, F.: Continuity of a deformation as a function of its Cauchy-Green tensor. In: Archive for rational mechanics and analysis, Jg. 167 (2003) Nr. 3, S. 255–269.
- [Cow-2006] Cowling, Ian D., James F. Whidborne, and Alastair K. Cooke (Hrsg.): Optimal trajectory planning and LQR control for a quadrotor UAV, 2006.
- [Cri-1990] Crisfield, M. A.: A consistent co-rotational formulation for non-linear, three-dimensional, beam-elements. In: Computer methods in applied mechanics and engineering, Jg. 81 (1990) Nr. 2, S. 131–150.

- [Die-2006] Diebel, J.: Representing attitude: Euler angles, unit quaternions, and rotation vectors. In: Matrix, Jg. 58 (2006) Nr. 15-16, S. 1–35.
- [Elk-1995] Elkaranshawy, H. A.; Dokainish, M. A.: Corotational finite element analysis of planar flexible multibody systems. In: Computers & structures, Jg. 54 (1995) Nr. 5, S. 881–890.
- [Fan-2016] Fang, H.; Qi, Z.: A Hybrid Interpolation Method for Geometric Nonlinear Spatial Beam Elements with Explicit Nodal Force. In: Mathematical Problems in Engineering, Jg. 2016 (2016)
- [Gao-2020] Gao, L., Zhuo, Y., Kleeberger, M., Peng, H. (Hrsg.): Modeling and Simulation of Long Boom Manipulator based on Geometrically Exact Beam Theory, 2020.
- [Gar-2003] Garcia-Vallejo, D.; Escalona, J. L.; Mayo, J.; Dominguez, J.: Describing rigid-flexible multibody systems using absolute coordinates. In: Nonlinear Dynamics, Jg. 34 (2003) Nr. 1, S. 75–94.
- [Ger-1973] Germain, P.: The method of virtual power in continuum mechanics. Part 2: Microstructure. In: SIAM Journal on Applied Mathematics, Jg. 25 (1973) Nr. 3, S. 556–575.
- [Gün-1997] Günthner, W. A.; Kleeberger, M.: Zum Stand der Berechnung von Gittermast-Fahrzeugkranen. In: dhf (1997) Nr. 03, S. 56–61.
- [Hen-2017] Hendzel, Z.; Rykała, Ł.: Modelling of dynamics of a wheeled mobile robot with mecanum wheels with the use of Lagrange equations of the second kind. In: International Journal of Applied Mechanics and Engineering, Jg. 22 (2017) Nr. 1
- [Hul-1990] Hulsen, M. A.: A sufficient condition for a positive definite configuration tensor in differential models. In: Journal of non-newtonian fluid mechanics, Jg. 38 (1990) Nr. 1, S. 93–100.
- [Jon-1990] Jonker, J. B.; Meijaard, J. P. (Hrsg.): Multibody systems handbook. Springer, 1990.
- [Kam-2015] Kammer, D. C.; Allen, M. S.; Mayes, R. L.: Formulation of an experimental substructure model using a Craig–Bampton based transmission simulator. In: Journal of Sound and Vibration, Jg. 359 (2015), S. 179–194.

- [Kha-2014] Khatoon, Shahida, Dhiraj Gupta, and L. K. Das (Hrsg.): PID & LQR control for a quadrotor: Modeling and simulation, 2014.
- [Kle-1996] Kleeberger, M.: Nichtlineare dynamische Berechnung von Gittermast-Fahrzeugkranen (en: Nonlinear dynamic calculation of lattice boom mobile cranes), PhD Dissertation, Technical University of Munich, 1996.
- [Kle-2006] Kleeberger, M.; Hübner, K.-T.: Using Superelements in the Calculation of Lattice-Boom Cranes. In: Logistics Journal: referierte Veröffentlichungen, Jg. 2006 (2006) Nr. Dezember
- [Kou-2007] Koutsovasilis, P.; Beitelschmidt, M.: Model Reduction of Large Elastic Systems (2007)
- [Kov-2012] Kovács, E. (Hrsg.): Rotation about an arbitrary axis and reflection through an arbitrary plane, 2012.
- [Lew-2012] Lewis, F. L.; Vrabie, D.; Syrmos, V. L.: Optimal control. John Wiley & Sons, 2012.
- [Li-2007] Li, Z. X.: A co-rotational formulation for 3D beam element using vectorial rotational variables. In: Computational Mechanics, Jg. 39 (2007) Nr. 3, S. 309–322.
- [Lim-1999] Lim, Andrew EB, and Xun Yu Zhou: Stochastic optimal LQR control with integral quadratic constraints and indefinite control weights. In: IEEE Transactions on automatic control, Jg. 44 (1999) Nr. 7, S. 1359–1369.
- [Luo-2008] Luo, Y.: An efficient 3d timoshenko beam element with consistent shape functions. In: Adv. Theor. Appl. Mech, Jg. 1 (2008) Nr. 3, S. 95–106.
- [Neu-2010] Neupert, J.; Arnold, E.; Schneider, K.; Sawodny, O.: Tracking and anti-sway control for boom cranes. In: Control Engineering Practice, Jg. 18 (2010) Nr. 1, S. 31–44.
- [Ped-2005] Pedersen, P.: Analytical stiffness matrices with Green–Lagrange strain measure. In: International journal for numerical methods in engineering, Jg. 62 (2005) Nr. 3, S. 334–352.

- [Pio-1966] Pio, R.: Euler angle transformations. In: IEEE Transactions on automatic control, Jg. 11 (1966) Nr. 4, S. 707–715.
- [Rot-1981] Rothenburg, L.; Selvadurai, A. P.: A micromechanical definition of the Cauchy stress tensor for particulate media. In: Mechanics of structured media (1981), S. 469–486.
- [San-2020] Santarpia, E.; Demasi, L.: Large displacement models for composites based on Murakami's Zig-Zag Function, Green-Lagrange Strain Tensor, and Generalized Unified Formulation. In: Thin-Walled Structures, Jg. 150 (2020), S. 106460.
- [Sch-2014] Schaper, U.; Sawodny, O.; Zeitz, M.; Schneider, K.: Load position estimation for crane anti-sway control systems. In: Journal of Dynamic Systems, Measurement, and Control, Jg. 136 (2014) Nr. 3
- [Sur-2016] Surana, K. S.; Joy, A. D.; Reddy, J. N.: A non-classical internal polar continuum theory for finite deformation of solids using first Piola-Kirchhoff stress tensor. In: Journal of Pure and Applied Mathematics: Advances and Applications, Jg. 16 (2016) Nr. 1, S. 1–41.
- [Tup-1987] Tupling, S. J.; Pierrynowski: Use of cardan angles to locate rigid bodies in three-dimensional space. In: Medical and Biological Engineering and computing, Jg. 25 (1987) Nr. 5, S. 527–532.
- [Vuj-1978] Vujanovic, B.: Conservation laws of dynamical systems via D'Alembert's principle. In: International Journal of Non-Linear Mechanics, Jg. 13 (1978) Nr. 3, S. 185–197.
- [Wan-2015] Wang, G.; Qi, Z.; Kong, X.: Geometrical nonlinear and stability analysis for slender frame structures of crawler cranes. In: Engineering Structures, Jg. 83 (2015), S. 209–222.
- [Yus-1998] Yushkov, M. P.; Zegzhda, S. A.: A new method of vibration analysis of elastic systems, based on the Lagrange equations of the first kind. In: Technische Mechanik-European Journal of Engineering Mechanics, Jg. 18 (1998) Nr. 2, S. 153–160.

List of Figures

Figure 2-1:	Structure of Model Predictive Control	10
Figure 3-1:	Definition of truss elements and truss order	28
Figure 3-2:	Flow chart of dynamic calculation of super truss element	30
Figure 4-1:	Butcher Tableau	42
Figure 5-1:	Flow Chart of Dynamics Calculation	46
Figure 5-2:	Rigid-body Minimum-Degree-of-Freedom Models a) Folding Boom System b) Single Jib Pendulum c) Double Jib Pendulum d) Triple Jib Pendulum	46
Figure 5-3:	Co-Simulation Logic of Hydraulic System and Mechanism Dynamics System	47
Figure 5-4:	Deep Reinforcement Learning Framework for Optimal Control based on the Multi-body Dynamics Model	47
Figure 6-1:	Quasi-Static Optimal Trajectory Tracking Strategy	51
Figure 6-2:	Static State Mapping	52
Figure 6-3:	Discrete Experimental Data from Statics Calculation	53
Figure 6-4:	Generation of Optimal Control Trajectory	55
Figure 7-1:	The Composition, Model Types of Elements and the number of the Elements of the Lattice Boom Crane	57
Figure 7-2:	Locations and Types of Constraints and Drive Configuration displayed on the Calculation Model	60
Figure 8-1:	Cantilever Beam Static Bending Test	64
Figure 8-2:	Vibration Test of Cantilever Beam under Self-gravity	64
Figure 8-3:	Fixed Axis Rotation under Torque Control	65
Figure 8-4:	Fixed Axis Rotation under Angle Control	66
Figure 8-5:	Vibration Test of Cantilever Truss Boom under Self-gravity	67
Figure 8-6:	Super Truss Element Fixed Axis Rotation under Torque Control	67
Figure 8-7:	Super Truss Element Fixed Axis Rotation under Angle Control	68
Figure 8-8:	Super Truss Element Equivalent Stiffness Test	68
Figure 8-9:	Super Truss Element Equivalent Mass Test	69
Figure 8-10:	Position and Velocity of the Load by Lifting Stage of the Crane	70
Figure 8-11:	Position and Velocity of the Load by Luffing Stage of the Crane	71
Figure 8-12:	Position and Velocity of the Load by Slewing Stage of the Crane	72

Figure 8-13:	Position and Velocity of the Load by Combined Motion of the Crane	73
Figure 8-14:	Experimental Data and Fitted Surface as Actual Mapping Relationship	74
Figure 8-15:	Optimal Trajectory of End Point from NMPC	75
Figure 8-16:	Projection of Trajectory on Mapping Surface and Optimal Control Trajectory	76
Figure 8-17:	Expansion and Fitting of Optimal Control Trajectory	76
Figure 8-18:	Theoretical Optimal Trajectory and Experimental Trajectory using Quasi-Static Optimal Control	77
Figure D-1:	Display of Lattice Boom Crane	D-11
Figure E-1:	Trapezoidal Velocity Three Stage Function	E-2
Figure E-2:	Trigonometric Cosine Step Function	E-3
Figure E-3:	Trigonometric Cosine Full Function	E-4
Figure E-4:	Hyperbolic Tangent Function	E-5

List of Tables

Table 2-1:	Deformation Tensor	8
Table 2-2:	Stress Tensor	9
Table 5-1:	Parameters for Dynamics Model	49
Table 5-2:	Parameters for Solving Route	49
Table 7-1:	Properties of different Types of Super Truss Elements	58
Table 7-2:	Locations and Types of Constraints for Lattice Boom Crane	60
Table 7-3:	Definition of Control Variables for Lattice Crane Model	61
Tabelle 8-1:	Parameters of Single Beam	63
Tabelle 8-2:	Beschriftung der Tabelle im Hauptteil	74
Table A-1:	Weight and Integration Point of Standard Format of Gaussian Numerical Integral	A-1
Table D-1:	Frame Parameter for Lattice Boom Crane Model	D-1
Table D-2:	Pedestal Parameter for Lattice Boom Crane Model	D-1
Table D-3:	Main Boom Parameter for Lattice Boom Crane Model	D-2
Table D-4:	Main Boom Initial State Parameter for Lattice Boom Crane Model	D-3
Table D-5:	Main Boom Head Parameter for Lattice Boom Crane Model	D-3
Table D-6:	Derrick Boom Parameter for Lattice Boom Crane Model	D-4
Table D-7:	Derrick Boom Initial State Parameter for Lattice Boom Crane Model	D-5
Table D-8:	Strut Tie Model Parameter for Lattice Boom Crane Model	D-6
Table D-9:	Luffing Rope Parameter for Lattice Boom Crane Model	D-6
Table D-10:	Sub-Cable Parameter for Lattice Boom Crane Model	D-7
Table D-11:	Lifting Cable Parameter for Lattice Boom Crane Model	D-7
Table D-12:	Load Parameter for Lattice Boom Crane Model	D-8
Table D-13:	Constraint Parameter for Lattice Boom Crane Model	D-8
Table D-14:	Nodal Force Parameter for Lattice Boom Crane Model	D-9
Table D-15:	Solver Parameter for Lattice Boom Crane Model	D-9
Table D-16:	Plot Parameter for Lattice Boom Crane Model	D-10
Table E-1:	Confidence Coefficient of Hyperbolic Tangent Function	E-4

Appendix A Mathematical Convention

A.1 Mathematical Convention

Skew symmetric matrix

$$\tilde{\underline{a}} = \text{skew}(\underline{a}) = \text{skew}\left(\begin{bmatrix} a_1 \\ a_2 \\ a_3 \end{bmatrix}\right) = \begin{bmatrix} 0 & -a_3 & a_2 \\ a_3 & 0 & -a_1 \\ -a_2 & a_1 & 0 \end{bmatrix} \quad (\text{A-1})$$

Properties of cross product

$$\underline{a} \times (\underline{b} \times \underline{c}) = \underline{b}(\underline{a} \cdot \underline{c}) - \underline{c}(\underline{a} \cdot \underline{b}) \Leftrightarrow \underline{\tilde{a}}\underline{\tilde{b}}\underline{c} = \underline{b}\underline{a}^T\underline{c} - \underline{c}\underline{a}^T\underline{b} = (\underline{b}\underline{c}^T - \underline{c}\underline{b}^T)\underline{a} \quad (\text{A-2})$$

$$\underline{a} \times (\underline{b} \times (\underline{b} \times \underline{a})) = \underline{b} \times (\underline{a} \times (\underline{b} \times \underline{a})) \Leftrightarrow \underline{\tilde{a}}\underline{\tilde{b}}\underline{\tilde{b}}\underline{a} = \underline{\tilde{b}}\underline{\tilde{a}}\underline{\tilde{b}}\underline{a} \quad (\text{A-3})$$

$$\underline{a} \times \underline{b} = \underline{c} \Leftrightarrow \underline{a} = -\left(\underline{b}\underline{b}^T - \underline{b}^T\underline{b}I\right)^{-1}\underline{\tilde{b}}\underline{c} \quad (\text{A-4})$$

A.2 Gaussian Numerical Integral

Standard format of Gaussian numerical integral

$$\int_{-1}^1 f(t)dt = \sum_{i=1}^n w[i]f(x[i]) \quad (\text{A-5})$$

Table A-1: Weight and Integration Point of Standard Format of Gaussian Numerical Integral

Order	Weight	Integration Point
$n = 1$	$w = 2$	$x = 0$
$n = 2$	$\underline{w} = \begin{bmatrix} 1 \\ 1 \end{bmatrix}$	$\underline{x} = \frac{1}{\sqrt{3}} \begin{bmatrix} -1 \\ 1 \end{bmatrix}$
$n = 3$	$\underline{w} = \frac{1}{9} \begin{bmatrix} 5 \\ 8 \\ 5 \end{bmatrix}$	$\underline{x} = \frac{\sqrt{3}}{\sqrt{5}} \begin{bmatrix} -1 \\ 0 \\ 1 \end{bmatrix}$

Order	Weight	Integration Point
$n = 4$	$\underline{w} = \frac{1}{36} \begin{bmatrix} 18 - \sqrt{30} \\ 18 + \sqrt{30} \\ 18 + \sqrt{30} \\ 18 - \sqrt{30} \end{bmatrix}$	$\underline{x} = \frac{1}{35} \begin{bmatrix} -\sqrt{525 + 70\sqrt{30}} \\ -\sqrt{525 - 70\sqrt{30}} \\ \sqrt{525 - 70\sqrt{30}} \\ \sqrt{525 + 70\sqrt{30}} \end{bmatrix}$
$n = 5$	$\underline{w} = \frac{1}{900} \begin{bmatrix} 322 - 13\sqrt{70} \\ 322 + 13\sqrt{70} \\ 512 \\ 322 + 13\sqrt{70} \\ 322 - 13\sqrt{70} \end{bmatrix}$	$\underline{x} = \frac{1}{21} \begin{bmatrix} -\sqrt{245 + 14\sqrt{70}} \\ -\sqrt{245 - 14\sqrt{70}} \\ 0 \\ \sqrt{245 - 14\sqrt{70}} \\ \sqrt{245 + 14\sqrt{70}} \end{bmatrix}$
$n = 6$	$\underline{w} = \frac{1}{10} \begin{bmatrix} 1.713244923791703 \\ 3.607615730481388 \\ 4.679139345726909 \\ 4.679139345726909 \\ 3.607615730481388 \\ 1.713244923791703 \end{bmatrix}$	$\underline{x} = \frac{1}{10} \begin{bmatrix} -9.324695142031521 \\ -6.612093864662646 \\ -2.386191860831968 \\ 2.386191860831968 \\ 6.612093864662646 \\ 9.324695142031521 \end{bmatrix}$
$n = 7$	$\underline{w} = \frac{1}{10} \begin{bmatrix} 1.294849661688696 \\ 2.797053914892767 \\ 3.818300505051183 \\ 4.179591836734694 \\ 3.818300505051183 \\ 2.797053914892767 \\ 1.294849661688696 \end{bmatrix}$	$\underline{x} = \frac{1}{10} \begin{bmatrix} -9.491079123427586 \\ -7.415311855993945 \\ -4.058451513773977 \\ 0 \\ 4.058451513773977 \\ 7.415311855993945 \\ 9.491079123427586 \end{bmatrix}$
$n = 8$	$\underline{w} = \frac{1}{10} \begin{bmatrix} 1.012285362903761 \\ 2.223810344533746 \\ 3.137066458778871 \\ 3.626837833783620 \\ 3.626837833783620 \\ 3.137066458778871 \\ 2.223810344533746 \\ 1.012285362903761 \end{bmatrix}$	$\underline{x} = \frac{1}{10} \begin{bmatrix} -9.602898564975363 \\ -7.966664774136270 \\ -5.255324099163293 \\ -1.834346424956495 \\ 1.834346424956495 \\ 5.255324099163293 \\ 7.966664774136270 \\ 9.602898564975363 \end{bmatrix}$
$n = 9$	$\underline{w} = \frac{1}{10} \begin{bmatrix} 0.812743883615745 \\ 1.806481606948574 \\ 2.606106964029354 \\ 3.123470770400029 \\ 3.302393550012598 \\ 3.123470770400029 \\ 2.606106964029354 \\ 1.806481606948574 \\ 0.812743883615745 \end{bmatrix}$	$\underline{x} = \frac{1}{10} \begin{bmatrix} -9.681602395076261 \\ -8.360311073266357 \\ -6.133714327005904 \\ -3.242534234038089 \\ 0 \\ 3.242534234038089 \\ 6.133714327005904 \\ 8.360311073266357 \\ 9.681602395076261 \end{bmatrix}$

Order	Weight	Integration Point
$n = 10$	$w = \frac{1}{10} \begin{bmatrix} 0.6667134430868785 \\ 1.494513491505809 \\ 2.190863625159821 \\ 2.692667193099963 \\ 2.955242247147528 \\ 2.955242247147528 \\ 2.692667193099963 \\ 2.190863625159821 \\ 1.494513491505809 \\ 0.6667134430868785 \end{bmatrix}$	$\underline{x} = \frac{1}{10} \begin{bmatrix} -9.739065285171719 \\ -8.650633666889848 \\ -6.794095682990241 \\ -4.333953941292476 \\ -1.488743389816309 \\ 1.488743389816309 \\ 4.333953941292476 \\ 6.794095682990241 \\ 8.650633666889848 \\ 9.739065285171719 \end{bmatrix}$
$n = 11$	$w = \frac{1}{10} \begin{bmatrix} 0.5566856711617369 \\ 1.255803694649046 \\ 1.862902109277342 \\ 2.331937645919904 \\ 2.628045445102470 \\ 2.729250867779006 \\ 2.628045445102470 \\ 2.331937645919904 \\ 1.862902109277342 \\ 1.255803694649046 \\ 0.5566856711617369 \end{bmatrix}$	$\underline{x} = \frac{1}{10} \begin{bmatrix} -9.782286581460570 \\ -8.870625997680953 \\ -7.301520055740494 \\ -5.190961292068118 \\ -2.695431559523450 \\ 0 \\ -2.695431559523450 \\ -5.190961292068118 \\ -7.301520055740494 \\ -8.870625997680953 \\ -9.782286581460570 \end{bmatrix}$

For non-standard Gaussian numerical integration

$$\int_{lb}^{ub} f(t) dt = \sum_{i=1}^n w[i] f(\hat{x}[i]) \quad \text{with } \hat{x}[i] = \frac{x[i] + 1}{2(ub - lb)} + lb \quad (\text{A-6})$$

A.3 Cubic Hermite Interpolation

In numerical analysis, a cubic Hermite spline or cubic Hermite interpolator is a spline where each piece is a third-degree polynomial specified in Hermite form, that is, by its values and first derivatives at the end points of the corresponding domain interval.

$$\begin{aligned} y(x) &= N_1^0 y(x_0) + N_2^0 y(x_e) + N_1^1 y'(x_0) + N_2^1 y'(x_e) \quad \text{with } y' = \partial y / \partial x \\ y'(x) &= N'_1^0 y(x_0) + N'_2^0 y(x_e) + N'_1^1 y'(x_0) + N'_2^1 y'(x_e) \\ y''(x) &= N''_1^0 y(x_0) + N''_2^0 y(x_e) + N''_1^1 y'(x_0) + N''_2^1 y'(x_e) \end{aligned} \quad (\text{A-7})$$

which can also be written as

$$\underline{y}(x) = \underline{\underline{N}} \underline{y}_\partial \quad \underline{y}'(x) = \underline{\underline{N}}' \underline{y}_\partial \quad \underline{y}''(x) = \underline{\underline{N}}'' \underline{y}_\partial \quad (\text{A-8})$$

where $\underline{y}_\partial = [y(x_0) \quad y'(x_0) \quad y(x_e) \quad y'(x_e)]^T$.

The shape function can be written as

$$\underline{\underline{N}} = \begin{bmatrix} N_1^0 I & N_1^1 I & N_2^0 I & N_2^1 I \end{bmatrix}$$

$$N_1^0 = 1 - 3\xi^2 + 2\xi^3 \quad N_2^0 = 3\xi^2 - 2\xi^3 \quad (\text{A-9})$$

$$N_1^1 = L(\xi - 2\xi^2 + \xi^3) \quad N_2^1 = L(\xi^3 - \xi^2)$$

The first derivative of the shape function can be written as

$$\underline{\underline{N'}} = \begin{bmatrix} N'_1 I & N'_1 I & N'_2 I & N'_2 I \end{bmatrix}$$

$$N'_1^0 = (-6\xi + 6\xi^2)/L \quad N'_2^0 = (6\xi - 6\xi^2)/L \quad (\text{A-10})$$

$$N'_1^1 = 1 - 4\xi + 3\xi^2 \quad N'_2^1 = 3\xi^2 - 2\xi$$

The second derivative of the shape function can be written as

$$\underline{\underline{N''}} = \begin{bmatrix} N''_1 I & N''_1 I & N''_2 I & N''_2 I \end{bmatrix}$$

$$N''_1^0 = (-6 + 12\xi)/L^2 \quad N''_1^1 = (-4 + 6\xi)/L \quad (\text{A-11})$$

$$N''_2^0 = (6 - 12\xi)/L^2 \quad N''_2^1 = (6\xi - 2)/L$$

A.4 Lagrange Polynomial

Lagrange polynomials are used for polynomial interpolation for a given set of points $(x_1, y_1), (x_2, y_2), \dots, (x_N, y_N), N \in \mathbb{Z}^+$ with $x_i \neq x_j, \forall i, j \in [1, N]$. The interpolation value can be written as

$$y(x) = \sum_{i=1}^N l_i(x)y_i \quad \text{with} \quad l_i(x) = \prod_{j=1, j \neq i}^N \frac{x - x_j}{x_i - x_j} \quad (\text{A-12})$$

The first derivative

$$y'(x) = \sum_{i=1}^N l'_i(x)y_i \quad \text{with} \quad l'_i(x) = \sum_{k=1, k \neq i}^N \frac{1}{x_i - x_k} \prod_{j=1, j \neq i, j \neq k}^N \frac{x - x_j}{x_i - x_j} \quad (\text{A-13})$$

Appendix B Spatial Rotation and Kinematics

B.1 Derivative of Rotation Matrix

B.1.1 Angular Velocity

First derivative of rotation matrix respect to time

$$I\underline{\underline{R}}_B = I\underline{\underline{\tilde{\omega}}}^B I\underline{\underline{R}}_B = I\underline{\underline{R}}_{BB} \underline{\underline{\tilde{\omega}}}^B \quad B\underline{\underline{R}}_I = -I\underline{\underline{R}}_B^T I\underline{\underline{\tilde{\omega}}}^B = -B\underline{\underline{\tilde{\omega}}}^B I\underline{\underline{R}}_B^T \quad (\text{B-1})$$

Angular velocity in different coordinate

$$I\underline{\underline{\tilde{\omega}}}^B = I\underline{\dot{R}}_{BB} \underline{\underline{R}}_I \quad B\underline{\underline{\tilde{\omega}}}^B = B\underline{\underline{R}}_I I\underline{\dot{R}}_B \quad (\text{B-2})$$

Relationship of angular velocity in different coordinate

$$\begin{aligned} B\underline{\underline{\omega}}^B &= B\underline{\underline{R}}_I I\underline{\underline{\omega}}^B \\ B\underline{\underline{\tilde{\omega}}}^B &= B\underline{\underline{R}}_{II} \underline{\underline{\tilde{\omega}}}^B I\underline{\underline{R}}_B \end{aligned} \quad \begin{aligned} I\underline{\underline{\omega}}^B &= I\underline{\underline{R}}_{BB} \underline{\underline{\omega}}^B \\ I\underline{\underline{\tilde{\omega}}}^B &= I\underline{\underline{R}}_{BB} \underline{\underline{\tilde{\omega}}}^B B\underline{\underline{R}}_I \end{aligned} \quad (\text{B-3})$$

B.1.2 Curvature

First derivative of rotation matrix respect to arc coordinate

$$I\underline{\underline{R}}'_B = I\underline{\underline{\tilde{\kappa}}}^B I\underline{\underline{R}}_B = I\underline{\underline{R}}_{BB} \underline{\underline{\tilde{\kappa}}}^B \quad B\underline{\underline{R}}'_I = -I\underline{\underline{R}}_B^T I\underline{\underline{\tilde{\kappa}}}^B = -B\underline{\underline{\tilde{\kappa}}}^B I\underline{\underline{R}}_B^T \quad (\text{B-4})$$

Curvature in different coordinate

$$I\underline{\underline{\tilde{\kappa}}}^B = I\underline{\underline{R}}'_{BB} \underline{\underline{R}}_I \quad B\underline{\underline{\tilde{\kappa}}}^B = B\underline{\underline{R}}_I I\underline{\underline{R}}'_B \quad (\text{B-5})$$

Relationship of curvature in different coordinate

$$\begin{aligned} B\underline{\underline{\kappa}}^B &= B\underline{\underline{R}}_I I\underline{\underline{\kappa}}^B \\ B\underline{\underline{\tilde{\kappa}}}^B &= B\underline{\underline{R}}_{II} \underline{\underline{\tilde{\kappa}}}^B I\underline{\underline{R}}_B \end{aligned} \quad \begin{aligned} I\underline{\underline{\kappa}}^B &= I\underline{\underline{R}}_{BB} \underline{\underline{\kappa}}^B \\ I\underline{\underline{\tilde{\kappa}}}^B &= I\underline{\underline{R}}_{BB} \underline{\underline{\tilde{\kappa}}}^B B\underline{\underline{R}}_I \end{aligned} \quad (\text{B-6})$$

B.2 Spatial Angle Representation

B.2.1 Axis-Angle Representation

Rotation Matrix and Rodrigues' rotation formula

$$\underline{\underline{R}}_B = \underline{\underline{I}} + \frac{\sin \theta}{\theta} \tilde{\underline{\underline{\varphi}}} + \frac{1 - \cos \theta}{\theta^2} \tilde{\underline{\underline{\varphi}}} \tilde{\underline{\underline{\varphi}}} , \quad \theta = \|\underline{\underline{\varphi}}\| \quad (\text{B-7})$$

The relationship between first derivative of angle and angular velocity and curvature

$$\begin{aligned} {}_B \underline{\underline{\kappa}}^B &= \underline{\underline{T}} \underline{\underline{\varphi}}' & {}_B \underline{\omega}^B &= \underline{\underline{T}} \dot{\underline{\underline{\varphi}}} \\ \underline{\underline{T}}(\underline{\underline{\varphi}}) &= \underline{\underline{I}} + \frac{\cos \theta - 1}{\theta^2} \tilde{\underline{\underline{\varphi}}} + \frac{\theta - \sin \theta}{\theta^3} \tilde{\underline{\underline{\varphi}}} \tilde{\underline{\underline{\varphi}}} \end{aligned} \quad (\text{B-8})$$

The second derivative of angle

$$\begin{aligned} {}_B \dot{\underline{\omega}}^B &= \underline{\underline{T}} \dot{\underline{\underline{\varphi}}} + \dot{\underline{\underline{T}}} \dot{\underline{\underline{\varphi}}} \\ {}_B \dot{\underline{\underline{\kappa}}}^B &= {}_B \tilde{\underline{\omega}}^B \underline{\underline{T}} \underline{\underline{\varphi}}' + \underline{\underline{T}} \dot{\underline{\underline{\varphi}}}' + \dot{\underline{\underline{T}}} \underline{\underline{\varphi}}' \end{aligned} \quad (\text{B-9})$$

The derivative of $\underline{\underline{T}}$ can also be written as

$$\dot{\underline{\underline{T}}} \underline{\underline{\varphi}}' = \hat{\underline{\underline{T}}} \dot{\underline{\underline{\varphi}}} \quad \underline{\underline{T}}' \dot{\underline{\underline{\varphi}}} = \dot{\underline{\underline{T}}} \underline{\underline{\varphi}}' \quad (\text{B-10})$$

where

$$\begin{aligned} \dot{\underline{\underline{T}}}(\underline{\underline{\varphi}}, \dot{\underline{\underline{\varphi}}}) &= \underline{\underline{\varphi}}^T \dot{\underline{\underline{\varphi}}} \left[\frac{(1 - \cos \theta)\theta - 3(1 - \sin \theta)}{\theta^5} \tilde{\underline{\underline{\varphi}}} - \frac{\theta \sin \theta + 2(\cos \theta - 1)}{\theta^4} \underline{\underline{I}} \right] \tilde{\underline{\underline{\varphi}}} \\ &\quad + \frac{\cos \theta - 1}{\theta^2} \tilde{\underline{\underline{\varphi}}} + \frac{\theta - \sin \theta}{\theta^3} (\dot{\underline{\underline{\varphi}}} \tilde{\underline{\underline{\varphi}}} + \tilde{\underline{\underline{\varphi}}} \dot{\underline{\underline{\varphi}}}) \\ \hat{\underline{\underline{T}}}(\underline{\underline{\varphi}}, \underline{\underline{\varphi}}') &= \frac{\theta - \sin \theta}{\theta^3} (\underline{\underline{\varphi}} \underline{\underline{\varphi}}'^T - \underline{\underline{\varphi}}' \underline{\underline{\varphi}}^T - \tilde{\underline{\underline{\varphi}}} \tilde{\underline{\underline{\varphi}}}') - \frac{\cos \theta - 1}{\theta^2} \tilde{\underline{\underline{\varphi}}} \\ &\quad + \left[\frac{(1 - \cos \theta)\theta - 3(1 - \sin \theta)}{\theta^5} \tilde{\underline{\underline{\varphi}}} - \frac{\theta \sin \theta + 2(\cos \theta - 1)}{\theta^4} \underline{\underline{I}} \right] \tilde{\underline{\underline{\varphi}}} \underline{\underline{\varphi}}' \underline{\underline{\varphi}}^T \end{aligned} \quad (\text{B-11})$$

B.2.2 Tait-Bryan (Cardan) Angles

Sequence of the rotation

$$I \xrightarrow[\theta]{} {}^1\!Z \xrightarrow[\psi]{} {}^1\!Y \xrightarrow[\varphi]{} {}^2\!X \xrightarrow{} B \quad (\text{B-12})$$

Elementary rotation matrix

$$\begin{aligned} \underline{\underline{R}}_x(\varphi) &= {}^2\underline{\underline{R}}_B(\varphi) = \begin{bmatrix} 1 & 0 & 0 \\ 0 & \cos \varphi & -\sin \varphi \\ 0 & \sin \varphi & \cos \varphi \end{bmatrix} \\ \dot{\underline{\underline{R}}}_x(\varphi, \dot{\varphi}) &= {}^2\dot{\underline{\underline{R}}}_B(\varphi, \dot{\varphi}) = \begin{bmatrix} 0 & 0 & 0 \\ 0 & -\sin \varphi & -\cos \varphi \\ 0 & \cos \varphi & -\sin \varphi \end{bmatrix} \dot{\varphi} = \underline{\underline{T}}_x(\varphi) \dot{\varphi} \end{aligned} \quad (\text{B-13})$$

$$\begin{aligned} \underline{\underline{R}}_y(\psi) &= {}^1\underline{\underline{R}}_2(\psi) = \begin{bmatrix} \cos \psi & 0 & \sin \psi \\ 0 & 1 & 0 \\ -\sin \psi & 0 & \cos \psi \end{bmatrix} \\ \dot{\underline{\underline{R}}}_y(\psi, \dot{\psi}) &= {}^1\dot{\underline{\underline{R}}}_2(\psi, \dot{\psi}) = \begin{bmatrix} -\sin \psi & 0 & \cos \psi \\ 0 & 0 & 0 \\ -\cos \psi & 0 & -\sin \psi \end{bmatrix} \dot{\psi} = \underline{\underline{T}}_y(\psi) \dot{\psi} \end{aligned} \quad (\text{B-14})$$

$$\begin{aligned} \underline{\underline{R}}_z(\theta) &= {}^1\underline{\underline{R}}_1(\theta) = \begin{bmatrix} \cos \theta & -\sin \theta & 0 \\ \sin \theta & \cos \theta & 0 \\ 0 & 0 & 1 \end{bmatrix} \\ \dot{\underline{\underline{R}}}_z(\theta, \dot{\theta}) &= {}^1\dot{\underline{\underline{R}}}_1(\theta, \dot{\theta}) = \begin{bmatrix} -\sin \theta & -\cos \theta & 0 \\ \cos \theta & -\sin \theta & 0 \\ 0 & 0 & 0 \end{bmatrix} \dot{\theta} = \underline{\underline{T}}_z(\theta) \dot{\theta} \end{aligned} \quad (\text{B-15})$$

Rotation matrix

$$\begin{aligned} \underline{\underline{R}}_B &= {}^1\underline{\underline{R}}_B \\ &= \begin{bmatrix} \cos \psi \cos \theta & \sin \varphi \sin \psi \cos \theta - \cos \varphi \sin \theta & \cos \varphi \sin \psi \cos \theta + \sin \varphi \sin \theta \\ \cos \psi \sin \theta & \sin \varphi \sin \psi \sin \theta + \cos \varphi \cos \theta & \cos \varphi \sin \psi \sin \theta - \sin \varphi \cos \theta \\ -\sin \psi & \sin \varphi \cos \psi & \cos \varphi \cos \psi \end{bmatrix} \\ &= {}^1\underline{\underline{R}}_1(\theta) {}^1\underline{\underline{R}}_2(\psi) {}^2\underline{\underline{R}}_B(\varphi) \end{aligned} \quad (\text{B-16})$$

Angular velocity and curvature can be written as

$$\begin{aligned} {}_B\underline{\underline{\omega}} &= \begin{bmatrix} \dot{\phi} \\ 0 \\ 0 \end{bmatrix} + {}_B\underline{\underline{R}}_2 \begin{bmatrix} 0 \\ \dot{\psi} \\ 0 \end{bmatrix} + {}_B\underline{\underline{R}}_2 \underline{\underline{R}}_1 \begin{bmatrix} 0 \\ 0 \\ \dot{\theta} \end{bmatrix} = \underline{\underline{T}}\dot{\underline{\underline{\varphi}}} = \begin{bmatrix} \dot{\phi} - \sin \psi \dot{\theta} \\ \cos \psi \dot{\phi} + \sin \psi \cos \psi \dot{\theta} \\ -\sin \psi \dot{\phi} + \cos \psi \cos \psi \dot{\theta} \end{bmatrix} \\ {}_B\underline{\underline{\kappa}} &= \begin{bmatrix} \dot{\varphi}' \\ 0 \\ 0 \end{bmatrix} + {}_B\underline{\underline{R}}_2 \begin{bmatrix} 0 \\ \dot{\psi}' \\ 0 \end{bmatrix} + {}_B\underline{\underline{R}}_2 \underline{\underline{R}}_1 \begin{bmatrix} 0 \\ 0 \\ \dot{\theta}' \end{bmatrix} = \underline{\underline{T}}\dot{\underline{\underline{\varphi}}}' \end{aligned} \quad (\text{B-17})$$

Derivative of angular velocity and curvature

$$\begin{aligned} {}_B\underline{\dot{\omega}} &= \underline{\underline{T}}\dot{\underline{\underline{\varphi}}} + \dot{\underline{\underline{T}}}\dot{\underline{\underline{\varphi}}} \\ {}_B\underline{\omega}' &= \underline{\underline{T}}\dot{\underline{\underline{\varphi}}}' + \dot{\underline{\underline{T}}}\dot{\underline{\underline{\varphi}}} = \underline{\underline{T}}\dot{\underline{\underline{\varphi}}}' + \dot{\underline{\underline{T}}}\dot{\underline{\underline{\varphi}}}' \end{aligned} \quad (\text{B-18})$$

where

$$\begin{aligned} \underline{\underline{T}}(\underline{\underline{\varphi}}) &= \begin{bmatrix} 1 & 0 & -\sin \psi \\ 0 & \cos \psi & \sin \psi \cos \psi \\ 0 & -\sin \psi & \cos \psi \cos \psi \end{bmatrix} \\ \dot{\underline{\underline{T}}}(\underline{\underline{\varphi}}, \dot{\underline{\underline{\varphi}}}) &= \begin{bmatrix} 0 & 0 & -\cos \psi \dot{\psi} \\ 0 & -\sin \psi \dot{\phi} & \cos \psi \cos \psi \dot{\phi} - \sin \psi \sin \psi \dot{\psi} \\ 0 & -\cos \psi \dot{\phi} & -\sin \psi \cos \psi \dot{\phi} - \cos \psi \sin \psi \dot{\psi} \end{bmatrix} \\ \dot{\underline{\underline{T}}}(\underline{\underline{\varphi}}, \dot{\underline{\underline{\varphi}}}') &= \begin{bmatrix} 0 & 0 & -\cos \psi \dot{\psi}' \\ 0 & -\sin \psi \dot{\phi}' & \cos \psi \cos \psi \dot{\phi}' - \sin \psi \sin \psi \dot{\psi}' \\ 0 & -\cos \psi \dot{\phi}' & -\sin \psi \cos \psi \dot{\phi}' - \cos \psi \sin \psi \dot{\psi}' \end{bmatrix} \\ \dot{\underline{\underline{T}}} &= \begin{bmatrix} 0 & -\cos \psi \dot{\theta} & 0 \\ -\sin \psi \dot{\psi} + \cos \psi \cos \psi \dot{\theta} & -\sin \psi \sin \psi \dot{\theta} & 0 \\ -\cos \psi \dot{\psi} - \sin \psi \cos \psi \dot{\theta} & -\cos \psi \sin \psi \dot{\theta} & 0 \end{bmatrix} \end{aligned} \quad (\text{B-19})$$

Generally, the rotation matrix corresponds infinite cardan rotation vectors. However, for small rotation, the rotation matrix and the cardan rotation vector have a one-to-one correspondence.

The small cardan vector can be written as

$$\begin{aligned} \underline{\underline{\varphi}} &= [\varphi \ \psi \ \theta]^T \\ \varphi &= \sin^{-1} \frac{\underline{g}_z^T \underline{\underline{R}}_B \underline{g}_y}{\cos \psi} \quad \psi = -\sin^{-1} \frac{\underline{g}_z^T \underline{\underline{R}}_B \underline{g}_x}{\cos \psi} \quad \theta = \sin^{-1} \frac{\underline{g}_y^T \underline{\underline{R}}_B \underline{g}_x}{\cos \psi} \end{aligned} \quad (\text{B-20})$$

B.3 Kinematics of Co-rotational Coordinate

B.3.1 Co-rotational Coordinate

The generalized coordinate of flexible beam can be sometimes written as

$$\underline{q}_e = \begin{bmatrix} q_{e,1} \\ q_{e,2} \end{bmatrix} = \begin{bmatrix} {}_I\underline{r}^1 \\ \underline{\varphi}^1 \\ {}_I\underline{r}^2 \\ \underline{\varphi}^2 \end{bmatrix} \quad \underline{dq}_e = \begin{bmatrix} dq_{e,1} \\ dq_{e,2} \end{bmatrix} = \begin{bmatrix} {}_I\dot{\underline{r}}^1 \\ {}_1\omega^1 \\ {}_I\dot{\underline{r}}^2 \\ {}_2\omega^2 \end{bmatrix} \quad (\text{B-21})$$

The co-rotational coordinate can be written as

$$\underline{q}_B = \begin{bmatrix} {}_I\underline{r}^B \\ \underline{\varphi}^B \end{bmatrix} \quad \underline{dq}_B = \begin{bmatrix} {}_I\dot{\underline{r}}^B \\ {}_B\omega^B \end{bmatrix} \quad (\text{B-22})$$

The generalized velocity and acceleration can be written as

$$\underline{dq}_B = \underline{T}_B \underline{dq}_e \quad \underline{d}\dot{q}_B = \underline{T}_B \underline{d}\dot{q}_e + \underline{\dot{T}}_B \underline{dq}_e \quad (\text{B-23})$$

In order to make the calculation much simpler, the co-rotational coordinate is chosen as the coordinate at the end point of the beam element. If the first end point is selected, the relationship between the generalized coordinate and the co-rotational coordinate can be written as

$$\underline{\underline{T}}_B = \begin{bmatrix} I & 0 & 0 & 0 \\ 0 & I & 0 & 0 \\ 0 & 0 & I & 0 \\ 0 & 0 & 0 & I \end{bmatrix} \quad \begin{aligned} \underline{q}_B &= q_{e,1} & \underline{dq}_B &= \underline{dq}_{e,1} \\ \underline{\dot{T}}_B &= 0 & \underline{\dot{T}}_B &= 0 \end{aligned} \quad (\text{B-24})$$

If the first end point is selected, the relationship between the generalized coordinate and the co-rotational coordinate can be written as

$$\underline{\underline{T}}_B = \begin{bmatrix} 0 & 0 & I & 0 \\ 0 & 0 & 0 & I \\ 0 & 0 & 0 & I \\ 0 & 0 & 0 & I \end{bmatrix} \quad \begin{aligned} \underline{q}_B &= q_{e,2} & \underline{dq}_B &= \underline{dq}_{e,2} \\ \underline{\dot{T}}_B &= 0 & \underline{\dot{T}}_B &= 0 \end{aligned} \quad (\text{B-25})$$

B.3.2 Deformation Coordinate

Generalized Coordinate

Generalized coordinate of any point on the beam element

$$\begin{cases} {}_I \underline{r}^c = {}_I \underline{r}^B + \underline{R}_B ({}_B \underline{r}^{r,c} + {}_B \underline{u}^c) \\ \underline{\varphi}^c \leftarrow \underline{\underline{R}}_c = \underline{\underline{R}} (\underline{\varphi}^B) \underline{\underline{R}} ({}_B \underline{\psi}^c) = \underline{\underline{R}}_B \underline{\underline{R}} ({}_B \underline{\psi}^c) \end{cases}, \quad \underline{q}_c = \begin{bmatrix} {}_I \underline{r}^c \\ \underline{\varphi}^c \end{bmatrix} \quad (B-26)$$

Generalized deformation coordinate of any point on the beam element

$$\begin{cases} {}_B \underline{u}^c = \underline{R}_B^T ({}_I \underline{r}^c - {}_I \underline{r}^B) - {}_B \underline{r}^{r,c} \\ {}_B \underline{\psi}^c \leftarrow \underline{\underline{R}}_{d,c} = \underline{\underline{R}}_B^T \underline{\underline{R}}_c \end{cases}, \quad \underline{q}_{d,c} = \begin{bmatrix} {}_B \underline{u}^c \\ {}_B \underline{\psi}^c \end{bmatrix} \quad (B-27)$$

Generalized Velocity

Generalized velocity of any point on the beam element

$$\begin{cases} {}_I \dot{\underline{r}}^c = {}_I \dot{\underline{r}}^B + \underline{R}_B B \underline{\tilde{\omega}}^B ({}_B \underline{r}^{r,c} + {}_B \underline{u}^c) + \underline{R}_B B \dot{\underline{u}}^c \\ {}_c \underline{\omega}^c = \underline{R}_{d,c B}^T \underline{\omega}^B + {}_c \underline{\omega}^c \end{cases} \quad (B-28)$$

Generalized velocity coordinate of any point on the beam element

$$\begin{cases} {}_B \dot{\underline{u}}^c = \underline{\underline{R}}_B^T ({}_I \dot{\underline{r}}^c - {}_I \dot{\underline{r}}^B) - {}_B \underline{\tilde{\omega}}^B ({}_B \underline{r}^{r,c} + {}_B \underline{u}^c) \\ {}_c \underline{\tilde{\omega}}^c = {}_c \underline{\omega}^c - \underline{R}_{d,c B}^T \underline{\omega}^B \end{cases} \quad (B-29)$$

Generalized Acceleration

Generalized acceleration of any point on the beam element

$$\begin{aligned} {}_I \ddot{\underline{r}}^c &= {}_I \ddot{\underline{r}}^B + \underline{R}_B B \underline{\tilde{\omega}}^B ({}_B \underline{r}^{r,c} + {}_B \underline{u}^c) + \underline{R}_B B \ddot{\underline{u}}^c + \underline{R}_B B \underline{\tilde{\omega}}^B B \underline{\tilde{\omega}}^B ({}_B \underline{r}^{r,c} + {}_B \underline{u}^c) \\ &\quad + 2 \underline{R}_B B \underline{\tilde{\omega}}^B {}_B \dot{\underline{u}}^c \\ {}_c \dot{\underline{\omega}}^c &= \underline{R}_{d,c B}^T \underline{\dot{\omega}}^B + {}_c \underline{\dot{\omega}}^c - {}_c \underline{\tilde{\omega}}^c \underline{R}_{d,c B}^T \underline{\omega}^B \end{aligned} \quad (B-30)$$

Generalized acceleration coordinate of any point on the beam element

$$\begin{aligned} {}_B \underline{\dot{u}}^c &= \underline{\underline{R}}_B^T (\underline{\dot{r}}^c - \underline{\dot{r}}^B) - {}_B \underline{\tilde{\omega}}^B (\underline{\dot{r}}^{r,c} + {}_B \underline{u}^c) + {}_B \underline{\tilde{\omega}}^B {}_B \underline{\tilde{\omega}}^B (\underline{\dot{r}}^{r,c} + {}_B \underline{u}^c) \\ &\quad - 2 {}_B \underline{\tilde{\omega}}^B \underline{\underline{R}}_B^T (\underline{\dot{r}}^c - \underline{\dot{r}}^B) \\ {}_c \underline{\dot{\omega}}^c &= {}_c \underline{\dot{\omega}}^c - \underline{\underline{R}}_{d,cB}^T \underline{\dot{\omega}}^B + {}_c \underline{\tilde{\omega}}^c \underline{\underline{R}}_{d,cB}^T \underline{\omega}^B \end{aligned} \quad (\text{B-31})$$

B.3.3 Relationship between Global Coordinate and Deformation Coordinate

The deformation velocity can be written through generalized velocity of the beam element and point on the beam.

$$\underline{dq}_{d,c} = \begin{bmatrix} {}_B \dot{u}^c \\ {}_c \underline{\dot{\omega}}^c \end{bmatrix} = \begin{bmatrix} -\underline{\underline{R}}_B^T & {}_B \underline{\tilde{r}}^{r,c} + {}_B \underline{\tilde{u}}^c & \underline{\underline{R}}_B^T & \underline{\underline{0}} \\ \underline{\underline{0}} & -\underline{\underline{R}}_{d,c}^T & \underline{\underline{0}} & \underline{\underline{I}} \end{bmatrix} \begin{bmatrix} \underline{dq}_B \\ \underline{dq}_c \end{bmatrix} = \underline{\underline{T}}_{d,c} \begin{bmatrix} \underline{dq}_B \\ \underline{dq}_c \end{bmatrix} \quad (\text{B-32})$$

The deformation acceleration can be written through generalized acceleration of the beam element and point on the beam.

$$\begin{aligned} \underline{d\dot{q}}_{d,c} &= \begin{bmatrix} {}_B \ddot{u}^c \\ {}_c \underline{\ddot{\omega}}^c \end{bmatrix} = \underline{\underline{T}}_{d,c} \begin{bmatrix} \underline{d\dot{q}}_B \\ \underline{d\dot{q}}_c \end{bmatrix} + \underline{\dot{\underline{T}}}_{d,c} \begin{bmatrix} \underline{dq}_B \\ \underline{dq}_c \end{bmatrix} \\ \underline{\dot{\underline{T}}}_{d,c} &= \begin{bmatrix} 2 {}_B \underline{\tilde{\omega}}^B \underline{\underline{R}}_B^T & -{}_B \underline{\tilde{\omega}}^B (\underline{\dot{r}}^{r,c} + {}_B \underline{\tilde{u}}^c) & -2 {}_B \underline{\tilde{\omega}}^B \underline{\underline{R}}_B^T & \underline{\underline{0}} \\ \underline{\underline{0}} & {}_c \underline{\tilde{\omega}}^c \underline{\underline{R}}_{d,c}^T & \underline{\underline{0}} & \underline{\underline{0}} \end{bmatrix} \end{aligned} \quad (\text{B-33})$$

The generalized velocity of point on the beam can be written through generalized velocity of the beam element and deformation velocity.

$$\begin{aligned} \underline{dq}_c &= \begin{bmatrix} {}_I \dot{r}^c \\ {}_c \underline{\dot{\omega}}^c \end{bmatrix} = \begin{bmatrix} \underline{\underline{T}}_{d,r,c}^{-1} \\ \underline{\underline{T}}_{d,\varphi,c}^{-1} \end{bmatrix} \begin{bmatrix} \underline{dq}_B \\ \underline{dq}_{d,c} \end{bmatrix} = \underline{\underline{T}}_{d,c}^{-1} \begin{bmatrix} \underline{dq}_B \\ \underline{dq}_{d,c} \end{bmatrix} \\ \underline{\underline{T}}_{d,r,c}^{-1} &= \begin{bmatrix} \underline{\underline{I}} & -\underline{\underline{R}}_B (\underline{\dot{r}}^{r,c} + {}_B \underline{\tilde{u}}^c) & \underline{\underline{R}}_B & \underline{\underline{0}} \\ \underline{\underline{0}} & \underline{\underline{R}}_{d,c}^T & \underline{\underline{0}} & \underline{\underline{I}} \end{bmatrix} \\ \underline{\underline{T}}_{d,\varphi,c}^{-1} &= \begin{bmatrix} \underline{\underline{0}} & \underline{\underline{R}}_{d,c}^T & \underline{\underline{0}} & \underline{\underline{I}} \end{bmatrix} \end{aligned} \quad (\text{B-34})$$

The generalized acceleration of point on the beam can be written through generalized acceleration of the beam element and deformation acceleration.

$$\begin{aligned}
 \underline{\underline{d}\dot{q}_c} &= \begin{bmatrix} {}^I\ddot{r}^c \\ {}_c\dot{\omega}^c \end{bmatrix} = \underline{\underline{T}}_{d,c}^{-1} \begin{bmatrix} d\dot{q}_B \\ d\dot{q}_{d,c} \end{bmatrix} + \begin{bmatrix} \dot{\underline{\underline{T}}}_{d,r,c}^{-1} \\ \dot{\underline{\underline{T}}}_{d,\varphi,c}^{-1} \end{bmatrix} \begin{bmatrix} dq_B \\ dq_{d,c} \end{bmatrix} = \underline{\underline{T}}_{d,c}^{-1} \begin{bmatrix} d\dot{q}_B \\ d\dot{q}_{d,c} \end{bmatrix} + \dot{\underline{\underline{T}}}_{d,c}^{-1} \begin{bmatrix} dq_B \\ dq_{d,c} \end{bmatrix} \\
 \dot{\underline{\underline{T}}}_{d,r,c}^{-1} &= \begin{bmatrix} 0 & -R_{BB}\widetilde{\omega}^B \left({}_B\tilde{r}^{r,c} + {}_B\tilde{u}^c \right) & 2R_{BB}\widetilde{\omega}^B & 0 \end{bmatrix} \\
 \dot{\underline{\underline{T}}}_{d,\varphi,c}^{-1} &= \begin{bmatrix} 0 & -{}_c\widetilde{\omega}^c R_{d,c}^T & 0 & 0 \end{bmatrix}
 \end{aligned} \tag{B-35}$$

B.3.4 Deformation Coordinate at Boundary

The deformation coordinate of the end point can be written as

$$\underline{q}_{d,end} = \begin{bmatrix} q_{d,1} \\ q_{d,2} \end{bmatrix} \tag{B-36}$$

The deformation velocity of the end point can be written as

$$\begin{aligned}
 \underline{dq}_{d,end} &= \begin{bmatrix} dq_{d,1} \\ dq_{d,2} \end{bmatrix} = {}_{d,end} \underline{\underline{T}}_{Be} \begin{bmatrix} dq_B \\ dq_1 \\ dq_2 \end{bmatrix} = {}_{d,end} \underline{\underline{T}}_{Be} \underline{\underline{T}}_e \underline{dq}_e = \underline{\underline{T}}_{d,end} \underline{dq}_e \\
 {}_{d,end} \underline{\underline{T}}_{Be} &= \begin{bmatrix} -R_B^T & {}_B\tilde{r}^{r,1} + {}_B\tilde{u}^1 & R_B^T & 0 & 0 & 0 \\ 0 & -R_{d,1}^T & 0 & I & 0 & 0 \\ -R_B^T & {}_B\tilde{r}^{r,2} + {}_B\tilde{u}^2 & 0 & 0 & R_B^T & 0 \\ 0 & -R_{d,2}^T & 0 & 0 & 0 & I \end{bmatrix}, \quad {}_{Be} \underline{\underline{T}}_e = \begin{bmatrix} T_B \\ I \\ 0 \end{bmatrix}
 \end{aligned} \tag{B-37}$$

The deformation acceleration of the end point can be written as

$$\begin{aligned}
 \underline{d\dot{q}}_{d,end} &= \begin{bmatrix} d\dot{q}_{d,1}^T & d\dot{q}_{d,2}^T \end{bmatrix}^T = \underline{\underline{T}}_{d,end} \underline{d\dot{q}}_e + \dot{\underline{\underline{T}}}_{d,end} \underline{dq}_e \\
 &= \underline{\underline{T}}_{d,end} \begin{bmatrix} d\dot{q}_B^T & d\dot{q}_1^T & d\dot{q}_2^T \end{bmatrix}^T + \dot{\underline{\underline{T}}}_{d,end} \begin{bmatrix} dq_B^T & dq_1^T & dq_2^T \end{bmatrix}^T \\
 &= {}_{d,end} \underline{\underline{T}}_{Be} \underline{\underline{T}}_e \underline{d\dot{q}}_e + \left({}_{d,end} \underline{\underline{T}}_{Be} \underline{\underline{T}}_e \dot{\underline{\underline{T}}}_e + {}_{d,end} \dot{\underline{\underline{T}}}_{Be} \underline{\underline{T}}_e \right) \underline{dq}_e \\
 {}_{d,end} \dot{\underline{\underline{T}}}_{Be} &= \begin{bmatrix} 2 {}_B\widetilde{\omega}^B R_B^T & - {}_B\widetilde{\omega}^B \left({}_B\tilde{r}^{r,1} + {}_B\tilde{u}^1 \right) & -2 {}_B\widetilde{\omega}^B R_B^T & 0 & 0 & 0 \\ 0 & {}_1\widetilde{\omega}^1 R_{d,1}^T & 0 & 0 & 0 & 0 \\ 2 {}_B\widetilde{\omega}^B R_B^T & - {}_B\widetilde{\omega}^B \left({}_B\tilde{r}^{r,2} + {}_B\tilde{u}^2 \right) & 0 & 0 & -2 {}_B\widetilde{\omega}^B R_B^T & 0 \\ 0 & {}_2\widetilde{\omega}^2 R_{d,2}^T & 0 & 0 & 0 & 0 \end{bmatrix} \\
 {}_{Be} \dot{\underline{\underline{T}}}_e &= \begin{bmatrix} \dot{\underline{\underline{T}}}_B^T & 0 \end{bmatrix}^T
 \end{aligned} \tag{B-38}$$

Appendix C Detailed Dynamics Models of Different Types of Elements

C.1 Rigid Body Dynamic Model

C.1.1 Generalized Coordination and Generalized Velocity

$$\underline{q}_e = \begin{bmatrix} {}_I \underline{r}^0 \\ \underline{\varphi} \end{bmatrix} \quad \underline{dq}_e = \begin{bmatrix} {}_I \dot{\underline{r}}^0 \\ {}_B \underline{\omega} \end{bmatrix} = \begin{bmatrix} {}_I \dot{\underline{r}}^0 \\ {}_T \dot{\underline{\varphi}} \end{bmatrix} \quad (\text{C-1})$$

C.1.2 Kinematic

$$\begin{aligned} {}_I \underline{r}^k &= {}_I \underline{r}^0 + \underline{\underline{R}}_B \underline{r}^{0k} \\ {}_I \dot{\underline{r}}^k &= {}_I \dot{\underline{r}}^0 + \underline{\underline{R}}_B \underline{\tilde{\omega}}_B \underline{r}^{0k} = {}_I \dot{\underline{r}}^0 - \underline{\underline{R}}_B \underline{\tilde{r}}^{0k} \underline{B} \underline{\omega} \\ {}_I \ddot{\underline{r}}^k &= {}_I \ddot{\underline{r}}^0 + \left(\underline{\underline{R}}_B \dot{\underline{\tilde{\omega}}} + \underline{\underline{R}}_B \underline{\tilde{\omega}}_B \underline{\tilde{\omega}} \right) \underline{B} \underline{r}^{0k} = {}_I \ddot{\underline{r}}^0 - \underline{\underline{R}}_B \underline{\tilde{r}}^{0k} \underline{B} \underline{\dot{\omega}} + \underline{\underline{R}}_B \underline{\tilde{\omega}}_B \underline{\tilde{r}}^{0k} \underline{B} \underline{\omega} \end{aligned} \quad (\text{C-2})$$

C.1.3 Virtual inertial power

$$\begin{aligned} \delta p_{ine} &= - \int_{\Omega} \delta {}_I \dot{\underline{r}}^k {}^T {}_I \ddot{\underline{r}}^k \rho d\Omega = - \delta \underline{dq}_e^T \left(\underline{\underline{M}}_e \underline{d\dot{q}}_e + \underline{\underline{D}}_e \underline{dq}_e \right) \\ \underline{\underline{M}}_e &= \begin{bmatrix} m_{tot} \underline{\underline{I}} & -m_{tot} \underline{\underline{R}}^T \underline{\underline{B}} \underline{\tilde{r}}^{0C} \\ m_{tot} \underline{\underline{B}} \underline{\tilde{r}}^{0C} \underline{\underline{R}}^T & \underline{\underline{B}} \underline{\Theta}^0 \end{bmatrix} \\ \underline{\underline{D}}_e &= \begin{bmatrix} 0 & m_{tot} \underline{\underline{R}}_B \underline{\tilde{\omega}}_B \underline{\tilde{r}}^{0C} \\ 0 & \underline{\underline{B}} \underline{\tilde{\omega}}_B \underline{\underline{\Theta}}^0 \end{bmatrix} \quad \underline{F}_{ine} = \underline{\underline{D}}_e \underline{dq}_e \end{aligned} \quad (\text{C-3})$$

with

$$\begin{aligned} \int_{\Omega} \rho d\Omega &= m_{tot} & \int_{\Omega} \rho_B \underline{\underline{B}} \underline{\tilde{r}}^{0k} {}^T \underline{\underline{B}} \underline{\tilde{r}}^{0k} d\Omega &= - \underline{\underline{B}} \underline{\Theta}^0 \\ \int_{\Omega} \rho_B \underline{r}^{0k} d\Omega &= m_{tot} \underline{B} \underline{r}^{0C} & \int_{\Omega} \rho_B \underline{\tilde{r}}^{0k} d\Omega &= m_{tot} \underline{B} \underline{\tilde{r}}^{0C} \end{aligned} \quad (\text{C-4})$$

C.1.4 Virtual external power

$$\begin{aligned}\delta p_{ext} &= \int_{\Omega} \delta_I \dot{\underline{r}}^k {}^I g \rho d\Omega = -\delta \underline{d} \underline{q}_e^T \underline{V}_{ext,g} {}^I g \\ \underline{V}_{ext,g} &= -m_{tot} \begin{bmatrix} I \\ {}^B \underline{\tilde{r}}^0 C \underline{\underline{R}}^T \end{bmatrix} \quad \underline{F}_{ext,g} = \underline{V}_{ext,g} {}^I g\end{aligned}\quad (\text{C-5})$$

C.1.5 Virtual power principle for Rigid Body

$$\begin{aligned}\delta p_e &= \delta p_{ine} + \delta p_{int} + \delta p_{ext} = \delta p_{ine} + \delta p_{ext,g} \\ &= -\delta \underline{d} \underline{q}_e^T (M_e \underline{d} \dot{\underline{q}}_e + F_{ine} + F_{ext,g}) = -\delta \underline{d} \underline{q}_e^T (M_e \underline{d} \dot{\underline{q}}_e + F_e)\end{aligned}\quad (\text{C-6})$$

C.2 Spatial Timoshenko Beam Dynamic Model based on Co-rotational Coordination

C.2.1 Generalized coordination

$$\underline{q}_e = \begin{bmatrix} q_1 \\ q_2 \end{bmatrix} = \begin{bmatrix} {}^I \underline{r}^1 \\ \underline{\varphi}^1 \\ {}^I \underline{r}^2 \\ \underline{\varphi}^2 \end{bmatrix} \quad \underline{d} \underline{q}_e = \begin{bmatrix} \underline{d} q_1 \\ \underline{d} q_2 \end{bmatrix} = \begin{bmatrix} {}^I \dot{\underline{r}}^1 \\ {}^1 \underline{\omega}^1 \\ {}^I \dot{\underline{r}}^2 \\ {}^2 \underline{\omega}^2 \end{bmatrix} \quad (\text{C-7})$$

C.2.2 Co-rotational Coordination

$$\underline{q}_B = \begin{bmatrix} {}^I \underline{r}^B \\ \underline{\varphi}^B \end{bmatrix} \quad \underline{d} \underline{q}_B = \begin{bmatrix} {}^I \dot{\underline{r}}^B \\ {}^B \underline{\omega}^B \end{bmatrix} \quad (\text{C-8})$$

Here we choose

$$\begin{aligned}\underline{q}_B &= \begin{bmatrix} {}^I \underline{r}^1 \\ \underline{\varphi}^1 \end{bmatrix} \quad \underline{d} \underline{q}_B = \begin{bmatrix} {}^I \dot{\underline{r}}^1 \\ {}^1 \underline{\omega}^1 \end{bmatrix} \\ \underline{\underline{R}}_B &= {}^I \underline{\underline{R}}_B = \underline{\underline{R}}(\underline{\varphi}^B)\end{aligned}\quad (\text{C-9})$$

C.2.3 Timoshenko Beam Assumption

$$\begin{aligned} {}_I \underline{r}^* &= {}_I \underline{r}^c + \underline{\underline{R}}_B c \underline{t} = {}_I \underline{r}^B + \underline{\underline{R}}_B ({}_{\underline{B}} \underline{r}^{r,c} + {}_c \underline{t}) \\ {}_I \underline{r} &= {}_I \underline{r}^c + \underline{\underline{R}}_B \underline{R}_{d,c} c \underline{t} = {}_I \underline{r}^B + \underline{\underline{R}}_B ({}_{\underline{B}} \underline{r}^{r,c} + {}_B \underline{u}^c + \underline{\underline{R}}_{d,c} c \underline{t}) \end{aligned} \quad (\text{C-10})$$

$$\begin{aligned} {}_I \underline{u} &= {}_I \underline{r} - {}_I \underline{r}^* = \underline{\underline{R}}_B \left[{}_B \underline{u}^c + \left(\underline{\underline{R}}_{d,c} - \underline{\underline{I}} \right) c \underline{t} \right] \\ {}_B \underline{u} &= \underline{\underline{R}}_B^T {}_I \underline{u} = {}_B \underline{u}^c + \left(\underline{\underline{R}}_{d,c} - \underline{\underline{I}} \right) c \underline{t} \end{aligned} \quad (\text{C-11})$$

Small deformation assumption

$$\underline{\underline{R}}_{d,c} = \underline{\underline{R}} \left({}_B \underline{\psi}^c \right) \approx \underline{\underline{I}} + {}_B \underline{\tilde{\psi}}^c \quad (\text{C-12})$$

$${}_B \underline{u} \approx {}_B \underline{u}^c + {}_B \underline{\tilde{\psi}}^c c \underline{t} = \begin{bmatrix} {}_B u^c - {}_B \theta^c {}_c y + {}_B \psi^c {}_c z \\ {}_B v^c - {}_B \varphi^c {}_c z \\ {}_B w^c + {}_B \varphi^c {}_c y \end{bmatrix} = \begin{bmatrix} {}_B u \\ {}_B v \\ {}_B w \end{bmatrix} \quad (\text{C-13})$$

C.2.4 Kinematic

$$\begin{aligned} {}_I \dot{\underline{r}} &= {}_I \dot{\underline{r}}^c + \underline{\underline{\Omega}}_c c \underline{t} = \left(\underline{\underline{H}}_t + \underline{\underline{H}}_{r,t} \right) \begin{bmatrix} \frac{dq_B}{dq_{d,c}} \\ \vdots \end{bmatrix} \\ \underline{\underline{\Omega}}_c &= \underline{\underline{R}}_B \underline{\tilde{\omega}}^B \underline{R}_{d,c} + \underline{\underline{R}}_B \underline{R}_{d,c} c \underline{\tilde{\omega}}^c \\ \underline{\underline{H}}_t &= \underline{\underline{T}}_{d,r,c}^{-1} = \begin{bmatrix} \underline{\underline{I}} & -\underline{\underline{R}}_B \left({}_B \tilde{r}^{r,c} + {}_B \tilde{u}^c \right) & \underline{\underline{R}}_B & \underline{\underline{0}} \\ \underline{\underline{0}} & -\underline{\underline{R}}_c c \underline{\tilde{t}} \underline{R}_{d,c}^T & \underline{\underline{0}} & -\underline{\underline{R}}_c c \underline{\tilde{t}} \end{bmatrix} \\ \underline{\underline{H}}_{r,t} &= \begin{bmatrix} \underline{\underline{0}} & -\underline{\underline{R}}_c c \underline{\tilde{t}} R_{d,c}^T & \underline{\underline{0}} & -\underline{\underline{R}}_c c \underline{\tilde{t}} \end{bmatrix} \end{aligned} \quad (\text{C-14})$$

$$\begin{aligned} {}_I \ddot{\underline{r}} &= {}_I \ddot{\underline{r}}^c + \underline{\underline{A}}_c c \underline{t} = \left(\underline{\underline{H}}_t + \underline{\underline{H}}_{r,t} \right) \begin{bmatrix} \frac{d\dot{q}_B}{dq_{d,c}} \\ \vdots \end{bmatrix} + \left(\underline{\underline{D}}_t + \underline{\underline{D}}_{r,t} \right) \begin{bmatrix} \frac{dq_B}{dq_{d,c}} \\ \vdots \end{bmatrix} \\ \underline{\underline{A}}_c &= \underline{\underline{R}}_B \underline{\tilde{\omega}}^B \underline{R}_{d,c} + \underline{\underline{R}}_B \underline{R}_{d,c} c \underline{\tilde{\omega}}^c + \underline{\underline{R}}_B \underline{\tilde{\omega}}^B {}_B \underline{\tilde{\omega}}^B \underline{R}_{d,c} + 2 \underline{\underline{R}}_B \underline{\tilde{\omega}}^B \underline{R}_{d,c} c \underline{\tilde{\omega}}^c \\ &\quad + \underline{\underline{R}}_B \underline{R}_{d,c} c \underline{\tilde{\omega}}^c c \underline{\tilde{\omega}}^c \\ \underline{\underline{D}}_t &= \underline{\underline{T}}_{d,r,c}^{-1} = \begin{bmatrix} \underline{\underline{0}} & -\underline{\underline{R}}_B \underline{\tilde{\omega}}^B \left({}_B \tilde{r}^{r,c} + {}_B \tilde{u}^c \right) & 2 \underline{\underline{R}}_B \underline{\tilde{\omega}}^B & \underline{\underline{0}} \\ \underline{\underline{0}} & -\underline{\underline{R}}_B \underline{\tilde{\omega}}^B \underline{R}_{d,c} c \underline{\tilde{t}} \underline{R}_{d,c}^T & \underline{\underline{0}} & -\left(2 \underline{\underline{R}}_B \underline{\tilde{\omega}}^B \underline{R}_{d,c} + \underline{\underline{R}}_c c \underline{\tilde{\omega}}^c \right) c \underline{\tilde{t}} \end{bmatrix} \end{aligned} \quad (\text{C-15})$$

C.2.5 Strain

Because of the small deformation assumption

$$\begin{aligned}
 {}_B\epsilon_{ij} &= \frac{1}{2} \left(\frac{\partial_B u_i}{\partial_B x_j} + \frac{\partial_B u_j}{\partial_B x_i} \right) \approx \frac{1}{2} \left(\frac{\partial_B u_i}{\partial_c x_j} + \frac{\partial_B u_j}{\partial_c x_i} \right) \\
 \left\{ \begin{array}{l} {}_B\epsilon_{xx} = \frac{\partial_B u}{\partial_c x} = {}_B u^{c'} - {}_B \theta^{c'} {}_c y + {}_B \psi^{c'} {}_c z \\ {}_B\epsilon_{xy} = \frac{1}{2} \left(\frac{\partial_B u}{\partial_c y} + \frac{\partial_B v}{\partial_c x} \right) = \frac{1}{2} ({}_B v^{c'} - {}_B \varphi^{c'} {}_c z - {}_B \theta^c) \\ {}_B\epsilon_{xz} = \frac{1}{2} \left(\frac{\partial_B u}{\partial_c z} + \frac{\partial_B w}{\partial_c x} \right) = \frac{1}{2} ({}_B w^{c'} + {}_B \varphi^{c'} {}_c y + {}_B \psi^c) \\ {}_B\epsilon_{yy} = {}_B\epsilon_{yz} = {}_B\epsilon_{zz} = 0 \end{array} \right. \quad (C-16)
 \end{aligned}$$

C.2.6 Shape function

$$\begin{aligned}
 \underline{q}_{d,c} &= \underline{\underline{N}}_c \underline{q}_{d,end} & \dot{\underline{q}}_{d,c} &= \underline{\underline{N}}_c \dot{\underline{q}}_{d,end} \\
 \underline{\underline{N}}_c &= [\underline{\underline{N}}_{c,1} \quad \underline{\underline{N}}_{c,2}] = \begin{bmatrix} \underline{\underline{N}}_{c,u,u1} & \underline{\underline{N}}_{c,u,\varphi 1} & \underline{\underline{N}}_{c,u,u2} & \underline{\underline{N}}_{c,u,\varphi 2} \\ \underline{\underline{N}}_{c,\varphi,u1} & \underline{\underline{N}}_{c,\varphi,\varphi 1} & \underline{\underline{N}}_{c,\varphi,u2} & \underline{\underline{N}}_{c,\varphi,\varphi 2} \end{bmatrix} \quad (C-17)
 \end{aligned}$$

As it is assumed that no external force is applied on the element, and external virtual work only contributes to the inhomogeneous terms, therefore, the homogeneous equations are obtained as

$$\begin{aligned}
 & -\underline{\underline{H}}_1 \underline{q}_c'' + \left(\underline{\underline{H}}_3 - \underline{\underline{H}}_2 \right) \underline{q}_c' + \underline{\underline{H}}_4 \underline{q}_c = \underline{0} \\
 & \underline{k} \underline{u}'' {}_c = 0 \\
 & \underline{k} \underline{v}'' {}_c - \theta' = 0 \\
 & \underline{k} \underline{w}'' {}_c + \psi' = 0 \\
 & \underline{\varphi}'' = 0 \\
 \left\{ \begin{array}{l} \frac{4EI_z}{GA} \psi'' - \underline{k} \underline{w}' {}_c - \psi = k_z \psi'' - \underline{k} \underline{w}' {}_c - \psi = 0 \\ \frac{4EI_y}{GA} \theta'' + \underline{k} \underline{v}' {}_c - \theta = k_y \theta'' + \underline{k} \underline{v}' {}_c - \theta = 0 \end{array} \right. \quad (C-18)
 \end{aligned}$$

$$\begin{aligned}
 \underline{q}_{uc} &= \underline{\underline{N}} \underline{q}_{uce} & \dot{\underline{q}}_{uc} &= \underline{\underline{N}} \dot{\underline{q}}_{uce} \\
 \underline{q}'_{uc} &= \underline{\underline{N}'} \underline{q}_{uce} & \underline{q}''_{uc} &= \underline{\underline{N}''} \underline{q}_{uce} \quad (C-19)
 \end{aligned}$$

To simplify the shape function, we define the following parameter

$$\begin{aligned}\xi &= \frac{x}{L} & \alpha_y &= \frac{48EI_y}{AGL^2} & \beta_y &= \frac{1}{\alpha_y + 1} \\ \alpha_z &= \frac{48EI_z}{AGL^2} & \beta_z &= \frac{1}{\alpha_z + 1}\end{aligned}\quad (\text{C-20})$$

$$\begin{aligned}{}_k u''_c &= 0 \rightarrow {}_k u_c = N_{u,u} {}_k u_{ce} = \xi {}_k u_{ce} \\ N_{u,u} &= \xi & N'_{u,u} &= 1 & N''_{u,u} &= 0\end{aligned}\quad (\text{C-21})$$

$$\begin{aligned}\varphi'' &= 0 \rightarrow \varphi = N_{\varphi,\varphi} \varphi_e = \xi \varphi_e \\ N_{\varphi,\varphi} &= \xi & N_{\varphi,\varphi} &= 1 & N_{\varphi,\varphi} &= 0\end{aligned}\quad (\text{C-22})$$

$$\begin{aligned}\begin{cases} {}_k v''_c - \theta' = 0 \\ {}_k \theta'' + {}_k v'_c - \theta = 0 \end{cases} &\rightarrow \begin{cases} {}_k v_c = N_{v,v} {}_k v_{ce} + N_{v,\theta} \theta_e \\ \theta = N_{\theta,v} {}_k v_{ce} + N_{\theta,\theta} \theta_e \end{cases} \\ N_{v,v} &= \beta_y (-2\xi^3 + 3\xi^2 + \alpha_y \xi) & N_{v,\theta} &= \beta_y L \left(\xi^3 + \frac{\alpha_y - 2}{2} \xi^2 - \frac{\alpha_y}{2} \xi \right) \\ N'_{v,v} &= \frac{\beta_y}{L} (-6\xi^2 + 6\xi + \alpha_y) & N'_{v,\theta} &= \beta_y \left(3\xi^2 + (\alpha_y - 2)\xi - \frac{\alpha_y}{2} \right) \\ N''_{v,v} &= \frac{\beta_y}{L^2} (-12\xi + 6) & N''_{v,\theta} &= \frac{\beta_y}{L} (6\xi + (\alpha_y - 2)) \\ N_{\theta,v} &= -\frac{6\beta_y}{L} (\xi^2 - \xi) & N_{\theta,\theta} &= \beta_y (3\xi^2 + (\alpha_y - 2)\xi) \\ N'_{\theta,v} &= -\frac{6\beta_y}{L^2} (2\xi - 1) & N'_{\theta,\theta} &= \frac{\beta_y}{L} (6\xi + (\alpha_y - 2)) \\ N'_{\theta,v} &= -\frac{12\beta_y}{L^3} & N'_{\theta,\theta} &= \frac{6\beta_y}{L^2}\end{aligned}\quad (\text{C-23})$$

$$\begin{aligned}\begin{cases} {}_k w''_c + \psi' = 0 \\ {}_k z \psi'' - {}_k w'_c - \psi = 0 \end{cases} &\rightarrow \begin{cases} {}_k w_c = N_{w,w} {}_k w_{ce} + N_{w,\psi} \psi_e \\ {}_k z \psi_c = N_{w,w} {}_k w_{ce} + N_{w,\psi} \psi_e \end{cases} \\ N_{w,w} &= \beta_z (-2\xi^3 + 3\xi^2 + \alpha_z \xi) & N_{w,\psi} &= -\beta_z L \left(\xi^3 + \frac{\alpha_z - 2}{2} \xi^2 - \frac{\alpha_z}{2} \xi \right) \\ N'_{w,w} &= \frac{\beta_z}{L} (-6\xi^2 + 6\xi + \alpha_z) & N'_{w,\psi} &= -\beta_z \left(3\xi^2 + (\alpha_z - 2)\xi - \frac{\alpha_z}{2} \right) \\ N''_{w,w} &= \frac{\beta_z}{L^2} (-12\xi + 6) & N''_{w,\psi} &= -\frac{\beta_z}{L} (6\xi + (\alpha_z - 2)) \\ N_{\psi,w} &= \frac{6\beta_z}{L} (\xi^2 - \xi) & N_{\psi,\psi} &= \beta_z (3\xi^2 + (\alpha_z - 2)\xi) \\ N'_{\psi,w} &= \frac{6\beta_z}{L^2} (2\xi - 1) & N'_{\psi,\psi} &= \frac{\beta_z}{L} (6\xi + (\alpha_z - 2)) \\ N'_{\psi,w} &= \frac{12\beta_z}{L^3} & N''_{\psi,\psi} &= \frac{6\beta_z}{L^2}\end{aligned}\quad (\text{C-24})$$

$$\begin{aligned}
 \underline{\underline{N}} &= \begin{bmatrix} N_{u,u} & 0 & 0 & 0 & 0 & 0 \\ 0 & N_{v,v} & 0 & 0 & 0 & N_{v,\theta} \\ 0 & 0 & N_{w,w} & 0 & N_{w,\psi} & 0 \\ 0 & 0 & 0 & N_{\varphi,\varphi} & 0 & 0 \\ 0 & 0 & N_{\psi,w} & 0 & N_{\psi,\psi} & 0 \\ 0 & N_{\theta,v} & 0 & 0 & 0 & N_{\theta,\theta} \end{bmatrix} \\
 \underline{\underline{N'}} &= \begin{bmatrix} N'_{u,u} & 0 & 0 & 0 & 0 & 0 \\ 0 & N'_{v,v} & 0 & 0 & 0 & N'_{v,\theta} \\ 0 & 0 & N'_{w,w} & 0 & N'_{w,\psi} & 0 \\ 0 & 0 & 0 & N'_{\varphi,\varphi} & 0 & 0 \\ 0 & 0 & N'_{\psi,w} & 0 & N'_{\psi,\psi} & 0 \\ 0 & N'_{\theta,v} & 0 & 0 & 0 & N'_{\theta,\theta} \end{bmatrix} \\
 \underline{\underline{N''}} &= \begin{bmatrix} N''_{u,u} & 0 & 0 & 0 & 0 & 0 \\ 0 & N''_{v,v} & 0 & 0 & 0 & N''_{v,\theta} \\ 0 & 0 & N''_{w,w} & 0 & N''_{w,\psi} & 0 \\ 0 & 0 & 0 & N''_{\varphi,\varphi} & 0 & 0 \\ 0 & 0 & N''_{\psi,w} & 0 & N''_{\psi,\psi} & 0 \\ 0 & N''_{\theta,v} & 0 & 0 & 0 & N''_{\theta,\theta} \end{bmatrix}
 \end{aligned} \tag{C-25}$$

C.2.7 Internal Node with small deformation assumption

$$\underline{dq}_c = \underline{T}_{d,c}^{-1} \left[\frac{dq_B}{dq_{d,c}} \right] = \underline{T}_{d,c}^{-1} \left[\frac{\underline{T}_B}{\underline{N}_c \underline{T}_{d,end}} \right] \underline{dq}_e = \underline{T}_c \underline{dq}_e \tag{C-26}$$

$$\begin{aligned}
 \underline{d\dot{q}}_c &= \underline{\underline{T}}_{d,c}^{-1} \left[\frac{d\dot{q}_B}{d\dot{q}_{d,c}} \right] + \underline{\dot{T}}_{d,c}^{-1} \left[\frac{dq_B}{dq_{d,c}} \right] \\
 &= \underline{T}_c \underline{d\dot{q}}_e + \left(\underline{T}_{d,c}^{-1} \left[\frac{\dot{T}_B}{\underline{N}_c \dot{T}_{d,end}} \right] \underline{dq}_e + \underline{\dot{T}}_{d,c}^{-1} \left[\frac{\underline{T}_B}{\underline{N}_c \underline{T}_{d,end}} \right] \right) \underline{dq}_e \\
 &= \underline{T}_c \underline{d\dot{q}}_e + \underline{\dot{T}}_c \underline{dq}_e
 \end{aligned} \tag{C-27}$$

C.2.8 Virtual internal power

$$\begin{aligned}\delta p_{int} &= - \iiint_V \sum_i \sum_j \delta_B \dot{\epsilon}_{ijB} \sigma_{ij} dV = - \int_0^L \iint_{A(s)} \sum_i \sum_j \delta_B \dot{\epsilon}_{ijB} \sigma_{ij} dA ds \\ &= - \int_0^L \iint_{A(s)} (\delta_B \dot{\epsilon}_{xx} E_B \epsilon_{xx} + \delta_B \dot{\epsilon}_{xy} G_B \epsilon_{xy} + \delta_B \dot{\epsilon}_{xz} G_B \epsilon_{xz}) dA ds\end{aligned}\quad (C-28)$$

$$\begin{aligned}\delta p_{int} &= - \int_0^L \delta \underline{\dot{q}}_{d,c}'^T (\underline{\underline{H}}_1 \underline{q}'_{d,c} + \underline{\underline{H}}_2 \underline{q}_{d,c}) ds + \int_0^L \delta \underline{\dot{q}}_{d,c}^T (\underline{\underline{H}}_3 \underline{q}'_{d,c} + \underline{\underline{H}}_4 \underline{q}_{d,c}) ds \\ &= - \delta \underline{\dot{q}}_{d,c}^T (\underline{\underline{H}}_1 \underline{q}'_{d,c} + \underline{\underline{H}}_2 \underline{q}_{d,c}) \Big|_0^L\end{aligned}\quad (C-29)$$

$$+ \int_0^L \delta \underline{\dot{q}}_{d,c}^T \left[-\underline{\underline{H}}_1 \underline{q}''_{d,c} + (\underline{\underline{H}}_3 - \underline{\underline{H}}_2) \underline{q}'_{d,c} + \underline{\underline{H}}_4 \underline{q}_{d,c} \right] ds$$

$$\begin{aligned}\underline{\underline{H}}_1 &= diag \left(\begin{bmatrix} EA & \frac{GA}{4} & \frac{GA}{4} & \frac{G(I_y + I_z)}{4} & EI_z & EI_y \end{bmatrix} \right) \\ \underline{\underline{H}}_2 &= \begin{bmatrix} 0 & 0 & 0 & 0 & 0 & 0 \\ 0 & 0 & 0 & 0 & 0 & -\frac{GA}{4} \\ 0 & 0 & 0 & 0 & \frac{GA}{4} & 0 \\ 0 & 0 & 0 & 0 & 0 & 0 \\ 0 & 0 & 0 & 0 & 0 & 0 \\ 0 & 0 & 0 & 0 & 0 & 0 \end{bmatrix} \quad \underline{\underline{H}}_3 = \underline{\underline{H}}_2^T \\ \underline{\underline{H}}_4 &= diag \left(\begin{bmatrix} 0 & 0 & 0 & 0 & \frac{GA}{4} & \frac{GA}{4} \end{bmatrix} \right)\end{aligned}\quad (C-30)$$

$$\delta p_{int} = - \delta \underline{\dot{q}}_{d,c}^T (\underline{\underline{H}}_1 \underline{q}'_{d,c} + \underline{\underline{H}}_2 \underline{q}_{d,c}) \Big|_0^L = - \delta \underline{\dot{q}}_{d,end}^T \underline{\underline{N}}_c^T (\underline{\underline{H}}_1 \underline{\underline{N}}'_c + \underline{\underline{H}}_2 \underline{\underline{N}}_c) \Big|_0^L \underline{q}_{d,end} \quad (C-31)$$

Apply small deformation assumption

$$\underline{\dot{q}}_{d,end} = \underline{dq}_{d,end} = \underline{\underline{T}}_{d,end} \underline{dq}_e \quad (C-32)$$

$$\begin{aligned}\delta p_{int} &= - \delta \underline{dq}_e^T \underline{\underline{T}}_{d,end}^T \underline{\underline{N}}_c^T (\underline{\underline{H}}_1 \underline{\underline{N}}'_c + \underline{\underline{H}}_2 \underline{\underline{N}}_c) \Big|_0^L \underline{q}_{d,end} = - \delta \underline{dq}_e^T \underline{F}_{int} \\ \underline{F}_{int} &= \underline{\underline{T}}_{d,end}^T \underline{\underline{N}}_c^T (\underline{\underline{H}}_1 \underline{\underline{N}}'_c + \underline{\underline{H}}_2 \underline{\underline{N}}_c) \Big|_0^L \underline{q}_{d,end} = \underline{\underline{T}}_{d,end}^T \underline{\underline{K}}_{d,end} \underline{q}_{d,end}\end{aligned}\quad (C-33)$$

C.2.9 Virtual inertial power

$$\begin{aligned}
 \delta p_{ine} &= - \iiint_V \delta_I \underline{\dot{r}}^T I \ddot{r} \rho dV = - \int_0^L \iint_{A(s)} \delta \left(I \dot{\underline{r}}^c + \underline{\underline{\Omega}}_c c \underline{t} \right)^T \left(I \ddot{\underline{r}}^c + \underline{\underline{A}}_c c \underline{t} \right) \rho dA ds \\
 &= - \int_0^L \left(\delta_I \dot{\underline{r}}^{cT} I \ddot{r}^c A + \delta_I \dot{\underline{r}}^{cT} \underline{\underline{A}}_c \iint_{A(s)} c \underline{t} dA + \iint_{A(s)} c \underline{t}^T dA \delta \underline{\underline{\Omega}}_c^T I \ddot{r}^c \right. \\
 &\quad \left. + \iint_{A(s)} c \underline{t}^T \delta \underline{\underline{\Omega}}_c^T \underline{\underline{A}}_c c \underline{t} dA \right) ds \quad (\text{C-34})
 \end{aligned}$$

For symmetrical sections

$$\iint_{A(s)} c \underline{t} dA = \left(\iint_{A(s)} c \underline{t}^T dA \right)^T = \begin{bmatrix} 0 \\ c A_y \\ c A_z \end{bmatrix} = \underline{0} \quad (\text{C-35})$$

$$\begin{aligned}
 \delta p_{ine} &= - \iiint_V \delta_I \underline{\dot{r}}^T I \ddot{r} \rho dV = - \int_0^L \iint_{A(s)} \delta \left(I \dot{\underline{r}}^c + \underline{\underline{\Omega}}_c c \underline{t} \right)^T \left(I \ddot{\underline{r}}^c + \underline{\underline{A}}_c c \underline{t} \right) \rho dA ds \\
 &= - \int_0^L \left[\delta_I \dot{\underline{r}}^{cT} I \ddot{r}^c A + I_y \delta \left(\underline{\underline{\Omega}}_c g_y \right)^T \underline{\underline{A}}_c g_y + I_z \delta \left(\underline{\underline{\Omega}}_c g_z \right)^T \underline{\underline{A}}_c g_z \right] \rho ds \quad (\text{C-36}) \\
 &= - \int_0^L \delta \left[\frac{dq_B}{dq_{d,c}} \right]^T \left(\underline{\underline{M}}_{B,c} \left[\frac{dq_B}{dq_{d,c}} \right] + \underline{\underline{D}}_{B,c} \left[\frac{dq_B}{dq_{d,c}} \right] \right) ds
 \end{aligned}$$

$$\begin{aligned}
 \underline{\underline{M}}_{B,c} &= \rho A \underline{\underline{H}}_t^T \underline{\underline{H}}_t + \rho I_y \underline{\underline{H}}_{r,y}^T \underline{\underline{H}}_{r,y} + \rho I_z \underline{\underline{H}}_{r,z}^T \underline{\underline{H}}_{r,z} \\
 \underline{\underline{D}}_{B,c} &= \rho A \underline{\underline{H}}_t^T \underline{\underline{D}}_t + \rho I_y \underline{\underline{H}}_{r,y}^T \underline{\underline{D}}_{r,y} + \rho I_z \underline{\underline{H}}_{r,z}^T \underline{\underline{D}}_{r,z} \quad (\text{C-37})
 \end{aligned}$$

$$\begin{aligned}
 \left[\frac{dq_B}{dq_{d,c}} \right] &= \left[\frac{dq_B}{\dot{q}_{d,c}} \right] = \begin{bmatrix} \underline{\underline{I}} & \underline{\underline{0}} \\ \underline{\underline{0}} & \underline{\underline{N}}_c \end{bmatrix} \left[\frac{dq_B}{\dot{q}_{d,end}} \right] = \begin{bmatrix} \underline{\underline{I}} & \underline{\underline{0}} \\ \underline{\underline{0}} & \underline{\underline{N}}_c \end{bmatrix} \left[\frac{dq_B}{dq_{d,end}} \right] \\
 &= \begin{bmatrix} \underline{\underline{I}} & \underline{\underline{0}} \\ \underline{\underline{0}} & \underline{\underline{N}}_c \end{bmatrix} \left[\frac{\underline{\underline{T}}_B}{T_{d,end}} \right] dq_e = \begin{bmatrix} \underline{\underline{T}}_B \\ \underline{\underline{N}}_c T_{d,end} \end{bmatrix} dq_e \quad (\text{C-38})
 \end{aligned}$$

$$\begin{aligned}
 \begin{bmatrix} \underline{d\dot{q}_B} \\ \underline{\dot{q}_{d,c}} \end{bmatrix} &= \begin{bmatrix} \underline{d\dot{q}_B} \\ \underline{\dot{q}_{d,c}} \end{bmatrix} = \begin{bmatrix} I & 0 \\ \underline{0} & \underline{N_c} \end{bmatrix} \begin{bmatrix} \underline{d\dot{q}_B} \\ \underline{\dot{q}_{d,end}} \end{bmatrix} = \begin{bmatrix} I & 0 \\ \underline{0} & \underline{N_c} \end{bmatrix} \begin{bmatrix} \underline{d\dot{q}_B} \\ \underline{d\dot{q}_{d,end}} \end{bmatrix} \\
 &= \begin{bmatrix} I & 0 \\ \underline{0} & \underline{N_c} \end{bmatrix} \begin{bmatrix} \underline{T_B} \\ \underline{T_{d,end}} \end{bmatrix} \underline{d\dot{q}_e} + \begin{bmatrix} I & 0 \\ \underline{0} & \underline{N_c} \end{bmatrix} \begin{bmatrix} \underline{\dot{T}_B} \\ \underline{\dot{T}_{d,end}} \end{bmatrix} \underline{dq_e} \quad (C-39) \\
 &= \begin{bmatrix} I & 0 \\ \underline{0} & \underline{N_c} \end{bmatrix} \begin{bmatrix} \underline{T_B} \\ \underline{T_{d,end}} \end{bmatrix} \underline{d\dot{q}_e} + \begin{bmatrix} \underline{\dot{T}_B} \\ N_c \underline{\dot{T}_{d,end}} \end{bmatrix} \underline{dq_e}
 \end{aligned}$$

$$\begin{aligned}
 \delta p_{ine} &= -\delta \underline{dq_e^T} \begin{bmatrix} \underline{T_B} \\ \underline{T_{d,end}} \end{bmatrix}^T \left[\int_0^L \begin{bmatrix} I & 0 \\ \underline{0} & \underline{N_c} \end{bmatrix}^T \left(\underline{\underline{M}_{B,c}} \begin{bmatrix} I & 0 \\ \underline{0} & \underline{N_c} \end{bmatrix} \right) ds \begin{bmatrix} \underline{T_B} \\ \underline{T_{d,end}} \end{bmatrix} \underline{d\dot{q}_e} \right. \\
 &\quad \left. + \int_0^L \begin{bmatrix} I & 0 \\ \underline{0} & \underline{N_c} \end{bmatrix}^T \left(\underline{\underline{M}_{B,c}} \begin{bmatrix} \underline{\dot{T}_B} \\ N_c \underline{\dot{T}_{d,end}} \end{bmatrix} + \underline{\underline{D}_{B,c}} \begin{bmatrix} \underline{T_B} \\ N_c \underline{T_{d,end}} \end{bmatrix} \right) ds \underline{dq_e} \right] = \quad (C-40) \\
 &= -\delta \underline{dq_e^T} \left(\underline{\underline{M}_e} \underline{d\dot{q}_e} + \underline{\underline{D}_e} \underline{dq_e} \right)
 \end{aligned}$$

$$\begin{aligned}
 \underline{\underline{M}_e} &= \begin{bmatrix} \underline{T_B} \\ \underline{T_{d,end}} \end{bmatrix}^T \int_0^L \begin{bmatrix} I & 0 \\ \underline{0} & \underline{N_c} \end{bmatrix}^T \underline{\underline{M}_{B,c}} \begin{bmatrix} I & 0 \\ \underline{0} & \underline{N_c} \end{bmatrix} ds \begin{bmatrix} \underline{T_B} \\ \underline{T_{d,end}} \end{bmatrix} \\
 \underline{\underline{D}_e} &= \begin{bmatrix} \underline{T_B} \\ \underline{T_{d,end}} \end{bmatrix}^T \int_0^L \begin{bmatrix} I & 0 \\ \underline{0} & \underline{N_c} \end{bmatrix}^T \left(\underline{\underline{M}_{B,c}} \begin{bmatrix} \underline{\dot{T}_B} \\ N_c \underline{\dot{T}_{d,end}} \end{bmatrix} + \underline{\underline{D}_{B,c}} \begin{bmatrix} \underline{T_B} \\ N_c \underline{T_{d,end}} \end{bmatrix} \right) ds \quad (C-41)
 \end{aligned}$$

C.2.10 Virtual external power

$$\begin{aligned}
 \delta p_{ext} &= \iiint_V \delta_I \dot{\underline{r}}^T \underline{g} \rho dV = \int_0^L \iint_{A(s)} \delta \left(\underline{I} \dot{\underline{r}}^c + \underline{\underline{\Omega}_c} \underline{t} \right)^T \rho dA ds \underline{I} \underline{g} = \int_0^L \delta_I \dot{\underline{r}}^c \rho A ds \underline{I} \underline{g} \\
 &= \int_0^L \delta \left[\frac{\underline{dq_B}}{\underline{dq_{d,c}}} \right]^T \underline{\underline{H}_f^T} \underline{I} \underline{g} \rho A ds
 \end{aligned} \quad (C-42)$$

Apply small deformation assumption

$$\begin{aligned}
 \delta p_{ine} &= \delta \underline{dq_e^T} \begin{bmatrix} \underline{T_B} \\ \underline{T_{d,end}} \end{bmatrix}^T \int_0^L \begin{bmatrix} I & 0 \\ \underline{0} & \underline{N_c} \end{bmatrix}^T \underline{\underline{H}_f^T} \rho A ds \underline{I} \underline{g} = -\delta \underline{dq_e^T} \underline{\underline{V}_{ext,g}} \underline{I} \underline{g} \\
 &= -\delta \underline{dq_e^T} \underline{F}_{ext,g}
 \end{aligned} \quad (C-43)$$

$$\begin{aligned}\underline{\underline{V}}_{ext,g} &= - \left[\begin{matrix} \underline{\underline{T}}_B \\ \underline{\underline{T}}_{d,end} \end{matrix} \right]^T \int_0^L \begin{bmatrix} \underline{\underline{I}} & \underline{\underline{0}} \\ \underline{\underline{0}} & \underline{\underline{N}}_c \end{bmatrix}^T \underline{\underline{H}}_t^T \rho A ds \\ \underline{\underline{F}}_{ext,g} &= \underline{\underline{V}}_{ext,g} \underline{\underline{I}} g\end{aligned}\quad (\text{C-44})$$

C.2.11 Virtual power principle for Timoshenko Beam

$$\begin{aligned}\delta p_e &= \delta p_{ine} + \delta p_{int} + \delta p_{ext} = \delta p_{ine} + \delta p_{int} + \delta p_{ext,g} \\ &= -\delta \underline{\underline{d}}q_e^T \left[\underline{\underline{M}}_e \underline{\underline{d}}\dot{q}_e + \underline{\underline{D}}_e \underline{\underline{d}}q_e + \underline{\underline{F}}_{int} + \underline{\underline{F}}_{ext,g} \right]\end{aligned}\quad (\text{C-45})$$

C.2.12 Small deformation assumption

$${}_B\underline{\underline{u}}^c \ll {}_B\underline{\underline{r}}^{r,c} \quad {}_B\underline{\underline{r}}^{r,c} + {}_B\underline{\underline{u}}^c \approx {}_B\underline{\underline{r}}^{r,c} \quad (\text{C-46})$$

$${}_B\underline{\underline{r}}^{r,c} = s \underline{\underline{g}}_x \quad (\text{C-47})$$

$$\begin{aligned}{}_B\underline{\underline{\psi}}^c &\rightarrow \underline{\underline{0}} & \underline{\underline{R}}_{d,c} &\approx \underline{\underline{I}} \\ \underline{\underline{R}}_B &= \underline{\underline{R}}_{d,c} \underline{\underline{R}}_c \approx \underline{\underline{R}}_c\end{aligned}\quad (\text{C-48})$$

$${}_c\underline{\underline{\tilde{\omega}}}^c \approx {}_B\underline{\underline{\psi}}^c \approx \begin{bmatrix} \underline{\underline{0}} & \underline{\underline{I}} \end{bmatrix} \underline{\underline{N}}_c \underline{\underline{q}}_{d,end} \quad (\text{C-49})$$

Mass Matrix

$$\begin{aligned}\underline{\underline{M}}_{B,c} &= \rho A \underline{\underline{H}}_t^T \underline{\underline{H}}_t + \rho I_y \underline{\underline{H}}_{r,y}^T \underline{\underline{H}}_{r,y} + \rho I_z \underline{\underline{H}}_{r,z}^T \underline{\underline{H}}_{r,z} \\ \underline{\underline{D}}_{B,c} &= \rho A \underline{\underline{H}}_t^T \underline{\underline{D}}_t + \rho I_y \underline{\underline{H}}_{r,y}^T \underline{\underline{D}}_{r,y} + \rho I_z \underline{\underline{H}}_{r,z}^T \underline{\underline{D}}_{r,z}\end{aligned}\quad (\text{C-50})$$

$$\begin{aligned}\underline{\underline{M}}_e &= \left[\begin{matrix} \underline{\underline{T}}_B \\ \underline{\underline{T}}_{d,end} \end{matrix} \right]^T \int_0^L \begin{bmatrix} \underline{\underline{I}} & \underline{\underline{0}} \\ \underline{\underline{0}} & \underline{\underline{N}}_c \end{bmatrix}^T \underline{\underline{M}}_{B,c} \begin{bmatrix} \underline{\underline{I}} & \underline{\underline{0}} \\ \underline{\underline{0}} & \underline{\underline{N}}_c \end{bmatrix} ds \left[\begin{matrix} \underline{\underline{T}}_B \\ \underline{\underline{T}}_{d,end} \end{matrix} \right] \\ \underline{\underline{D}}_e &= \left[\begin{matrix} \underline{\underline{T}}_B \\ \underline{\underline{T}}_{d,end} \end{matrix} \right]^T \int_0^L \begin{bmatrix} \underline{\underline{I}} & \underline{\underline{0}} \\ \underline{\underline{0}} & \underline{\underline{N}}_c \end{bmatrix}^T \left(\underline{\underline{M}}_{B,c} \begin{bmatrix} \underline{\underline{T}}_B \\ \underline{\underline{N}}_c \underline{\underline{T}}_{d,end} \end{bmatrix} + \underline{\underline{D}}_{B,c} \begin{bmatrix} \underline{\underline{T}}_B \\ \underline{\underline{N}}_c \underline{\underline{T}}_{d,end} \end{bmatrix} \right) ds\end{aligned}\quad (\text{C-51})$$

$$\underline{\underline{H}}_t \approx \begin{bmatrix} I & -\underline{\underline{R}}_B \tilde{r}^{r,c} & \underline{\underline{R}}_B & 0 \\ \underline{\underline{I}} & -s \underline{\underline{R}}_B \tilde{g}_x & \underline{\underline{R}}_B & 0 \\ s \tilde{g}_x \underline{\underline{R}}_B^T & -s^2 \underline{\underline{g}}_x \tilde{g}_x & s \tilde{g}_x & 0 \\ \underline{\underline{R}}_B^T & -s \underline{\underline{g}}_x & I & 0 \\ 0 & 0 & 0 & 0 \end{bmatrix} \quad (C-52)$$

$$\underline{\underline{H}}_{r,y} \approx \begin{bmatrix} 0 & -\underline{\underline{R}}_B \tilde{g}_y & 0 & -\underline{\underline{R}}_B \tilde{g}_y \\ 0 & 0 & 0 & 0 \\ 0 & -\underline{\underline{g}}_y \tilde{g}_y & 0 & -\underline{\underline{g}}_y \tilde{g}_y \\ 0 & 0 & 0 & 0 \\ 0 & -\underline{\underline{g}}_y \tilde{g}_y & 0 & -\underline{\underline{g}}_y \tilde{g}_y \end{bmatrix} \quad (C-53)$$

$$\underline{\underline{H}}_{r,z} \approx \begin{bmatrix} 0 & -\underline{\underline{R}}_B \tilde{g}_z & 0 & -\underline{\underline{R}}_B \tilde{g}_z \\ 0 & 0 & 0 & 0 \\ 0 & -\underline{\underline{g}}_z \tilde{g}_z & 0 & -\underline{\underline{g}}_z \tilde{g}_z \\ 0 & 0 & 0 & 0 \\ 0 & -\underline{\underline{g}}_z \tilde{g}_z & 0 & -\underline{\underline{g}}_z \tilde{g}_z \end{bmatrix} \quad (C-54)$$

$$\underline{\underline{M}}_{B,c} = \rho \begin{bmatrix} AI & -As \underline{\underline{R}}_B \tilde{g}_x & AR_B & 0 \\ As \tilde{g}_x \underline{\underline{R}}_B^T & -As^2 \underline{\underline{g}}_x \tilde{g}_x + J & As \tilde{g}_x & J \\ AR_B^T & -As \underline{\underline{g}}_x & AI & 0 \\ 0 & J & 0 & J \end{bmatrix} \quad (C-55)$$

$$\underline{\underline{J}} \triangleq -I_y \underline{\underline{g}}_y \underline{\underline{g}}_y - I_z \underline{\underline{g}}_z \underline{\underline{g}}_z = \begin{bmatrix} I_y + I_z & 0 & 0 \\ 0 & I_z & 0 \\ 0 & 0 & I_y \end{bmatrix} \quad (C-56)$$

$$\begin{aligned} \underline{\underline{M}}_e &= \left[\frac{T_B}{T_{d,end}} \right]^T \int_0^L \begin{bmatrix} I & 0 & 0 \\ 0 & \underline{\underline{N}}_{c,1} & \underline{\underline{N}}_{c,2} \end{bmatrix}^T \underline{\underline{M}}_{B,c} \begin{bmatrix} I & 0 & 0 \\ 0 & \underline{\underline{N}}_{c,1} & \underline{\underline{N}}_{c,2} \end{bmatrix} ds \left[\frac{T_B}{T_{d,end}} \right] \\ &= \left[\frac{T_B}{T_{d,end}} \right]^T \underline{\underline{M}}_{B,end} \left[\frac{T_B}{T_{d,end}} \right] \end{aligned} \quad (C-57)$$

Inertial Force

$$\begin{aligned}
 \underline{\underline{F}}_{ine} &= \underline{\underline{D}}_e \underline{dq}_e = \left[\begin{array}{c} \underline{\underline{T}}_B \\ \underline{\underline{T}}_{d,end} \end{array} \right]^T \int_0^L \begin{bmatrix} \underline{\underline{I}} & \underline{\underline{0}} \\ \underline{\underline{0}} & \underline{\underline{N}}_c \end{bmatrix}^T \left(\begin{array}{c} \underline{\underline{M}}_{B,c} \begin{bmatrix} \dot{\underline{\underline{T}}}_B \\ \underline{\underline{N}}_c \dot{\underline{\underline{T}}}_{d,end} \end{bmatrix} \\ + \underline{\underline{D}}_{B,c} \begin{bmatrix} \underline{\underline{T}}_B \\ \underline{\underline{N}}_c \underline{\underline{T}}_{d,end} \end{bmatrix} \end{array} \right) ds \underline{dq}_e \\
 &= \left[\begin{array}{c} \underline{\underline{T}}_B \\ \underline{\underline{T}}_{d,end} \end{array} \right]^T \left(\begin{array}{c} \underline{\underline{M}}_{B,end} \begin{bmatrix} \dot{\underline{\underline{T}}}_B \\ \dot{\underline{\underline{T}}}_{d,end} \end{bmatrix} \\ + \int_0^L \begin{bmatrix} \underline{\underline{I}} & \underline{\underline{0}} \\ \underline{\underline{0}} & \underline{\underline{N}}_c \end{bmatrix}^T \underline{\underline{D}}_{B,c} \begin{bmatrix} \underline{\underline{I}} & \underline{\underline{0}} \\ \underline{\underline{0}} & \underline{\underline{N}}_c \end{bmatrix} ds \begin{bmatrix} \underline{\underline{T}}_B \\ \underline{\underline{T}}_{d,end} \end{bmatrix} \end{array} \right) \underline{dq}_e \quad (C-58)
 \end{aligned}$$

$$\underline{\underline{D}}_{B,c} = \rho A \underline{\underline{H}}_t^T \underline{\underline{D}}_t + \rho I_y \underline{\underline{H}}_{r,y}^T \underline{\underline{D}}_{r,y} + \rho I_z \underline{\underline{H}}_{r,z}^T \underline{\underline{D}}_{r,z} \quad (C-59)$$

$$\begin{aligned}
 \underline{\underline{D}}_t &= \begin{bmatrix} \underline{\underline{0}} & -s \underline{\underline{R}}_{B,B} \widetilde{\omega}^B \widetilde{g}_x & 2 \underline{\underline{R}}_{B,B} \widetilde{\omega}^B & \underline{\underline{0}} \end{bmatrix} = \underline{\underline{R}}_{B,B} \widetilde{\omega}^B \begin{bmatrix} \underline{\underline{0}} & -s \widetilde{g}_x & 2 \underline{\underline{I}} & \underline{\underline{0}} \end{bmatrix} \\
 \underline{\underline{H}}_t^T \underline{\underline{D}}_t &= \begin{bmatrix} \underline{\underline{0}} & -s \underline{\underline{R}}_{B,B} \widetilde{\omega}^B \widetilde{g}_x & 2 \underline{\underline{R}}_{B,B} \widetilde{\omega}^B & \underline{\underline{0}} \\ \underline{\underline{0}} & -s_B \widetilde{r}^{r,c} \underline{\underline{B}} \widetilde{\omega}^B \widetilde{g}_x & 2_B \widetilde{r}^{r,c} \underline{\underline{B}} \widetilde{\omega}^B & \underline{\underline{0}} \\ \underline{\underline{0}} & -s_B \widetilde{\omega}^B \widetilde{g}_x & 2_B \widetilde{\omega}^B & \underline{\underline{0}} \\ \underline{\underline{0}} & \underline{\underline{0}} & \underline{\underline{0}} & \underline{\underline{0}} \end{bmatrix} \quad (C-60)
 \end{aligned}$$

$$\begin{aligned}
 \underline{\underline{D}}_{r,y} &= \begin{bmatrix} \underline{\underline{0}} & -\underline{\underline{R}}_{B,B} \widetilde{\omega}^B \widetilde{g}_y & \underline{\underline{0}} & -\underline{\underline{R}}_B (2_B \widetilde{\omega}^B + c \widetilde{\omega}^c) \widetilde{g}_y \end{bmatrix} \\
 &= \underline{\underline{R}}_B \begin{bmatrix} \underline{\underline{0}} & -\underline{\underline{B}} \widetilde{\omega}^B & \underline{\underline{0}} & - (2_B \widetilde{\omega}^B + c \widetilde{\omega}^c) \end{bmatrix] \widetilde{g}_y \\
 &= \underline{\underline{R}}_B \begin{bmatrix} \underline{\underline{0}} & -\underline{\underline{B}} \widetilde{\omega}^B & \underline{\underline{0}} & - (2_B \widetilde{\omega}^B + B \dot{\psi}^c) \end{bmatrix] \widetilde{g}_y \\
 &= \underline{\underline{R}}_B \begin{bmatrix} \underline{\underline{0}} & -\underline{\underline{B}} \widetilde{\omega}^B & \underline{\underline{0}} & - (2_B \widetilde{\omega}^B + [\underline{\underline{0}} \quad \underline{\underline{I}}] \underline{\underline{N}}_c \dot{\underline{\underline{q}}}_{d,end}) \end{bmatrix] \widetilde{g}_y \quad (C-61) \\
 \underline{\underline{H}}_{r,y}^T \underline{\underline{D}}_{r,y} &= \begin{bmatrix} \underline{\underline{0}} & \underline{\underline{0}} & \underline{\underline{0}} & \underline{\underline{0}} \\ \underline{\underline{0}} & -\widetilde{g}_{yB} \widetilde{\omega}^B \widetilde{g}_y & \underline{\underline{0}} & -\widetilde{g}_y (2_B \widetilde{\omega}^B + c \widetilde{\omega}^c) \widetilde{g}_y \\ \underline{\underline{0}} & \underline{\underline{0}} & \underline{\underline{0}} & \underline{\underline{0}} \\ \underline{\underline{0}} & -\widetilde{g}_{yB} \widetilde{\omega}^B \widetilde{g}_y & \underline{\underline{0}} & -\widetilde{g}_y (2_B \widetilde{\omega}^B + c \widetilde{\omega}^c) \widetilde{g}_y \end{bmatrix}
 \end{aligned}$$

$$\underline{\underline{D}}_{r,z} = \begin{bmatrix} 0 & -R_B B \tilde{\omega}^B \tilde{g}_z & 0 & -R_B (2_B \tilde{\omega}^B + c \tilde{\omega}^c) \tilde{g}_z \\ 0 & 0 & 0 & 0 \\ 0 & -\tilde{g}_{zB} \tilde{\omega}^B \tilde{g}_z & 0 & -\tilde{g}_z (2_B \tilde{\omega}^B + c \tilde{\omega}^c) \tilde{g}_z \\ 0 & 0 & 0 & 0 \\ 0 & -\tilde{g}_{zB} \tilde{\omega}^B \tilde{g}_z & 0 & -\tilde{g}_z (2_B \tilde{\omega}^B + c \tilde{\omega}^c) \tilde{g}_z \end{bmatrix} \quad (C-62)$$

$$\begin{aligned} \underline{\underline{D}}_e &= \left[\begin{array}{c} T_B \\ \underline{\underline{T}}_{d,end} \end{array} \right]^T \int_0^L \left[\begin{array}{cc} I & 0 \\ \underline{\underline{0}} & \underline{\underline{N}}_c \end{array} \right]^T \left(\underline{\underline{M}}_{B,c} \begin{bmatrix} I & 0 \\ \underline{\underline{0}} & \underline{\underline{N}}_c \end{bmatrix} \begin{bmatrix} \dot{T}_B \\ \dot{\underline{\underline{T}}}_{d,end} \end{bmatrix} + \underline{\underline{D}}_{B,c} \begin{bmatrix} I & 0 \\ \underline{\underline{0}} & \underline{\underline{N}}_c \end{bmatrix} \begin{bmatrix} T_B \\ \underline{\underline{T}}_{d,end} \end{bmatrix} \right) ds \\ &= \left[\begin{array}{c} T_B \\ \underline{\underline{T}}_{d,end} \end{array} \right]^T \left(\int_0^L \left[\begin{array}{cc} I & 0 \\ \underline{\underline{0}} & \underline{\underline{N}}_c \end{array} \right]^T \underline{\underline{M}}_{B,c} \begin{bmatrix} I & 0 \\ \underline{\underline{0}} & \underline{\underline{N}}_c \end{bmatrix} ds \begin{bmatrix} \dot{T}_B \\ \dot{\underline{\underline{T}}}_{d,end} \end{bmatrix} \right. \\ &\quad \left. + \int_0^L \left[\begin{array}{cc} I & 0 \\ \underline{\underline{0}} & \underline{\underline{N}}_c \end{array} \right]^T \underline{\underline{D}}_{B,c} \begin{bmatrix} I & 0 \\ \underline{\underline{0}} & \underline{\underline{N}}_c \end{bmatrix} ds \begin{bmatrix} T_B \\ \underline{\underline{T}}_{d,end} \end{bmatrix} \right) \\ &= \left[\begin{array}{c} T_B \\ \underline{\underline{T}}_{d,end} \end{array} \right]^T \left(\underline{\underline{M}}_{B,end} \begin{bmatrix} \dot{T}_B \\ \dot{\underline{\underline{T}}}_{d,end} \end{bmatrix} + \underline{\underline{D}}_{B,end} \begin{bmatrix} T_B \\ \underline{\underline{T}}_{d,end} \end{bmatrix} \right) \end{aligned} \quad (C-63)$$

$$\underline{\underline{D}}_{B,end} = \int_0^L \left[\begin{array}{cc} I & 0 \\ \underline{\underline{0}} & \underline{\underline{N}}_c \end{array} \right]^T \underline{\underline{D}}_{B,c} \begin{bmatrix} I & 0 \\ \underline{\underline{0}} & \underline{\underline{N}}_c \end{bmatrix} ds \quad (C-64)$$

Gravity

$$\underline{\underline{V}}_{ext,g} = -\rho A \left[\begin{array}{c} T_B \\ \underline{\underline{T}}_{d,end} \end{array} \right]^T \int_0^L \left[\begin{array}{cc} I & 0 \\ \underline{\underline{0}} & \underline{\underline{N}}_c \end{array} \right]^T \underline{\underline{H}}_t^T ds \quad (C-65)$$

C.3 Two Nodes Strut Tie Dynamic Model based on Absolute Coordination

C.3.1 Ideal Strut Tie Model Assumption

The strut tie model described in this part is an ideal strut tie model, which satisfies the following assumptions:

5. Only the normal stress from axial tension and compression is considered, and other internal forces that may exist in the real rod are ignored;
6. the normal stress is evenly distributed with the length of the rod;
7. the cross section of the rod is symmetrical about the y- and z-axis of the section local coordinate;
8. the density and total mass of the rod remain unchanged.

C.3.2 Generalized Coordinate and Generalized Velocity

According to the above assumptions, the generalized coordinates and generalized velocity of the two nodes strut tie model can be expressed by the position vectors and translational velocity of the two nodes.

$$\underline{q}_e = \begin{bmatrix} {}_I\dot{r}^1 \\ {}_I\dot{r}^2 \end{bmatrix} \quad d\underline{q}_e = \dot{\underline{q}}_e = \begin{bmatrix} {}_I\ddot{r}^1 \\ {}_I\ddot{r}^2 \end{bmatrix} \quad (\text{C-66})$$

Since only the x-axis is determined (parallel to the line connected the two end nodes), according to the third assumption the posture of the rod can be determined only based on the x-axis.

$$\underline{\varphi}^B = \varphi^B \underline{n}_\varphi^B \quad \underline{\underline{R}}_B = \underline{\underline{R}}(\underline{\varphi}^B) \quad (\text{C-67})$$

where

$$\begin{aligned} \sin \varphi^B &= \left\| \underline{\underline{\tilde{g}}}_x \underline{n}_x \right\| / l_{\varphi,B} & \cos \varphi^B &= \underline{g}_x^T \underline{n}_x / l_{\varphi,B} \\ \underline{n}_\varphi^B &= \underline{\underline{\tilde{g}}}_x \underline{n}_x / \left\| \underline{\underline{\tilde{g}}}_x \underline{n}_x \right\| & l_{\varphi,B} &= \sqrt{\left\| \underline{\underline{\tilde{g}}}_x \underline{n}_x \right\|^2 + \left(\underline{g}_x^T \underline{n}_x \right)^2} \end{aligned} \quad (\text{C-68})$$

According to the relationship between the translational velocities of the two end nodes, the angular velocity of the rod and the velocity of the axial deformation can be obtained.

$$\begin{aligned} {}_B \underline{\dot{r}}^{12} &= \underline{g}_x \underline{n}_x^T \begin{bmatrix} -I & I \end{bmatrix} \underline{d}\underline{q}_e = \underline{\underline{T}}_r \underline{d}\underline{q}_e \\ {}_B \underline{\omega}^B &= \frac{1}{\left\| {}_I \underline{r}^{12} \right\|} \underline{\underline{R}}_{x,90^\circ} \left(\underline{\underline{R}}_B^T - \underline{g}_x \underline{n}_x^T \right) \begin{bmatrix} -I & I \end{bmatrix} \underline{d}\underline{q}_e = \underline{\underline{T}}_\varphi \underline{d}\underline{q}_e \end{aligned} \quad (\text{C-69})$$

where

$${}_I \underline{r}^{12} = {}_I \underline{r}^2 - {}_I \underline{r}^1 \quad \underline{n}_x = \underline{\underline{R}}_B \underline{g}_x \quad \underline{\underline{R}}_{x,90^\circ} = \underline{\underline{R}} \left(\begin{bmatrix} \frac{\pi}{2} & 0 & 0 \end{bmatrix}^T \right) \quad (\text{C-70})$$

The angular acceleration of the rod can be written as

$${}_B \dot{\underline{\omega}}^B = \underline{\underline{T}}_\varphi \underline{d}q_e + \underline{\underline{T}}_\varphi \underline{d}\dot{q}_e \quad (\text{C-71})$$

where

$$\underline{\underline{T}}_\varphi = \underline{\underline{R}}_{x,90^\circ} \left[\frac{{}_I \underline{r}^{12T} {}_I \dot{\underline{r}}^{12}}{\|{}_I \underline{r}^{12}\|^2} \underline{\underline{I}} - {}_B \widetilde{\underline{\omega}}^B \right] \underline{\underline{g}}_x \underline{\underline{T}}_\varphi \quad {}_I \dot{\underline{r}}^{12} = {}_I \dot{\underline{r}}^2 - {}_I \dot{\underline{r}}^1 \quad (\text{C-72})$$

C.3.3 Kinematics and Deformation of Points on the Beam

Since for the strut tie model only the axial deformation is considered, there is no relative rotation with the local coordinate on any cross section. The position, velocity and acceleration of any point on any section of the rod can be expressed as

$$\begin{aligned} {}_I \underline{r} &= {}_I \underline{r}^c + \underline{\underline{R}}_{Bc} \underline{t} \\ {}_I \dot{\underline{r}} &= {}_I \dot{\underline{r}}^c + \underline{\underline{R}}_{BB} \widetilde{\underline{\omega}}^B \underline{c} \underline{t} \\ {}_I \ddot{\underline{r}} &= {}_I \ddot{\underline{r}}^c + \underline{\underline{R}}_{BB} \widetilde{\underline{\omega}}^B \underline{c} \underline{t} + \underline{\underline{R}}_{BB} \widetilde{\underline{\omega}}^B {}_B \widetilde{\underline{\omega}}^B \underline{c} \underline{t} \end{aligned} \quad (\text{C-73})$$

According to the definition of strain in absolute coordinates, the axial strain of the rod can be written as

$${}_I \varepsilon = \|{}_I \underline{r}^{c'}\| - 1 \quad (\text{C-74})$$

The velocity and acceleration of the axial strain can be expressed as

$$\begin{aligned} {}_I \dot{\varepsilon} &= \frac{1}{\|{}_I \underline{r}'\|} {}_I \underline{r}'^T \underline{\underline{N}}' \underline{d}q_e = \frac{1}{\|{}_I \underline{r}'\|} \underline{q}_e^T \underline{\underline{N}}'^T \underline{\underline{N}}' \underline{d}q_e \triangleq \underline{\underline{T}}_\varepsilon^T \underline{d}q_e \\ {}_I \ddot{\varepsilon} &= \frac{1}{\|{}_I \underline{r}'\|} \underline{q}_e^T \underline{\underline{N}}'^T \underline{\underline{N}}' \underline{d}\dot{q}_e + {}_I \dot{\underline{r}}'^T \frac{1}{\|{}_I \underline{r}'\|} \left(\underline{\underline{I}} - \frac{{}_I \underline{r}' {}_I \underline{r}'^T}{\|{}_I \underline{r}'\|^2} \right) \underline{\underline{N}}' \underline{d}q_e \triangleq \underline{\underline{T}}_\varepsilon^T \underline{d}\dot{q}_e + \underline{\underline{T}}_\varepsilon^T \underline{d}q_e \end{aligned} \quad (\text{C-75})$$

The stress can be obtained from the constitutive relationship with strain. In order to avoid the high-frequency oscillation of the rod caused by strain, the average stress is

used to replace the instantaneous stress by introducing smooth factor h . The average stress in inertial coordinate can be expressed as

$${}_I\bar{\sigma} = E {}_I\bar{\epsilon} = E \left({}_I\epsilon + \frac{h}{2} {}_I\dot{\epsilon} + \frac{h^2}{6} {}_I\ddot{\epsilon} \right) = E {}_I\epsilon + E \left(\frac{h}{2} \underline{T}_{\epsilon}^T + \frac{h^2}{6} \underline{\dot{T}}_{\epsilon}^T \right) \underline{dq}_e + E \frac{h^2}{6} \underline{T}_{\epsilon}^T \underline{d\dot{q}}_e \quad (\text{C-76})$$

C.3.4 Discretization

In order to satisfy the second assumption, the first derivative of the position vector of the center of any section on the rod should be constant. Therefore, its position vector can be expressed by linear interpolation of position vectors of two end section. The position, velocity and acceleration of this center point can be expressed as

$${}_I\underline{r}^c \triangleq \underline{\underline{N}} \underline{q}_e \quad {}_I\dot{\underline{r}}^c = \underline{\underline{N}} \underline{dq}_e \quad {}_I\ddot{\underline{r}}^c = \underline{\underline{N}} \underline{d\dot{q}}_e \quad (\text{C-77})$$

Where $\underline{\underline{N}}$ is the shape function, and its specific expression is

$$\underline{\underline{N}} = [(1 - \xi) \underline{\underline{I}} \quad \xi \underline{\underline{I}}] \quad (\text{C-78})$$

with $\xi = s/L$. The first derivative of its position and velocity vector with respect to the arc length coordinate s can be written as

$${}_I\underline{r}^{c'} \triangleq \underline{\underline{N'}} \underline{q}_e \quad {}_I\dot{\underline{r}}^{c'} = \underline{\underline{N'}} \underline{\dot{q}}_e \quad (\text{C-79})$$

with

$$\underline{\underline{N'}} = \frac{1}{L} [-\underline{\underline{I}} \quad \underline{\underline{I}}] \quad (\text{C-80})$$

C.3.5 The Virtual Power of Strut Tie Model

The inertial virtual power of strut tie model can be written as

$$\begin{aligned}\delta p_{ine} &= - \iiint_V \delta_I \dot{\underline{r}}^T I \ddot{\underline{r}} \rho dV = -\delta \underline{dq}_e^T (\underline{\underline{M}}_{e,ine} \underline{d}\dot{q}_e + \underline{\underline{D}}_{e,ine} \underline{dq}_e) \\ &= -\delta \underline{dq}_e^T (\underline{\underline{M}}_{e,ine} \underline{d}\dot{q}_e + \underline{F}_{ine})\end{aligned}\quad (C-81)$$

The mass matrix and damping matrix generated from the virtual inertial power can be expressed as

$$\underline{\underline{M}}_{e,ine} = \rho L \left(\frac{A}{6} \begin{bmatrix} 2I & I \\ I & 2I \end{bmatrix} + \underline{T}_{\varphi}^T \underline{\underline{J}} \underline{T}_{\varphi} \right) \quad \underline{\underline{D}}_{e,ine} = -\rho L \underline{T}_{\varphi}^T \left(\underline{\underline{J}} \dot{\underline{T}}_{\varphi} + \underline{\underline{J}} \underline{T}_{\varphi} \right) \quad (C-82)$$

where $\underline{\underline{J}}$ is the moment of inertia of section

$$\underline{\underline{J}} = diag([I_y + I_z \quad I_z \quad I_y]) \quad \underline{\underline{J}}_B \underline{\omega}^B = \underline{\underline{\tilde{\omega}}}^B \underline{\underline{J}}_B \underline{\omega}^B \quad (C-83)$$

The virtual internal power with the smooth factor can be written as

$$\begin{aligned}\delta p_{int} &= - \int_0^L \delta_I \dot{\varepsilon} I \bar{\sigma} A ds = -\delta \underline{dq}_e^T (\underline{\underline{M}}_{e,int} \underline{d}\dot{q}_e + \underline{\underline{D}}_{e,int} \underline{dq}_e + \underline{\underline{K}}_e \underline{q}_e) \\ &= -\delta \underline{dq}_e^T (\underline{\underline{M}}_{e,int} \underline{d}\dot{q}_e + \underline{F}_{int})\end{aligned}\quad (C-84)$$

The mass matrix, the damping matrix and the stiffness matrix obtained through the virtual internal power can be expressed as

$$\begin{aligned}\underline{\underline{M}}_{e,int} &= EAL \frac{h^2}{6} \underline{T}_{\varepsilon} \underline{T}_{\varepsilon}^T \quad \underline{\underline{D}}_{e,int} = EAL \left(\frac{h}{2} \underline{T}_{\varepsilon} \underline{T}_{\varepsilon}^T + \frac{h^2}{6} \underline{T}_{\varepsilon} \dot{\underline{T}}_{\varepsilon}^T \right) \\ \underline{\underline{K}}_e &= \frac{1}{\|I_r'\|} \underline{\underline{N}}'^T \underline{\underline{N}}' EA_I \varepsilon L\end{aligned}\quad (C-85)$$

As the external force here only gravity is considered. The virtual power of gravity can be written as

$$\delta p_{ext,g} = \iiint_V \delta_I \dot{\underline{r}}^T I \underline{g} \rho dV = \delta \underline{dq}_e^T \rho A \int_0^L \underline{\underline{N}}^T ds_I \underline{g} = -\delta \underline{dq}_e^T \underline{F}_{ext,g} \quad (C-86)$$

The virtual power of strut tie model is

$$\delta p_e = \delta p_{ine} + \delta p_{int} + \delta p_{ext,g} = -\underline{\delta q}_e^T (\underline{\underline{M}}_e \underline{d}\dot{q}_e + \underline{F}_e) \quad (C-87)$$

where the total generalized mass and generalized force can be written as

$$\underline{\underline{M}}_e = \underline{\underline{M}}_{e,ine} + \underline{\underline{M}}_{e,int} \quad \underline{F}_e = \underline{F}_{ine} + \underline{F}_{int} + \underline{F}_{ext,g} \quad (C-88)$$

C.3.6 Body Parameter of Strut Tie Model after Deformation

According to the forth assumption, we assume the density ρ and the total mass m before and after the deformation remain unchanged. Here we assume the cross section of the rod is circular with outer diameter r_a and inner diameter r_i , the ratio of outer diameter to inner diameter remains unchanged. Therefore, the section parameters after the deformation can be expressed as

$$r_a = \sqrt{\frac{m}{\rho\pi\|\underline{I}\underline{r}^{12}\|(r_a^{*2} - r_i^{*2})}} r_a^* \quad r_i = \sqrt{\frac{m}{\rho\pi\|\underline{I}\underline{r}^{12}\|(r_a^{*2} - r_i^{*2})}} r_i^* \quad (C-89)$$

where r_a^* and r_i^* is the outer diameter and inner diameter before deformation.

C.4 Cubic Spline Beam Dynamic Model

C.4.1 Generalized coordinate

$$\underline{q}_e = \begin{bmatrix} q_1 \\ q_2 \end{bmatrix} = \begin{bmatrix} \underline{\underline{I}}^1 \\ \|\underline{I}\underline{r}'^1\| \\ \underline{\underline{I}}^2 \\ \|\underline{I}\underline{r}'^2\| \end{bmatrix} \quad \underline{dq}_e = \begin{bmatrix} \underline{d}q_1 \\ \underline{d}q_2 \end{bmatrix} = \begin{bmatrix} \underline{\dot{I}}^1 \\ \|\underline{I}\dot{\underline{r}}'^1\| \\ \underline{\dot{I}}^2 \\ \|\underline{I}\dot{\underline{r}}'^2\| \end{bmatrix} \quad (C-90)$$

$$\begin{aligned} \underline{\underline{R}}_2 &= \underline{\underline{R}}_1 \underline{\underline{R}}_2 = \underline{\underline{R}}_1 \underline{\underline{R}} \left({}_1 \underline{\varphi}^{12} \right) & {}_1 \underline{\varphi}^{12} &= [{}_1 \varphi^{12} \quad {}_1 \psi^{12} \quad {}_1 \theta^{12}]^T \\ {}_1 \psi^{12} &= -\sin^{-1} \underline{g}_z^T \underline{\underline{R}}_2 \underline{g}_x & {}_1 \varphi^{12} &= \sin^{-1} \frac{\underline{g}_z^T \underline{\underline{R}}_2 \underline{g}_y}{\cos {}_1 \psi^{12}} \end{aligned} \quad (C-91)$$

$$\begin{aligned}
 {}_2\omega^2 &= {}_1\underline{\underline{R}}_2^T {}_1\underline{\omega}^1 + \underline{\underline{T}} \left({}_1\underline{\varphi}^{12} \right) {}_1\underline{\dot{\varphi}}^{12} \\
 {}_1\underline{\dot{\varphi}}^{12} &= \underline{\underline{T}}^{-1} \left({}_1\underline{\varphi}^{12} \right) \left({}_2\omega^2 - \underline{\underline{R}}_2^T \underline{\underline{R}}_1 {}_1\underline{\omega}^1 \right) = \underline{\underline{T}}_{\varphi^{12}} d\underline{q}_e \\
 \underline{\underline{T}}_{\varphi^{12}} &= \underline{\underline{T}}^{-1} \left({}_1\underline{\varphi}^{12} \right) \left(\underline{\underline{T}}_{\omega^2} - \underline{\underline{R}}_2^T \underline{\underline{R}}_1 \underline{\underline{T}}_{\omega^1} \right)
 \end{aligned} \tag{C-92}$$

$$\begin{aligned}
 {}_2\dot{\omega}^2 &= \underline{\underline{R}}_2^T \underline{\underline{R}}_1 {}_1\dot{\omega}^1 + \underline{\underline{T}} \left({}_1\underline{\varphi}^{12} \right) {}_1\dot{\varphi}^{12} - {}_2\widetilde{\omega}^2 \underline{\underline{R}}_2^T \underline{\underline{R}}_1 {}_1\omega^1 + \underline{\underline{R}}_2^T \underline{\underline{R}}_1 {}_1\widetilde{\omega}^1 {}_1\omega^1 \\
 &\quad + \underline{\underline{T}} \left({}_1\underline{\varphi}^{12}, {}_1\dot{\varphi}^{12} \right) {}_1\dot{\varphi}^{12} \\
 {}_1\underline{\dot{\varphi}}^{12} &= \underline{\underline{T}}^{-1} \left({}_1\underline{\varphi}^{12} \right) \left({}_2\dot{\omega}^2 - \underline{\underline{R}}_2^T \underline{\underline{R}}_1 {}_1\dot{\omega}^1 \right) \\
 &\quad + \underline{\underline{T}}^{-1} \left({}_1\underline{\varphi}^{12} \right) \left[{}_2\widetilde{\omega}^2 \underline{\underline{R}}_2^T \underline{\underline{R}}_1 {}_1\omega^1 - \underline{\underline{R}}_2^T \underline{\underline{R}}_1 {}_1\widetilde{\omega}^1 {}_1\omega^1 \right. \\
 &\quad \left. - \underline{\underline{T}} \left({}_1\underline{\varphi}^{12}, {}_1\dot{\varphi}^{12} \right) {}_1\dot{\varphi}^{12} \right] \\
 &= \underline{\underline{T}}^{-1} \left({}_1\underline{\varphi}^{12} \right) \left(\underline{\underline{T}}_{\omega^2} - \underline{\underline{R}}_2^T \underline{\underline{R}}_1 \underline{\underline{T}}_{\omega^1} \right) d\underline{q}_e \\
 &\quad + \underline{\underline{T}}^{-1} \left({}_1\underline{\varphi}^{12} \right) \left[{}_2\widetilde{\omega}^2 \underline{\underline{R}}_2^T \underline{\underline{R}}_1 \underline{\underline{T}}_{\omega^1} - \underline{\underline{R}}_2^T \underline{\underline{R}}_1 {}_1\widetilde{\omega}^1 \underline{\underline{T}}_{\omega^1} \right. \\
 &\quad \left. - \underline{\underline{T}} \left({}_1\underline{\varphi}^{12}, {}_1\dot{\varphi}^{12} \right) \underline{\underline{T}}_{\varphi^{12}} \right] d\underline{q}_e = \underline{\underline{T}}_{\varphi^{12}} d\underline{q}_e + \underline{\underline{T}}_{\varphi^{12}} d\underline{q}_e \\
 \dot{\underline{\underline{T}}}_{\varphi^{12}} &= \underline{\underline{T}}^{-1} \left({}_1\underline{\varphi}^{12} \right) \left[{}_2\widetilde{\omega}^2 \underline{\underline{R}}_2^T \underline{\underline{R}}_1 \underline{\underline{T}}_{\omega^1} - \underline{\underline{R}}_2^T \underline{\underline{R}}_1 {}_1\widetilde{\omega}^1 \underline{\underline{T}}_{\omega^1} - \underline{\underline{T}} \left({}_1\underline{\varphi}^{12}, {}_1\dot{\varphi}^{12} \right) \underline{\underline{T}}_{\varphi^{12}} \right]
 \end{aligned} \tag{C-93}$$

C.4.2 Shape function

$$\begin{aligned}
 {}_I\underline{r}^c &= N_0^1 {}_I\underline{r}^1 + N_0^2 {}_I\underline{r}^2 + N_1^1 {}_I\underline{r}'^1 + N_1^2 {}_I\underline{r}'^2 = \\
 &= N_0^1 {}_I\underline{r}^1 + N_0^2 {}_I\underline{r}^2 + N_1^1 \| {}_I\underline{r}'^1 \|_I \underline{n}_x^1 + N_1^2 \| {}_I\underline{r}'^2 \|_I \underline{n}_x^2
 \end{aligned} \tag{C-94}$$

$$\begin{aligned}
 {}_I\dot{\underline{r}}^c &= N_0^1 {}_I\dot{\underline{r}}^1 + N_0^2 {}_I\dot{\underline{r}}^2 + N_1^1 \left(\| {}_I\dot{\underline{r}}'^1 \|_I \underline{n}_x^1 - \| {}_I\dot{\underline{r}}'^1 \|_I \tilde{\underline{n}}_x^1 \underline{\underline{R}}_1 {}_1\omega^1 \right) \\
 &\quad + N_1^2 \left(\| {}_I\dot{\underline{r}}'^2 \|_I \underline{n}_x^2 - \| {}_I\dot{\underline{r}}'^2 \|_I \tilde{\underline{n}}_x^2 \underline{\underline{R}}_2 {}_2\omega^2 \right) = \underline{\underline{N}} D d\underline{q}_e \\
 \underline{\underline{N}} &= \begin{bmatrix} N_0^1 I & N_1^1 I & N_0^2 I & N_1^2 I \\ \underline{\underline{I}} & \underline{\underline{0}} & \underline{\underline{0}} & \underline{\underline{0}} \\ \underline{\underline{0}} & -\| {}_I\dot{\underline{r}}'^1 \|_I \tilde{\underline{n}}_x^1 \underline{\underline{R}}_1 & \underline{n}_x^1 & \underline{\underline{0}} \\ \underline{\underline{0}} & \underline{\underline{0}} & \underline{\underline{I}} & \underline{\underline{0}} \\ \underline{\underline{0}} & \underline{\underline{0}} & \underline{\underline{0}} & -\| {}_I\dot{\underline{r}}'^2 \|_I \tilde{\underline{n}}_x^2 \underline{\underline{R}}_2 \end{bmatrix} \\
 D &= \begin{bmatrix} I & \underline{\underline{0}} & \underline{\underline{0}} & \underline{\underline{0}} & \underline{\underline{0}} & \underline{\underline{0}} \\ \underline{\underline{0}} & -\| {}_I\dot{\underline{r}}'^1 \|_I \tilde{\underline{n}}_x^1 \underline{\underline{R}}_1 & \underline{n}_x^1 & \underline{\underline{0}} & \underline{\underline{0}} & \underline{\underline{0}} \\ \underline{\underline{0}} & \underline{\underline{0}} & \underline{\underline{0}} & \underline{\underline{I}} & \underline{\underline{0}} & \underline{\underline{0}} \\ \underline{\underline{0}} & \underline{\underline{0}} & \underline{\underline{0}} & \underline{\underline{0}} & -\| {}_I\dot{\underline{r}}'^2 \|_I \tilde{\underline{n}}_x^2 \underline{\underline{R}}_2 & \underline{n}_x^2 \end{bmatrix} \\
 &= \begin{bmatrix} I & \underline{\underline{0}} & \underline{\underline{0}} & \underline{\underline{0}} & \underline{\underline{0}} & \underline{\underline{0}} \\ \underline{\underline{0}} & -{}_I\tilde{\underline{r}}'^1 \underline{\underline{R}}_1 & \underline{n}_x^1 & \underline{\underline{0}} & \underline{\underline{0}} & \underline{\underline{0}} \\ \underline{\underline{0}} & \underline{\underline{0}} & \underline{\underline{0}} & \underline{\underline{I}} & \underline{\underline{0}} & \underline{\underline{0}} \\ \underline{\underline{0}} & \underline{\underline{0}} & \underline{\underline{0}} & \underline{\underline{0}} & -{}_I\tilde{\underline{r}}'^2 \underline{\underline{R}}_2 & \underline{n}_x^2 \end{bmatrix}
 \end{aligned} \tag{C-95}$$

$$\begin{aligned}
 & {}_I\ddot{\underline{r}}^c = \underline{\underline{N}} \underline{D} d\dot{q}_e + \underline{\underline{N}} \dot{\underline{D}} d\dot{q}_e \\
 & \underline{\underline{D}} = \\
 & = \begin{bmatrix} 0 & 0 & 0 & 0 & 0 \\ 0 & -\|{}_I\underline{r}'^1\| \underline{\underline{R}}_{11} \tilde{\omega}^1 \underline{\underline{\tilde{g}}}_x & -2{}_I\underline{\underline{n}}_x^1 \underline{\underline{R}}_{11} \underline{\omega}^1 & 0 & 0 \\ 0 & 0 & 0 & 0 & 0 \\ 0 & 0 & 0 & 0 & 0 \\ 0 & 0 & 0 & -\|{}_I\underline{r}'^2\| \underline{\underline{R}}_{22} \tilde{\omega}^2 \underline{\underline{\tilde{g}}}_x & -2{}_I\underline{\underline{n}}_x^2 \underline{\underline{R}}_{22} \underline{\omega}^2 \end{bmatrix} \quad (\text{C-96})
 \end{aligned}$$

$${}_I\underline{r}'^c = N'_0{}_I\underline{r}^1 + N'_0{}_I\underline{r}^2 + N'_1 \|{}_I\underline{r}'^1\| {}_I\underline{n}_x^1 + N'_1 \|{}_I\underline{r}'^2\| {}_I\underline{n}_x^2 \quad (\text{C-97})$$

$$\begin{aligned}
 & {}_I\dot{\underline{r}}'^c = \underline{\underline{N}}' \underline{\underline{D}} d\dot{q}_e \\
 & \underline{\underline{N}}' = [N'_0 \underline{\underline{I}} \quad N'_1 \underline{\underline{I}} \quad N'_0 \underline{\underline{I}} \quad N'_1 \underline{\underline{I}}] \quad (\text{C-98})
 \end{aligned}$$

$${}_I\ddot{\underline{r}}'^c = \underline{\underline{N}}' \underline{\underline{D}} d\dot{q}_e + \underline{\underline{N}}' \underline{\underline{D}} d\dot{q}_e \quad (\text{C-99})$$

$${}_I\underline{r}''^c = N''_0{}_I\underline{r}^1 + N''_0{}_I\underline{r}^2 + N''_1 \|{}_I\underline{r}'^1\| {}_I\underline{n}_x^1 + N''_1 \|{}_I\underline{r}'^2\| {}_I\underline{n}_x^2 \quad (\text{C-100})$$

$$\begin{aligned}
 & {}_I\dot{\underline{r}}''^c = \underline{\underline{N}}'' \underline{\underline{D}} d\dot{q}_e \\
 & \underline{\underline{N}}'' = [N''_0 \underline{\underline{I}} \quad N''_1 \underline{\underline{I}} \quad N''_0 \underline{\underline{I}} \quad N''_1 \underline{\underline{I}}] \quad (\text{C-101})
 \end{aligned}$$

C.4.3 X-axis

$${}_I\underline{n}_x = \frac{1}{\|{}_I\underline{r}'^c\|} {}_I\underline{r}'^c \quad (\text{C-102})$$

$${}_I\underline{n}'_x = \frac{1}{\|{}_I\underline{r}'^c\|} \left(\underline{\underline{I}} - {}_I\underline{n}_x {}_I\underline{n}_x^T \right) {}_I\underline{r}''^c \quad (\text{C-103})$$

$${}_I\dot{\underline{n}}_x = \frac{1}{\|{}_I\underline{r}'^c\|} \left(\underline{\underline{I}} - {}_I\underline{n}_x {}_I\underline{n}_x^T \right) {}_I\dot{\underline{r}}'^c = \frac{1}{\|{}_I\underline{r}'^c\|} \left(\underline{\underline{I}} - {}_I\underline{n}_x {}_I\underline{n}_x^T \right) \underline{\underline{N}}' \underline{\underline{D}} d\dot{q}_e = \underline{T}_{nx} d\dot{q}_e \quad (\text{C-104})$$

$$\begin{aligned}
 {}_I\dot{\underline{n}}'_x &= -\frac{1}{\|{}_I\underline{r}'^c\|} \left[{}_I\underline{n}'_x {}_I\underline{n}_x^T {}_I\dot{\underline{r}}'^c + \left({}_I\underline{n}_x^T {}_I\underline{r}''^c \underline{I} + {}_I\underline{n}_x {}_I\underline{r}''^c {}^T \right) {}_I\dot{\underline{n}}_x \right. \\
 &\quad \left. - \left(\underline{I} - {}_I\underline{n}_x {}_I\underline{n}_x^T \right) {}_I\dot{\underline{r}}''^c \right] \\
 &= -\frac{1}{\|{}_I\underline{r}'^c\|} \left[{}_I\underline{n}'_x {}_I\underline{n}_x^T \underline{N}' \underline{D} + \left({}_I\underline{n}_x^T {}_I\underline{r}''^c \underline{I} + {}_I\underline{n}_x {}_I\underline{r}''^c {}^T \right) \underline{T}_{nx} \right. \\
 &\quad \left. - \left(\underline{I} - {}_I\underline{n}_x {}_I\underline{n}_x^T \right) \underline{N}'' \underline{D} \right] \underline{d}q_e = \underline{T}_{dnx} \underline{d}q_e
 \end{aligned} \tag{C-105}$$

$$\begin{aligned}
 {}_I\ddot{\underline{n}}_x &= -\frac{1}{\|{}_I\underline{r}'^c\|} \left[\left(2 {}_I\dot{\underline{n}}_x {}_I\underline{n}_x^T + {}_I\underline{n}_x {}_I\dot{\underline{n}}_x^T \right) {}_I\dot{\underline{r}}'^c - \left(\underline{I} - {}_I\underline{n}_x {}_I\underline{n}_x^T \right) {}_I\ddot{\underline{r}}'^c \right] \\
 &= -\frac{1}{\|{}_I\underline{r}'^c\|} \left[\left(2 {}_I\dot{\underline{n}}_x {}_I\underline{n}_x^T + {}_I\underline{n}_x {}_I\dot{\underline{n}}_x^T \right) \underline{N}' \underline{D} \right. \\
 &\quad \left. - \left(\underline{I} - {}_I\underline{n}_x {}_I\underline{n}_x^T \right) \underline{N}' \underline{D} \right] \underline{d}q_e + \frac{1}{\|{}_I\underline{r}'^c\|} \left(\underline{I} - {}_I\underline{n}_x {}_I\underline{n}_x^T \right) \underline{N}' \underline{D} \underline{d}\dot{q}_e \\
 &= \dot{\underline{T}}_{nx} \underline{d}q_e + \underline{T}_{nx} \underline{d}\dot{q}_e
 \end{aligned} \tag{C-106}$$

C.4.4 Angle

$$\underline{n}_x = \underline{\underline{R}}_1 \underline{\underline{R}}_Z ({}^1\theta) \underline{\underline{R}}_y ({}^1\psi) \underline{g}_x = \underline{\underline{R}}_1 \begin{bmatrix} \cos {}^1\psi \cos {}^1\theta \\ \cos {}^1\psi \sin {}^1\theta \\ -\sin {}^1\psi \end{bmatrix} \tag{C-107}$$

Bending angle

$${}^1\psi = -\sin^{-1} \underline{g}_z^T \underline{\underline{R}}_1^T {}_I\underline{n}_x \quad {}^1\theta = \sin^{-1} \frac{\underline{g}_y^T \underline{\underline{R}}_1^T {}_I\underline{n}_x}{\cos {}^1\psi} \tag{C-108}$$

The first derivative of s

$$\begin{aligned}
 {}^1\psi' &= -\frac{\underline{g}_z^T \underline{\underline{R}}_1^T}{\sqrt{1 - \sin^2 {}^1\psi}} \underline{n}'_x \\
 {}^1\theta' &= \frac{\underline{g}_y^T \underline{\underline{R}}_1^T}{\cos {}^1\psi \sqrt{1 - \sin^2 {}^1\theta}} ({}^1n'_x + {}^1n_x \tan {}^1\psi {}^1\psi')
 \end{aligned} \tag{C-109}$$

First derivative with respect to t

$$\begin{aligned}
 {}_1\dot{\psi} &= -\frac{\underline{g}_z^T \underline{R}_1^T}{\sqrt{1 - \sin^2 {}_1\psi}} \left({}_I \dot{n}_x + {}_I \tilde{n}_x \underline{R}_1 \underline{\omega}^1 \right) \\
 &= -\frac{\underline{g}_z^T \underline{R}_1^T}{\sqrt{1 - \sin^2 {}_1\psi}} \left(\underline{T}_{nx} + {}_I \tilde{n}_x \underline{R}_1 \underline{T}_{\omega 1} \right) \underline{dq}_e = \underline{T}_{\psi}^T \underline{dq}_e \\
 {}_1\dot{\theta} &= \frac{\underline{g}_y^T \underline{R}_1^T}{\cos {}_1\psi \sqrt{1 - \sin^2 {}_1\theta}} \left({}_I \tilde{n}_x \underline{R}_1 \underline{\omega}^1 + {}_I \dot{n}_x + {}_I n_x \tan {}_1\psi {}_1\dot{\psi} \right) \quad (\text{C-110}) \\
 &= \frac{\underline{g}_y^T \underline{R}_1^T}{\cos {}_1\psi \sqrt{1 - \sin^2 {}_1\theta}} \left({}_I \tilde{n}_x \underline{R}_1 \underline{T}_{\omega 1} + \underline{T}_{nx} + {}_I n_x \underline{T}_{\psi}^T \tan {}_1\psi {}_1\dot{\psi} \right) \underline{dq}_e \\
 &= \underline{T}_{\theta}^T \underline{dq}_e
 \end{aligned}$$

Derivative to s, t

$$\begin{aligned}
 {}_1\dot{\psi}' &= -\frac{\underline{g}_z^T \underline{R}_1^T}{\sqrt{1 - \sin^2 {}_1\psi}} \left[{}_I \dot{n}'_x + {}_I \tilde{n}'_x \underline{R}_1 \underline{\omega}^1 + {}_I n'_x \tan {}_1\psi {}_1\dot{\psi} \right] \\
 &= -\frac{\underline{g}_z^T \underline{R}_1^T}{\sqrt{1 - \sin^2 {}_1\psi}} \left[\underline{T}_{dnx} + {}_I \tilde{n}'_x \underline{R}_1 \underline{T}_{\omega 1} + {}_I n'_x \tan {}_1\psi \underline{T}_{\psi}^T \right] \underline{dq}_e \\
 &= \underline{T}_{d\psi}^T \underline{dq}_e \\
 {}_1\dot{\theta}' &= \frac{\underline{g}_y^T \underline{R}_1^T}{\cos {}_1\psi \sqrt{1 - \sin^2 {}_1\theta}} \left[{}_I \tilde{n}'_x \underline{R}_1 \underline{\omega}^1 + {}_I \dot{n}'_x \right. \\
 &\quad \left. + ({}_I n'_x \tan {}_1\psi + {}_I n_x \sec^2 {}_1\psi {}_1\psi') {}_1\dot{\psi} + {}_I n_x \tan {}_1\psi {}_1\dot{\psi}' \right. \quad (\text{C-111}) \\
 &\quad \left. + (\tan {}_1\psi {}_1\psi' + \tan {}_1\theta {}_1\theta') \left({}_I \tilde{n}_x \underline{R}_1 \underline{\omega}^1 + {}_I \dot{n}_x + {}_I n_x \tan {}_1\psi {}_1\dot{\psi} \right) \right] \\
 &= \frac{\underline{g}_y^T \underline{R}_1^T}{\cos {}_1\psi \sqrt{1 - \sin^2 {}_1\theta}} \left[{}_I \tilde{n}'_x \underline{R}_1 \underline{T}_{\omega 1} + \underline{T}_{dnx} \right. \\
 &\quad \left. + ({}_I n'_x \tan {}_1\psi + {}_I n_x \sec^2 {}_1\psi {}_1\psi') \underline{T}_{\psi}^T + {}_I n_x \tan {}_1\psi \underline{T}_{d\psi}^T \right. \\
 &\quad \left. + (\tan {}_1\psi {}_1\psi' + \tan {}_1\theta {}_1\theta') \left({}_I \tilde{n}_x \underline{R}_1 \underline{T}_{\omega 1} + \underline{T}_{nx} \right. \right. \\
 &\quad \left. \left. + {}_I n_x \tan {}_1\psi \underline{T}_{\psi}^T \right) \right] \underline{dq}_e = \underline{T}_{d\theta}^T \underline{dq}_e
 \end{aligned}$$

Second derivative with respect to t

$$\begin{aligned}
 {}_1\ddot{\psi} &= -\frac{1}{\sqrt{1-\sin^2 {}_1\psi}} \left(\underline{g}_z^T \underline{R}_1^T {}_I \ddot{n}_x + \underline{g}_z^T \underline{R}_1^T {}_I \tilde{n}_x \underline{R}_{11} \underline{\omega}^1 \right) \\
 &\quad - \frac{\underline{g}_z^T \underline{R}_1^T}{\sqrt{1-\sin^2 {}_1\psi}} \left[\left(2 {}_I \dot{\tilde{n}}_x - \underline{R}_{11} \underline{\tilde{\omega}}^1 \underline{R}_1^T {}_I \tilde{n}_x \right) \underline{R}_{11} \underline{\omega}^1 \right. \\
 &\quad \left. + \left({}_I \dot{n}_x + {}_I \tilde{n}_x \underline{R}_{11} \underline{\omega}^1 \right) \tan {}_1\psi {}_1\dot{\psi} \right] = \\
 &= -\frac{\underline{g}_z^T \underline{R}_1^T}{\sqrt{1-\sin^2 {}_1\psi}} \left(\underline{T}_{nx} + {}_I \tilde{n}_x \underline{R}_{11} \underline{T}_{\omega 1} \right) \underline{d}\dot{q}_e \\
 &\quad - \frac{\underline{g}_z^T \underline{R}_1^T}{\sqrt{1-\sin^2 {}_1\psi}} \left[\underline{\dot{T}}_{nx} + \left(2 {}_I \dot{\tilde{n}}_x - \underline{R}_{11} \underline{\tilde{\omega}}^1 \underline{R}_1^T {}_I \tilde{n}_x \right) \underline{R}_{11} \underline{T}_{\omega 1} \right. \\
 &\quad \left. + \left({}_I \dot{n}_x + {}_I \tilde{n}_x \underline{R}_{11} \underline{\omega}^1 \right) \tan {}_1\psi \underline{T}_{\psi}^T \right] \underline{dq}_e = \underline{T}_{\psi}^T \underline{d}\dot{q}_e + \underline{\dot{T}}_{\psi}^T \underline{dq}_e \\
 {}_1\ddot{\theta} &= \underline{T}_{\theta}^T \underline{d}\dot{q}_e + \underline{\dot{T}}_{\theta}^T \underline{dq}_e
 \end{aligned} \tag{C-112}$$

$$\begin{aligned}
 \underline{\dot{T}}_{\psi}^T &= -\frac{\underline{g}_z^T \underline{R}_1^T}{\sqrt{1-\sin^2 {}_1\psi}} \left[\underline{\dot{T}}_{nx} + \left(2 {}_I \dot{\tilde{n}}_x - \underline{R}_{11} \underline{\tilde{\omega}}^1 \underline{R}_1^T {}_I \tilde{n}_x \right) \underline{R}_{11} \underline{T}_{\omega 1} \right. \\
 &\quad \left. + \left({}_I \dot{n}_x + {}_I \tilde{n}_x \underline{R}_{11} \underline{\omega}^1 \right) \tan {}_1\psi \underline{T}_{\psi}^T \right] \\
 \underline{\dot{T}}_{\theta}^T &= \frac{\underline{g}_y^T}{\cos {}_1\psi \sqrt{1-\sin^2 {}_1\theta}} \left[\underline{R}_1^T \underline{\dot{T}}_{nx} + \underline{R}_1^T {}_I \underline{n}_x \tan {}_1\psi \underline{T}_{\psi}^T - {}_1 \underline{\tilde{\omega}}^1 \underline{R}_1^T {}_I \tilde{n}_x \underline{R}_{11} \underline{T}_{\omega 1} \right. \\
 &\quad - 2 {}_1 \underline{\tilde{\omega}}^1 \underline{R}_1^T \underline{T}_{nx} \\
 &\quad + \left(2 \underline{R}_1^T {}_I \dot{n}_x \tan {}_1\psi - 2 {}_1 \underline{\tilde{\omega}}^1 \underline{R}_1^T {}_I \underline{n}_x \tan {}_1\psi + \underline{R}_1^T {}_I \underline{n}_x \sec^2 {}_1\psi {}_1\dot{\psi} \right. \\
 &\quad \left. + \underline{R}_1^T {}_I \underline{n}_x \tan^2 {}_1\psi {}_1\dot{\psi} \right) \underline{T}_{\psi}^T \\
 &\quad \left. + \left(- {}_1 \underline{\tilde{\omega}}^1 \underline{R}_1^T {}_I \underline{n}_x + \underline{R}_1^T {}_I \dot{n}_x + \underline{R}_1^T {}_I \underline{n}_x \tan {}_1\psi {}_1\dot{\psi} \right) \tan {}_1\theta \underline{T}_{\theta}^T \right]
 \end{aligned} \tag{C-113}$$

$$\begin{aligned}
 {}_1\varphi &= \xi {}_1\varphi^{12} & {}_1\varphi' &= \frac{1}{L} {}_1\varphi^{12} \\
 {}_1\dot{\varphi} &= \xi {}_1\dot{\varphi}^{12} = \xi \underline{g}_x^T \underline{T}_{\varphi 12} \underline{dq}_e & \underline{T}_{\varphi}^T \underline{dq}_e &= \underline{T}_{\varphi}^T \underline{dq}_e \\
 {}_1\dot{\varphi}' &= \frac{1}{L} {}_1\dot{\varphi}^{12} = \frac{1}{L} \underline{g}_x^T \underline{T}_{\varphi 12} \underline{dq}_e & \underline{T}_{d\varphi}^T \underline{dq}_e &= \underline{T}_{d\varphi}^T \underline{dq}_e
 \end{aligned} \tag{C-114}$$

$${}_1\ddot{\varphi} = \xi {}_1\ddot{\varphi}^{12} = \xi \underline{g}_x^T \underline{T}_{\varphi 12} \underline{d}\dot{q}_e + \xi \underline{g}_x^T \underline{\dot{T}}_{\varphi 12} \underline{dq}_e = \underline{T}_{\varphi}^T \underline{d}\dot{q}_e + \underline{\dot{T}}_{\varphi}^T \underline{dq}_e \tag{C-115}$$

$${}_1\underline{\varphi} = [{}_1\varphi \quad {}_1\psi \quad {}_1\theta]^T \quad {}_1\underline{\varphi}' = [{}_1\varphi' \quad {}_1\psi' \quad {}_1\theta']^T \tag{C-116}$$

$$\begin{aligned}
 {}_1\dot{\underline{\phi}} &= \begin{bmatrix} {}_1\dot{\phi} \\ {}_1\dot{\psi} \\ {}_1\dot{\theta} \end{bmatrix} = \begin{bmatrix} T_{\phi}^T \\ T_{\psi}^T \\ T_{\theta}^T \end{bmatrix} \underline{dq}_e = \underline{T}_{Angle} \underline{dq}_e \\
 {}_1\dot{\underline{\phi}'} &= \begin{bmatrix} {}_1\dot{\phi}' \\ {}_1\dot{\psi}' \\ {}_1\dot{\theta}' \end{bmatrix} = \begin{bmatrix} T_{d\phi}^T \\ T_{d\psi}^T \\ T_{d\theta}^T \end{bmatrix} \underline{dq}_e = \underline{T}_{dAngle} \underline{dq}_e \\
 {}_1\ddot{\underline{\phi}} &= \begin{bmatrix} {}_1\ddot{\phi} \\ {}_1\ddot{\psi} \\ {}_1\ddot{\theta} \end{bmatrix} = \begin{bmatrix} T_{\phi}^T \\ T_{\psi}^T \\ T_{\theta}^T \end{bmatrix} \underline{d\dot{q}}_e + \begin{bmatrix} \dot{T}_{\phi}^T \\ \dot{T}_{\psi}^T \\ \dot{T}_{\theta}^T \end{bmatrix} \underline{dq}_e = \underline{T}_{Angle} \underline{d\dot{q}}_e + \dot{\underline{T}}_{Angle} \underline{dq}_e
 \end{aligned} \tag{C-117}$$

C.4.5 Kinematic

$$\begin{aligned}
 {}_1\underline{R}_c &= \underline{\underline{R}}_d = \underline{\underline{R}} \left({}_1\underline{\phi} \right) & {}_c\underline{\omega}_d^c &= \underline{\underline{T}} \left({}_1\underline{\phi} \right) {}_1\underline{\dot{\phi}} \\
 \underline{\underline{T}}_d &= \underline{\underline{T}} \left({}_1\underline{\phi} \right) & \underline{\underline{T}}_d &= \dot{\underline{\underline{T}}} \left({}_1\underline{\phi}, {}_1\underline{\dot{\phi}} \right)
 \end{aligned} \tag{C-118}$$

$$\begin{aligned}
 {}_c\underline{\omega}^c &= \underline{\underline{R}}_d^T {}_1\underline{\omega}^1 + \underline{\underline{T}}_d {}_1\underline{\dot{\phi}} = \underline{\underline{T}}_\omega \underline{dq}_e \\
 \underline{\underline{T}}_\omega &= \underline{\underline{R}}_d^T \underline{\underline{T}}_{\omega 1} + \underline{\underline{T}}_d \underline{\underline{T}}_{Angle}
 \end{aligned} \tag{C-119}$$

$$\begin{aligned}
 \frac{\partial {}_c\underline{\omega}^c}{\partial t} &= \underline{\underline{R}}_d^T {}_1\underline{\dot{\omega}}^1 - {}_c\widetilde{\omega}_d^c \underline{\underline{R}}_d^T {}_1\underline{\omega}^1 + \dot{\underline{\underline{T}}}_d {}_1\underline{\dot{\phi}} + \underline{\underline{T}}_d {}_1\underline{\ddot{\phi}} \\
 &= \left(\underline{\underline{R}}_d^T \underline{\underline{T}}_{\omega 1} + \underline{\underline{T}}_d \underline{\underline{T}}_{Angle} \right) \underline{d\dot{q}}_e \\
 &+ \left(\dot{\underline{\underline{T}}}_d \underline{\underline{T}}_{Angle} + \underline{\underline{T}}_d \dot{\underline{\underline{T}}}_{Angle} - {}_c\widetilde{\omega}_d^c \underline{\underline{R}}_d^T \underline{\underline{T}}_{\omega 1} \right) \underline{dq}_e = \underline{\underline{T}}_\omega \underline{d\dot{q}}_e + \dot{\underline{\underline{T}}}_\omega \underline{dq}_e \\
 \dot{\underline{\underline{T}}}_\omega &= \dot{\underline{\underline{T}}}_d \underline{\underline{T}}_{Angle} + \underline{\underline{T}}_d \dot{\underline{\underline{T}}}_{Angle} - {}_c\widetilde{\omega}_d^c \underline{\underline{R}}_d^T \underline{\underline{T}}_{\omega 1}
 \end{aligned} \tag{C-120}$$

$$\begin{aligned}
 {}_I\underline{\dot{\omega}}^c &= \underline{\underline{R}}_c \frac{\partial {}_c\underline{\omega}^c}{\partial t} + \underline{\underline{R}}_c {}_c\widetilde{\omega}^c {}_c\underline{\omega}^c \\
 {}_c\underline{\dot{\omega}}^c &= \underline{\underline{R}}_c^T {}_I\underline{\dot{\omega}}^c = \frac{\partial {}_c\underline{\omega}^c}{\partial t} + {}_c\widetilde{\omega}^c {}_c\underline{\omega}^c = \frac{\partial {}_c\underline{\omega}^c}{\partial t}
 \end{aligned} \tag{C-121}$$

C.4.6 Strain

Axial stress

$${}_I\varepsilon = \| {}_I\underline{r}'^c \| - 1 = {}_B\varepsilon \tag{C-122}$$

$$I\dot{\varepsilon} = \frac{1}{\|I\dot{r}'^c\|} I\dot{r}'^{cT} I\dot{r}'^c = \underline{\underline{R}}_c \underline{g}_x I\dot{r}'^c = \frac{1}{\|I\dot{r}'^c\|} I\dot{r}'^{cT} \underline{\underline{N}}' \underline{\underline{D}} d\underline{q}_e = \underline{\underline{T}}_{\varepsilon}^T d\underline{q}_e \quad (\text{C-123})$$

Curvature

$$\begin{aligned} B\underline{\underline{\kappa}} &= \underline{\underline{T}} \left({}_1 \underline{\varphi} \right) {}_1 \underline{\varphi}' \\ \frac{\partial B\underline{\underline{\kappa}}}{\partial t} &= \underline{\underline{T}} \left({}_1 \underline{\varphi} \right) {}_1 \dot{\underline{\varphi}} + \underline{\underline{T}} \left({}_1 \underline{\varphi}, {}_1 \dot{\underline{\varphi}} \right) {}_1 \underline{\varphi}' = \underline{\underline{T}} \left({}_1 \underline{\varphi} \right) {}_1 \dot{\underline{\varphi}} + \underline{\underline{T}}' \left({}_1 \underline{\varphi}, {}_1 \underline{\varphi}' \right) {}_1 \dot{\underline{\varphi}} \\ &= \left[\underline{\underline{T}} \left({}_1 \underline{\varphi} \right) \underline{\underline{T}}_{dAngle} + \underline{\underline{T}}' \left({}_1 \underline{\varphi}, {}_1 \underline{\varphi}' \right) \underline{\underline{T}}_{Angle} \right] d\underline{q}_e = \underline{\underline{T}}_{\kappa} d\underline{q}_e \end{aligned} \quad (\text{C-124})$$

$$\begin{aligned} I\dot{\underline{\kappa}} &= \underline{\underline{R}}_c \frac{\partial c\underline{\underline{\kappa}}}{\partial t} + \underline{\underline{R}}_c c \underline{\tilde{\omega}}^c c\underline{\underline{\kappa}} \\ \frac{d c\underline{\underline{\kappa}}}{dt} &= \underline{\underline{R}}_c^T I\dot{\underline{\kappa}} = \frac{\partial B\underline{\underline{\kappa}}}{\partial t} + c \underline{\tilde{\omega}}^c c\underline{\underline{\kappa}} = \frac{\partial B\underline{\underline{\kappa}}}{\partial t} - c \underline{\tilde{\kappa}} c \underline{\omega}^c \end{aligned} \quad (\text{C-125})$$

C.4.7 Virtual Internal Power

$$\underline{\underline{\varepsilon}} = \begin{bmatrix} I^{\underline{\varepsilon}} \\ B\underline{\underline{\kappa}} \end{bmatrix} \quad (\text{C-126})$$

$$\dot{\underline{\varepsilon}} = \begin{bmatrix} I\dot{\underline{\varepsilon}} \\ B\dot{\underline{\kappa}} \end{bmatrix} = \begin{bmatrix} \underline{\underline{T}}_{\varepsilon}^T \\ \underline{\underline{T}}_{\kappa} \end{bmatrix} d\underline{q}_e = \underline{\underline{T}}_{Strain} d\underline{q}_e \quad (\text{C-127})$$

$$\underline{\sigma} = \begin{bmatrix} EA & 0 & 0 & 0 \\ 0 & GJ & 0 & 0 \\ 0 & 0 & EI_y & 0 \\ 0 & 0 & 0 & EI_z \end{bmatrix} \begin{bmatrix} I^{\underline{\varepsilon}} \\ B\underline{\kappa}_x \\ B\underline{\kappa}_y \\ B\underline{\kappa}_z \end{bmatrix} = \underline{\underline{K}}_{\varepsilon} \underline{\underline{\varepsilon}} \quad (\text{C-128})$$

$$\delta p_{int} = - \int_0^L \delta \dot{\underline{\varepsilon}}^T \underline{\sigma} ds = - \delta \underline{dq}_e^T \int_0^L \underline{\underline{T}}_{Strain}^T \underline{\underline{K}}_{\varepsilon} \underline{\underline{\varepsilon}} ds = - \delta \underline{dq}_e^T \underline{F}_{int} \quad (\text{C-129})$$

C.4.8 Virtual Inertial Power

$$\begin{aligned}
 \delta p_{ine,tra} &= -\rho A \int_0^L \delta_I \underline{\dot{r}}^c T \underline{\dot{r}}^c ds = -\delta \underline{dq}_e^T (\underline{\underline{M}}_{e,ine,tra} \underline{d\dot{q}}_e + \underline{\underline{D}}_{ine,tra} \underline{dq}_e) \\
 &= -\delta \underline{dq}_e^T \left(\rho A \underline{\underline{D}}^T \int_0^L \underline{\underline{N}}^T \underline{\underline{N}} ds \underline{\underline{D}} \underline{d\dot{q}}_e + \rho A \underline{\underline{D}}^T \int_0^L \underline{\underline{N}}^T \underline{\underline{N}} ds \underline{\underline{D}} \underline{dq}_e \right) \\
 &= -\delta \underline{dq}_e^T (\underline{\underline{M}}_{e,ine,tra} \underline{d\dot{q}}_e + \underline{F}_{ine,tra}) \\
 \underline{\underline{M}}_{e,ine,tra} &= \rho A \underline{\underline{D}}^T \int_0^L \underline{\underline{N}}^T \underline{\underline{N}} ds \underline{\underline{D}} \quad \underline{F}_{ine,tra} = \underline{\underline{D}}_{ine,tra} \underline{dq}_e \\
 \underline{\underline{D}}_{ine,tra} &= \rho A \underline{\underline{D}}^T \int_0^L \underline{\underline{N}}^T \underline{\underline{N}} ds \underline{\underline{D}}
 \end{aligned} \tag{C-130}$$

$$\begin{aligned}
 \delta p_{ine,rot} &= -\rho \int_0^L \delta_I \underline{\omega}^c T \underline{J}_I \underline{\dot{\omega}}^c ds = -\rho \int_0^L \delta_c \underline{\omega}^c T \underline{\underline{R}}_c^T \underline{J}_I \underline{\underline{R}}_c (\underline{c\dot{\omega}}^c + \underline{c\tilde{\omega}}^c \underline{c\omega}^c) ds \\
 &= -\rho \int_0^L \delta_c \underline{\omega}^c T (\underline{J}_c \underline{\dot{\omega}}^c + \underline{c\tilde{\omega}}^c \underline{J}_c \underline{\omega}^c) ds \\
 &= -\delta \underline{dq}_e^T (\underline{\underline{M}}_{e,ine,rot} \underline{d\dot{q}}_e + \underline{F}_{ine,rot}) \\
 \underline{\underline{M}}_{e,ine,rot} &= \rho \int_0^L \underline{\underline{T}}_\omega^T \underline{\underline{J}}_\omega ds \quad \underline{F}_{ine,rot} = \underline{\underline{D}}_{ine,rot} \underline{dq}_e \\
 \underline{\underline{D}}_{ine,rot} &= \rho \int_0^L \underline{\underline{T}}_\omega^T (\underline{\underline{J}}_\omega \dot{\underline{\underline{\omega}}} + \underline{c\tilde{\omega}}^c \underline{\underline{J}}_\omega \underline{\omega}) ds
 \end{aligned} \tag{C-131}$$

$$\begin{aligned}
 \delta p_{ine} &= \delta p_{ine,tra} + \delta p_{ine,rot} \\
 &= -\delta \underline{dq}_e^T [(\underline{\underline{M}}_{e,ine,tra} + \underline{\underline{M}}_{e,ine,rot}) \underline{d\dot{q}}_e + (\underline{F}_{ine,tra} + \underline{F}_{ine,rot})] \\
 &= -\delta \underline{dq}_e^T (\underline{\underline{M}}_{e,ine} \underline{d\dot{q}}_e + \underline{F}_{ine})
 \end{aligned} \tag{C-132}$$

C.4.9 Virtual External Power

$$\delta p_{ext,g} = \rho A \int_0^L \delta_I \underline{\dot{r}}^c T ds_I g = \delta \underline{dq}_e^T \rho A \underline{\underline{D}}^T \int_0^L \underline{\underline{N}}^T ds_I g = -\delta \underline{dq}_e^T \underline{\underline{V}}_e I g \tag{C-133}$$

$$\underline{\underline{V}_e} = -\rho A \underline{\underline{D}}^T \int_0^L \underline{\underline{N}}^T ds \quad \underline{F}_{ext,g} = \underline{\underline{V}_e} \underline{\underline{I}} \underline{\underline{g}} \quad (C-134)$$

C.4.10 Virtual power principle of Cubic Spline Beam

$$\begin{aligned} \delta p_e &= \delta p_{ine} + \delta p_{int} + \delta p_{ext} = \delta p_{ine} + \delta p_{int} + \delta p_{ext,g} \\ &= -\delta \underline{\underline{dq}}_e^T \left[\left(\underline{\underline{M}}_{e,ine,tra} + \underline{\underline{M}}_{e,ine,rot} \right) \underline{\underline{d}\dot{q}}_e + \underline{\underline{F}}_{ine} + \underline{\underline{F}}_{int} + \underline{\underline{F}}_{ext,g} \right] \quad (C-135) \\ &= -\delta \underline{\underline{dq}}_e^T \left(\underline{\underline{M}}_e \underline{\underline{d}\dot{q}}_e + \underline{\underline{F}}_e \right) \end{aligned}$$

C.4.11 Coordinate of Internal Node with no End Axial Strain Assumption

$$\begin{aligned} \underline{\underline{r}}^c &= N_0^1 \underline{\underline{r}}^1 + N_0^2 \underline{\underline{r}}^2 + N_1^1 \underline{\underline{r}}'^1 + N_1^2 \underline{\underline{r}}'^2 \approx N_0^1 \underline{\underline{r}}^1 + N_0^2 \underline{\underline{r}}^2 + N_1^1 \underline{\underline{n}}_x^1 + N_1^2 \underline{\underline{n}}_x^2 \\ &= N_0^1 \underline{\underline{r}}^1 + N_0^2 \underline{\underline{r}}^2 + N_1^1 \underline{\underline{R}}_1 g_x + N_1^2 \underline{\underline{R}}_2 g_x \end{aligned} \quad (C-136)$$

$$\begin{aligned} \underline{\underline{\dot{r}}}^c &= N_0^1 \underline{\underline{\dot{r}}}^1 + N_0^2 \underline{\underline{\dot{r}}}^2 + N_1^1 \underline{\underline{R}}_{1,1} \widetilde{\omega}^1 g_x + N_1^2 \underline{\underline{R}}_{2,2} \widetilde{\omega}^2 g_x \\ &= N_0^1 \underline{\underline{\dot{r}}}^1 + N_0^2 \underline{\underline{\dot{r}}}^2 - N_1^1 \underline{\underline{\tilde{n}}}_x^1 \underline{\underline{R}}_{1,1} \underline{\underline{\omega}}^1 - N_1^2 \underline{\underline{\tilde{n}}}_x^2 \underline{\underline{R}}_{2,2} \underline{\underline{\omega}}^2 = \underline{\underline{ND}} \underline{\underline{dq}}_e \\ \underline{\underline{D}} &= \begin{bmatrix} \underline{\underline{I}} & \underline{\underline{0}} & \underline{\underline{0}} & \underline{\underline{0}} \\ \underline{\underline{0}} & -\underline{\underline{I}} \underline{\underline{\tilde{n}}}_x^1 \underline{\underline{R}}_1 & \underline{\underline{0}} & \underline{\underline{0}} \\ \underline{\underline{0}} & \underline{\underline{0}} & \underline{\underline{I}} & \underline{\underline{0}} \\ \underline{\underline{0}} & \underline{\underline{0}} & \underline{\underline{0}} & -\underline{\underline{I}} \underline{\underline{\tilde{n}}}_x^2 \underline{\underline{R}}_2 \end{bmatrix} \end{aligned} \quad (C-137)$$

$$\begin{aligned} \underline{\underline{\ddot{r}}}^c &= N_0^1 \underline{\underline{\ddot{r}}}^1 + N_0^2 \underline{\underline{\ddot{r}}}^2 + N_1^1 \underline{\underline{R}}_{1,1} \dot{\underline{\underline{\omega}}}^1 g_x + N_1^2 \underline{\underline{R}}_{2,2} \dot{\underline{\underline{\omega}}}^2 g_x + N_1^1 \underline{\underline{R}}_{1,1} \dot{\underline{\underline{\omega}}}^1 \dot{\underline{\underline{\omega}}}^1 g_x \\ &\quad + N_1^2 \underline{\underline{R}}_{2,2} \dot{\underline{\underline{\omega}}}^2 \dot{\underline{\underline{\omega}}}^2 g_x \\ &= N_0^1 \underline{\underline{\ddot{r}}}^1 + N_0^2 \underline{\underline{\ddot{r}}}^2 - N_1^1 \underline{\underline{\tilde{n}}}_x^1 \underline{\underline{R}}_{1,1} \underline{\underline{\omega}}^1 - N_1^2 \underline{\underline{\tilde{n}}}_x^2 \underline{\underline{R}}_{2,2} \underline{\underline{\omega}}^2 = \underline{\underline{ND}} \underline{\underline{dq}}_e \\ \underline{\underline{\dot{D}}} &= \begin{bmatrix} \underline{\underline{0}} & \underline{\underline{0}} & \underline{\underline{0}} & \underline{\underline{0}} \\ \underline{\underline{0}} & -\underline{\underline{R}}_{1,1} \dot{\underline{\underline{\omega}}}^1 \underline{\underline{\tilde{g}}}_x & \underline{\underline{0}} & \underline{\underline{0}} \\ \underline{\underline{0}} & \underline{\underline{0}} & \underline{\underline{0}} & \underline{\underline{0}} \\ \underline{\underline{0}} & \underline{\underline{0}} & \underline{\underline{0}} & -\underline{\underline{R}}_{2,2} \dot{\underline{\underline{\omega}}}^2 \underline{\underline{\tilde{g}}}_x \end{bmatrix} \end{aligned} \quad (C-138)$$

C.4.12 Cubic Spline Body and Section Parameter Recognition

$$\begin{aligned}
 \delta p_e &= \delta p_{ine} + \delta p_{int} + \delta p_{ext,g} \\
 &= -\delta \underline{d} \underline{q}_e^T \left\{ \int_0^L \left(\underline{\underline{D}}^T \underline{\underline{N}}^T \rho A \underline{\underline{AND}} + \underline{\underline{T}}_\omega^T \rho J \underline{\underline{T}}_\omega \right) ds \underline{d} \dot{q}_e \right. \\
 &\quad + \int_0^L \left[\underline{\underline{T}}_{strain}^T \underline{\underline{K}}_\varepsilon \underline{\varepsilon} - \underline{\underline{D}}^T \underline{\underline{N}}^T \rho A_I g \right. \\
 &\quad \left. \left. + \left(\underline{\underline{D}}^T \underline{\underline{N}}^T \rho A \underline{\underline{AND}} \dot{+} \underline{\underline{T}}_\omega^T \rho J \dot{\underline{\underline{T}}}_\omega + \underline{\underline{T}}_\omega^T c \tilde{\underline{\underline{\omega}}}^c \rho J \underline{\underline{T}}_\omega \right) \underline{d} q_e \right] ds \right\} \\
 \end{aligned} \tag{C-139}$$

With Gauss Interpolation

$$\begin{aligned}
 \delta p_e &= \delta p_{ine} + \delta p_{int} + \delta p_{ext,g} \\
 &= -\delta \underline{d} \underline{q}_e^T \sum_{i=1}^n w \left[\left(\underline{\underline{D}}^T \underline{\underline{N}}^T \rho A \underline{\underline{IND}} + \underline{\underline{T}}_\omega^T \rho J \underline{\underline{T}}_\omega \right) \Big|_x \right] \underline{d} \dot{q}_e \\
 &\quad - \delta \underline{d} \underline{q}_e^T \sum_{i=1}^n w \left\{ \left[\underline{\underline{T}}_{strain}^T \underline{\underline{K}}_\varepsilon \underline{\varepsilon} - \underline{\underline{D}}^T \underline{\underline{N}}^T \rho A I_I g \right. \right. \\
 &\quad \left. \left. + \left(\underline{\underline{D}}^T \underline{\underline{N}}^T \rho A \underline{\underline{IND}} \dot{+} \underline{\underline{T}}_\omega^T \rho J \dot{\underline{\underline{T}}}_\omega + \underline{\underline{T}}_\omega^T c \tilde{\underline{\underline{\omega}}}^c \rho J \underline{\underline{T}}_\omega \right) \underline{d} q_e \right] \Big|_x \right\} \\
 &\underline{\underline{M}}_e = \sum_{i=1}^n w \left[\left(\underline{\underline{D}}^T \underline{\underline{N}}^T \rho A \underline{\underline{IND}} + \underline{\underline{T}}_\omega^T \rho J \underline{\underline{T}}_\omega \right) \Big|_x \right] \\
 &\quad = \sum_{i=1}^n w \left[\left(\underline{\underline{D}}^T \underline{\underline{N}}^T \underline{\underline{\mathfrak{P}}}_{ine}^{t,i} \underline{\underline{ND}} + \underline{\underline{T}}_\omega^T \underline{\underline{\mathfrak{P}}}_{ine}^{r,i} \underline{\underline{T}}_\omega \right) \Big|_x \right]
 \end{aligned} \tag{C-140}$$

C.5 Cubic Spline Rope Dynamic Model

C.5.1 Generalized coordinate

$$\underline{q}_e = \begin{bmatrix} q_1 \\ q_2 \end{bmatrix} = \begin{bmatrix} \underline{l} \underline{r}^1 \\ \underline{l} \underline{r}'^1 \\ \underline{l} \underline{r}^2 \\ \underline{l} \underline{r}'^2 \end{bmatrix} \quad \underline{d} \underline{q}_e = \begin{bmatrix} d q_1 \\ d q_2 \end{bmatrix} = \begin{bmatrix} \underline{l} \dot{\underline{r}}^1 \\ \underline{l} \dot{\underline{r}}'^1 \\ \underline{l} \dot{\underline{r}}^2 \\ \underline{l} \dot{\underline{r}}'^2 \end{bmatrix} \tag{C-141}$$

C.5.2 Shape function

$${}_I \underline{r}^c = N_0^1 {}_I \underline{r}^1 + N_1^1 {}_I \underline{r}'^1 + N_0^2 {}_I \underline{r}^2 + N_1^2 {}_I \underline{r}'^2 = \underline{\underline{N}} q_e$$

$$\underline{\underline{N}} = [N_0^1 \underline{\underline{I}} \quad N_1^1 \underline{\underline{I}} \quad N_0^2 \underline{\underline{I}} \quad N_1^2 \underline{\underline{I}}] \quad (\text{C-142})$$

$${}_I \dot{\underline{r}}^c = N_0^1 {}_I \dot{\underline{r}}^1 + N_1^1 {}_I \dot{\underline{r}}'^1 + N_0^2 {}_I \dot{\underline{r}}^2 + N_1^2 {}_I \dot{\underline{r}}'^2 = \underline{\underline{N}} d q_e \quad (\text{C-143})$$

$${}_I \ddot{\underline{r}}^c = N_0^1 {}_I \ddot{\underline{r}}^1 + N_1^1 {}_I \ddot{\underline{r}}'^1 + N_0^2 {}_I \ddot{\underline{r}}^2 + N_1^2 {}_I \ddot{\underline{r}}'^2 = \underline{\underline{N}} d \dot{q}_e \quad (\text{C-144})$$

$${}_I \underline{r}'^c = N'^1_0 {}_I \underline{r}^1 + N'^1_1 {}_I \underline{r}'^1 + N'^2_0 {}_I \underline{r}^2 + N'^2_1 {}_I \underline{r}'^2 = \underline{\underline{N'}} q_e$$

$$\underline{\underline{N'}} = [N'^1_0 \underline{\underline{I}} \quad N'^1_1 \underline{\underline{I}} \quad N'^2_0 \underline{\underline{I}} \quad N'^2_1 \underline{\underline{I}}] \quad (\text{C-145})$$

$${}_I \dot{\underline{r}}'^c = N'^1_0 {}_I \dot{\underline{r}}^1 + N'^1_1 {}_I \dot{\underline{r}}'^1 + N'^2_0 {}_I \dot{\underline{r}}^2 + N'^2_1 {}_I \dot{\underline{r}}'^2 = \underline{\underline{N'}} d q_e \quad (\text{C-146})$$

$${}_I \ddot{\underline{r}}'^c = N'^1_0 {}_I \ddot{\underline{r}}^1 + N'^1_1 {}_I \ddot{\underline{r}}'^1 + N'^2_0 {}_I \ddot{\underline{r}}^2 + N'^2_1 {}_I \ddot{\underline{r}}'^2 = \underline{\underline{N'}} d \dot{q}_e \quad (\text{C-147})$$

$${}_I \underline{r}''^c = N''^1_0 {}_I \underline{r}^1 + N''^1_1 {}_I \underline{r}'^1 + N''^2_0 {}_I \underline{r}^2 + N''^2_1 {}_I \underline{r}'^2 = \underline{\underline{N''}} q_e$$

$$\underline{\underline{N''}} = [N''^1_0 \underline{\underline{I}} \quad N''^1_1 \underline{\underline{I}} \quad N''^2_0 \underline{\underline{I}} \quad N''^2_1 \underline{\underline{I}}] \quad (\text{C-148})$$

$${}_I \dot{\underline{r}}''^c = \underline{\underline{N''}} d q_e \quad (\text{C-149})$$

C.5.3 Strain

Axial stress

$${}_I \varepsilon = \| {}_I \dot{\underline{r}}'^c \| - 1 \quad (\text{C-150})$$

$${}_I \dot{\varepsilon} = \frac{1}{\| {}_I \dot{\underline{r}}'^c \|} {}_I \underline{r}'^{cT} {}_I \dot{\underline{r}}'^c = \frac{1}{\| {}_I \dot{\underline{r}}'^c \|} {}_I \underline{r}'^{cT} \underline{\underline{N'}} d q_e = \underline{T}_{\varepsilon}^T d q_e \quad (\text{C-151})$$

C.5.4 Virtual Internal Power

$${}_I \sigma = E A {}_I \varepsilon \quad (\text{C-152})$$

$$\delta p_{int} = - \int_0^L \underline{\delta}_I \underline{\varepsilon}^T \underline{\sigma} ds = - \underline{\delta} \underline{dq}_e^T EA \int_0^L \underline{T}_{\underline{\varepsilon}}^T \underline{\varepsilon} ds = - \underline{\delta} \underline{dq}_e^T \underline{F}_{int} \quad (C-153)$$

C.5.5 Virtual Inertial Power

$$\begin{aligned} \delta p_{ine} &= - \underline{\delta} \underline{dq}_e^T \underline{\underline{M}}_{e,ine} \underline{d}\dot{\underline{q}}_e \approx \delta p_{ine,tra} = - \rho A \int_0^L \underline{\delta}_I \underline{\dot{r}}^c \underline{\dot{r}}^c ds \\ &= - \underline{\delta} \underline{dq}_e^T \rho A \int_0^L \underline{\underline{N}}^T \underline{\underline{N}} ds \underline{d}\dot{\underline{q}}_e = - \underline{\delta} \underline{dq}_e^T \underline{\underline{M}}_{e,ine,tra} \underline{d}\dot{\underline{q}}_e \\ \underline{\underline{M}}_{e,ine} &\approx \underline{\underline{M}}_{e,ine,tra} = \rho A \int_0^L \underline{\underline{N}}^T \underline{\underline{N}} ds \end{aligned} \quad (C-154)$$

C.5.6 Virtual External Power

$$\begin{aligned} \delta p_{ext,g} &= \rho A \int_0^L \underline{\delta}_I \underline{\dot{r}}^c \underline{ds} \underline{Ig} = \underline{\delta} \underline{dq}_e^T \rho A \int_0^L \underline{\underline{N}}^T \underline{ds} \underline{Ig} = - \underline{\delta} \underline{dq}_e^T \underline{\underline{V}}_e \underline{Ig} \\ \underline{\underline{V}}_e &= - \rho A \int_0^L \underline{\underline{N}}^T \underline{ds} \quad F_{ext,g} = \underline{\underline{V}}_e \underline{Ig} \end{aligned} \quad (C-155)$$

C.5.7 Virtual power principle of Cubic Spline Rope

$$\begin{aligned} \delta p_e &= \delta p_{ine} + \delta p_{int} + \delta p_{ext} = \delta p_{ine} + \delta p_{int} + \delta p_{ext,g} \\ &= - \underline{\delta} \underline{dq}_e^T \left[\underline{\underline{M}}_{e,ine} \underline{d}\dot{\underline{q}}_e + \underline{F}_{int} + \underline{F}_{ext,g} \right] = - \underline{\delta} \underline{dq}_e^T \left(\underline{\underline{M}}_e \underline{d}\dot{\underline{q}}_e + \underline{F}_e \right) \quad (C-156) \\ \underline{\underline{M}}_e &= \underline{\underline{M}}_{e,ine} \quad \underline{F}_e = \underline{F}_{int} + \underline{F}_{ext,g} \end{aligned}$$

Appendix D Detailed Modelling Information of Lattice Boom Crane

D.1 Body Element, Joint Configuration and Initial State

D.1.1 Frame and Pedestal

Frame is a virtual element and only the joints of the frame should be defined. In addition, the initial state of the frame should always be zero.

Table D-1: Frame Parameter for Lattice Boom Crane Model

Parameter		Frame
Model Type	-	
Element Number	0	
Joints	Quantity	1
	Joint 1	$\underline{B}r_j = [0 \ 0 \ 0]^T, \underline{B}\varphi_j = [0 \ 0 \ 0]^T$
Initial State	State variables	$\underline{x}_f = [\underline{q}_f^T \ \underline{dq}_f^T]^T = [\underline{r}^T \ \underline{B}\varphi^T \ \underline{dq}_e^T]^T$ with $\underline{dq}_f = 0$
	Position	$\underline{I}r = [0 \ 0 \ 0]^T$
	Posture	$\underline{B}\varphi = [0 \ 0 \ 0]^T$

The pedestal is regarded as a rigid body. The parameters of pedestal are shown as follows

Table D-2: Pedestal Parameter for Lattice Boom Crane Model

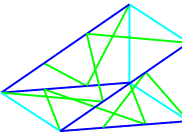
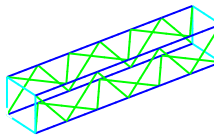
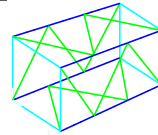
Parameter		Body 1
Model Type	Rigid Body	
Section Size	Type	Custom defined
	Length	30
	Mass	100
	Moment of inertia	1000 x diag([1,1,1])
	Centroid position	[1;0;0]
Joints	Quantity	2
	Joint 1	$\underline{B}r_j = [0 \ 0 \ 0]^T \quad \underline{B}\varphi_j = [0 \ 0 \ 0]^T$
	Joint 2	$\underline{B}r_j = [11 \ 0 \ 0]^T \quad \underline{B}\varphi_j = [0 \ 0 \ 0]^T$

Parameter		Type 1
Initial State	State variables	$\underline{x}_e = [\underline{q}_e^T \quad \underline{d}\underline{q}_e^T]^T = [\underline{l}\underline{r}^T \quad \underline{B}\underline{\varphi}^T \quad \underline{d}\underline{q}_e^T]^T$ with $d\underline{q}_e = \underline{0}$
	Position	$\underline{l}\underline{r} = [0 \quad 0 \quad 0]^T$
	Posture	$\underline{B}\underline{\varphi} = [0 \quad 0 \quad 0]^T$

D.1.2 Main Boom

The main boom consists of 5 super truss elements in 3 types.

Table D-3: Main Boom Parameter for Lattice Boom Crane Model

Parameter		Type 1	Type 2	Type 3	
Structure		  			
Model Type		Super Truss Element	Super Truss Element	Super Truss Element	
Element Number		2	3,4,5	6	
Truss Parameters	Truss Order	3	6	3	
	Truss Length	5	15	5	
Truss Parameters	Nodes on Cross	x-Position y-Position z-Position	0,0 1.5,-1.5 0,0	0,0,0,0 1.5,-1.5,-1.5,1.5 1.4,1.4,-1.4,-1.4	
	Nodes on Cross	x-Position y-Position z-Position	0,0,0,0 1.5,-1.5,-1.5,1.5 1.4,1.4,-1.4,-1.4	0,0,0,0 1.5,-1.5,-1.5,1.5 1.4,1.4,-1.4,-1.4	
	Main Beam	Nodes Nr. 1 Nodes Nr. 2	1,2,2,1 1,2,3,4	1,2,3,4 1,2,3,4	
	Cross Section Beam	Nodes Nr. 1 Nodes Nr. 2	1,2 1,2;2,3;3,4;4,1	1,2;2,3;3,4;4,1 1,2;2,3;3,4;4,1	
	SB Connection Form	TP Type1	Type1	Type1	
	Main Beam	Type ra ri	Round Tube 0.1 0.08	Round Tube 0.1 0.08	
	Cross Section Beam	Type ra ri	Round Tube 0.1 0.08	Round Tube 0.1 0.08	
	Sub-Beam	Type ra ri	Round Tube 0.05 0.04	Round Tube 0.05 0.04	

	Parameter	Type 1	Type 2	Type 3
Material Properties	Density	7800	7800	7800
	Elastic modulus	2060000000000	2060000000000	2060000000000
	Poisson's ratio	0.25	0.25	0.25

Only two joints are on the flexible beam, and located at the ends of the beam elements. The initial state of the super truss elements consists of generalized coordinate and generalized velocity. The generalized velocity at initial state is zero. The generalized coordinate is shown as follows

Table D-4: Main Boom Initial State Parameter for Lattice Boom Crane Model

	Initial State	Body 2	Body 3	Body 4	Body 5	Body 6
Generalized Coordinate	Point 1	\underline{r}^1	$\begin{bmatrix} 0 \\ 0 \\ 0 \end{bmatrix}$	$\begin{bmatrix} -0.43578 \\ 0 \\ 4.980973 \end{bmatrix}$	$\begin{bmatrix} -1.7431 \\ 0 \\ 19.9239 \end{bmatrix}$	$\begin{bmatrix} -3.05045 \\ 0 \\ 34.86681 \end{bmatrix}$
		$\underline{\varphi}^1$	$\begin{bmatrix} 0 \\ -rad(95^\circ) \\ 0 \end{bmatrix}$	$\begin{bmatrix} 0 \\ -rad(95^\circ) \\ 0 \end{bmatrix}$	$\begin{bmatrix} 0 \\ -rad(95^\circ) \\ 0 \end{bmatrix}$	$\begin{bmatrix} 0 \\ -rad(95^\circ) \\ 0 \end{bmatrix}$
	Point 2	\underline{r}^2	$\begin{bmatrix} -0.43578 \\ 0 \\ 4.980973 \end{bmatrix}$	$\begin{bmatrix} -1.74311 \\ 0 \\ 19.92389 \end{bmatrix}$	$\begin{bmatrix} -3.0505 \\ 0 \\ 34.8668 \end{bmatrix}$	$\begin{bmatrix} -4.35779 \\ 0 \\ 49.80973 \end{bmatrix}$
		$\underline{\varphi}^2$	$\begin{bmatrix} 0 \\ -rad(95^\circ) \\ 0 \end{bmatrix}$	$\begin{bmatrix} 0 \\ -rad(95^\circ) \\ 0 \end{bmatrix}$	$\begin{bmatrix} 0 \\ -rad(95^\circ) \\ 0 \end{bmatrix}$	$\begin{bmatrix} 0 \\ -rad(95^\circ) \\ 0 \end{bmatrix}$

D.1.3 Main Boom Head

Because of the complexity of the main beam head, it is regarded as a rigid body and its configuration is shown as

Table D-5: Main Boom Head Parameter for Lattice Boom Crane Model

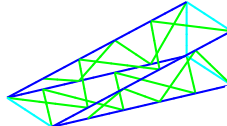
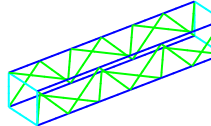
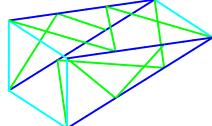
	Parameter	Body 7
	Model Type	Rigid Body
Section Size	Type	Custom defined
	Length	2
	Mass	1
	Moment of inertia	$1 \times \text{diag}([1,1,1])$
	Centroid position	[0.5;0;0]

	Parameter	Body 7
Joints	Quantity	13
	Joint 1	$B\vec{r}_j = [0 \ 0 \ 0]^T$ $B\vec{\varphi}_j = [0 \ 0 \ 0]^T$
	Joint 2	$B\vec{r}_j = [0 \ 0 \ -1.2]^T$ $B\vec{\varphi}_j = [0 \ 0 \ 0]^T$
	Joint 3	$B\vec{r}_j = [1.75 \ 0 \ -1.4]^T$ $B\vec{\varphi}_j = [0 \ 0 \ 0]^T$
	Joint 4	$B\vec{r}_j = [2.2 \ 0 \ 1.7]^T$ $B\vec{\varphi}_j = [0 \ 0 \ 0]^T$
	Joint 5	$B\vec{r}_j = [0 \ 0 \ 1.2]^T$ $B\vec{\varphi}_j = [0 \ 0 \ 0]^T$
	Joint 6	$B\vec{r}_j = [0 \ 1.3 \ 1.2]^T$ $B\vec{\varphi}_j = [0 \ 0 \ 0]^T$
	Joint 7	$B\vec{r}_j = [0 \ -1.3 \ 1.2]^T$ $B\vec{\varphi}_j = [0 \ 0 \ 0]^T$
	Joint 8	$B\vec{r}_j = [0 \ 1.3 \ -1.2]^T$ $B\vec{\varphi}_j = [0 \ 0 \ 0]^T$
	Joint 9	$B\vec{r}_j = [0 \ -1.3 \ -1.2]^T$ $B\vec{\varphi}_j = [0 \ 0 \ 0]^T$
	Joint 10	$B\vec{r}_j = [1.75 \ 1.4 \ -1.4]^T$ $B\vec{\varphi}_j = [0 \ 0 \ 0]^T$
	Joint 11	$B\vec{r}_j = [1.75 \ -1.4 \ -1.4]^T$ $B\vec{\varphi}_j = [0 \ 0 \ 0]^T$
	Joint 12	$B\vec{r}_j = [2.2 \ 1.5 \ 1.7]^T$ $B\vec{\varphi}_j = [0 \ 0 \ 0]^T$
	Joint 13	$B\vec{r}_j = [2.2 \ -1.5 \ 1.7]^T$ $B\vec{\varphi}_j = [0 \ 0 \ 0]^T$
Initial State	State variables	$\underline{x}_e = [\underline{q}_e^T \ \underline{dq}_e^T]^T = [\underline{l}\underline{r}^T \ B\underline{\varphi}^T \ \underline{dq}_e^T]^T$ with $\underline{dq}_e = \underline{0}$
	Position	$\underline{l}\underline{r} = [-4.7936 \ 0 \ 54.7907]^T$
	Posture	$B\underline{\varphi} = [0 \ -rad(95^\circ) \ 0]^T$

D.1.4 Derrick Boom

The derrick boom consists of 3 super truss elements in 3 types.

Table D-6: *Derrick Boom Parameter for Lattice Boom Crane Model*

	Parameter	Type 4	Type 5	Type 6
Structure				
Model Type		Super Truss Element	Super Truss Element	Super Truss Element
Element Number	8	9	10	
Section Size	Type	Round Tube	Round Tube	Round Tube
	Main Beam ra	0.1	0.1	0.1
	ri	0.08	0.08	0.08
	Cross Section Beam Type	Round Tube	Round Tube	Round Tube
	ra	0.1	0.1	0.1
	ri	0.08	0.08	0.08
Sub-Beam	Type	Round Tube	Round Tube	Round Tube
	ra	0.05	0.05	0.05
	ri	0.04	0.04	0.04

	Parameter	Type 4	Type 5	Type 6
Material Properties	Density	7800	7800	7800
	Elastic modulus	2060000000000	2060000000000	2060000000000
	Poisson's ratio	0.25	0.25	0.25
Truss Parameters	Truss Order	5	6	3
	Truss Length	8	13	5
	Nodes on Cross Section 1	x-Position y-Position z-Position	0,0 1.3,-1.3 0,0	0,0,0,0 1.3,-1.3,-1.3,1.3 1.1,1.1,-1.1,-1.1
	Nodes on Cross Section 1	x-Position y-Position z-Position	0,0,0,0 1.3,-1.3,-1.3,1.3 1.1,1.1,-1.1,-1.1	0,0 1.3,-1.3 0,0
	Main Beam	Nodes Nr. 1 Nodes Nr. 2	1,2,2,1 1,2,3,4	1,2,3,4 1,2,2,1
	Cross Section Beam	Nodes Nr. 1 Nodes Nr. 2	1,2 1,2;2,3;3,4;4,1	1,2;2,3;3,4;4,1 1,2
	SB Connection Form	TP Type1	Type1	TP Anti Type1

The generalized coordinate in initial state is shown as follows

Table D-7: Derrick Boom Initial State Parameter for Lattice Boom Crane Model

	Initial State	Body 8	Body 9	Body 10
Generalized Coordinate	Point 1	\underline{r}^1 $\begin{bmatrix} 0 \\ 0 \\ 0 \end{bmatrix}$	$\begin{bmatrix} 3.38095 \\ 0 \\ 7.25046 \end{bmatrix}$	$\begin{bmatrix} 8.87498 \\ 0 \\ 19.0325 \end{bmatrix}$
		$\underline{\varphi}^1$ $\begin{bmatrix} 0 \\ -rad(65^\circ) \\ 0 \end{bmatrix}$	$\begin{bmatrix} 0 \\ -rad(65^\circ) \\ 0 \end{bmatrix}$	$\begin{bmatrix} 0 \\ -rad(65^\circ) \\ 0 \end{bmatrix}$
	Point 2	\underline{r}^2 $\begin{bmatrix} 3.38095 \\ 0 \\ 7.25046 \end{bmatrix}$	$\begin{bmatrix} 8.87498 \\ 0 \\ 19.0325 \end{bmatrix}$	$\begin{bmatrix} 10.9881 \\ 0 \\ 23.564 \end{bmatrix}$
		$\underline{\varphi}^2$ $\begin{bmatrix} 0 \\ -rad(65^\circ) \\ 0 \end{bmatrix}$	$\begin{bmatrix} 0 \\ -rad(65^\circ) \\ 0 \end{bmatrix}$	$\begin{bmatrix} 0 \\ -rad(65^\circ) \\ 0 \end{bmatrix}$

D.1.5 Luffing Cable System

The luffing cable system consists of 3 elements, namely 2 strut tie models and 1 cubic spline rope. The parameters of 2 strut tie models are shown as follows

Table D-8: Strut Tie Model Parameter for Lattice Boom Crane Model

Parameter		Type 11	Type 12
Model Type		Strut Tie Model	Strut Tie Model
Section Size	Type	Round Tube	Round Tube
	Length	15	15
	Outer Diameter	0.05	0.05
	Inner Diameter	0	0
Material Properties	Density	7800	7800
	Elastic modulus	206000000000	206000000000
Generalized Coordinate	Poisson's ratio	0.25	0.25
	Point 1	\underline{r}^1 $[-3.551 \ 0 \ 56.656]^T$	$[2.482 \ 0 \ 42.923]^T$
	Point 2	\underline{r}^2 $[2.482 \ 0 \ 42.923]^T$	$[8.516 \ 0 \ 29.190]^T$

The cubic spline rope is used to adjust the length of luffing cable system. The parameters of the cubic spline rope are shown as follows

Table D-9: Luffing Rope Parameter for Lattice Boom Crane Model

Parameter		Type 13
Model Type		Cubic Spline Rope
Section Size	Type	Round Tube
	Length	6.1453
	Outer Diameter	0.05
	Inner Diameter	0
Material Properties	Density	7800
	Elastic modulus	100000000000
Generalized Coordinate	Poisson's ratio	0.25
	Point 1	\underline{r}^1 $[10.988 \ 0 \ 23.564]^T$
		φ^1 $[0 \ -1.985 \ 0]^T$
		$\ \underline{r}'^1 \ $ 1
		\underline{r}^2 $[8.516 \ 0 \ 29.190]^T$
	Point 2	φ^2 $[0 \ -1.985 \ 0]^T$
		$\ \underline{r}'^2 \ $ 1

D.1.6 Sub-Cable

The sub-cable is modeled as a cubic spline rope, whose parameter is shown as follows

Table D-10: Sub-Cable Parameter for Lattice Boom Crane Model

Parameter		Type 14
	Model Type	Cubic Spline Rope
Section Size	Type	Round Tube
	Length	23.5640
	Outer Diameter	0.05
	Inner Diameter	0
Material Properties	Density	7800
	Elastic modulus	1000000000000
	Poisson's ratio	0.25
Generalized Coordinate	\underline{r}^1	$[11 \ 0 \ 0]^T$
	Point 1 $\underline{\varphi}^1$	$[0 \ -rad(90^\circ) \ 0]^T$
	$\ \underline{r}'^1\ $	1
	\underline{r}^2	$[10.988 \ 0 \ 23.564]^T$
	Point 2 $\underline{\varphi}^2$	$[0 \ -rad(90^\circ) \ 0]^T$
	$\ \underline{r}'^2\ $	1

D.1.7 Lifting Cable

The lifting cable is modeled as a cubic spline rope, whose parameter is shown as follows

Table D-11: Lifting Cable Parameter for Lattice Boom Crane Model

Parameter		Type 15
	Model Type	Cubic Spline Rope
Section Size	Type	Round Tube
	Length	54.8342
	Outer Diameter	0.05
	Inner Diameter	0
Material Properties	Density	7800
	Elastic modulus	1000000000000
	Poisson's ratio	0.25
Generalized Coordinate	\underline{r}^1	$[0 \ 0 \ 0]^T$
	Point 1 $\underline{\varphi}^1$	$[0 \ -rad(95^\circ) \ 0]^T$
	$\ \underline{r}'^1\ $	1
	\underline{r}^2	$[-0.43578 \ 0 \ 4.980973]^T$
	Point 2 $\underline{\varphi}^2$	$[0 \ -rad(95^\circ) \ 0]^T$
	$\ \underline{r}'^2\ $	1

D.1.8 Load

The load is basically a rigid body. Simply it is treated a cylinder, whose total mass nears to 400 tons. The parameter is shown as follows

Table D-12: Load Parameter for Lattice Boom Crane Model

Parameter		Body 16
Model Type		Rigid Body
Section Size	Type	Round Tube
	Length	2
	Outer Diameter	2.82095
	Inner Diameter	0
Joints	Quantity	2
	Joint 1	$B\vec{r}_j = [0 \ 0 \ 0]^T$ $B\vec{\varphi}_j = [0 \ 0 \ 0]^T$
	Joint 2	$B\vec{r}_j = [2 \ 0 \ 0]^T$ $B\vec{\varphi}_j = [0 \ 0 \ 0]^T$
Initial State	State variables	$\underline{x}_e = [\underline{q}_e^T \ \underline{dq}_e^T]^T = [\underline{l}r^T \ B\varphi^T \ \underline{dq}_e^T]^T$ with $\underline{dq}_e = 0$
	Position	$\underline{l}r = [-6.6788 \ 0 \ 2]^T$
	Posture	$B\varphi = [0 \ rad(90^\circ) \ 0]^T$

D.2 Constraint and Nodal Force

Constraints Configuration

There are totally 18 constraints for lattice boom crane. The configuration of constraints is shown as follows

Table D-13: Constraint Parameter for Lattice Boom Crane Model

Nr.	Body Nr. 1	Joint Nr. 1	Body Nr. 2	Joint Nr. 2	Constraint Type	Reduced
1	0	1	1	1	Fixed	
2	1	1	2	1	Revolute_y	✓
3	2	2	3	1	Fixed	✓
4	3	2	4	1	Fixed	✓
5	4	2	5	1	Fixed	✓
6	5	2	6	1	Fixed	✓
7	7	1	6	2	Fixed	✓
8	1	1	8	1	Revolute_y	✓
9	8	2	9	1	Fixed	✓
10	9	2	10	1	Fixed	✓
11	7	3	11	1	Spherical	

Nr.	Body Nr. 1	Joint Nr. 1	Body Nr. 2	Joint Nr. 2	Constraint Type	Reduced
12	11	2	12	1	Spherical	
13	12	2	13	2	Spherical	✓
14	10	2	13	1	Spherical	✓
15	1	2	14	1	Spherical	
16	14	2	10	2	Spherical	✓
17	7	4	15	1	Spherical	
18	16	1	15	2	Spherical	

Among them, the fixed constraints, revolute constraints and the spherical constraints can be realized by using public computing nodes, which can reduce the overall degree of freedom. The final lattice boom crane model has 8 constraints.

Nodal Force

No external nodal force for lattice boom crane model. The structure of the nodal force parameter table is shown as follows

Table D-14: Nodal Force Parameter for Lattice Boom Crane Model

Nr.	Body Nr.	Joint Nr.	Force				Moment			
			Fx	Fy	Fz	F-Coordinate	Mx	My	Mz	M-Coordinate
1										

The coordinate of force and moment can be chosen as “Inertial” or “Body”.

D.3 Solver Parameter

The solver parameter consists of several parts, which consider the global parameter, solver, solving consequence and postprocessing method. The detailed information is shown as follows

Table D-15: Solver Parameter for Lattice Boom Crane Model

	Parameter	Value
Jacobian Matrix	Calculation Jacobian Matrix	false
Gravity Setting	Direction of gravity	0; 0; -1
	Gravity Magnitude	9.8

	Parameter	Value
ODE Setting	ODE Solver	ode23tb
	ODE Solver Method	-
	ODE Solver Order	-
	ODE Solver Option	-
	Calculation Time Start	0
	Calculation Time End	100
	Absolute Tolerance	0.01
	Relative Tolerance	0.01
Static Position	Max Step	0.01
	ODE Output Function	MechanismPlot
	Calculation Static Position	true
	Max Tolerance for Velocity and Acceleration	1e-9
Display by Computing	Display Current Time	true
	Plot Mechanism by Computing	true
	Plot Start Iteration	0
	Plot Iteration Interval	100
Result	Save Result	true
	Result Existence	false
	Result Saving Dictionary	[]
Plot Configuration	Axes Size	-30, 30, -30, 30, 0, 60
	Grid	on, MINOR
	Observation	x-z
Post Processing	Post Processing Method	none

D.4 Plot Parameter

The plot parameters of the elements describe the sequence of the joints for drawing the elements and the configuration of the printed lines. For the flexible beam, it is also needed to set the number of displayed interpolation points, which can more detailed show the shape of the elements after the deformation.

Table D-16: Plot Parameter for Lattice Boom Crane Model

Parameter	Body 1	Body 2	Body 3	Body 4	Body 5
Sequence	1,2	-	-	-	-
Interpolation Number	-	5	5	5	5
Configuration	k.-	b-, c-, g-	b-, c-, g-	b-, c-, g-	b-, c-, g-

Parameter	Body 6	Body 8	Body 9	Body 10	Body 11
Sequence	-	-	-	-	-
Interpolation Number	5	5	5	5	2
Configuration	b-, c-, g	b-, c-, g-	b-, c-, g-	b-, c-, g-	y-
Parameter	Body 12	Body 13	Body 14	Body 15	Body 16
Sequence	-	-	-	-	1,2
Interpolation Number	2	5	5	5	-
Configuration	y-	r-	r-	r-	k-
Parameter	Body 7				
Sequence	6,7,9,8,6,12,13,7,13,11,9,11,10,8,10,12				
Interpolation Number	-				
Configuration	y-				

Since the flexible beam has only two joints, it is not necessary to define the sequence of the flexible beam.

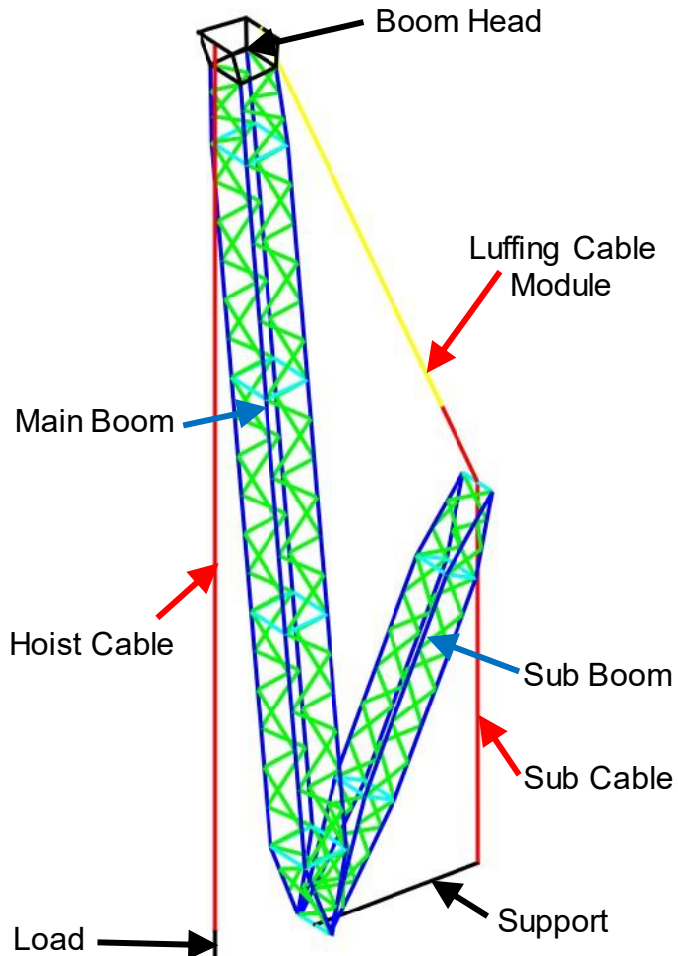


Figure D-1: Display of Lattice Boom Crane

Appendix E Specified Drive Function

E.1 Trapezoidal Velocity Three Stage Function

Acceleration phase t_1

$$s_1 = \frac{1}{2} a_1 t_1^2 \quad v_{max} = a_1 t_1 \quad (\text{E-1})$$

Uniform speed phase t_2

$$s_2 = v_{max} t_2 \quad (\text{E-2})$$

Deceleration phase t_3

$$s_3 = v_{max} t_3 + \frac{1}{2} a_3 t_3^2 \quad v_{max} + a_3 t_3 = 0 \quad (\text{E-3})$$

Relationship

$$\begin{aligned} t_0 &= t_1 + t_2 + t_3 \\ s_0 &= s_1 + s_2 + s_3 = \frac{1}{2} a_1 t_1 (2t_0 - t_1 - t_3) \end{aligned} \quad (\text{E-4})$$

Assume s_0, t_0, t_1, t_3 are known

$$a_1 = \frac{2s_0}{t_1(2t_0 - t_1 - t_3)} \quad a_3 = -\frac{2s_0}{t_3(2t_0 - t_1 - t_3)} \quad (\text{E-5})$$

For example: $s_0 = 10m, t_0 = 40s, t_1 = 5s, t_3 = 5s$

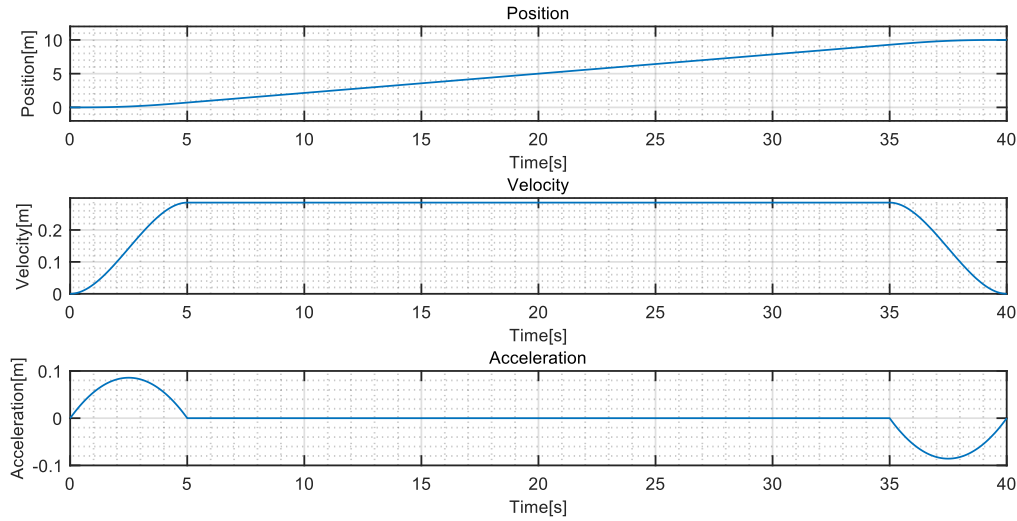


Figure E-1: Trapezoidal Velocity Three Stage Function

E.2 Trigonometric Cosine Function (\cos)

Trigonometric cosine function is used in the transition section from start value y_{start} to end value y_{end} in the certain time span t_{start} to t_{end} . The function can be written as

$$y_h(t) = \begin{cases} y_{start}, & t < t_{start} \\ \frac{y_{start} + y_{end}}{2} + \frac{y_{start} - y_{end}}{2} \cos \frac{(t - t_{start})\pi}{t_{start} - t_{end}}, & t_{start} \leq t \leq t_{end} \\ y_{end}, & t > t_{end} \end{cases} \quad (\text{E-6})$$

$$\dot{y}_h(t) = \begin{cases} 0, & t < t_{start} \\ -\frac{\pi}{2} \frac{y_{start} - y_{end}}{t_{start} - t_{end}} \sin \frac{(t - t_{start})\pi}{t_{start} - t_{end}}, & t_{start} \leq t \leq t_{end} \\ 0, & t > t_{end} \end{cases} \quad (\text{E-7})$$

$$\ddot{y}_h(t) = \begin{cases} 0, & t < t_{start} \\ -\frac{\pi^2}{2} \frac{y_{start} - y_{end}}{(t_{start} - t_{end})^2} \cos \frac{(t - t_{start})\pi}{t_{start} - t_{end}}, & t_{start} \leq t \leq t_{end} \\ 0, & t > t_{end} \end{cases} \quad (\text{E-8})$$

For example: $y_{start} = 10$, $y_{end} = 20$, $t_{start} = 5$, $t_{end} = 15$

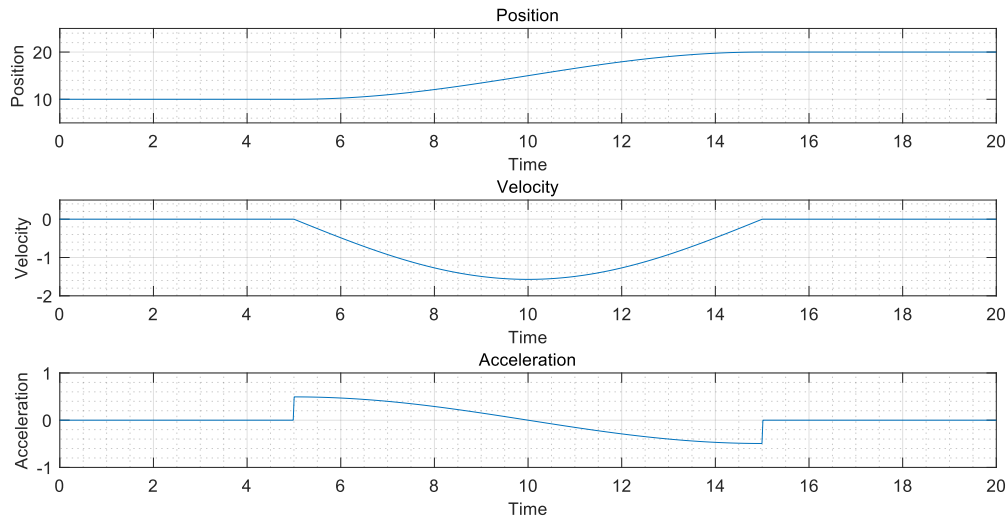


Figure E-2: Trigonometric Cosine Step Function

Also, the cosine function can be used to generate a smooth transition section from value y_1 to value y_2 and then return to value y_1 in the certain time span t_1 to t_2 . The value y_2 will be reached at $(t_1 + t_2)/2$. The function can be written as

$$y_f(t) = \begin{cases} y_1, & t < t_1 \\ \frac{y_1 + y_2}{2} + \frac{y_1 - y_2}{2} \cos \frac{2\pi(t - t_1)}{t_1 - t_2}, & t_1 \leq t \leq t_2 \\ y_1, & t > t_2 \end{cases} \quad (\text{E-9})$$

$$\dot{y}_f(t) = \begin{cases} 0, & t < t_1 \\ -\pi \frac{y_1 - y_2}{t_1 - t_2} \sin \frac{2\pi(t - t_1)}{t_1 - t_2}, & t_1 \leq t \leq t_2 \\ 0, & t > t_2 \end{cases} \quad (\text{E-10})$$

$$\ddot{y}_f(t) = \begin{cases} 0, & t < t_1 \\ -2\pi^2 \frac{y_1 - y_2}{(t_1 - t_2)^2} \cos \frac{2\pi(t - t_1)}{t_1 - t_2}, & t_1 \leq t \leq t_2 \\ 0, & t > t_2 \end{cases} \quad (\text{E-11})$$

For example: $y_1 = 10$, $y_2 = 20$, $t_1 = 5$, $t_2 = 15$

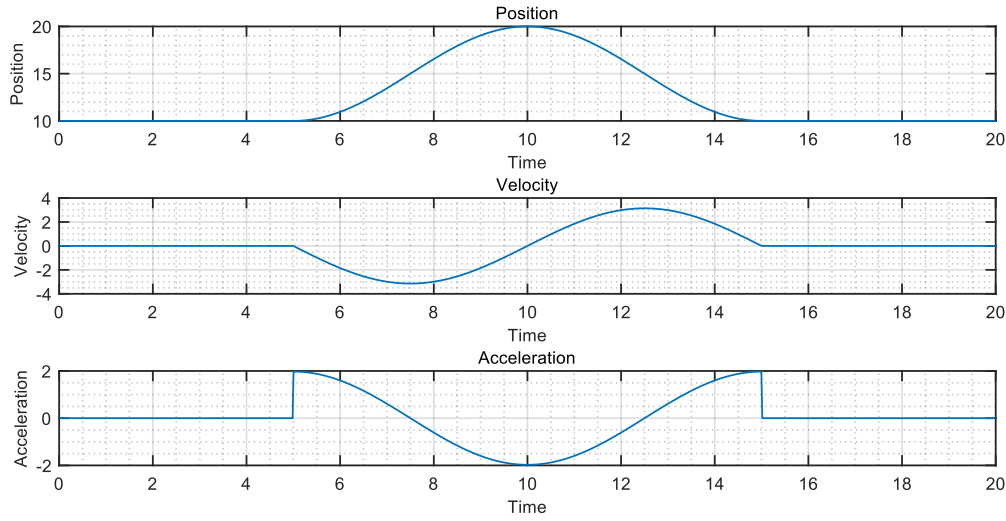


Figure E-3: Trigonometric Cosine Full Function

E.3 Hyperbolic Tangent Function (\tanh)

The hyperbolic tangent function (\tanh) can be written as

$$\tanh t = \frac{\sinh t}{\cosh t} = \frac{e^t - e^{-t}}{e^t + e^{-t}}$$

$$\lim_{t \rightarrow 0} \tanh t = 0 \quad \lim_{t \rightarrow \infty} \tanh t = 1 \quad (\text{E-12})$$

The hyperbolic tangent function can never reach 0 or 1 in practical situation. According to the deviation from the limit value, different confidence interval coefficients and confidence intervals are designed.

Table E-1: Confidence Coefficient of Hyperbolic Tangent Function

Nr.	Confidence c	Coefficient $\lambda(c)$	Variable Interval	Value Interval
1	90.0%	1.4765	[-1.4765; 1.4765]	[0.100; 0.900]
2	95.0%	1.8368	[-1.8368; 1.8368]	[0.050; 0.950]
3	99.0%	2.6476	[-2.6476; 2.6476]	[0.010; 0.990]
4	99.5%	2.9980	[-2.9980; 2.9980]	[0.005; 0.995]
5	99.9%	3.8088	[-3.8088; 3.8088]	[0.001; 0.999]

The transition function from value y_1 to value y_2 in the certain time span t_1 to t_2 with the confidence c can be written as

$$y(t) = \frac{1}{2}(y_1 + y_2) + \frac{1}{2}(y_2 - y_1) \tanh \frac{\lambda[2t - (t_1 + t_2)]}{t_2 - t_1} \quad \text{with } \lambda = \lambda(c) \quad (\text{E-13})$$

$$\dot{y}(t) = \lambda \frac{y_2 - y_1}{t_2 - t_1} \left(1 - \tanh^2 \frac{\lambda[2t - (t_1 + t_2)]}{t_2 - t_1} \right) \quad (\text{E-14})$$

$$\begin{aligned} \ddot{y}(t) &= -4\lambda^2 \frac{y_2 - y_1}{(t_2 - t_1)^2} \tanh \frac{\lambda[2t - (t_1 + t_2)]}{t_2 - t_1} \left(1 - \tanh^2 \frac{\lambda[2t - (t_1 + t_2)]}{t_2 - t_1} \right) \\ &= -4\lambda \frac{1}{t_2 - t_1} \tanh \frac{\lambda[2t - (t_1 + t_2)]}{t_2 - t_1} \dot{y}(t) \end{aligned} \quad (\text{E-15})$$

For example: $y_1 = 10$, $y_2 = 20$, $t_1 = 5$, $t_2 = 15$

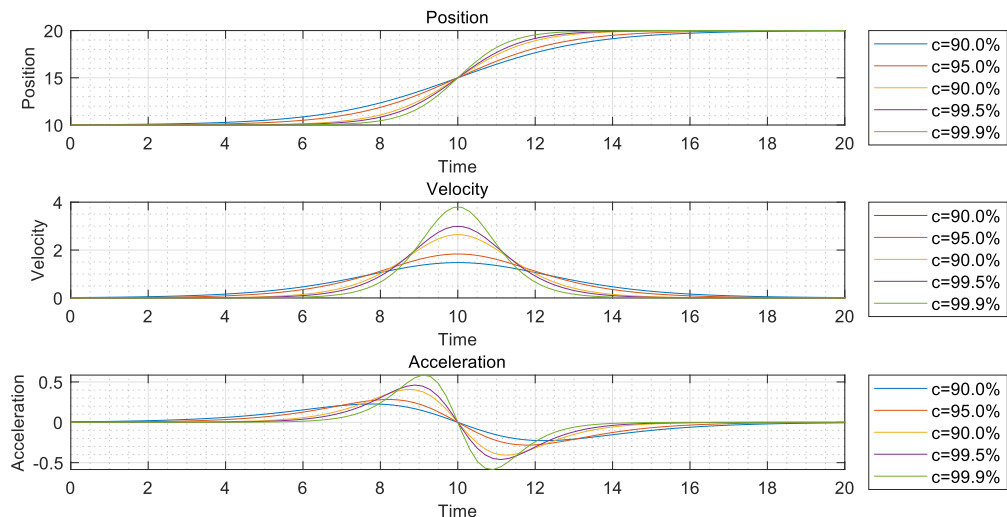


Figure E-4: Hyperbolic Tangent Function

Eidesstattliche Erklärung

Ich versichere hiermit, dass ich die von mir eingereichte Abschlussarbeit selbstständig verfasst und keine anderen als die angegebenen Quellen und Hilfsmittel benutzt habe.

München, 31, Mai, 2021

Ort, Datum, Unterschrift

Dai Xiaobing

Statutory Declaration

I hereby affirm that I wrote the submitted thesis myself and that I did not use any other sources and aids than those in bibliography.

Munich, 31, May, 2021

Place, Date, Signature

Dai Xiaobing